The role of Orai inhibition in acute pancreatitis

Thesis submitted in accordance with the requirements of the University of Liverpool for the degree of Doctor of Philosophy

By

Li Wen

August 2015

Dedicated to my father, my mother &

my husband

Statement of originality

The work described in this thesis was carried out when I was doing the PhD study in the NIHR Liverpool Pancreas Biomedical Research Unit and Department of Molecular and Clinical Cancer Medicine, Institute of Translational Medicine, University of Liverpool. All the work described in this thesis was done by me and the thesis was written entirely by me, except for the specific contributions listed below.

Prof Robert Sutton supervised all aspects of experimental design and planning as well as advised on revision of all the chapters of this thesis. Dr Wei Huang taught me the techniques for the induction of experimental AP when I firstly started my PhD study. Dr Svetlana Voronina and Dr Michael Chvanov conducted the experiments for measuring $[Ca^{2+}]_c$ in pancreatic acinar cells; Miss Diane Latawiec as one independent observer blindly scored pancreatic histopathological slides with me. Mr Muhammad Ahsan Javed and Dr Muhammad Awais assisted in the experiments for measuring necrotic cell death pathway activation. Dr John Barrett, GlaxoSmithKline (GSK) assisted to measure the levels of GSK-7975A and GSK-6288B in the blood and pancreas as well as protein binding of GSK-7975A in the blood and pancreas; Calcimedica assisted to measure the levels of CM_128 in the plasma, pancreas and lung. Dr Jane Amstrong helped to proof-read the English used in this thesis. I take full responsibility for any errors in the data within or compilation of this thesis, as well as any errors in the use of English.

Abstract

Background and aims: Prolonged elevation of cytosolic Ca^{2+} concentration is the key trigger of pancreatic damage and acute pancreatitis (AP). Ca^{2+} release-activated Ca^{2+} modulator Orai1 channel is the most abundant store-operated Ca^{2+} entry (SOCE) channel in pancreatic acinar cells; it sustains calcium overload in mice exposed to toxins that induce AP. The studies in this thesis investigated the roles of Orai1channel in pancreatic acinar cell injury and the development of AP in mice.

Methods: Freshly isolated mouse and human acinar cells were hyper-stimulated or incubated with human bile acid orthapsigargin to induce Ca^{2+} entry. Effects of GSK-7975A or CM_128 on Ca^{2+} entry and necrotic cell death pathway activation were analysed by confocal and video microscopy. Experimental acute pancreatitis was induced in C57BL/6J mice by 1) ductal injections of taurolithocholic acid 3-sulphate (TLCS-AP); 2) intraperitoneal (IP) administration of caerulein (CER-AP) or 3) a combined IP administration of ethanol and palmitoleic acid (FAEE-AP). Two Orai1 inhibitors were administrated at different time points and the disease severity was assessed by various local and systemic parameters, including pancreatic trypsin and myeloperoxidase (MPO) activity, serum interleukin (IL)-6 and lung MPO activityas well as blinded histopathology.

Results: GSK-7975A and CM_128 each separately inhibited toxin-induced activation of SOCE via Orai1 channels in a concentration dependent manner, in mouse and human pancreatic acinar cells (inhibition >90% the levels observed in control cells). GSK-7975A and CM_128 each inhibited all local and systemic features of AP in all three representative models, in dose- and time-dependent manners. The agents were significantly more effective, in a range of parameters, when given early versus late after induction of AP.

Conclusion: Cytosolic Ca^{2+} overload mediated via Orai1 plays a pivotal role in the pathogenesis of AP. Inhibition of Orai1 channel is a useful therapeutic approach for human acute pancreatitis.

Acknowledgements

Firstly, I would like to tremendously thank my supervisor Prof Robert Sutton for his great, constructive and never-ending supervision, guidance, inspiration and support throughout my entire PhD study. Prof Sutton is the best supervisor I have ever met, pursuing excellent educational strategies. All his efforts have made my PhD training splendid, productive, meaningful and memorable. His intelligence, passion, hard-work and great personality as well as his considerable scientific thinking have influenced me deeply. My PhD study in the NIHR Liverpool Pancreas Biomedical Research Unit has firmly reinforced my desire to become an international pancreatologist in the future, which may take my entire life to become!

Secondly, I would like to thank my co-supervisor, Dr David Criddle, who is friendly, easily approachable and always ready to give advice; Prof Qing Xia, in the Department of Integrated Traditional Chinese and Western Medicine, West China Hospital, Sichuan University, who supported and encouraged me to come to study in the United Kingdom and Prof Alexei Tepikin for kindly letting me work in Blue Block in the Physiological Laboratory and for his scientific advice on my projects.

I would also like to hugely thank Dr Svetlana Voronina and Dr Michael Chvanov in Blue Block for providing invaluable technical support; Miss Diane Latawiec, who has undertaken histopathological scoring with me of countless slides with great enthusiasm; and Mr Muhammad Ahsan Javed and Dr Muhammad Awais, who helped in the experiments measuring necrotic cell death pathway activation. Many thanks to Dr Wei Huang, who taught me the techniques for induction of experimental acute pancreatitis; to Dr Jane Amstrong, who taught me the ELISA assay (for this

project) as well as many other assays and to Dr Brian Lane, Dr Li Yan, Dr Vicki Elliott, Mr Peter Szatmary, Mr Rajarshi Mukherjee, Mr Ajay Sud and all the other members from NIHR Liverpool Pancreas Biomedical Research Unit for their valuable time for discussion and general advice, hospitality and wisdom. Special thanks to Ms Becky Taylor for all her generous help to make my life much easier in Liverpool.

I would also like to thank the staff in the Biomedical Services Unit for their assistance during my *in vivo* experiments; Mr Michael Neil from the Department of Pathology for helping with preparing the histological samples in a timely manner and Mr William Taylor and Ms Jean Devine from the Department of Clinical Biochemistry for helping with amylase analyses.

Thanks very much to my parents for their continuous support and inspiration, and to my husband, Lei Jiang who has been encouraging me all the time using ‘his special method’. All this has helped my resolve, sustaining me in meaningful PhD studies.

Finally, I would like to thank Chinese Scholarship Council (CSC) for funding my tuition fees and living costs in United Kingdom; to the NIHR Liverpool Pancreas Biomedical Research Unit for funding my research and to West China Hospital, Sichuan University for offering the invaluable opportunity. Also many thanks to our industrial collaborators-GlaxoSmithKline and CalciMedica for providing study tools and financial support.

Table of Contents

Statement of originality ***3***

Abstract ***4***

Acknowledgements ***5***

Table of Contents ***7***

List of tables ***13***

List of figures ***14***

List of abbreviations ***17***

Chapter 1 Introduction ***22***

1.1 Acute pancreatitis (AP) *23*

1.2 Current understanding about the pathogenesis of AP *27*

1.3 Status of treatment development in AP *30*

1.4 An ideal drug target for AP *32*

1.5 Physiological Ca^{2+} signals, calcium overload and AP *35*

1.5.1 Physiological Ca^{2+} signals in PACs *35*

1.5.2 Calcium overload and AP *36*

1.6 Mitochondrial dysfunction and AP *40*

1.7 Store-operated Ca^{2+} entry channels are potential therapeutic target *44*

1.7.1 STIM, a Ca^{2+} sensor of the level of Ca^{2+} in the ER *46*

1.7.2 Orai1 is the component of the CRAC channel *48*

1.7.3 Development of Orai channel inhibitors *50*

1.7.4 SOCE and AP *54*

1.8 Hypothesis and study aims *55*

Chapter 2 Methods ***57***

2.1 Animal *58*

2.2 Isolation of murine PACs *58*

2.3 Isolation of human PACs *59*

2.4 Necrotic cell death pathway activation measurement *60*

2.5 Induction of experimental AP *60*

2.5.1 Hyperstimulation AP *60*

2.5.2 Biliary AP *61*

2.5.3 Alcohol/fatty acid AP *62*

2.6 Drug delivery by mini-osmotic pump *63*

2.6.1 Working mechanism of mini-osmotic pump *63*

2.6.2 Selecting compatible solvent *65*

2.6.3 Filling mini-osmotic pumps *65*

2.6.4 Priming mini-osmotic pumps *66*

2.6.5 Implanting mini-osmotic pumps *66*

2.6.6 Verifying the accuracy of mini-osmotic pump drug delivery *67*

2.7 Evaluation of experimental AP severity *67*

2.7.1 Serum amylase and IL-6 *68*

2.7.2 Trypsin activity *68*

2.7.3 Myeloperoxidase activity *68*

2.7.4 Histology *69*

2.8 Chemicals *70*

2.9 Statistical analysis *71*

2.10 Study approval *71*

Results: Chapter 3	**Effects of novel Orai inhibitors on store-operated Ca^{2+} entry and cell fate in mouse and human pancreatic acinar cells**	***72***
3.1	Introduction	*73*
3.2	Methods	*74*
3.2.1	*Measurement of cytosolic Ca^{2+} concentrations*	*74*
3.2.2	*Measurement of necrotic cell death pathway activation*	*74*
3.3	Results	*75*
3.3.1	*Effects of GSK-7975A on store-operated Ca^{2+} entry in mouse PACs*	*75*
3.3.2	*Effects of GSK-7975A on store-operated Ca^{2+} entry in human PACs*	*81*
3.3.3	*Effects of GSK-7975A on necrotic cell death pathway activation in mouse and human PACs*	*83*
3.3.4	*Effects of CM_128 on store-operated Ca^{2+} entry in mouse PACs*	*85*
3.3.5	*Effects of CM_128 on store-operated Ca^{2+} entry in human PACs*	*87*
3.3.6	*Effects of CM_128 on necrotic cell death pathway activation in mouse and human PACs*	*89*
3.4	Discussion	*91*
3.5	Summary	*92*
Results: Chapter 4	**Effects of GSK-7975A given as prodrug GSK-6288B in experimental acute pancreatitis**	***93***
4.1	Introduction	*94*

4.2	Methods	*94*
4.2.1	*Measurement of GSK-7975A in vivo*	*95*
4.2.2	*Protein binding of GSK-7975A*	*95*
4.2.3	*Induction of experimental AP*	*96*
4.2.4	*Administration of GSK-7975A*	*96*
4.2.5	*Assessment of experimental AP severity*	*96*
4.3	Results	*96*
4.3.1	*Pharmacokinetic study of GSK-7975A*	*96*
4.3.2	*Protein binding of GSK-7975A in the blood and pancreas*	*99*
4.3.3	*Effects of GSK-7975A on disease severity in CER-AP*	*100*
4.3.4	*Effects of GSK-7975A on disease severity in two clinically representative models*	*105*
4.4	Discussion	*110*
4.5	Summary	*111*
Results: Chapter 5	**Effects of GSK-7975A administered late in experimental acute pancreatitis**	***112***
5.1	Introduction	*113*
5.2	Methods	*118*
5.2.1	*Induction of experimental AP*	*118*
5.2.2	*Administration of GSK-7975A*	*118*
5.2.3	*Assessment of experimental AP severity*	*118*
5.2.4	*Statistical analysis*	*118*
5.3	Results	*119*
5.3.1	*Effects of GSK-7975A administered late on disease severity in*	*119*

TLCS-AP

5.3.2 *Effects of GSK-7975A administered late on disease severity in FAEE-AP* *124*

5.3.3 *The extent of experimental AP when late administration of GSK-7975A was begun* *129*

5.4 Discussion *134*

5.5 Summary *135*

Results: Chapter 6 **Effects of CM_128, a novel Orai inhibitor, in experimental acute pancreatitis** ***136***

6.1 Introduction *137*

6.2 Methods *138*

6.2.1 *Measurement of CM_128 in vivo* *138*

6.2.2 *Protein binding of CM_128* *138*

6.2.3 *Induction of experimental AP* *139*

6.2.4 *Administration of CM_128* *139*

6.2.5 *Assessment of experimental AP severity* *139*

6.2.6 *Statistical analysis* *140*

6.3 Results *140*

6.3.1 *Effects of CM_128 administered 1 h or 6 h after disease induction on disease severity in TLCS-AP and FAEE-AP* *140*

6.3.2 *The extent of experimental AP when late administration of CM_128 was begun* *147*

6.4 Discussion *152*

6.5 Summary *153*

Chapter 7 Overview ***154***

7.1 Targeting Ca^{2+} signalling to treat AP *155*

7.2 Other strategies to treat AP *159*

7.3 SOCE mediated via Orai1 is a valid drug target for protecting against AP *162*

7.4 Inhibitors of Orai1 have translational potential as a treatment for human AP *164*

7.5 Door-to-needle time is critical for the treatment of AP *166*

7.6 Conclusion *169*

References ***171***

Publications arising from this thesis ***207***

List of tables

1.1 Severity classifications of acute pancreatitis ***25***

1.2 Summary of Orai channel inhibitors ***53***

2.1 Pancreatic histopathological grading criteria ***70***

4.1 Binding fractions of GSK-7975A to murine/human blood and pancreas ***99***

5.1 Summary of agents applied prophylactically and therapeutically in murine experimental AP ***115***

5.2 Summary of agents administered therapeutically at early or late after disease induction in murine experimental AP ***117***

List of figures

1.1	Pathogenesis of AP	***29***
1.2	Time course of the progression of AP	***34***
1.3	Mechanism of Ca^{2+} overload and AP	***37***
1.4	Diagram of the MPTP formed by dimers of the F_0F_1 ATP synthase	***43***
1.5	STIM1/Orai1-mediated store-operated Ca^{2+} entry	***45***
1.6	Functional domains of STIM1	***47***
1.7	Functional domains of Orai1	***49***
2.1	A representative photo from TLCS-AP induction	***62***
2.2	A schematic illustration of a mini-pump	***64***
2.3	Procedures of mini-pump implantation	***67***
3.1	Effects of GSK-7975A on CCK-induced Ca^{2+} plateau in mouse PACs	***76***
3.2	Effects of GSK-7975A on CCK-induced Ca^{2+} plateau maintained by physiological Ca^{2+} concentration in mouse PACs	***78***
3.3	Effects of GSK-7975A on TLCS-induced Ca^{2+} plateau in mouse PACs	***79***
3.4	Effects of GSK-7975A on thapsigargin-induced Ca^{2+} entry in human PACs	***82***
3.5	Effects of GSK-7975A on necrotic cell death pathway activation in human PACs	***84***
3.6	Effects of CM_128 on thapsigargin-induced Ca^{2+} entry in mouse PACs	***86***
3.7	Effects of CM_128 on thapsigargin-induced Ca^{2+} entry in human PACs	***88***
3.8	Effects of CM_128 on necrotic cell death pathway activation in mouse and human PACs	***90***
4.1	Blood and pancreatic levels of GSK-7975A	***97***
4.2	Effects of GSK-7975A on pancreatic parameters in CER-AP	***101***

4.3	Effects of GSK-7975A on systemic biochemical parameters in CER-AP	***102***
4.4	Typical histopathology from CER-AP	***103***
4.5	Histopathological scores from CER-AP	***104***
4.6	Effects of GSK-7975A on pancreatic parameters in TLCS-AP and FAEE-AP	***106***
4.7	Effects of GSK-7975A on systemic biochemical parameters in TLCS-AP and FAEE-AP	***107***
4.8	Typical histopathology from TLCS-AP and FAEE-AP	***108***
4.9	Histopathological scores from TLCS-AP and FAEE-AP	***109***
5.1	Effects of GSK-7975A administered late on pancreatic parameters in TLCS-AP	***120***
5.2	Effects of GSK-7975A administered late on systemic biochemical parameters in TLCS-AP	***121***
5.3	Typical histopathology of TLCS-AP following late administration of GSK-7975A	***122***
5.4	Histopathological scores of TLCS-AP comparing early versus late administration of GSK-7975A	***123***
5.5	Effects of GSK-7975A administered late on pancreatic parameters in FAEE-AP	***125***
5.6	Effects of GSK-7975A administered late on systemic biochemical parameters in FAEE-AP	***126***
5.7	Typical histopathology of FAEE-AP following late administration of GSK-7975A	***127***
5.8	Histopathological scores of FAEE-AP comparing early versus late administration of GSK-7975A	***128***

5.9 Pancreatic parameters at 6 h and 24 h in TLCS-AP and FAEE-AP ***130***

5.10 Systemic biochemical parameters at 6 h and 24 h in TLCS-AP and FAEE-AP ***131***

5.11 Typical histopathology at 6 h and 24 h from TLCS-AP and FAEE-AP including effects of late administration of GSK-7975A ***132***

5.12 Histopathological scores at 6 h and 24 h in TLCS-AP and FAEE-AP including effects of late administration of GSK-7975A ***133***

6.1 Levels of CM_128 in the plasma, pancreas and lung ***142***

6.2 Effects of CM_128 administered early or late on pancreatic parameters in TLCS-AP and FAEE-AP ***143***

6.3 Effects of CM_128 administered early or late on systemic biochemical parameters in TLCS-AP and FAEE-AP ***144***

6.4 Typical histopathology from TLCS-AP and FAEE-AP following early or late administration of CM_128 ***145***

6.5 Histopathological scores of CM_128 administered early or late in TLCS-AP and FAEE-AP ***146***

6.6 Pancreatic parameters at 6 h and 24 h in TLCS-AP and FAEE-AP ***148***

6.7 Systemic biochemical parameters at 6 h and 24 h in TLCS-AP and FAEE-AP ***149***

6.8 Typical histopathology from TLCS-AP and FAEE-AP showing extent of injury at 6 h and following late administration of CM_128 ***150***

6.9 Histopathological scores of TLCS-AP and FAEE-AP showing extent of injury at 6 h and following late administration of CM_128 ***151***

7.1 Optimal therapeutic window for the drug that targets the pathogenesis of AP ***168***

List of abbreviations

$[Ca^{2+}]_C$	Cytosolic Ca^{2+} concentration
$\Delta\Psi_M$	Mitochondrial membrane potential
2-APB	2-amino-ethoxydiphenylborate
AP	Acute pancreatitis
AT	Angiotensin
ACh	Acetylcholine
ACG	American College of Gastroenterology
ADP	Adenosine diphosphate
ANT	Adenine nucleotide translocator
APA	American Pancreatic Association
ATP	Adenosine triphosphate
ATF	Activating transcription factor
BA	Bile acid
BiP/GPR78	Immunoglobulin heavy chain binding protein
BTP	Bis(trifluoromethyl) pyrazole derivatives
BPDOE-CDL	Bilio-pancreatic-duct-outlet-exclusion closed-duodenal-loops
cADPR	Cyclic ADP ribose
CM	CalciMedica
CAD	CRAC activation domain
CCK	Cholecystokinin
CDE	Choline-defient, ethionine supplemented
CRP	C-reactive protein
Cyp D	Cyclophilin D
CAPE	Caffeic acid phenethyl ester

CHOP	C/EBP homologous protein
CRAC	Ca^{2+} release-activated Ca^{2+}
CCK1R	Cholecystokinin 1 receptor
CER-AP	Hyperstimulation AP
DAMPs	Damage-associated molecule patterns
DAG	Diacyle glycerol
DBC	Determinant-based classification
DMSO	Dimethylsulfoxide
eIF2α	eukaryotic translation initiation factor 2 alpha
ER	Endoplasmic reticulum
ER-PM	ER-plasma membrane
EAE	Experimental autoimmune encephalomyelitis
EAP	Experimental AP
EMA	European Medicine Agency
ETC	Electron transport chain
ERCP	Endoscopic retrograde cholangiopancreatography
FA	Fatty acid
FAEE	Fatty acid ethyl esters
FAEE-AP	Alcoholic AP
FDA	Food and drug administration
GA	Golgi apparatus
GITR	Glucocorticoid induced TNF receptor family-related protein
GPBAR1	G-protein coupled bile acid receptor 1
H&E	Hematoxylin and eosin
HO-1	Heme oxygenase-1

HEPES	4-(2-hydroxyethyl)-1 piperazineethanesulfonic acid
HMGB1	High mobility group box 1
I_{Na}	Sodium current
IL	Interleukin
IP_3	Inositol-1,4,5- trisphosphate
IAP	International Association of Pancreatology
ICE	interleukin 1β-converting enzyme
IL1R	Interleukin-1 receptor
IP_3R	IP_3 receptor
IMM	Inner mitochondrial membrane
IRE1α	Inositol-requiring kinase 1 alpha
LPS	lipopolysaccharide
LC-MS	Liquid chromatography mass spectrometry
MCU	Mitochondrial Ca^{2+} uniporter
MCI-727	(Z)-2-(4-methylpiperazin-1-yl)-1-[4-(2-phenyl-ethyl)phenyl]-eth anone oxime hydrochloride monohydrate
Me_2Spm	Bismethylspermine
MOF	Multiple organ failure
MOPS	4-morpholinepropane sulfonic acid
MPO	Myeloperoxidase
MLKL	Mixed lineage kinase domain-like protein
MPTP	Mitochondrial permeability transition pore
NET	Neutrophil extracellular trap
NLR	NOD-like receptor
NOD	Nucleotide binding domain

NAADP	Nicotinic acid adenine dinucleotide phosphate
NADPH	Nicontinamide adenine dinucleotide phosphate
OMM	Outer mitochondrial membrane
OSCP	Oligomycin sensitivity-conferring protein
PI	Propidium iodide
PM	Plasma membrane
PAC	Pancreatic acinar cell
PBS	Phospate buffer saline
PCA	Passive cutaneous anaphylaxis
PiC	Phosphate carrier
PLC	Phospholipase
PAR-2	Proteinase-activated receptor-2
PARP	Poly(ADP-ribose) polymerase
PBMC	Peripheral blood mononuclear cell
PERK	Protein kinase-like ER kinase
PMCA	Plasma membrane Ca^{2+}-ATPase
PPAR	Peroxisome proliferator-activated receptor
POA	Palmitoleic acid
POAEE	Palmitoleic acid ethyl ester
RAC	Revised Atlanta classification
RCD	Regulated cell death
RCT	Randomised clinical trial
RED	Rapid equilibrium dialysis
ROS	Reactive oxygen species
RyR	Rynadine receptor

RNAi	RNA interference
RAGE	Receptor for advanced glycation end-products
SAM	Sterile α motif
SCID	Severe combined immune deficiency
SERCA	Sarcoendoplasmic reticulum Ca^{2+}-ATPase
SIRS	Systemic inflammatory response syndrome
SMWC	Small molecular weight chemical
SOAR	STIM1 Orai1 activation region
SOCE	Store-operated Ca^{2+} entry
SOFA	Sepsis-related organ failure assessment
sPLA$_2$	Secretory phospholipase A_2
STIM	Stromal interacting molecule
Treg	Regulator T cell
TM	Transmembrane
TLR	Toll-like receptor
TNF	Tumor necrosis factor
TLCS	Taurolithocholic acid 3-sulfate
TRPC	Transient receptor potential canonical channel
TUDCA	Taurousodeoxycholic acid
TLCS-AP	Biliary AP
TNFR-bp	Tumor necrosis factor receptor binding protein
UPR	Unfolded protein response
VDAC	Voltage-dependent anion channel
XBP1	X box binding protein 1
ZG	Enzymogen granule

Chapter 1

Introduction

1.1 Acute pancreatitis

Acute pancreatitis (AP) is a worldwide common inflammatory disease with a substantial morbidity, mortality and financial burden on health care services (Peery et al., 2012). A recent publication from the United States evaluating the burden of gastrointestinal (GI) disorders revealed that AP is the commonest causes of GI-related hospitalization with an estimated annual cost of $2.6 billion (Peery et al., 2012). Gallstone and alcohol abuse account for 70-80% of cases of AP; other causes include drugs, viral infection, hyperlipidemia, hypercalcemia, trauma, etc.(Pandol et al., 2007). There are also genetic susceptibility, including mutations of human cationic trypsinogen (PRSS1), chymotrypsin C (CTRC), serine protease inhibitor, Kazal type1 (SPINK) and cystic fibrosis transmembrane conductance regulator (CFTR) for recurrent AP and chronic pancreatitis (Mounzer and Whitcomb, 2013). Incidences vary from 10~100 per 100,000 annually with a geographical variation (about 50 per 100,000 in United Kingdom) and there has been a steadily rise worldwide, partly due to increased alcohol consumption (Goldacre and Roberts, 2004, Roberts et al., 2008, Lowenfels et al., 2009). One out of five AP patients develops a severe form of the disease with significantly higher mortality, morbidity and prolonged hospital stay (Pandol et al., 2007). The overall mortality of AP is approximately 5% in patients with AP; higher mortality is seen in patients with necrotizing AP (~15%)(Pandol et al., 2007, van Santvoort et al., 2011). Despite such a major burden of the disease, there is no licensed drug therapy for AP, requiring the development of an effective therapy based on better understanding of the pathophysiology of AP.

The diagnosis of AP requires at least 2 of the following: typical upper abdominal pain, serum levels of amylase or lipase ≥3 times the upper limit of normal and confirmatory findings from cross-sectional imaging (Working Group, 2013, Wu and Banks, 2013). Better understanding of organ failure and necrosis and their outcomes, as well as the improvement of diagnostic imaging, have led to the expansion of disease categories from the original Atlanta Classification (mild and severe) into the revised Atlanta Classification (RAC) and Determinant-Based Classification (DBC) (Bradley, 1993, Banks et al., 2013, Dellinger et al., 2012). Patients with AP have been classified as mild, moderate and severe (three categories) in the RAC (Banks et al., 2013); and as mild, moderate, severe and critical (four categories) in the DBC (Dellinger et al., 2012), see **Table 1.1**. Two main differences between these two new classification systems are 1) infected pancreatic necrosis is not considered severe in the RAC; 2) exacerbations of co-morbid disease are not considered to determine severity in the DBC (Windsor et al., 2015, Bakker et al., 2014, Gomatos et al., 2014).

Table 1.1 Severity classifications of acute pancreatitis

Atlanta Classification 1992 (Bradley, 1993)	**Mild**	No organ failure **and** No local complications
	Severe	Ranson criteria ≥3 in first 48 hours: APACHE II ≥ 8 at any time **and/or** Local complications
Revised Atlanta Classification 2012 (Banks et al., 2013)	**Mild**	No organ failure **and** No local and systemic complications
	Moderately severe	Transient organ failure (<48 h) **and/or** Local or systemic complications without persistent organ failure (>48 h) **and/or** exacerbation of pre-existing co-morbidity
	Severe	Persistent organ failure (>48 h): single or multiple organ failure **with/without** Local complications **with/without** exacerbation of pre-existing comorbidity
Determinant-Based Classification 2012 (Dellinger et al., 2012)	**Mild**	No organ failure **and** No (peri)pancreatic necrosis
	Moderate	Transient organ failure (<48 h) **and/or** Sterile (peri)pancreatic necrosis

	Severe	Persistent organ failure (>48 h) **or** Infected (peri)pancreatic necrosis
	Critical	Persistent organ failure (>48 h) **and** Infected (peri)pancreatic necrosis

Note: In Atlanta Classification 1992, local complications were defined as necrosis (⩾3 cm diameter or 30% volume), abscess (>4 weeks after onset) or pseudocyst (>4 weeks after onset); severe = three or more Ranson criteria in first 48 hours: 8 or more APACHE II at any time: systolic blood pressure <90 mm Hg; PaO2 ⩽ 60 mm Hg; creatinine >177 μmol/L or 2 mg/dL after rehydration; >500 ml/24 h blood loss; platelets ⩽ 100,000 mm3; fibrinogen <1.0 g/L; fibrin split products >80 μg/mL; calcium ⩽1.87 mmol/L (7.5 mg/dL). In revised Atlanta Classification 2012, local complications are defined as acute peripancreatic fluid collection, pancreatic pseudocyst, acute necrotic collection, walled-off necrosis, infected pancreatic (acute and wall-off) necrosis and other local complications including gastric outlet dysfunction, splenic or portal vein thrombosis and colonic necrosis; systemic complications are defined as transient or persistent organ failure and exacerbation of pre-existing co-morbidity and organ failure is assessed by >2 modified Marshall score (Marshall et al., 1995) for respiratory, cardiovascular and renal organ systems. In Determinant-based Classification 2012, organ failure is assessed by >2 sepsis-related organ failure assessment (SOFA) (Vincent et al., 1996).

1.2 Current understanding about the pathogenesis of AP

Over last few decades, the basic research on AP has advanced our knowledge and provides the understanding of disease mechanism. The initial injury during AP starts within pancreatic acinar cells (PACs) and/or ductal cells, which make up the bulk of the organ (Sutton et al., 2003, Hegyi et al., 2011). Calcium toxicity characterized as the sustained elevation of cytosolic Ca^{2+} concentration ($[Ca^{2+}]_C$), is the earliest intracellular event (Ward et al., 1995) and contributes to almost all subsequent pathophysiological events, including premature enzyme activation, vacuolization and necrosis (Petersen and Sutton, 2006). Mitochondria supply cellular energy in the form of adenosine triphosphate (ATP) and are also critical determinants of cell death pathway activation. Cytosolic Ca^{2+} overload followed by mitochondrial Ca^{2+} overload results in uncoupled oxidative phosphorylation, mitochondrial membrane potential ($\Delta\Psi_M$) depletion and impaired ATP production. Mitochondrial dysfunction has been found to play critical and central role in the pathogenesis of AP (Mukherjee et al., 2008, Gerasimenko and Gerasimenko, 2012, Maleth et al., 2013). Intra-acinar trypsinogen activation has been shown to mediate early stage pancreatic injury, together with intra-acinar nuclear factor-kappa B (NF-κB) activation plays an important role in mediating the severity of AP (Rakonczay et al., 2008, Ji et al., 2009, Dawra et al., 2011).

Patterns of cell death are the key determinants of disease severity in AP. Necrosis is characterized by mitochondrial swelling, impaired ATP production, plasmalemmal disruption and spillage of cellular contents, which triggers acute inflammation and exacerbates pancreatitis. Apoptosis features chromatin condensation, nuclear fragmentation and the formation of plasma-membrane blebs without the leakage of

intracellular contents (Criddle et al., 2007, Hotchkiss et al., 2009). The severity of pancreatic damage correlates directly with the extent of necrosis and largely but not entirely inversely with apoptosis in distinct *in vivo* models of experimental AP (Kaiser et al., 1995, Criddle et al., 2007). Both forms of cell death (necrosis and apoptosis) can be triggered by cytosolic Ca^{2+} overload and mitochondrial dysfunction followed by Ca^{2+} overload (Criddle et al., 2007, Pandol et al., 2007, Mukherjee et al., 2008, Booth et al., 2011). Most recently, a form of programmed necrotic cell death termed necroptosis has been suggested to play a role in the pathogenesis of AP (He et al., 2009). Autophagy, a multiple lysosome-driven process that degrades long-lived protein, lipids and cytoplasmic organelles, has been shown to be impaired during AP (Mareninova et al., 2009).

On the other hand, injured PACs can act as inflammatory cells to produce, release and respond to cytokines, such as tumour necrosis factor (TNF)-α (Saluja et al., 2007, Gukovskaya et al., 1997). Inflammatory mediators, such as TNF-α and interleukin (IL)-1, activate macrophages and neutrophils, resulting in a cascade of systemic inflammatory responses, followed by further excessive local and systemic damage (Raraty et al., 2005, Bhatia, 2005, Vonlaufen et al., 2007). Recently, damage-associated molecular patterns (DAMPs) have been implicated in mediating pancreatic and distant organ damage (Hoque et al., 2012). DAMPs, such as extracelluar ATP, high mobility group box 1 (HMGB1) and S100A can be endogenously released from dead or dying cells and bind to specific sensors on/in inflammatory cells, subsequently leading to sterile inflammation (Chen and Nunez, 2010). Taken together, intra-acinar and immunological events are two independent, but synergic components that contribute to AP severity.

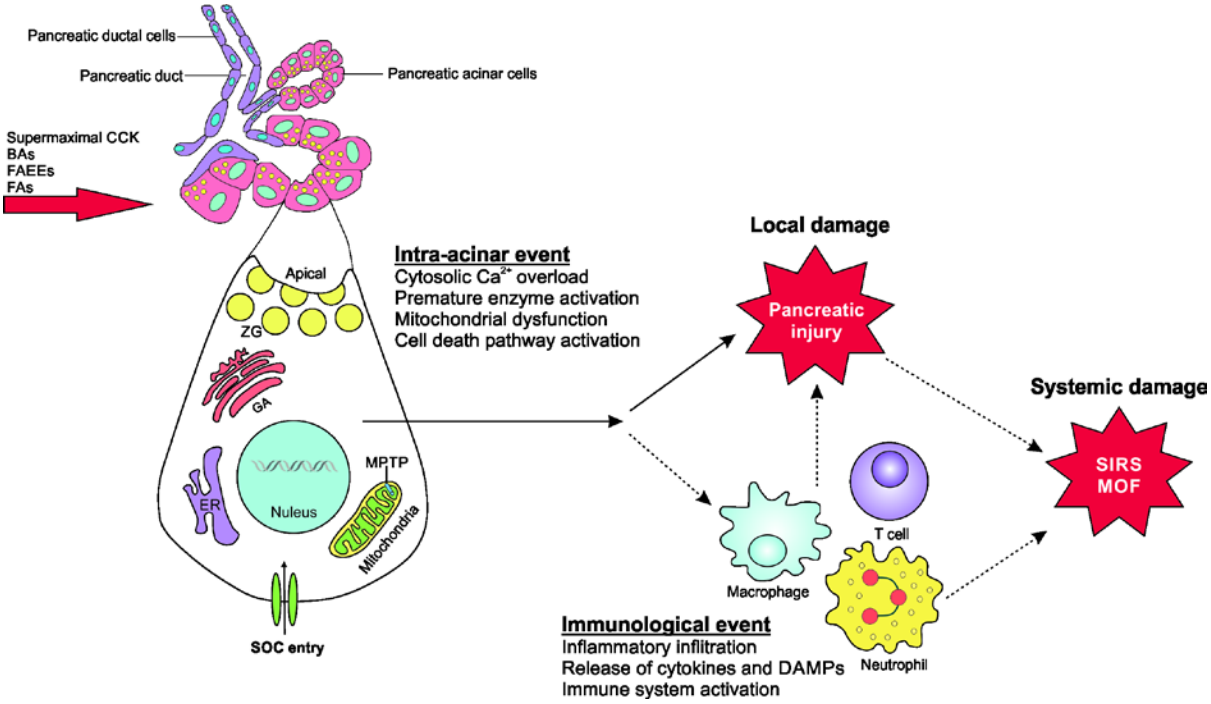

Figure 1.1 Pathogenesis of AP. Pancreatitis-associated toxins include supermaximal cholecystokinin (CCK), bile acids (BAs), fatty acid ethyl esters (FAEEs) and fatty acids (FAs). The initial site of injury is within pancreatic acinar and/or ductal cells after toxin stimulation. Cytosolic Ca^{2+} overload mediated by store-operated Ca^{2+} entry (SOCE) is the trigger of AP. Subsequent intra-cellular events including premature enzyme activation, mitochondrial dysfunction and cell death pathway activation are all Ca^{2+}-dependent processes. Injured PACs release cytokines, chemokines and damage-associated molecular patterns (DAMPs) to activate inflammatory cells, resulting in a cascade of systemic inflammatory responses. All these events lead to further local damage and distant organ dysfunction. **Abbreviations:** ZG, zymogen granule; GA, golgi apparatus; ER, endoplasmic reticulum; MPTP, mitochondrial permeability transition pore; SIRS, systemic inflammatory response syndrome; MOF, multiple organ failure

1.3 Status of treatment development in AP

Over last decade, substantial improvement of the management of AP has led to revised guidelines for patient management published in 2013 by the International Association of Pancreatology (IAP)/American Pancreatic Association (APA) (Working Group, 2013) and American College of Gastroenterology (ACG) (Tenner et al., 2013) separately. Therapeutic strategies at the early stage of the disease remain as basic supportive treatments including fluid resuscitation, pain management and nutritional support. Intensive care support including mechanical ventilation and renal replacement therapy are given to patients with severe AP if necessary. A well-designed prospective randomized trial has demonstrated early fluid resuscitation with Ringer's lactate, but not normal saline, significantly reduced systemic inflammation measured by levels of systemic inflammatory response syndrome (SIRS) and C-reactive protein (CRP) (Wu et al., 2011). Early aggressive fluid resuscitation is most beneficial during the first 12-24 h; aggressive fluid hydration is defined as 5-10 mL/kg/h in the IAP/APA guidelines and 250-500 mL/h in the ACG guidelines (Working Group, 2013, Tenner et al., 2013). Pain management is a priority in the management of patients with AP on admission. However, findings from a systemic review of eight RCTs showed that the randomised controlled trials comparing different analgesics were of low quality and did not favour clearly any particular analgesic for pain relief in AP (Meng et al., 2013). Nutritional support is accepted as therapeutic that provide energy suppliers, leading to the increased ATP production within PACs to better copy with cytosolic Ca^{2+} overload during AP. Findings from a systematic review including fifteen RCTs have shown either enteral or parenteral nutrition is associated with a lower risk of death compared with no supplementary nutrition (Petrov et al., 2008). A Cochrane systematic review and

meta-analysis has shown enteral nutrition significantly reduced mortality, multiple organ failure, systemic infection and the need for operative interventions in comparison with parenteral nutrition (Al-Omran et al., 2010), but there is insufficient evidence to support the use of any specific enteral nutrition formulation (Poropat et al., 2015) and the optimal delivery route for enteral nutrition is still a subject of investigation (Wu and Banks, 2013). An early initiation (within 48 h) of enteral nutrition is associated with significantly improved outcomes (Petrov et al., 2009, Bakker et al., 2014, Lankisch et al., 2015). Glutamine supplementation was found to significantly reduce the risk of mortality and total infective complications, but not length of hospital stay in patients receiving parenteral nutrition in a systematic review of twelve RCTs (Asrani et al., 2013). Several RCTs and meta-analyses have indicated that antioxidants are ineffective in improving the outcomes of AP (Siriwardena et al., 2007, Mohseni Salehi Monfared et al., 2009). In patients with gallstone AP, a Cochrane systematic review has indicated early endoscopic retrograde cholangiopancreatography (ERCP) significantly reduced mortality, local and systemic complications, but only in patient group with co-existing cholangitis or biliary obstruction (Tse and Yuan, 2012).

Certainly, improvements of the surgical management of AP have emerged, resulting in the better management of patients with local complications such as infected necrosis at the later stage. Delayed intervention (performed after a median of ~4 weeks after onset of symptom) is more beneficial than early intervention; a minimally invasive approach is superior to open necrosectomy (van Santvoort et al., 2011, Wu and Banks, 2013, Lankisch et al., 2015). A multicentre randomised clinical trial (RCT) has shown a step-up approach consisting of percutaneous drainage followed, if

necessary, by minimally invasive retroperitoneal necrosectomy reduced the rate of major complication or death by 29% compared with open necrosectomy (van Santvoort et al., 2010). Another RCT of 20 patients analyzed showed endoscopic transgastric necrosectomy reduced the proinflammatory response as well as a composite clinical end-point compared with surgical necrosectomy (Bakker et al., 2012). Despite all these findings, there is still no specific drug treatment that targets the pathogenesis of AP to halt the progression of the disease.

1.4 An ideal drug target for AP

Several principal criteria are required for an ideal therapeutic target (Simmons, 2006, Gashaw et al., 2011). There are specific features in the pathophysiological processes of AP that should be exploited to yield good therapeutic targets. PACs are an initial site of pancreatic injury and ought to be the primary target to halt pancreatic damage during AP. PACs, depend heavily on subtle, small changes in Ca^{2+} for pronounced changes in function(Petersen and Tepikin, 2008), making PACs among the most sensitive cells within the body to abnormal Ca^{2+} signalling. The strategies that prevent abnormal Ca^{2+} overload/signalling and enhance/preserve the ability of Ca^{2+} handling are potentially useful approaches to protect against pancreatic injury, which could ultimately lead to a cure for AP. Apart from targeting Ca^{2+} signals in PACs, there are several other potential therapeutic approaches for treating AP, including increasing ATP production, inhibition of trypsinogen activation and inhibition of intra-acinar NF-κB activation. Moreover, the critical roles of ductal cells in mediating AP severity have been noted (Hegyi and Petersen, 2013). Preservation of ductal cells function by preventing Ca^{2+} overload and increasing ATP production are useful tools and the approach that increase ductal cell secretion is also important.

In addition, modulation of inflammatory responses by deletion of certain types of inflammatory cells such as neutrophils or by inhibition the core functions of inflammatory cells, such as NADPH oxidase activity (Gukovskaya et al., 2002). In clinical cases of AP, pancreatic necrosis and organ failure are two major determinants of the severity and the outcome of AP (Petrov et al., 2010). Multiple organ failure is the leading cause of death in the first two weeks after symptom onset, whereas infected necrosis with multiple organ failure is the main reason for death after that time. Thus, all the therapies applied at the early stage of the disease should take these factors into account. Unlike myocardial infarction or cerebral ischemic stroke that are typically caused by a sudden arterial occlusion, pancreatic necrosis and organ failure may take days to develop. This offers a potentially wider therapeutic window to explore any possible treatments, see **Figure 1.2**.

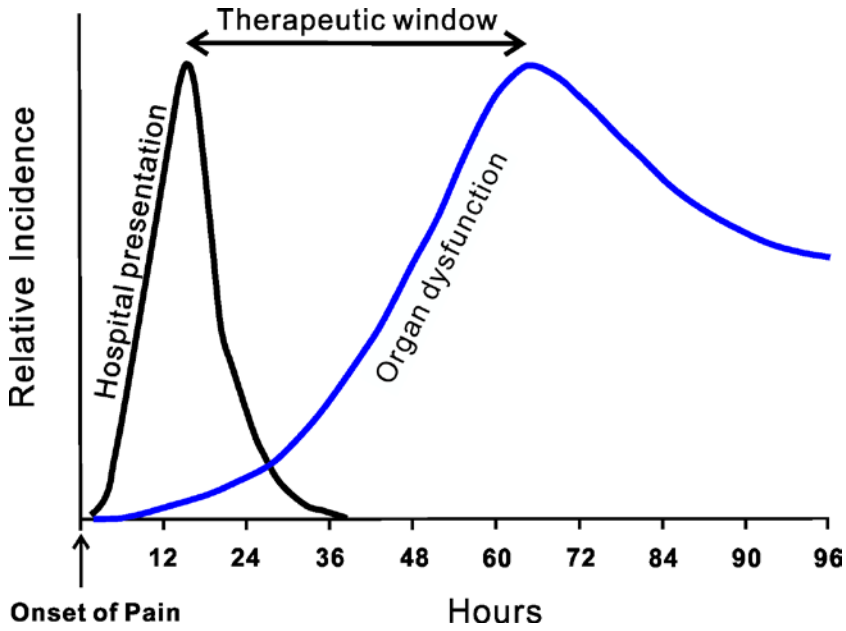

Figure 1.2 Time course of the progression of AP. This plot shows a potential therapeutic window for therapies targeting the pathogenesis of pancreatitis. Most patients with AP present to a hospital emergency department within several hours of the onset of pain. A minority of patients develop severe AP, developing distant organ dysfunction 2 to 4 days later, although distant organ failure may be manifest at the time of admission. Such presentation allows for a therapeutic window during which time specific targeted treatment could be administered to attenuate/prevent the progression of AP. *Adapted from* (Norman, 1998)

1.5 Physiological Ca^{2+} signals, calcium overload and AP

1.5.1 Physiological Ca^{2+} signals in PACs

Cytosolic Ca^{2+} signals are critical for fluid and enzyme secretion from the exocrine pancreas. The highly polarized PACs have a sophisticated and complex Ca^{2+} signalling toolkit. In response to physiological stimulation of acetylcholine (ACh) or cholecystokinin (CCK), PACs generate the second messenger, inositol triphospate (IP_3), cyclic ADP ribose (cADPR) and nicotinic acid adenine dinucleotide phosphate (NAADP). These second messengers cause Ca^{2+} release from internal Ca^{2+} stores through binding to IP_3 receptors (IP_3Rs) and rynadine receptors (RyRs) on the endoplasmic reticulum (ER) and also from other intracellular Ca^{2+} stores, such as acidic Ca^{2+} stores (Petersen, 2005, Petersen and Tepikin, 2008, Petersen, 2012). Repetitive local Ca^{2+} spikes are produced in the apical region and buffered by peri-apical mitochondria to elicit physiological functions of cells, such as secretion and protein synthesis. The normal basal cytosolic Ca^{2+} concentration is restored through two mechanisms, both of which are ATP-dependent processes, with the Na^{+}-Ca^{2+} exchanger being of little quantitative importance in these cells (Petersen and Sutton, 2006). The sarcoendoplasmic reticulum Ca^{2+}-ATPase (SERCA) pump refills the ER Ca^{2+} stores while the plasma membrane Ca^{2+}-ATPase (PMCA) pump extrudes Ca^{2+} to the outside of the cells. Ca^{2+} microdomains in PACs are responsible for regulating physiological Ca^{2+} spikes. In the functionally very important microdomain near the apical membrane, the opening of Ca^{2+} channels in the apical region would cause a rise in the local Ca^{2+} levels, whereas after channel closure, when the SERCA pump are working maximally, Ca^{2+} levels would deline (Petersen et al., 2006). Three distinct groups of mitochondria located in separate sub-cellular domains of PACs play specific roles: 1) peri-apical mitochondria act as a Ca^{2+} buffer barrier and the

uptake of Ca^{2+} into these mitochondria also stimulates mitochondrial ATP synthesis; 2) sub-plasmalemmal mitochondria support both Ca^{2+} entry at the base and the refilling of the ER Ca^{2+} stores; 3) peri-nuclear mitochondria confine Ca^{2+} signals primarily generated inside the nucleus (Park et al., 2001, Petersen, 2012).

1.5.2 Calcium overload and AP

Almost twenty years ago, the hypothesis was proposed that prolonged elevation of $[Ca^{2+}]_c$ is toxic and is the key trigger of auto-digestion of the pancreas and the onset of AP (Ward et al., 1995). Pancreatitis-associated toxins, including supramaximal CCK, BAs and non-oxidative alcohol metabolites, cause Ca^{2+} release through IR_3Rs and RyRs, resulting in the depletion of internal Ca^{2+} stores including within the ER (Raraty et al., 2000, Criddle et al., 2006, Gerasimenko et al., 2006). Following ER store depletion, Ca^{2+} influx (into the ER) is activated through store-operated Ca^{2+} entry (SOCE) as a compensatory mechanism for Ca^{2+} loss from internal cellular stores (Petersen and Sutton, 2006), allowing further release from the ER and so sustaining cytosolic Ca^{2+} overload. Sustained cytosolic Ca^{2+} overload leads to mitochondrial Ca^{2+} overload, causing mitochondrial membrane potential depletion, mitochondrial permeability transition induction and impaired ATP production (Mukherjee et al., 2008). Ca^{2+} extrusion from PACs is largely dependent on PMCA pump activity (Petersen and Sutton, 2006). Mitochondrial dysfunction/failure as a consequence of cytosolic Ca^{2+} overload eventually results in cell death pathway activation and severe pancreatic acinar injury (Mukherjee et al., 2008, Odinokova et al., 2008, Gerasimenko and Gerasimenko, 2012, Maleth et al., 2013), see **Figure 1.3**.

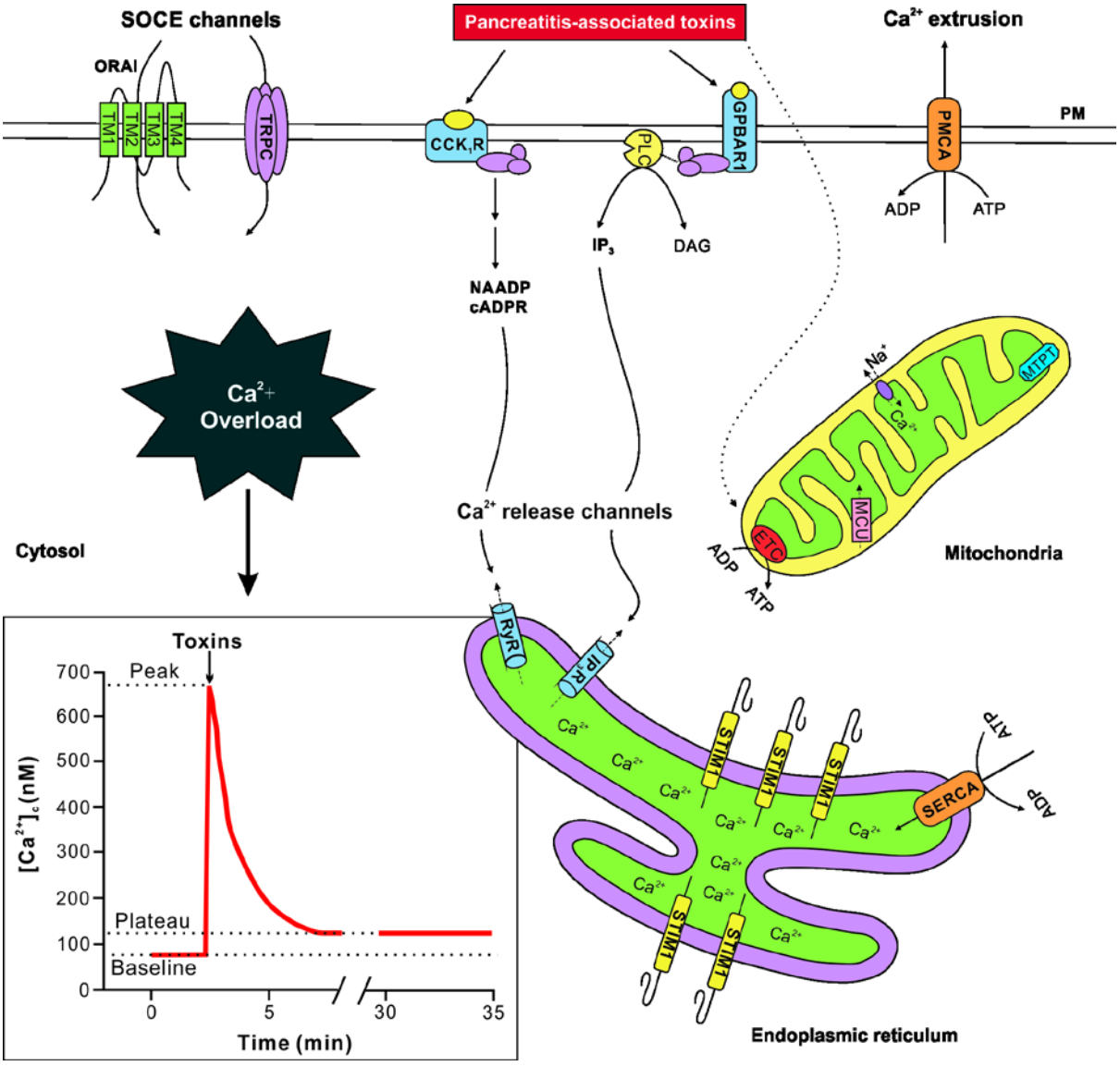

Figure 1.3 Mechanism of Ca^{2+} overload and AP. Upon pancreatitis-associated toxin exposure of PACs, the second messengers IP_3, cADPR and NAADP are generated or their receptors (IP_3Rs and RyRs) activated, leading to Ca^{2+} release from these receptors on the ER membrane. Depletion of ER Ca^{2+} stores activates redistribution of stromal interacting molecule 1 (STIM1) to form the puncta ER-plasma membrane (ER-PM) junctions with Ca^{2+} release-activated Ca^{2+} entry channels (ORAI and TRPC). Subsequent Ca^{2+} influx via SOCE channels sustains cytosolic Ca^{2+} overload (typical trace showing Ca^{2+} plateau induced by hyperstimulation). Ca^{2+} extrusion is mainly through PMCA to pump Ca^{2+} outside

PACs. Meanwhile SERCA also acts to refill the ER Ca^{2+} store, the activity of which is largely dependent on the amount of ATP production; if mitochondria are impaired by Ca^{2+} overload, ATP supply is reduced and SERCA activity diminished, exacerbating cytosolic Ca^{2+} overload.

Abreviations: SOCE, store-operated Ca^{2+} entry; TM, transmembrane; TPRC, transient potential receptor type C channel; CCK1R, cholecystokinin 1 receptor; PLC, phospholipase C; IP_3,inositol-1,4,5-trisphosphate; DAG, diacyle glycerol; GPBAR1, G-protein couple bile acid receptor 1; PMCA, plasma membrane Ca^{2+} ATPase; PM, plasma membrane; ETC, electron transport chain; MCU, mitochondrial Ca^{2+} uniporter; MPTP, mitochondrial permeability transition pore; ADP, adenosine diphosphate; ATP, adenosine triphosphate; RyR, rynadine receptors; IP_3R, inositol-1,4,5-trisphosphate receptor; STIM1, stromal interacting molecule 1; SERCA, sarcoendoplamic reticulum Ca^{2+} ATPase.

The Ca^{2+} release channels IP_3Rs and RyRs are expressed in the pancreas and mediate intracellular Ca^{2+} release. IP_3R type 2 and type 3 isoforms are widely expressed in various organs and play an essential role in regulating secretion and proliferation, whereas type 1 is more predominantly expressed in the nervous system (Futatsugi et al., 2005). RyRs are predominantly expressed in excitable cells, but also found in many other tissues; type 1 RyR is abundant in skeletal muscle, type 2 RyR in the heart. RyR-deficient mice have perinatal death (Takeshima et al., 1994), suggesting its fundamental role. There is clear evidence demonstrating inhibition of IP_3Rs and RyRs prevent PAC injury and AP in both *in vitro* and *in vivo*. PACs from IP_3R2-deficient mice and IP_3R2/IP_3R3 double-knockout mice have significantly reduced Ca^{2+} release and trypsinogen activation, with more dramatic reduction in cells from double-knockout mice (Gerasimenko et al., 2009). IP_3R2 knockout did not reduce the severity of caerulein-induced pancreatitis compared with wild-type mice (Orabi et al., 2012), but the effect of IP_3R2/IP_3R3 double-knockouts on AP severity remains to be investigated. RyR-mediated Ca^{2+} release modulates intra-acinar premature zymogen activation; inhibition of RyR by dantrolene reduces the severity of caerulein- and bile acid-induced pancreatitis (Husain et al., 2005, Orabi et al., 2010, Husain et al., 2012). Nevertheless, preventing Ca^{2+} overload by inhibition of primary Ca^{2+} release through IP_3Rs and RyRs is unlikely to be a safe therapeutic approach due to their ubiquitous expression and fundamentally important roles.

ATP-dependent Ca^{2+} uptake into cell stores and extrusion outside cells is the main mechanism of Ca^{2+} clearance in PACs, which explains why Ca^{2+} overload is particularly dangerous in these cells (Petersen and Sutton, 2006). Two studies have shown insulin protected against Ca^{2+} overload and pancreatic damage by

maintaining cellular ATP and thus PMCA activity through switching acinar cell metabolism from oxidative phospholation to gylcolysis (Mankad et al., 2012, Samad et al., 2014). Ferdek *et al* have demonstrated that the antiapoptotic protein Bcl-2 affects Ca^{2+} extrusion by regulating PMCA functions, thereby influencing cell fate (Ferdek et al., 2012). Apart from altering Ca^{2+} handling, preservation of mitochondrial function is potentially useful tool in order to maintain the ability of efficient Ca^{2+} handling of the cells.

1.6 Mitochondrial dysfunction and AP

Mitochondrial dysfunction as a consequence of cytosolic Ca^{2+} overload is a key determinant of the pattern of cell death and the severity of AP. Ca^{2+}- and mitochondria-dependent necrotic cell death pathway activation is correlated with the more severe forms of pancreatitis (Criddle et al., 2007, Mukherjee et al., 2008, Booth et al., 2011, Gerasimenko and Gerasimenko, 2012, Odinokova et al., 2008, Maleth et al., 2013). Accumulating evidence suggests pancreatitis-associated toxins such as BAs or non-oxidative metabolites of ethanol and FAs cause mitochondrial membrane potential depletion, uncoupling of oxidative phosphorylation and impairment of ATP production through Ca^{2+} overload of mitochondria (Voronina et al., 2002, Criddle et al., 2004, Criddle et al., 2006, Mukherjee et al., 2008). FAEEs are non-oxidative alcohol metabolites that can bind to and accumulate within the inner mitochondrial membrane, where hydrolases act to release high concentrations of FAs locally (Criddle et al., 2006). FAs, relevant to hypertriglyceridemic AP, also have direct effects on the electron transport chain without depolarization of the inner mitochondria membrane (Petersen et al., 2009).

The mitochondrial permeability transition pore (MPTP) is a 40 nm, multi-protein channel that forms in the inner mitochondrial membrane (IMM) in response to mitochondrial Ca^{2+} overload and oxidative stress. This results in a sudden, sustained increase of IMM permeability, allowing solutes with a molecular mass up to 1.5 kDa to pass in and out. Induction of the MPTP is known as the point of 'no return' in the chain of cell death pathway activation (Kroemer et al., 2007, Gukovsky et al., 2011). Several proposed components of the MPTP include adenine nucleotide translocator (ANT), voltage-dependent anion channel (VDAC) and phosphate carrier (PiC). Over the past decades, studies using genetic manipulation clearly demonstrated that ANT is not a MPTP component, but could be a regulator of MPTP induction (Kokoszka et al., 2004) and VDAC did not contribute to MPTP formation (Baines et al., 2007). Most recently, a study using cardiac-specific deletion of PiC suggests PiC is not a pore-forming component, but is a regulator of its activation (Kwong et al., 2014). The most recent evidence is that dimers of F_0F_1 ATP synthase form the MPTP and the regulator cyclophilin (Cyp D) binds to the F_0F_1 ATP synthase in the oligomycin sensitivity-conferring protein (OSCP) subunit (Giorgio et al., 2013). A further study concluded that the c-subunit ring of F_0 of F_0F_1 ATP synthase forms a voltage-sensitive channel that is the MPTP (Alavian et al., 2014).

Cyp D is a mitochondrial matrix protein with peptidylprolylcis-trans isomerase activity encoded by *Ppif* gene. Cyp D-deficient (*Ppif*$^{-/-}$) mice are viable, fertile and have no obvious abnormalities. Cells from *Ppif* $^{-/-}$ mice are largely protected from necrosis induced by Ca^{2+} -overload and oxidative stress. Cyp D-deficient mice have been found to have decreased infarction sizes in cardiac and cerebral I/R injury *in vivo* (Baines et al., 2005, Nakagawa et al., 2005, Schinzel et al., 2005). PACs from Ppif$^{-/-}$

mice have less necrosis and Cyp D-deficient mice develop less severe forms of AP in response to the combined administration of ethanol and CCK (Shalbueva et al., 2013). Most recent study demonstrated that genetic and pharmacological inhibition of Cyp D protect against pancreatic injury in mouse and human PAC and in four diverse experimental models of AP (Mukherjee et al., 2015). Preventing the opening of MPTP by specific Cyp D inhibition could be a useful therapeutic tool with significant therapeutic implications for other diseases.

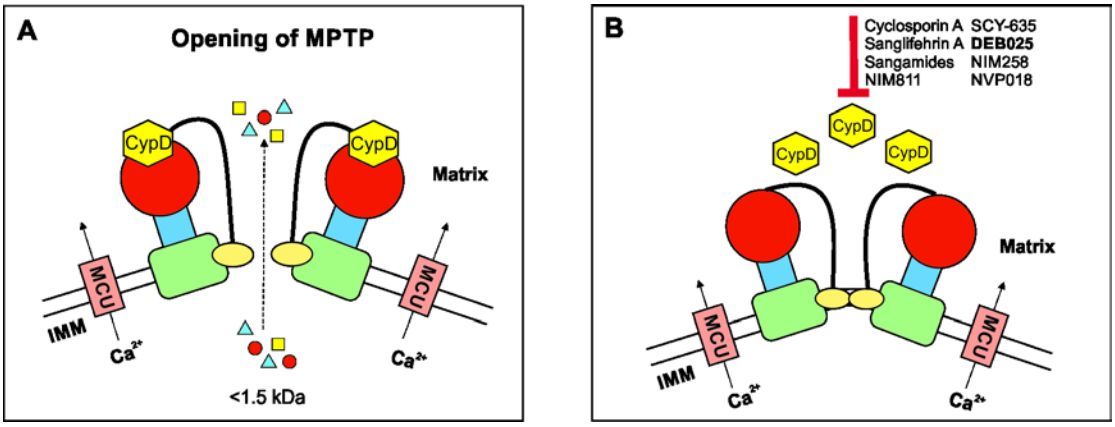

Figure 1.4 Diagram of the MPTP formed by dimers of the F_0F_1 ATP synthase. (A) Opening of the MPTP is induced by mitochondrial Ca^{2+} overload and oxidative stress, allowing solutes with a molecular mass up to 1.5 kDa to pass through the inner mitochondrial membrane. Cyp D binds to the F_0F_1 ATP synthase on the oligomycin sensitivity-conferring protein (OSCP) subunit. **(B)** Inhibition of Cyp D prevents the interaction of Cyp D with the F_0F_1 ATP synthase, increasing the threshold of MPTP opening. The listed agents are cyclophilin inhibitors, although these lack specificity for cyclophilin D, being general cyclophilin inhibitors.

Abbreviations: MPTP, mitochondrial permeability transition pore; ATP, adenosine triphosphate; Cyp D, cyclophilin D; IMM, inner mitochondrial membrane; MCU, mitochondrial Ca^{2+} uniporter

1.7 Store-operated Ca^{2+} entry channels are potential therapeutic targets

Intracellular Ca^{2+} store depletion stimulates compensatory Ca^{2+} entry from outside the cell to refill the emptied Ca^{2+} stores, known as store-operated Ca^{2+} entry (SOCE). SOCE is the principal mechanism of maintaining physiological Ca^{2+} homeostasis and cell functions in non-excitable cells such as endothelial cells (Abdullaev et al., 2008), hepatocytes (Jones et al., 2008), platelets (Tolhurst et al., 2008), T cells (Barr et al., 2008, Lioudyno et al., 2008) and PACs (Lur et al., 2009). Two key molecular components of this Ca^{2+} entry pathway have been identified a decade ago (Liou et al., 2005, Prakriya et al., 2006): firstly, the protein that senses Ca^{2+} store depletion on the endoplasmic reticulum referred as the STIM proteins, and secondly, the protein that forms the Ca^{2+} permeable ion channel on the plasma membrane referred to as Orai, see **Figure 1.5**.

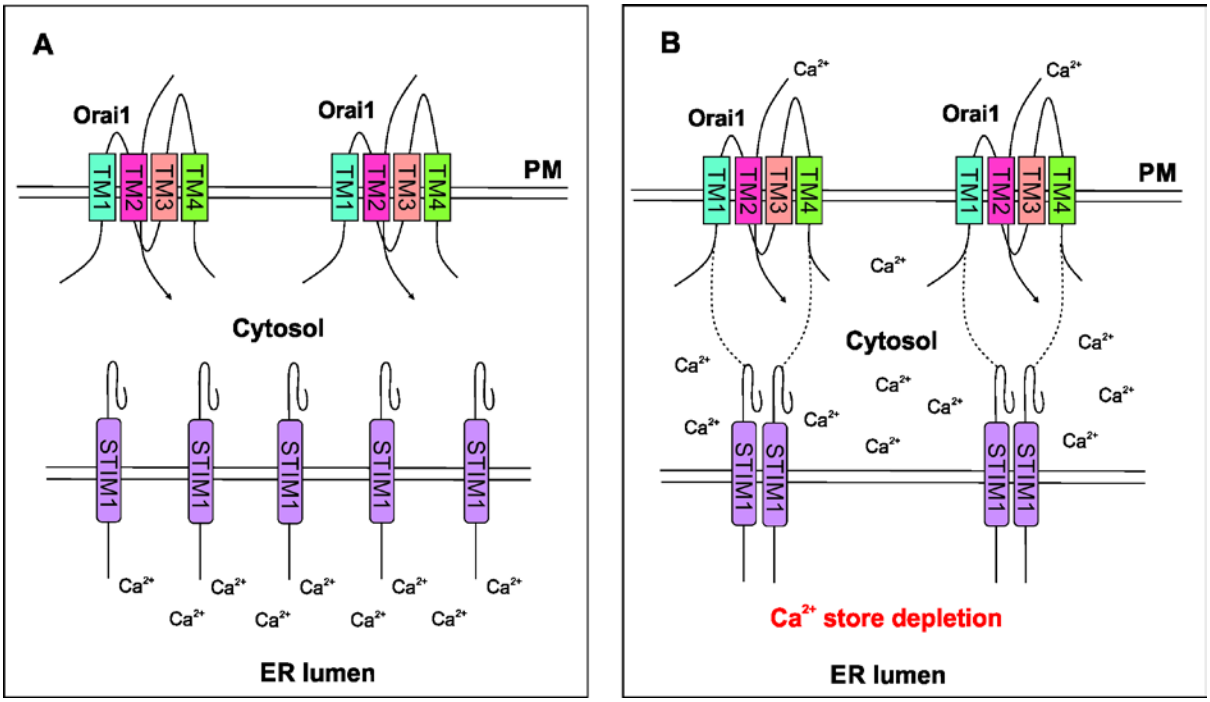

Figure 1.5 STIM1/Orai1-mediated SOCE. (A) At the resting state or before ER Ca^{2+} store depletion, STIM1 bound to Ca^{2+} and is distributed uniformly as monomers in the ER membrane. Orai1 is four transmembrane domains with both N and C termini facing into the cytosol and it is Ca^{2+} selective pore-forming subunit of Ca^{2+} release-activated Ca^{2+} channel located in the plasma membrane. Orai1 at resting state has been described as a dimer (Penna et al., 2008) or a tetramer (Ji et al., 2008). **(B)** Upon ER Ca^{2+} store depletion, Ca^{2+} dissociates with STIM1, enabling STIM1 oligomerisaion and migration to the ER-PM junctions to form distinct STIM1 puncta. This allows STIM1 aggregates, interacts with and activates Orai1 channels, resulting in Ca^{2+} entry from the outside of the cells.

Abbreviations: SOCE, store-operated Ca^{2+} entry; ER, endoplasmic reticulum; PM, plasma membrane.

1.7.1 STIM, a Ca^{2+} sensor of the level of Ca^{2+} in the ER

STIM proteins are single-pass, type I transmembrane proteins with two mammalian homologues, STIM1 and STIM2. Two studies have demonstrated that STIM1, acting as Ca^{2+} sensor for the level of Ca^{2+} in the ER, plays an essential role in controlling and activating the Ca^{2+} release-activated Ca^{2+} entry (CRAC) channel (Roos et al., 2005, Liou et al., 2005). The luminal N-terminal region of STIM1 including an EF-hand motif near the amino terminus is the Ca^{2+} binding site. Upon the depletion of the ER Ca^{2+} store, STIM1 redistributes from the ER site to form a puncta at the ER-plasma membrane (ER-PM) junctions, located 10-25 nm from the PM (Liou et al., 2005, Zhang et al., 2005, Luik et al., 2006). The luminal Ca^{2+} –binding EF hand dissociated from Ca^{2+} loses interaction with a sterile α motif domain (SAM), leading to partial unfolding of STIM1 and the formation of STIM1 oligomers. Oligomerization of STIM1 alone is sufficient to cause STIM1 accumulation at ER-PM junctions, but this is not enough to activate the CRAC channel (Luik et al., 2006, Stathopulos et al., 2008). A cytosolic region of STIM1, namely the 107-amino acid CRAC activation domain (CAD), is essential for CRAC activation and probably binds directly to both the N- and C-terminal of Orai1 to open the channels (Park et al., 2009), see **Figure 1.6**.

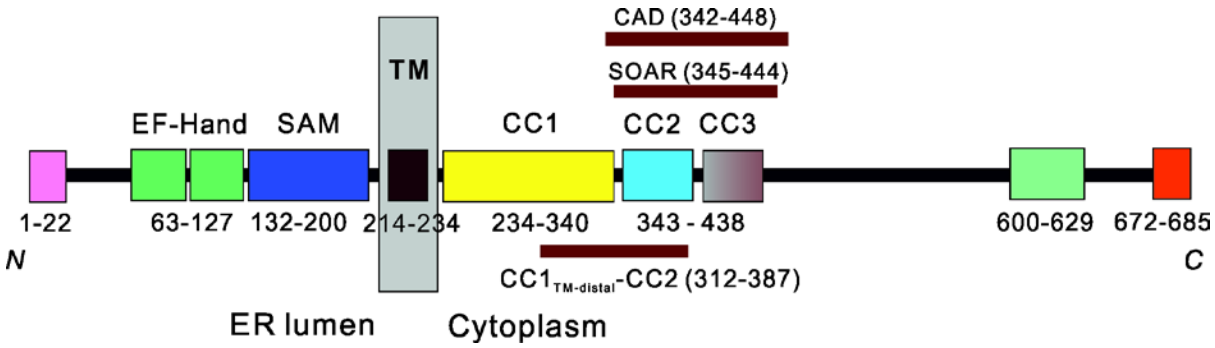

Figure 1.6 Functional domains of STIM1. STIM1 is a single-pass membrane protein of 77 kDa with N-terminus facing ER lumen and C-terminus facing cytosol. Of the ER domains, EF-hand motif imparts the protein with ER Ca^{2+} sensing functionality; SAM regulates STIM oligomerization. The cytosolic C-terminus is organized into several distinct functionally important modules including CAD and STIM1 Orai1 activation region (SOAR). Among them, the most critical functional domain of a roughly 100 amino acid regions called CAD, which is necessary and sufficient to activate I_{CRAC}. Adapted from (Shim et al., 2015).

Abbreviations: SAM, sterile α motif domain; ER, endoplasmic reticulum; TM, transmembrane; CAD, CRAC activation domain; SOAR, STIM Orai1 activation region.

1.7.2 Orai1 is the component of the CRAC channel

Orai are the keepers of the heaven gates in Greek mythology (Roberts-Thomson et al., 2010). Orai1 was firstly identified from patients with hereditary severe combined immune deficiency (SCID) syndrome, which is defective in SOCE and CRAC channel function. The defect of SCID is associated with replacement of a highly conserved arginine residue by tryptophan at R91 position (Feske et al., 2006). Two following studies have identified Orai1 as an essential pore subunit of the CRAC channel (Prakriya et al., 2006, Vig et al., 2006). Two conserved acidic residues, E106 and E190 in transmembrane helices 1 and 3, respectively determines the ion selectivity of CRAC channel (Prakriya et al., 2006). Orai1 is a four–transmembrane protein (TM1-TM4) expressed at the cell surface with its N- and C-terminal facing into the cytoplasm. The crystal structure of Orai was revealed in 2012 and shows a hexameric assembly of Orai subunits comprising the ion pore arranged around a central ion pore, which traverses the membrane and extends into the cytosol (Hou et al., 2012). Use of the crystal structure of Orai could facilitate the development of more selective Orai inhibitors. The selectivity of Orai is determined by glutamate residues on its extracellular side; the closed state is mediated by binding of anions to a basic region near the intracellular side (Yeromin et al., 2006, Hou et al., 2012). Orai1 interaction with the C-terminus of STIM induces Orai1 dimers to dimerize, forming tetramers that constitute the Ca^{2+}–selective pore (Penna et al., 2008). Another study has suggested that Orai1 forms tetramers in resting cells and the activated CRAC channels remain as tetramers (Ji et al., 2008), see **Figure 1.7**.

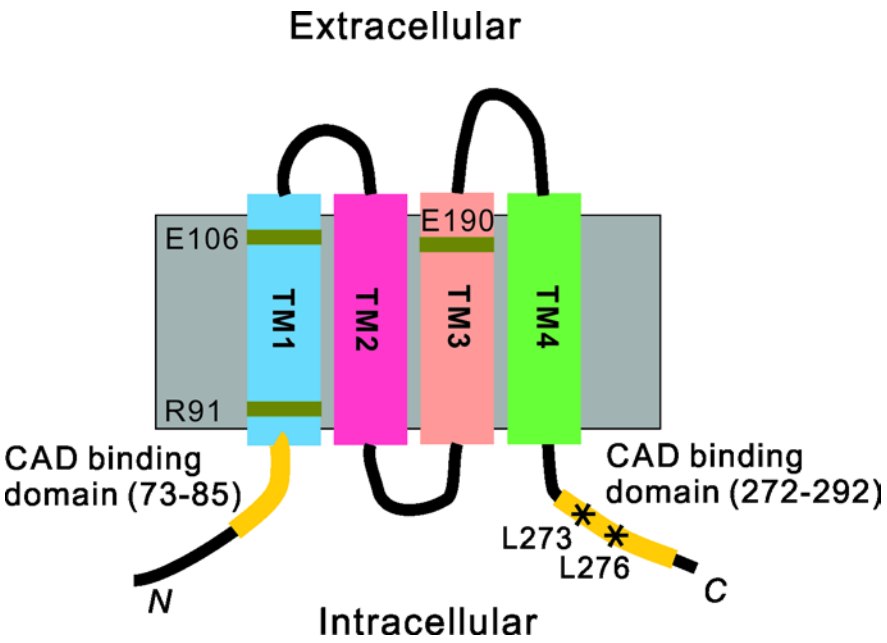

Figure 1.7 Structure of Orai1. Each Orai1 monomer includes four transmembrane domains (TM1-TM4). Early studies identified several acidic residues in TM1 (E106) and TM3 (E190) whose mutation changed ion selectivity or permeation. Future study confirmed residue E106 forming critical molecular determinant of the high Ca^{2+} selectivity of the CRAC channel. STIM1 interacts with two sites in Orai1; CAD binding regions of intracellular C- and N-termini are highlighted in yellow. Adapted from (Shim et al., 2015).

Abbreviations: TM, transmembrane; CAD, CRAC activation domain

Orai has three isoforms Orai1, Orai2 and Orai3. Orai proteins share no homology with any other known ion channel proteins (Roberts-Thomson et al., 2010). Orai1, Orai3 and STIM1 are almost ubiquitously expressed in the whole body while Orai2 is prominently expressed in the brain, lung, spleen and intestine (Gross et al., 2007). Orai1-deficient ($Orai1^{-/-}$) mice exhibit some clinically relevant phenotypes, including immunodeficiency with defective T- and B-cell function and impaired mast cell function (Vig et al., 2008, Gwack et al., 2008). The important roles of Orai1 have been noted and studied in different diseases over recent few years, including allergic disease (Vig et al., 2008), breast cancer (Yang et al., 2009), myocardial infarction and stroke (Braun et al., 2009), allograft rejection(McCarl et al., 2010) and autoimmune disease (Kim et al., 2014).

1.7.3 Development of Orai channel inhibitors

There are currently no specific I_{CRAC} inhibitors approved by the European Medicines Agency (EMA) or US Food and Drug Administration (FDA) for clinical use. 2-amino-ethoxydiphenylborate (2-APB) is a blocker of I_{CRAC} with multiple off-target effects, which has been used as a tool to study SOCE for many years (Bootman et al., 2002). DPB162-AE and 163-AE, chemical analogs of 2-APB, were identified by the Mikoshiba group with an IC_{50} of 27 nM and 42 nM respectively in DT-40 cells (Goto et al., 2010). Subsequent study indicated that the inhibitory effects of these two compounds target STIM1, though effects on the STIM1-Orai interaction are unknown (Jairaman and Prakriya, 2013). This prevents further development of these two compounds for clinical use since STIM1 plays such a fundamental role in maintaining physiological Ca^{2+} signals in the body. Bis(trifluoromethyl) pyrazole derivatives (BTPs) were first identified by Abbott Laboratories in a high-throughput

drug screen for inhibition of IL-2 production in Jurkat T cells (Djuric et al., 2000). YM-58483 is the same as BTP2, but synthesized independently by Yamanouchi pharmaceuticals with an IC_{50} value of ~100 nM inhibiting SOCE in Jurkat T cells (Ishikawa et al., 2003). Apart from inhibition of CRAC channels, various studies have shown BTP2 inhibited other ion channels including TRM4, TRPC3 and TRPC5 (Jairaman and Prakriya, 2013). The non-specific inhibitory effects of BTPs on several ion channels preclude their use in human diseases. 3-fluoropyridine-4-carboxylic acid (2',5'-dimethoxybiphenyl-4-yl)amide (Synta 66) was developed by Synta pharmaceuticals with a similar structure to BTP2 and an IC_{50} of ~3 μM (Jairaman and Prakriya, 2013). Synta 66 showed selectivity for CRAC inhibition over inhibition of Kv1.3, hERG, TRPM4 or TRPM7 channels (Sweeney et al., 2009), but its relatively high IC_{50} value may prevent its use in clinical setting (Parekh, 2010).

2,6-difluoro-N--benzamide (RO2959) is a potent SOCE inhibitor that completely inhibits SOCE, cytokine production and T cell proliferation in $CD4^+$ T cells. RO2959 has a 20-fold difference of IC_{50} between Orai1 and Orai2/3 (25 nM for Orai1 and 500 nM for Orai3) and did not have a significant inhibitory effect on a number of ion channels screened including TRPC1, TRPM2, TRPM4, hERG, hCav1.2, hKv1.5. This makes RO2959 a fairly selective CRAC channel inhibitor (Chen et al., 2013, Jairaman and Prakriya, 2013). 2,6-difluoro-N-(1-(4-hydroxy-2-(trifluoromethyl)benzyl)-1H-pyrazol-3-yl)benzamide (GSK-7975A) is a novel I_{CRAC} inhibitor that blocks Orai1 and Orai3 channels with an IC_{50} of approximately 4.1 μM and 3.8 μM, respectively. Inhibitory profiles of GSK-7975A on sixteen ion channels revealed only a slight inhibitory effect on L-type (CaV1.2) Ca^{2+} channels (Derler et al., 2013, Rice et al., 2013). CalciMedica (CM) has patented a series of compounds that

inhibit I_{CRAC} and Orai channels. CM2489 has completed Phase I clinical trials for the treatment of moderate-to-severe plaque psoriasis, which is the first CRAC inhibitor to be tested in humans (Jairaman and Prakriya, 2013). The multiple-dose Phase I study of CM2489 has shown this to be safe, well-tolerated and well-behaved with some evidence of clinical improvement (www.calcimedica.com), see **Table 1.3**.

Table 1.2 Summary of Orai channel inhibitors

Drug	Company/Institute	Drug class	Mechanism of action	Clinical phase
BTP2 (YM58483)	Abbott (Yamanouchi)	SMWC	Orai channel inhibitor, unknown selectivity	Preclinical (discontinued)
Synta 66	Synta	SMWC	Orai channel inhibitor, unknown selectivity	Preclinical (discontinued)
RO2959	Hoffmann-La Roche	SMWC	Orai1 channel inhibitor	Preclinical (unknown)
GSK-7975A	GlaxoSmithKline	SMWC	Orai1/3 channel inhibitor	Preclinical (discontinued)
CM compounds	CalciMedica	SMWC	Orai1/3 channel inhibitor	Phase I

Abbreviations: SMWC, small molecular weight chemical; CM, CalciMedica

1.7.4 SOCE and AP

Pathophysiological events induced by pancreatitis-associated toxins in PACs are all dependent on Ca^{2+} entry through SOCE on the plasma membrane, including premature digestive enzyme activation, vacuole formation, altered trafficking and secretion, skeletal disruption, mitochondrial dysfunction and necrotic cell death activation. All these processes do not occur if there is removal of external Ca^{2+} or intracellular Ca^{2+} chelation (Raraty et al., 2000, Criddle et al., 2004, Kim et al., 2002, Voronina et al., 2002). Orai1 is the principal SOCE channel in PACs, opening of which is coordinated by STIM1, following decrease in ER Ca^{2+} store concentrations. PACs contain two pools of Orai1: an apical pool that co-localizes and interacts with IP_3Rs and a basal pool that interacts with STIM1 following the Ca^{2+} store depletion (Lur et al., 2009). Previous studies have demonstrated that GSK-7975A inhibits SOCE induced by thapsigargin in isolated murine pancreatic acinar cells over the range of 1-50 µM (IC_{50} ~3.4 µM) (Gerasimenko et al., 2013). In addition, GSK-7975A inhibits endocytic vacuole formation (Voronina et al., 2015) and reduces necrosis induced by toxins that cause AP (Gerasimenko et al., 2013, Voronina et al., 2015).

Transient receptor potential canonical (TRPC) channels are another class of functional SOCE channels present on PACs. They can be activated subsequent to the activation of different isoforms of phospholipase (PLC) and also can be activated whenever intracellular Ca^{2+} stores are depleted, acting as a non-selective Ca^{2+}-permeable cation, SOC channels (Nilius et al., 2007). Acinar cells expressed TRPC1, TRPC3 and TRPC6(Parekh and Putney, 2005). TRPC3-deficient mice ($Trpc3^{-/-}$) are viable, fertile and have normal phenotype other than impaired synaptic transmission in Purkinje cells and motor coordination (Hartmann et al., 2008). Genetic depletion

and pharmacological inhibition of TRPC3 resulted in ~50% reduction Ca^{2+} influx in vitro and ~50% reduction of *in vivo* pancreatic damage induced by four injections of cerulein (Kim et al., 2009, Kim et al., 2011).

1.8 Hypotheses and study aims

Hypothesis 1: Cytosolic Ca^{2+} overload mediated via Orai1 channels has a pivotal role in the pathogenesis of AP.

Study aims 1) to determine the effects of Orai1 inhibition by GSK-7975A and CM_128 on SOCE and necrotic cell death pathway activation in isolated murine pancreatic acinar cells; 2) to evaluate the effects of Orai1 inhibition by GSK-7975A and CM_128 on disease severity in at least two experimental AP models.

Hypothesis 2: Prevention of Ca^{2+} overload by inhibition of Orai1 channel has translational potential as a treatment for human acute pancreatitis

Study aims: to examine the effects of Orai1 inhibition by GSK-7975A and CM_128 on SOCE and necrotic cell death pathway activation in isolated human pancreatic acinar cells.

Hypothesis 3: Door-to-needle time is critical for AP treatment targeting the pathogenesis of pancreatic injury.

Study aims: to compare the effects of early versus late administration of GSK-7975A and CM_128 on disease severity in two clinically representative models of AP.

In vitro and *in vivo* mouse AP models were used in my study since the study in my thesis was mainly focusing on PACs and the cells from mouse pancreas have similar

characteristics as human PACs to better mimic the settings of human diseases. Hyperstimulation AP (CER-AP) was well-established, wildly used and reproducible experimental model. Biliary AP (TLCS-AP) and alcohol/fatty acid AP (FAEE-AP) were chosen to model the major etiology of human AP (Lerch and Gorelick, 2013).

Chapter 2

Methods

2.1 Animals

CD-1 and C57BL/6J mice were from Charles River UK Ltd. Pancreatic acinar cells were isolated from CD-1 mice. For *in vivo* experiments 10-12 week old male C57BL/6J mice were used. All animals were allowed to acclimatize for 1 week under temperature-controlled conditions with a 12-hour light/dark cycle, with free access to water and standard laboratory chow during this time. All efforts were made to minimize animal suffering and to reduce the number of animals used.

2.2 Isolation of murine PACs

Mice were humanely killed by dislocation of the neck following the Code of Practice for the Humane Killing of Animals under Schedule 1 of the Animals (Scientific Procedure) Act 1986. The pancreas was dissected immediately and washed twice with sodium 4-(2-hydroxyethyl)-1 piperazineethanesulfonic acid (HEPES) solution, containing in mM: 140 NaCl, 4.7 KCl, 1.13 $MgCl_2$, 10 HEPES, 10 D-glucose and 1.2 $CaCl_2$; pH 7.35. The tissue was digested by injecting with 1 ml of collagenase (200 units/ml, Worthington) dissolved in sodium HEPES solution and incubated in the collagenase solution, in a shaking water bath, at 37°C for 17 min. After incubation, the tissue was poured into 15 ml falcon tube and washed with sodium HEPES solution once to remove the collagenase solution. Then the tissue was disrupted by either shaking by hand or pipetting through an enlarged 1 ml pipette tip. The cloudy supernatant was transferred into fresh falcon tubes and this step repeated several times until the tubes were filled and centrifuged at 1,000 rpm for 1 minute. The supernatant was discarded and the cell pellet was re-suspended in sodium HEPES solution. The cell re-suspension was filtered through a 70 µm cell strainer (BD Falcon) and centrifuged at 1,000 rpm for 1 minute. The supernatant was discarded

carefully and the cell pellet was re-suspended in sodium HEPES solution for *in vitro* experiments. All isolated cells were used within 4-6 hours.

2.3 Isolation of human PACs

Human pancreas was sampled and cells isolated as described (Murphy et al., 2008). Briefly, specimen was taken from patients undergoing surgery for left-sided or small un-obstructing pancreatic tumours. During surgery, a small piece (~1 cm x 1 cm x 1 mm) was cut with a fresh scalpel blade from the transaction margin of the pancreas *in situ*. The sample was washed immediately twice by sodium HEPES solution, then put straight into falcon tube containing sodium HEPES solution plus 5 µM trypsin inhibitor, 100 µM sodium pyruvate as well as protease inhibitor and taken into the laboratory. Pancreatic cell isolation in each case was started less than 10 minutes after sampling. Serial digestions of human tissue were required for high quantity and quality cell yields. For the first digestion, the tissue was injected with 1-2 ml of collagenase (200 units/ml, Worthington) and incubated in the collagenase solution in a shaking water bath at 37°C for 20-25 minute. After incubation, the tissue was poured into 15 ml falcon tube and washed with sodium HEPES solution once to remove the collagenase solution. Then the tissue was disrupted by either shaking by hand or pipetting through a 1 ml pipette tip. The cloudy supernatant was filtered with a 70 µm cell strainer (BD Falcon) before transfer into a fresh 50 ml falcon tube and this step was repeated several times until the 50 ml tube was filled and centrifuged at 1,000 rpm for 1 minute. The supernatant was discarded and the cell pellet re-suspended in sodium HEPES solution and stored at 4°C. The remaining tissue was subject to a second digestion by injecting with a stronger collagenase solution (4000 units/ml, Worthington) and incubated in the collagenase solution in a shaking water

bath at 37°C for 10-15 minute. After incubation, the previously described steps were repeated and the cell pellet from the second digestion was re-suspended in sodium HEPES solution and stored at 4°C. Whether a third digestion was required depended on the cells yielded from first two digestions and the amount of remaining tissue. If the first two digestions have yielded big cell pellets and the remaining tissue was small and almost disrupted, the third digestion was not required. If cell pellets from the first two digestions were not big enough and the remaining tissue was still comparatively large, further digestion was required. After serial digestions of tissue, the cells from each digestion were checked separately under microscopy before mixing together for *in vitro* experiments. All isolated cells were used within 4-6 hours.

2.4 Necrotic cell death pathway activation measurement

Cells were treated with various concentrations of test compounds together with 500 µM taurolithocholic acid 3-sulfate (TLCS) for 30 minutes, gently shaking at 1,000 rpm at room temperature. After washing with sodium HEPES solution once, cells were stained with propidium iodide (PI) and Hoechst 33342, placed onto a 96-well glass bottom plate (150 µl per well) and imaged using LSM710 systems. Hoechst 33342 (50 µg/ml; excitation 364 nm, emission 405-450 nm) was used to stain the nucleus, to count the total number of cells. PI (1 µM; excitation 488 nm, emission 630-693 nm) was used to assess plasma membrane rupture: the total number of cells displaying PI uptake was counted in 20 random fields of each isolate to give a percentage, averaged across fields as mean ± s.e.m. with ≥3 isolates/group.

2.5 Induction of experimental AP

2.5.1 Hyperstimulation AP

Hyperstimulation AP (CER-AP) was induced by seven hourly intraperitoneal injections of 50 µg/kg caerulein (Lerch and Gorelick, 2013), with humane killing 12 h after the first injection with no mortality. Analgesia was given by subcutaneous injection of 1 mg/kg buprenophine. The control mice were received seven hourly intraperitoneal injections of the same volume of saline.

2.5.2 Biliary AP

Biliary AP (TLCS-AP) was induced by retrograde pancreatic duct infusion of 3 mM TLCS at a speed of 5 µl/min over 10 min (50 µl TLCS in total) by infusion pump (Laukkarinen et al., 2007, Perides et al., 2010); humane killing 24 h later with no mortality. General anaesthesia was given using O_2 and isoflurane. Prior to laparotomy, the mice were given 1 mg/kg buprenophine subcutaneously. Methylene blue with a final concentration of 100 mg/ml was used to indicate satisfactory pancreatic infusion (see **Figure 2.1**). After surgery, the mice were recovered in 37ºC mini-thermacage (Datasand Group) for 30 min, then move to the cage on a warm heat pad and monitored carefully for at least 2-3 h. The control mice were received sham operation.

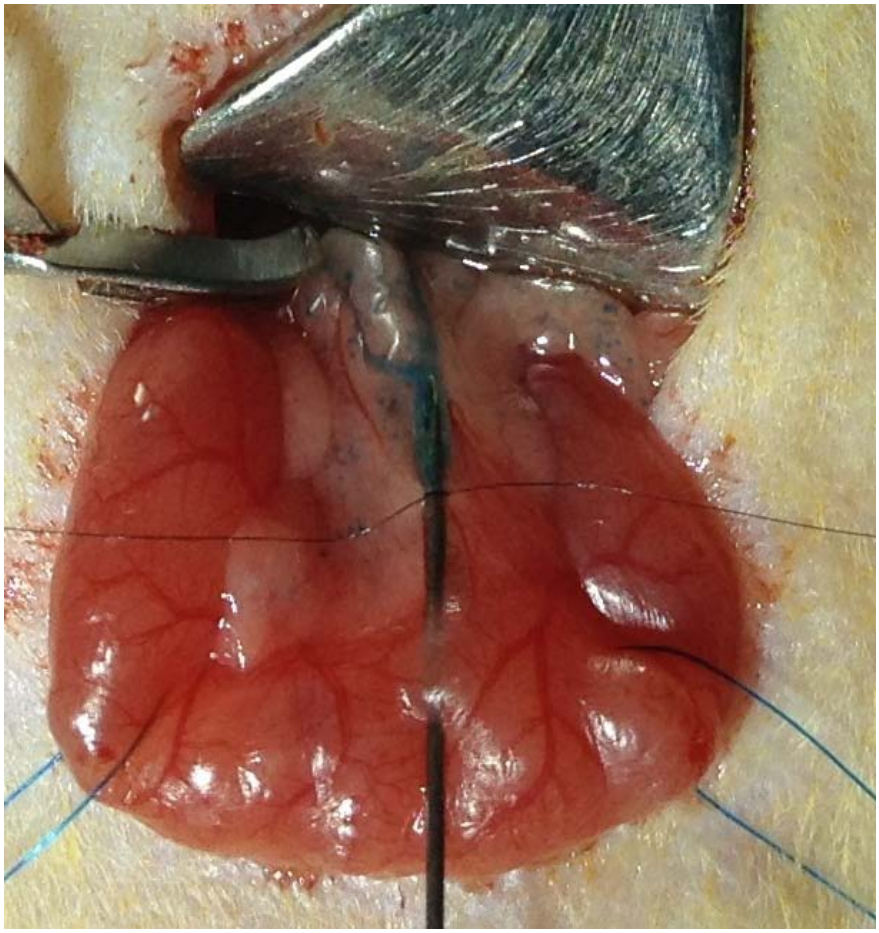

Figure 2.1 A representative photo of TLCS-AP induction. Photo from TLCS-AP at the end of retrograde pancreatic duct infusion, indicating successful infusion of TLCS into the pancreas.

2.5.3 Alcohol/fatty acid AP

Alcohol/fatty acid AP (FAEE-AP) was induced by two hourly intraperitoneal injections of 150 mg/kg palmitoleic acid (POA) and 1.35 g/kg ethanol (Huang et al., 2014), with humane killing 24 h later for assessment of the severity of AP. In order to avoid local damage by ethanol and/or POA, 200 µl of sterile saline was injected intraperitoneally at the site before each injection. Analgesia was given by subcutaneous injection of 1 mg/kg buprenophine every 12 h. The mice were kept on a warm heat pad during the procedure and monitored very carefully for the first 6 h after the first injection. During

the continuously monitoring, humane killing was applied to the mouse (1-2 out of 10 mice) when the mouse was considered to suffer too much pain and stresses. The contol mice were received two hourly intraperitoneal injections of the same volume of saline.

2.6 Drug delivery by mini-osmotic pump

As experimental procedures were done with mice and the time course of experiments was up to 24 h, ALZET mini-osmotic pump (Model 2001D) with 8 µL/h delivery rate over 24 h periods was selected for subcutaneous implantation for some experiments in which a drug with a very short half-life (GSK-7975A given as phosphate prodrug GSK-6288B) was tested. ALZET mini-osmotic pump was filled-in, primed and implanted according to the manufacturer's instructions. Good sterile technique was used during the filling, handling and surgical implantation of minipumps. During filling and implantation, minipumps were handled with surgical gloves because skin oils in large quantity may interfere with the performance of a pump if they accumulate on its surface.

2.6.1 Working mechanism of mini-osmotic pump

Minipumps operate because of an osmotic pressure difference between a compartment within the pump (called the salt sleeve) and the tissue environment in which the pump is implanted. The high osmolarity of the salt sleeve causes water to flux into the pump through a semipermeable membrane which forms the outer surface of the pump. As the water enters the salt sleeve, it compresses the flexible reservoir, displacing the test solution from the pump at a controlled, predetermined rate (see **Figure 2.2**).

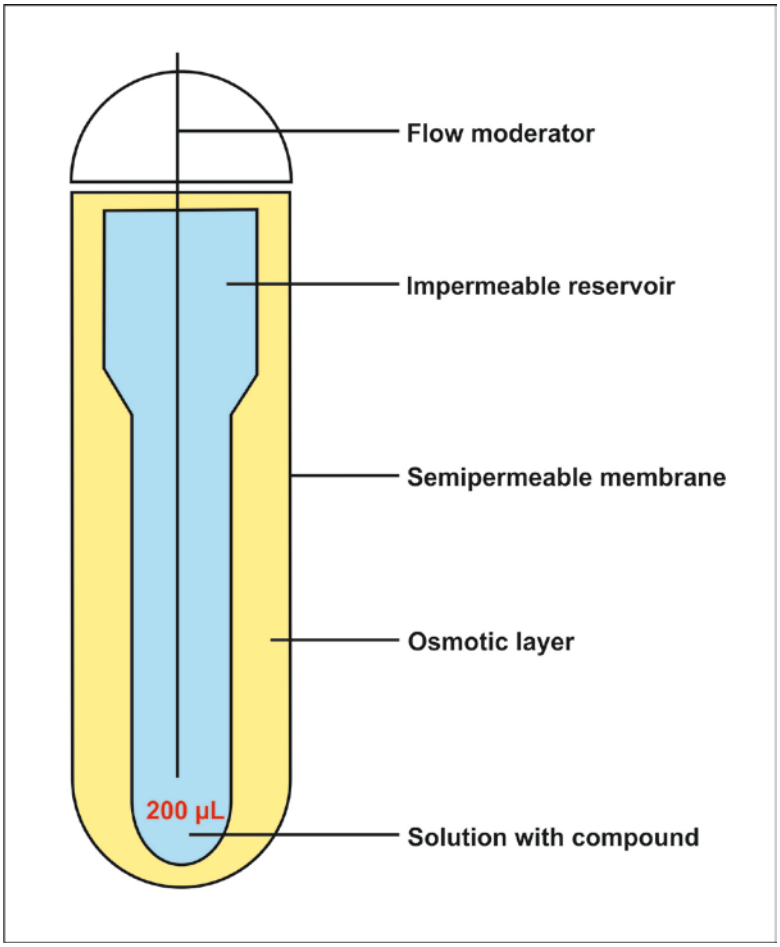

Figure 2.2 A Schematic illustration of a minipump. Tested compound is dissolved in a compatible solvent and loaded into the impermeable reservoir. The semi-permeable membrane allows water (from tissue fluid) to influx through the outer surface of the pump. The expanding layer in the salt sleeve compresses the flexible reservoir, pumping the tested solution at controlled rate through the flow moderator.

2.6.2 Selecting compatible solvent

The minipumps are compatible with aqueous solutions, dilute acids and bases, dilute or low concentrations of DMSO and alcohol, and up to 100% propylene and polyethylene glycol. A phosphate prodrug GSK-6288B with higher solubility in aqueous solvent was used in some studies. It was dissolved in phosphate buffer, which is compatible with the minipump used.

2.6.3 Filling mini-osmotic pumps

Minipumps were carefully filled as below:

1) The empty pump together with its flow moderator was weighed.
2) Filling the pump was accomplished with a small syringe (1.0 ml) and the provided blunt-tipped, 27 gauge filling tube.
3) With the flow moderator removed, the pump was held in an upright position and the filling tube was inserted through the opening at the top of the pump until it could go no further.
4) The plunger of the syringe was pushed very slowly to avoid air bubbles. When the solution appeared at the outlet, the filling was stopped and the syringe was carefully removed.
5) The excess solution was wiped off and the flow moderator was inserted until the white flange was flush with the top of the pump. The insertion of the flow moderator displaced some of the solution from the filled pump. To function properly, the flow moderator had to be fully inserted into the body of the pump.
6) The filled pump was weighed. The difference in the weights obtained in Step 1) and 6) was the net weight of the solution loaded, with the weight in

milligrams approximately the same as the volume in microliters for dilute aqueous solutions.

2.6.4 Priming mini-osmotic pumps

Before implantation, the prefilled pumps were put in 0.9% saline for at least 3 hours at 37°C in order to reach a steady state pumping rate immediately after implantation.

2.6.5 Implanting mini-osmotic pumps

Minipumps were implanted subcutaneously in mice under general anesthesia of O_2 and isoflurane. A small incision was made in the skin between the scapulae, and a small pocket formed using scissors by spreading the subcutaneous connective tissues apart. Minipumps were inserted into the pocket with the flow moderator pointing away from the incision. The skin incision was closed with sutures (see **Figure 2.3**).

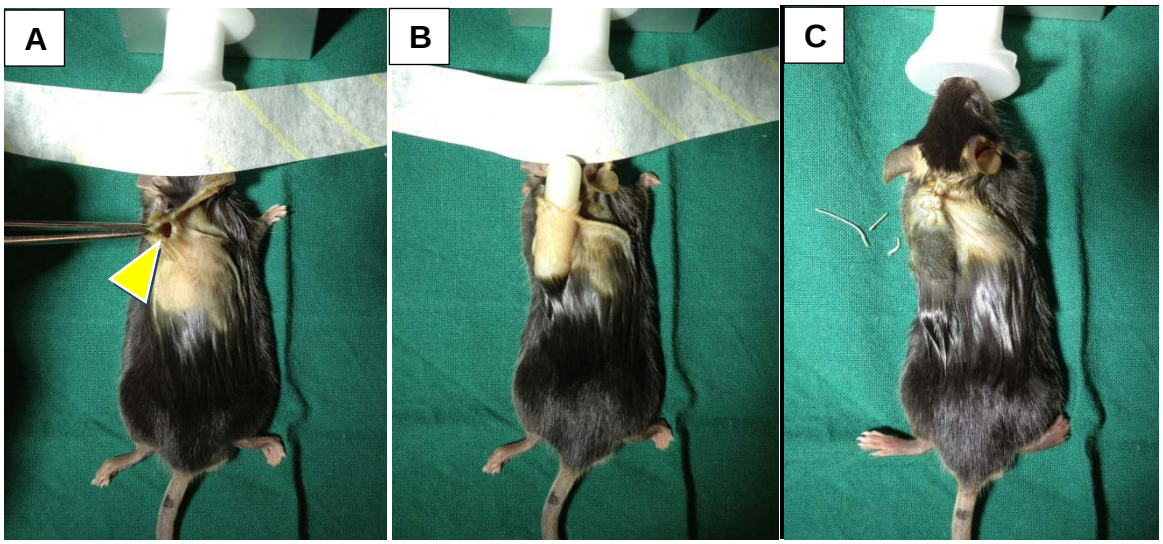

Figure 2.3 Procedure of mini-pump implantation. (A) Small pocket was made by spreading the subcutaneous connective tissues apart after a small incision was made (arrow showing towards the small pocket); **(B)** the pump was inserted into the pocket with flow moderator pointing away from the incision; **(C)** the incision was closed with sutures.

2.6.6 Verifying the accuracy of mini-osmotic pump drug delivery

The recommended method to verify the results from continuous administration is to measure the blood levels of drug at several points during the course of infusion. The levels of GSK-6288B and GSK-7975A in the blood and pancreas were measured at 1, 2, 4, 10 and 22 h after minipump implantation in the study prior to drug efficacy assessment.

2.7 Evaluation of experimental AP severity

Whether experiment AP was successfully developed was confirmed by serum amylase and pancreatic histology. AP severity was evaluated by local biochemical parameters, including pancreatic trypsin and MPO activity, a marker of inflammatory infiltration (Dawra et al., 2008). Pancreatitis-associated distant organ damage was

measured by IL-6 and lung MPO activity since respiratory failure is one of the commonest organ dysfunction in severe AP patients (Banks et al., 2013).

2.7.1 Serum amylase and IL-6

Blood was collected in a clean 2 ml tube, then centrifuged 1,500 ×g for 10 minutes. Serum amylase activity was determined by Roche automated clinical chemistry analyzers (Roche) and serum IL-6 was measured by Quantikine ELISA (R&D systems).

2.7.2 Trypsin activity

Pancreatic trypsin activity was measured by fluorogenic assay as previously described (Nathan et al., 2005), using Boc-Gln-Ala-Arg-MCA substrate (excitation 380 nm, emission 440 nm) converted by trypsin to a fluorescent product. Briefly, pancreatic tissue was homogenized in 5 mM 4-morpholinepropane sulfonic acid (MOPS) buffer, containing 250 mM sucrose and 1 mM magnesium sulphate, pH 6.5, centrifuged at 1,500 × g for 5 min at 4°C. The supernatant was added to each well of a 96-well plate containing pre-warmed pH 8.0 assay buffer, with 50 mM Tris, 150 mM NaCl, 1 mM $CaCl_2$ and 1% (w/v) bovine serum albumin and peptide substrate. Fluorescence was measured using a PLOARstar Omega microplate reader. Pancreatic trypsin activity was calculated as the difference of fluorescence intensity between 0 min and 5 min.

2.7.3 Myeloperoxidase activity

MPO activity was determined as described (Dawra et al., 2008). Briefly, pancreatic and lung tissue were homogenized in 100 mM phosphate buffer (pH 7.4) with

protease inhibitors, centrifuged at 16000 × g for 15 minutes at 4°C (twice for pancreas and three times for lung). The pellet was re-suspended in 100 mM phosphate buffer (pH 5.4), containing 0.5% hexadecyltrimethyl ammonium bromide, 10 mM EDTA and protease inhibitors, then freeze-thawed three times, sonicated for 30 sec and centrifuged at 16,000 × g for 15 minutes at 4°C. Myeloperoxidase activity was measured in the supernatants mixed with 3,3,5,5-tetramethylbenzidine as the substrate with freshly added 0.01% H_2O_2. Absorbance was measured at 655 nm and MPO activity calculated as the difference between the values at 0 and 3 min.

2.7.4 Histology

For morphological examination pancreatic tissues were fixed in 10% formalin, embedded in paraffin, and stained with hematoxylin and eosin (H&E). Histopathological evaluation was assessed blindly on 10 random fields (×10 high power fields) of each slide by two independent investigators, grading the degree and extent of oedema, inflammatory infiltration and necrosis from 0 to 3 (see **Table 2.1** for the details), calculating summated mean ± s.e.m, for ≥6 mice/group. The agreement of these scores between two indepedent investigators was evaluated and confirmed before assessing the slides from experimental groups.

Table 2.1 Pancreatic histopathological grading criteria (Wildi et al., 2007)

Parameter	Scores	Indications
1. Edema	0	Absent
	1	Focal increased between lobules
	2	Diffused increased
	3	Acini disrupted and separated
2. Inflammatory inflitration	0	Absent
	1	In ducts (around ductal margins)
	2	In the parachyma (<50% of the lobules)
	3	In the parachyma (>50% of the lobules)
3. Necrosis	0	Absent
	1	Periductal necrosis (<5)*
	2	Focal necrosis (5-20%)
	3	Diffused parachymal necrosis (>20%)

*Approximate percentage of cells involved per field examined.

2.8 Chemicals

CCK-8 was from American Peptide; other fluorescent dyes from Molecular Probes; Boc-Gln-Ala-Arg-MCA from Peptide Instutite (Osaka, Japan); protease inhibitors from Roche GmbH (Mannheim, Germany); IL-6 Quantikine ELISA Kit from R&D Systems; ALZET® osmotic mini-pump (2001D) from Charles River UK Ltd. Other reagents were from Sigma (Dorset, United Kingdom). 2,6-difluoro-N-(1-(4-hydroxy-2-(trifluoromethyl)benzyl)-1H-pyrazol-3-yl)benzamide (GSK-7975A) and pro-drug GSK-6288B were gifted by GlaxoSmithKline (Stevenage, United Kingdom). CM_128 was gifted by CalciMedica (La Jolla, United States).

2.9 Statistical analysis

Data were presented as mean ± s.e.m. Statistical evaluation was performed using OriginPro 9 (OriginLab corporation, USA). Two-tailed Student's t-test (two groups) and ANOVA (more than two groups) were performed for parametric data and $\chi 2$ test for non-parametric data; p values <0.05 were considered significant.

2.10 Study Approval

Human pancreatic samples were obtained with informed consent as approved by Liverpool Adult Local Research Ethics Committee (Ref: 03/12/242/A). All animal studies were ethically reviewed and conducted according to UK Animals (Scientific Procedures) Act 1986, approved by UK Home Office (PPL 40/3320, renewed as 70/8109) and Prof Sutton (my supervisor) is the project license holder.

Results: Chapter 3

Effect of novel Orai inhibitors on store-operated Ca^{2+} entry and cell fate in mouse and human pancreatic acinar cells

3.1 Introduction

Sustained elevation of the $[Ca^{2+}]_c$ is a critical trigger for pancreatic acinar cell injury and necrosis that depends on SOCE. All subsequent cellular injury does not occur if sustained Ca^{2+} entry via SOCE channels is prevented, either by the removal Ca^{2+} from external solution or by blocking Ca^{2+} entry channels on the plasma membrane (Raraty et al., 2000, Petersen and Sutton, 2006, Gerasimenko et al., 2013, Lankisch et al., 2015). The molecular component of the CRAC channel named Orai1 has been identified by 1) genotyping and analyzing cells from patients with hereditary SCID syndrome; 2) genome-wide RNA intereference (RNAi) screens followed by a secondary patch-clamp screens (Feske et al., 2006, Vig et al., 2006). Orai1 is the principal SOCE channel in PACs (Lur et al., 2009), opening of which is coordinated by STIM1 and STIM2 following decreases in ER Ca^{2+} store concentrations (Gerasimenko et al., 2013, Lur et al., 2009, Muik et al., 2012, Derler et al., 2013).

GSK-7975A and CM_128 were discovered independently as Orai channel inhibitors by GlaxoSmithKline (Derler et al., 2013, Rice et al., 2013) and CalciMedica, respectively. The inhibitory effects of GSK-7975A on SOCE have been evaluated in lung mast cells (Ashmole et al., 2012), platelets (van Kruchten et al., 2012) and glomerular mesangial cells (Chaudhari et al., 2014). Previous studies showed GSK-7975A inhibits thapsigargin- and palmitoleic acid ethyl ester (POAEE)-induced SOCE in isolated murine PACs over the range of 1-50 μM (IC_{50} ~3.4 μM) (Gerasimenko et al., 2013), inhibits endocytic vacuole formation (Voronina et al., 2015) and reduces necrosis induced by toxins that cause AP (Gerasimenko et al., 2013, Voronina et al., 2015). But, the effects of GSK7975A on SOCE and cell fate in

human PACs remain unknown. Until now, there are no published data on the effects of CM_128, a new molecular entity of Orai inhibitor.

The study described in this chapter was designed to evaluate the effects of GSK-7975A on CCK- and TLCS-induced Ca^{2+} entry in isolated mouse PACs and thapsigargin-induced Ca^{2+} entry in isolated human PACs as well as the effects of GSK-7975A and CM_128 on bile acid-induced necrotic cell death pathway activation in isolated mouse and human PACs.

3.2 Methods

3.2.1 Measurement of cytosolic Ca^{2+} concentrations

Cells isolated from mouse and human pancreata (details in 2.2 and 2.3) were loaded Fura-2 (5 µM; excitation 340 and 380, emission >490 nm) for 30-45 mins and imaged using a Till Photonics System to assess $[Ca^{2+}]_c$; ratio of fluorescence recorded from excitation at 340 and 380 nm were used for the analysis. Experiments were undertaken by Dr Svetlana Voronina and Dr Michael Chvanov.

3.2.2 Measurement of necrotic cell death pathway activation

Cells isolated from mouse and human pancreata (details in 2.2 and 2.3) were treated with 500 µM TLCS ± various concentrations of GSK-7975A and CM_128 for 30 min, shaking at 1,000 rpm, at room temperature. Control cells were treated with the same volume of dimethylsulfoxide (DMSO) used to dissolve GSK-7975A/CM_128, without TLCS, for 30 min under the same conditions. After washing, cells were stained with PI and Hoechst 33342, placed into a 96-well glass bottom plate (150 µl per well) and imaged using LSM710 systems. Hoechst 33342 (50 µg/ml; excitation 364 nm,

emission 405-450 nm) was used to stain the nucleus, to count the total number of cells. PI (1 µM; excitation 543 nm, emission 630-693 nm) was used to assess plasma membrane rupture: the total number of cells displaying PI uptake was counted in ≥ 3 wells and ≥ 12 random fields of each differently treated group of each isolate to give a percentage, averaged across fields as mean ± s.e.m. with ≥3 isolates/group, except where stated.

3.3 Results

3.3.1 Effects of GSK-7975A on store-operated Ca^{2+} entry in mouse PACs

Isolated mouse pancreatic acinar cells maintained in 5 mM external Ca^{2+} were perfused with supramaximal CCK (1 nM) or TLCS (500 µM) to induce sustained elevation of $[Ca^{2+}]_c$ dependent on SOCE (Raraty et al., 2000, Gerasimenko et al., 2013, Muik et al., 2012, Kim et al., 2009). Once a stable plateau in $[Ca^{2+}]_c$ had formed, a range of fixed concentrations (0-100 µM) of GSK-7975A were applied (at 700 s). Increasing concentrations of GSK-7975A lowered the $[Ca^{2+}]_c$ plateau progressively and increasingly rapidly. With CCK, suppression of $[Ca^{2+}]_c$ towards the initial baseline approached >95% using 15 µM GSK-7975A (see **Figure 3.1**), an effect also seen when cells were maintained in 1.8 mM external Ca^{2+} (see **Figure 3.2**); with TLCS, suppression to baseline was ~80% using 30 µM GSK-7975A (see **Figure 3.3**). With CCK and TLCS, GSK-7975A at 100 µM but not 50 µM there was loss of effect (see **Figure 3.1 and 3.3**).

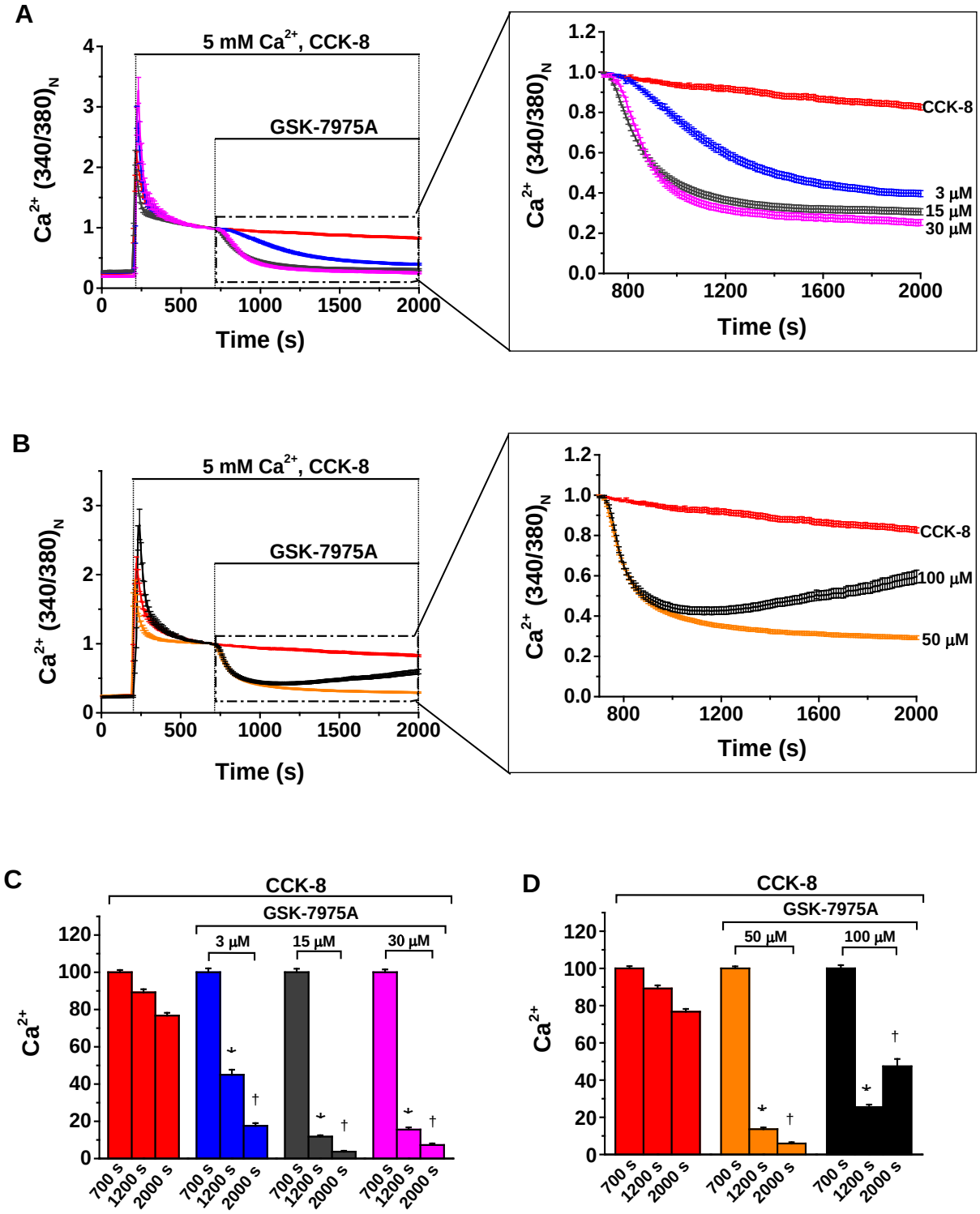

Figure 3.1 Effects of GSK-7975A on the CCK-induced Ca^{2+} plateau in mouse PACs. GSK-7975A concentration-dependently inhibited CRAC entry (Fura-2 340: 380 normalised at 700 s). **(A and B)** Changes in mouse pancreatic acinar $[Ca^{2+}]_c$ induced by 1 nM CCK, showing effects of GSK-7975A from 700 s, expanded. **(C and**

D) Mean (± s.e.m) $[Ca^{2+}]_c$ at 700, 1200 and 2000 s from **(A and B)**, showing progressive reduction with increasing concentration of GSK-7975A, but not 100 µM (≥38 cells/groups; *p<0.001, CCK vs CCK plus GSK-7975A at 1200 s; †p<0.001, at 2000 s). Note: **(A and B)** were analysed by Dr Svetlana Voronina and **(C and D)** were suggested and calculated by myself according to the data from **(A and B).**

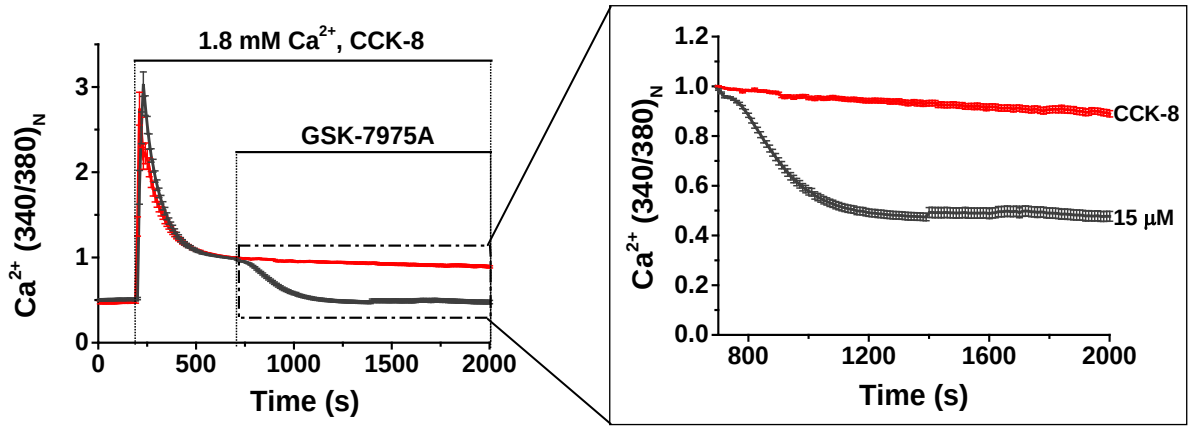

Figure 3.2 Effects of GSK-7975A on the CCK-induced Ca^{2+} plateau maintained in physiological Ca^{2+} concentration in mouse PACs. Changes in mouse pancreatic acinar $[Ca^{2+}]_c$ induced by 1 nM CCK with external physiological $[Ca^{2+}]$ (1.8 mM) applied, showing effect of 15 µM GSK-7975A from 700 s, expanded (≥79 cells/group). Note: this was done by Dr Svetlana Voronina.

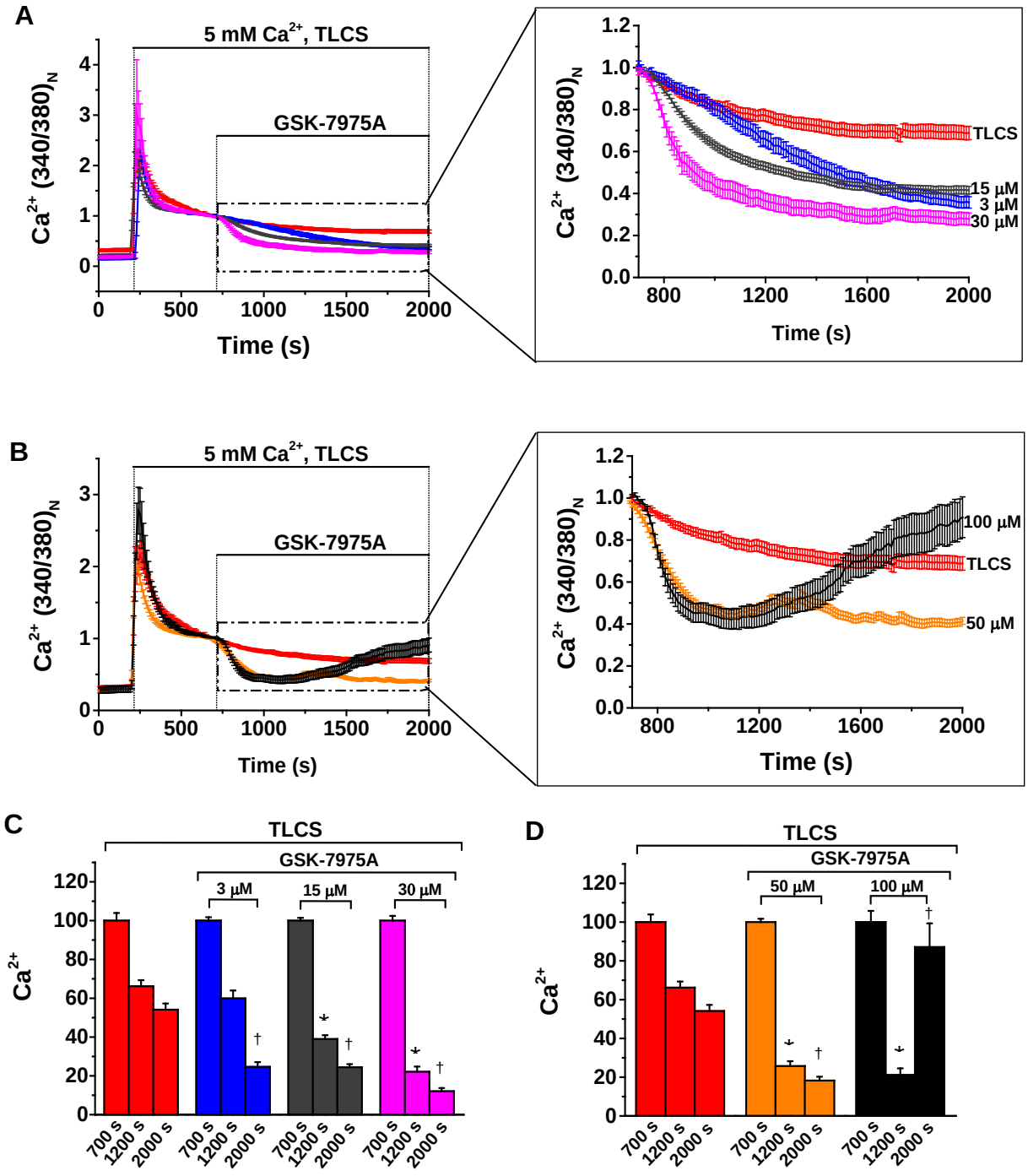

Figure 3.3 Effects of GSK-7975A on the TLCS-induced Ca^{2+} plateau in mouse PACs. GSK-7975A concentration-dependently inhibited CRAC entry (Fura-2 340: 380 normalised at 700 s). **(A and B)** Changes in mouse pancreatic acinar $[Ca^{2+}]_c$ induced by 500 µM TLCS, showing effects of GSK-7975A from 700 s, expanded. **(C and D)** Mean (± s.e.m) $[Ca^{2+}]_c$ at 700, 1200 and 2000 s from **(A and B)**, showing

progressive reduction with increasing concentration of GSK-7975A, but not 100 µM (≥19 cells/groups; *p<0.001, CCK vs CCK plus GSK-7975A at 1200 s; †p<0.001, at 2000 s). Note: **(A and B)** were analysed by Dr Svetlana Voronina and **(C and D)** were suggested and calculated by myself according to the data from **(A and B).**

3.3.2 Effects of GSK-7975A on store-operated Ca^{2+} entry in human PACs

Potential translation applications of SOCE inhibition as a treatment for clinical acute pancreatitis were evaluated by examination of the effects of GSK-7975A on isolated human pancreatic acinar cells (Murphy et al., 2008). Thapsigargin was used in zero external Ca^{2+} to empty Ca^{2+} stores, stimulate STIM-mediated Orai pore formation, and permit SOCE by the reintroduction of external Ca^{2+}. GSK-7975A (10-50 μM) significantly inhibited SOCE in these cells (see **Figure 3.4**).

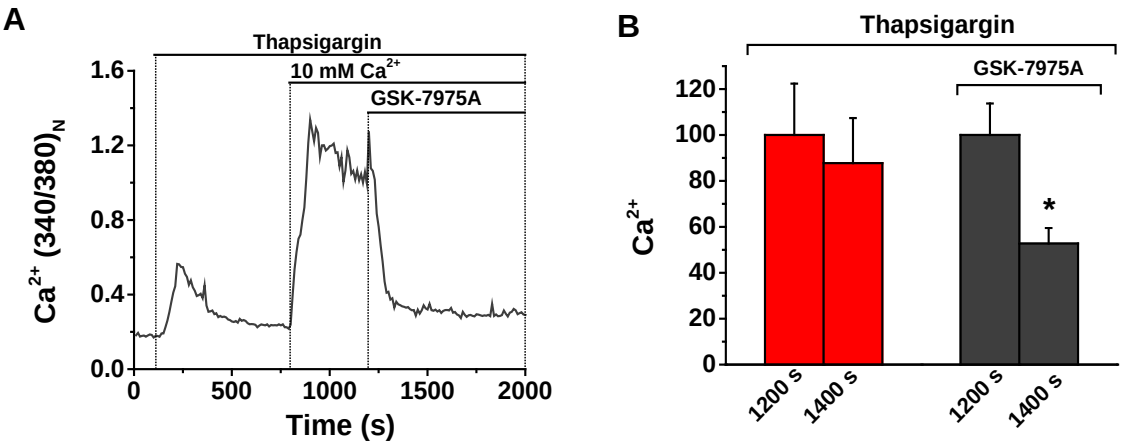

Figure 3.4 Effects of GSK-7975A on thapsigargin-induced Ca^{2+} entry in human PACs. (A) Typical trace showing inhibitory effect of GSK-7975A (50 µM) on thapsigargin-induced Ca^{2+} influx. **(B)** Mean (± s.e.m.) $[Ca^{2+}]_c$ at 1200 s and 1400 s from thapsigargin and thapsigargin plus GSK-7975A traces, showing marked reduction with GSK-7975A (≥20 cells/group; *p<0.001, thapsigargin vs thapsigargin plus GSK-7975A at 1400 s). Note: **(A)** were analysed by Dr Svetlana Voronina and **(B)** were suggested and calculated by myself according to the data from **(A).**

3.3.3 Effects of GSK-7975A on necrotic cell death pathway activation in mouse and human PACs

The percentage of PI uptake indicated necrotic cell death pathway activation; nuclei stained with Hoechst 33342 showed the total number of cells. GSK-7975A at 10 µM protected mouse PACs from necrotic cell death pathway activation induced by TLCS (500 µM), which induces acute pancreatitis *in vivo* (Laukkarinen et al., 2007, Lerch and Gorelick, 2013); GSK-7975A at 30 µM protected human PACs (See **Figure 3.5**).

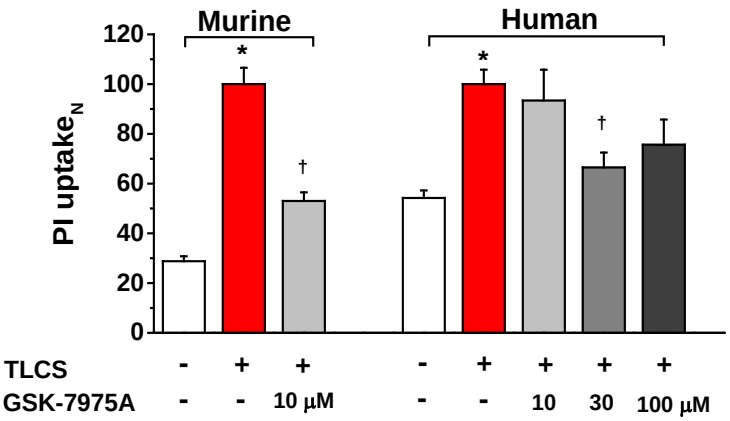

Figure 3.5 Effects of GSK-7975A on necrotic cell death pathway activation in human PACs. The percentage of PI uptake indicated necrotic cell death pathway activation; nuclei stained with Hochest 3342 showed the total number of cells. Treatment of GSK-7975A protected both mouse and human PACs from necrotic cell death pathway activation induced by TLCS (500 μM) (mean± s.e.m., normalised to TLCS at 100;≥3 experiments/group; *p<0.05, control vs TLCS; †p<0.05, TLCS vs TLCS plus GSK-7975A).

3.3.4 Effects of CM_128 on store-operated Ca^{2+} entry in mouse PACs

To determine the effect of CM_128 on SOCE in isolated mouse PACs, thapsigargin was used to empty Ca^{2+} stores and initiate STIM-mediated Orai pore formation, while maintaining cells in zero external Ca^{2+} until Ca^{2+} was reintroduced to enable SOCE (Raraty et al., 2000, Gerasimenko et al., 2013). Application of this protocol demonstrated that CM_128 markedly reduced SOCE, at a lower dose (1 µM; see **Figure 3.6**).

The effect of CM_128 on SOCE and its concentration-dependency was confirmed by a separate experimental protocol (Wen et al., 2015). Cyclopiazonic acid was used to empty Ca^{2+} stores within mouse PACs (Kim et al., 2009) (maintained in zero external Ca^{2+}) to stimulate STIM-mediated Orai opening. Upon reintroduction of external Ca^{2+} (1.8 mM), the rate of Ca^{2+} entry demonstrated concentration-dependent log proportionality, with IC_{50} ~0.7 µM and a complete inhibition at 10 µM; there was no loss of effect at higher concentrations (Wen et al., 2015).

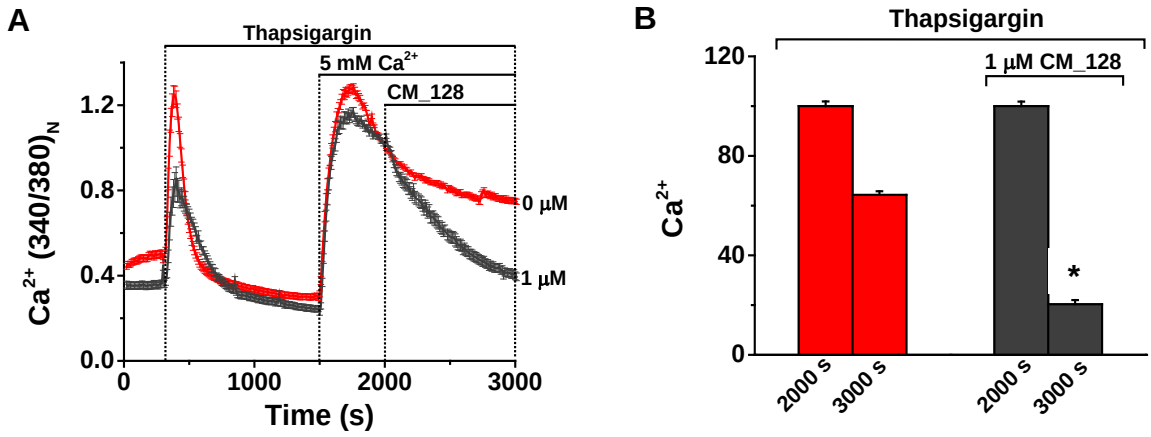

Figure 3.6 Effects of CM_128 on thapsigargin-induced Ca^{2+} entry in mouse PACs. (A) Changes in mouse pancreatic acinar $[Ca^{2+}]_c$ induced by thapsigargin (Fura-2 340:380 normalised at 2000 s), showing effect of 1 µM CM_128. **(B)** Mean (± s.e.m) $[Ca^{2+}]_c$ at 2000 s and 3000 s from **(A)**, showing marked reduction with 1 µM CM_128 (≥62 cells/group; *p<0.001, thapsigargin vs thapsigargin plus CM_128 at 3000 s). Note: **(A)** were analysed by Dr Michael Chvanov and **(B)** were suggested and calculated by myself according to the data from **(A).**

3.3.5 Effects of CM_128 on store-operated Ca^{2+} entry in human PACs

Potential translation applications of SOCE inhibition as a treatment for clinical acute pancreatitis were evaluated by examination of the effects of CM_128 on isolated human PACs (Murphy et al., 2008). Thapsigargin was used in zero external Ca^{2+} to empty Ca^{2+}, stimulate STIM-mediated Orai pore formation, and permit SOCE by the reintroduction of external Ca^{2+}. CM_128 inhibited SOCE in human PACs at low concentrations (1 µM; see **Figure 3.7**).

The inhibitory effect of CM_128 on human Orai1 was also verified using transfected HEK293 cells (Wen et al., 2015). HEK293 cells transfected with Orai1/STIM1 (Derler et al., 2013) were patched in zero extracelluar Ca^{2+} to measure ICRAC in response to extracellular addition of 10 mM Ca^{2+}, and the effect of a range of concentrations of CM_128 tested. CM_128 inhibited I_{CRAC} in a direct concentration-dependent manner, with IC_{50} ~0.1 µM and a complete inhibition at 1 µM; there was no loss of effect at higher concentrations (Wen et al., 2015).

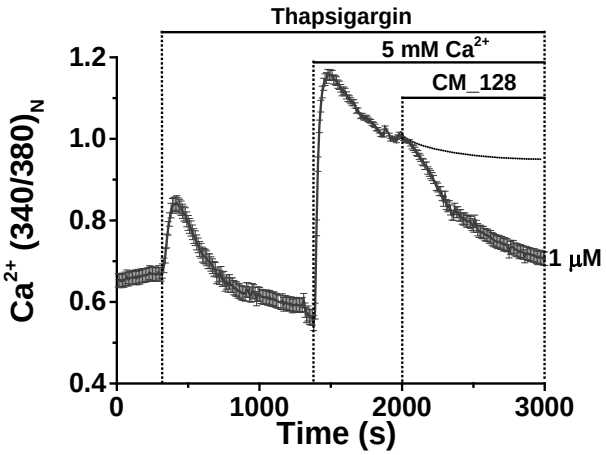

Figure 3.7 Effects of CM_128 on thapsigargin-induced Ca^{2+} entry in human PACs. Changes in human pancreatic acinar $[Ca^{2+}]_c$ induced by thapsigargin (Fura-2 340:380 normalised at 2000 s), showing inhibitory effect of 1 μM CM_128 (68 cells). Dash line was drawing to indicate the $[Ca^{2+}]_c$ in control human PACs as a reference line to compare with the inhibitory effects of CM_128.

3.3.6 Effects of CM_128 on necrotic cell death pathway activation in mouse and human PACs

The percentage of PI uptake indicated necrotic cell death pathway activation, nuclei stained with Hoechst 3342 showed the total number of cells. CM_128 at 1 µM protected both mouse and human PACs from necrotic cell death pathway activation induced by TLCS (500 µM; see **Figure 3.8**).

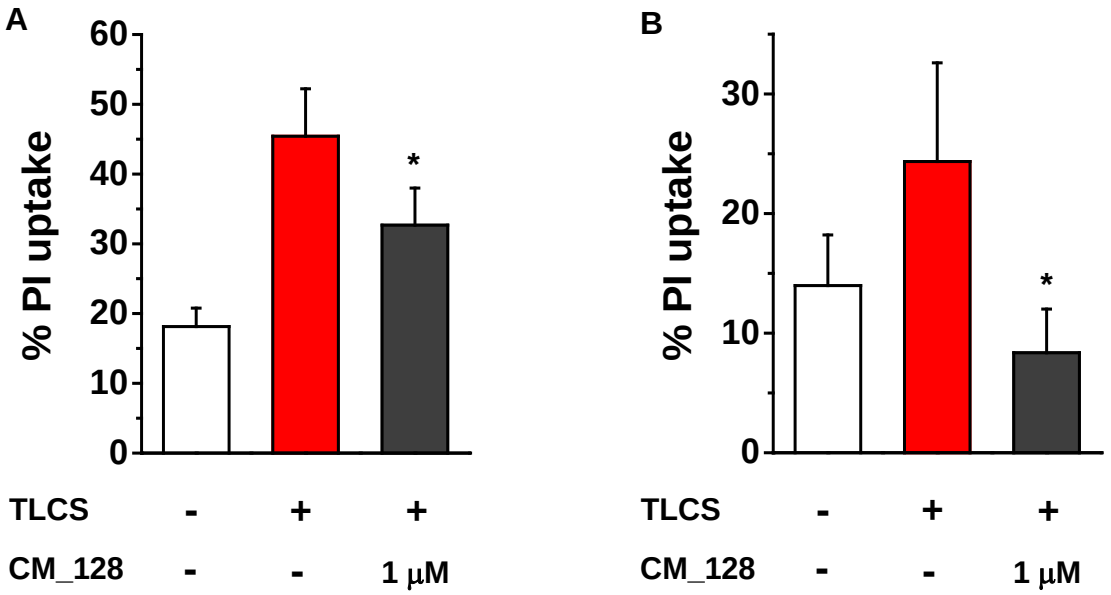

Figure 3.8 Effects of CM_128 on necrotic cell death pathway activation in mouse and human PACs. CM_128 protected isolated **(A)** mouse and **(B)** human PACs from necrotic cell death pathway activation induced by TLCS (500 μM) (mean ± s.e.m.; ≥3 experiments/group in mouse; 1 experiment/group (4 wells and 16 high power fields each, total 172 control cells, 97 TLCS, 110 TLCS and CM_128) in human; *p<0.05, TLCS vs TLCS plus CM_128).

3.4 Discussion

GSK-7975A was found to inhibit CCK-, TLCS- and thapsigargin-induced SOCE in mouse PACs in a concentration-dependent manner, exceeding >90% block of relative control values in some protocols. These findings are consistent with published data, showing the effects of GSK-7975A on SOCE in mouse PACs (Gerasimenko et al., 2013, Voronina et al., 2015). The same inhibitory effect on the Ca^{2+} plateau was observed when PACs were maintained in physiological external Ca^{2+} concentrations, which mimics physiological conditions around PACs. GSK-7975A at 100 µM showed a loss of inhibitory effect, resulting in an increase of $[Ca^{2+}]_c$ by an unknown mechanism. CM_128 (0.1- 10 µM) was found to inhibit thapsigargin- and cyclopiazonic acid-induced SOCE in mouse PACs, showing higher potency with IC_{50} ~0.7 µM, and unlike GSK-7975A, no loss of efficacy at higher concentrations.

Pancreatic necrosis is one determinant of severity in patients with AP (Petrov et al., 2010). The extent of necrosis is related to severity in experimental AP (Kaiser et al., 1995). The study reported in this chapter demonstrates GSK-7975A (10-30 µM) and CM_128 (1 µM) significantly reduce necrotic cell death pathway activation in mouse and human PACs exposed to TLCS, which induces AP *in vivo* (Laukkarinen et al., 2007) and is related to clinical gallstone AP (Pandol et al., 2007, Lerch and Gorelick, 2013).

GSK-7975A at various concentrations (10-100 µM) and CM_128 at a lower concentration (1 µM) showed similarly critical effects on thapsigargin-induced SOCE and necrotic cell death pathway activation in human PACs. The data here suggest the translational potential of Orai inhibitors as the treatment of clinical AP. CM_128

with higher potency inhibited I_{CRAC} in recombinant hOrai1/hSTIM1 HEK 293 cells in a concentration-dependent manner with an IC_{50} ~0.1 µM. Moreover, CM2489, a closely related analogue of CM_128 has been tested in a Phase I clinical trial for the treatment of moderate-to-severe plaque psoriasis and CM2489 has been shown to be safe and well-tolorated (www.calcimedica.com). All these data suggest further development of Orai inhibitors as a treatment for AP in man.

3.5 Summary

In this chapter, the data demonstrated that GSK-7975A significantly inhibited CCK- and TLCS-induced SOCE in mouse PACs in a concentration dependent manner. CM_128 significantly inhibited thapsigargin- and cyclopiazonic acid-induced Ca^{2+} influx in mouse pancreatic acinar cells in a concentration dependent manner. Both GSK-7975A and CM_128 inhibited thapsigargin-induced Ca^{2+} influx in human PACs and protected both mouse and human PACs from necrotic cell death pathway activation. Furthermore, CM_128 concentration-dependently inhibited I_{CRAC} current in hOrai1/hSTIM1 HEK 293 cells; unlike GSK-7975A, no loss of efficacy at high concentration. There are no published data of both compounds evaluated in the *in vivo* setting of AP.

Results: Chapter 4

Effects of GSK-7975A given as prodrug GSK-6288B in experimental acute pancreatitis

4.1 Introduction

In the previous chapter (Chapter 3), we have demonstrated GSK-7975A inhibited TLCS-, CCK- and thapsigargin-induced SOCE and protested against TLCS-induced necrotic cell death pathway activation in mouse and human PACs. The inhibitory effects on SOCE was concentration-dependent over the range from 3-100 μM, with increasing concentrations of GSK-7975A showing increasing reduction of Ca^{2+} entry, but not at 100 μM, which showed a loss of effect. Others also demonstrated inhibition of Orai channels by GSK-7975A protected against CCK- and POAEE-induced necrotic cell death pathway activation. However, the role of Orai channels in experimental AP *in vivo* has not yet been determined.

Genetic knockout of TRPC3 channel (Kim et al., 2009), a non-selective cation channel regulated in part by STIM1 via TRPC1 (Lee et al., 2014), resulted in ~50% reduction of *in vivo* serum amylase elevation and oedema formation induced by four hourly injections of caerulein. These experiments supported some role for SOCE in AP, but in a single, mild AP model with few parameters evaluated of disease severity.

The study described in this chapter was designed to investigate the effects of GSK-7975A on experimental AP *in vivo*. Due to the modest aqueous solubility of GSK-7975A, we used a phosphate pro-drug (GSK-6288B) that is rapidly cleaved *in vivo* to liberate GSK-7975A. As there are no preliminary pharmacokinetic data on GSK-7975A and GSK-6288B, a pharmacokinetic study against a background of AP was conducted prior to the assessment of drug efficacy.

4.2 Methods

4.2.1 Measurement of GSK-7975A *in vivo*

Sampling was at 1, 2, 4, 10 and 22 h after subcutaneous osmotic minipump insertion from three mice/time point. Immediately following humane killing, blood was collected into a heparinised tube and diluted 1:1 with sterile water; the pancreas was removed and homogenized in 2 ml Covaris tubes containing ceramic beads. Standards and study samples (50 µl from blood and 100 µl from pancreas) were extracted by protein precipitation and centrifuged. Supernatants were dried under heated nitrogen (40°C). Levels of GSK-7975A and GSK-6288B were determined by liquid chromatography mass spectrometry (LC-MS/MS; API4000 with Jasco X-LC and Ascentis express C18 column). Samples were prepared by me and measurement by LC-MS/MS was undertaken by GSK.

4.2.2 Protein binding of GSK-7975A

The protein binding of GSK-7975A in the blood and pancreas was determined at 1 µg/ml using a dialysis Teflon block with dialysis membrane strips and a rapid equilibrium dialysis (RED) device (Thermo Scientific) respectively. Blood was collected into a heparin pre-coated tube, diluted 1:1 with phosphate buffer saline (PBS, pH 7.4). Pancreas was homogenised in 500 µl PBS, diluted 1:10. Blood and pancreas homogenates were dialyzed against PBS in a buffer chamber, shaking gently at 37°C for 5 h (blood) and 4 h (pancreas homogenate). After equilibrium, samples from both sample chamber and buffer chamber were collected in a matrix-match manner and analyzed by liquid chromatography mass spectrometry (LC-MS/MS; AP14000, Applied Biosystems). Experiments were carried out in triplicate. The percentage of GSK-7975A bound was calculated by the equation: % bound= ([GSK-7975A]a- [GSK-7975A]b)/ [GSK-7975A]a ×100%, where [GSK-7975A]a was

the concentration of GSK-7975A in the sample chamber and [GSK-7975A]b was the concentration of GSK-7975A in the buffer chamber. Samples were prepared by me and measurement by LC-MS/MS was undertaken by GSK.

4.2.3 Induction of experimental AP

Experimental AP (CER-AP, TLCS-AP and FAEE-AP) was induced as previously described in 2.5.

4.2.4 Administration of GSK-7975A

Low (L, 28 mg/kg/h) and high (H, 110 mg/kg/h) doses of GSK-7975A were given as prodrug GSK-6288B subcutaneously by osmotic mini-pump implantation after disease induction; this was undertaken at the third injection of caerulein, 30 min after TLCS-AP induction or 1 h after FAEE-AP induction. Minipump preparation and implantation was as described in 2.6.

4.2.5 Assessment of experimental AP severity

Standard biochemical parameters and blind histopathology were used, as previously described in 2.7.

4.3 Results

4.3.1 Pharmacokinetic study of GSK-7975A

To ensure consistent delivery of GSK-7975A, levels of GSK-7975A in the blood and pancreas were measured at various time points after osmotic mini-pump insertion against a CER-AP background. Blood and pancreatic levels of GSK-7975A reached steady state within 4 h at all tested (see **Figure 4.1**). GSK-7975A at the low and high

doses achieved steady state blood concentrations of ~4.3 µM and ~13.3 µM and pancreatic concentrations of ~8.9 µM and 49.3 µM respectively, with no detectable prodrug GSK-6288B at all doses and time points.

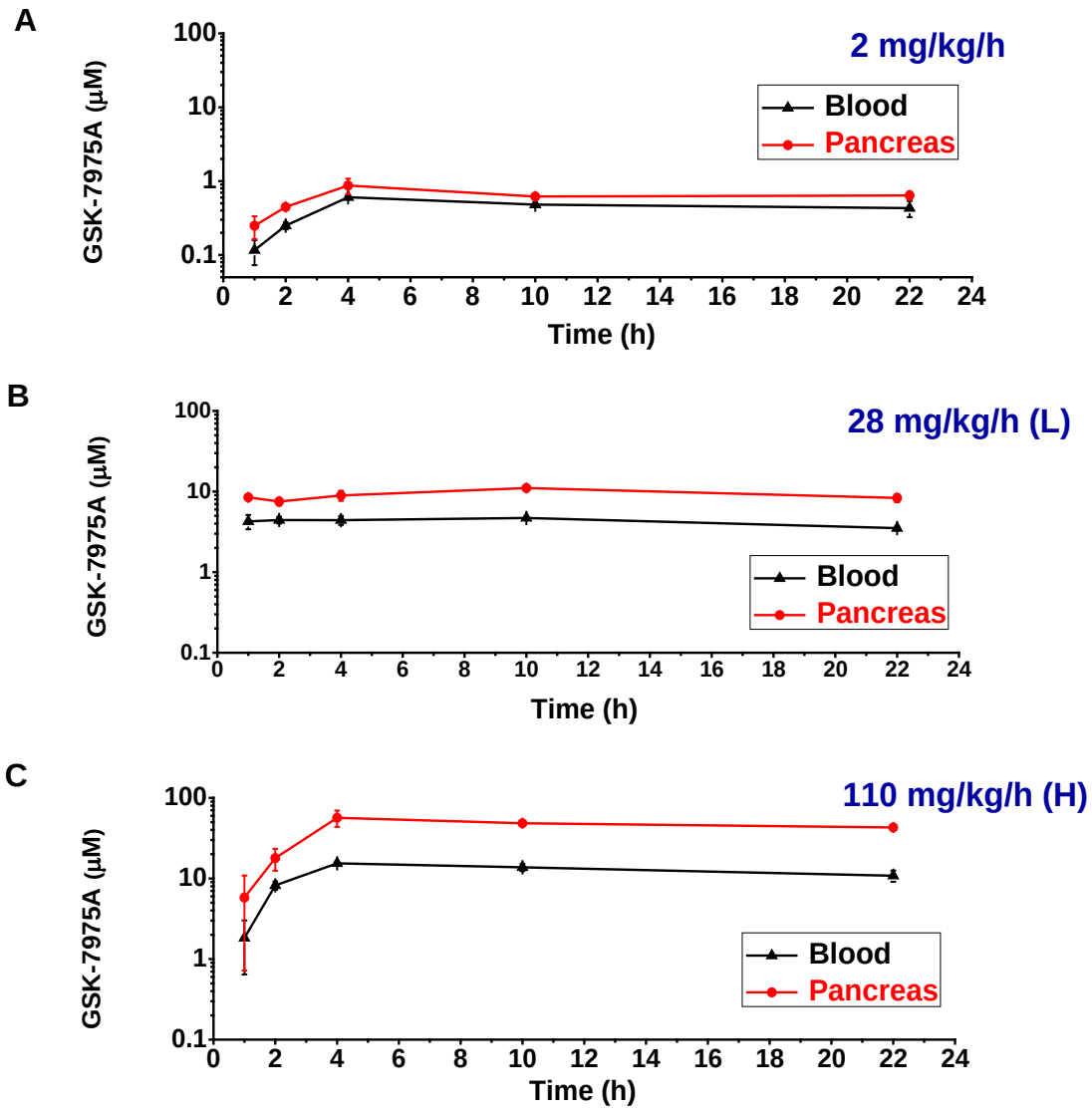

Figure 4.1 Blood and pancreatic levels of GSK-7975A. GSK-7975A given as prodrug GSK-6288B administered subcutaneously by osmotic mini-pump was consistently delivered to each mouse and maintained throughout the experimental period. There was no detectable GSK-6288B in the blood or pancreas, suggesting complete conversion into GSK-7975A. **(A)** Blood and pancreas levels of GSK-7975A

following administration of 2 mg/kg/h GSK-6288B showed a steady state 4 h after minipump implantation, when the mean concentrations in blood and pancreas were ~0.4 µM and ~0.6 µM respectively. **(B)** Blood and pancreas levels of GSK-7975A at the (lower) dose of 28 mg/kg/h GSK-6288B (L) reached a steady state 1 h after mini-pump implantation, when the mean concentrations in blood and pancreas were ~5 µM and ~10 µM respectively. **(C)** Blood and pancreas levels of GSK-7975A at the (higher) dose of 110 mg/kg/h GSK-6288B (H) reached a steady state 4 h after mini-pump implantation, when the mean concentrations in blood and pancreas were ~15 µM and ~50 µM respectively. Note: the raw data were provided by GSK and the calculation and graphs were made by me.

4.3.2 Protein binding of GSK-7975A in the blood and pancreas

To better understand the relationship between *in vivo* drug levels and pharmacological effects, bound and free fractions of GSK-7975A were measured in the blood and pancreas. GSK-7975A showed high protein binding, with >95% bound fraction in the blood and pancreas across species.

	Conc. (μg/ml)	**% Bound fraction**			**% Free fraction**		
		Blood		Pancreas	Blood		Pancreas
		Murine	Human	Murine	Murine	Human	Murine
GSK-7975A	1	96.8	97.5	96.5	3.2	2.5	3.5

Table 4.1 Binding fractions of GSK-7975A to murine/human blood and pancreas. Note: the raw data were provided by GSK and the table was made by myself.

4.3.3 Effects of GSK-7975A on disease severity in CER-AP

To evaluate the protective effects of GSK-7975A *in vivo*, hyperstimulation AP (CER-AP) was studied first since it is the most widely used, well-established and is an easily reproducible experimental AP model (Lerch and Gorelick, 2013). GSK-7975A administered subcutaneously at the third injection of caerulein significantly reduced all local (see **Figure 4.2**) and systemic biochemical parameters (see **Figure 4.3**), with more pronounced reduction at the high dose (110 mg/kg/h) ($p<0.05$). Similar significant improvements were observed in pancreatic histopathology with the high dose approaching control levels (see **Figure 4.4** and **Figure 4.5**).

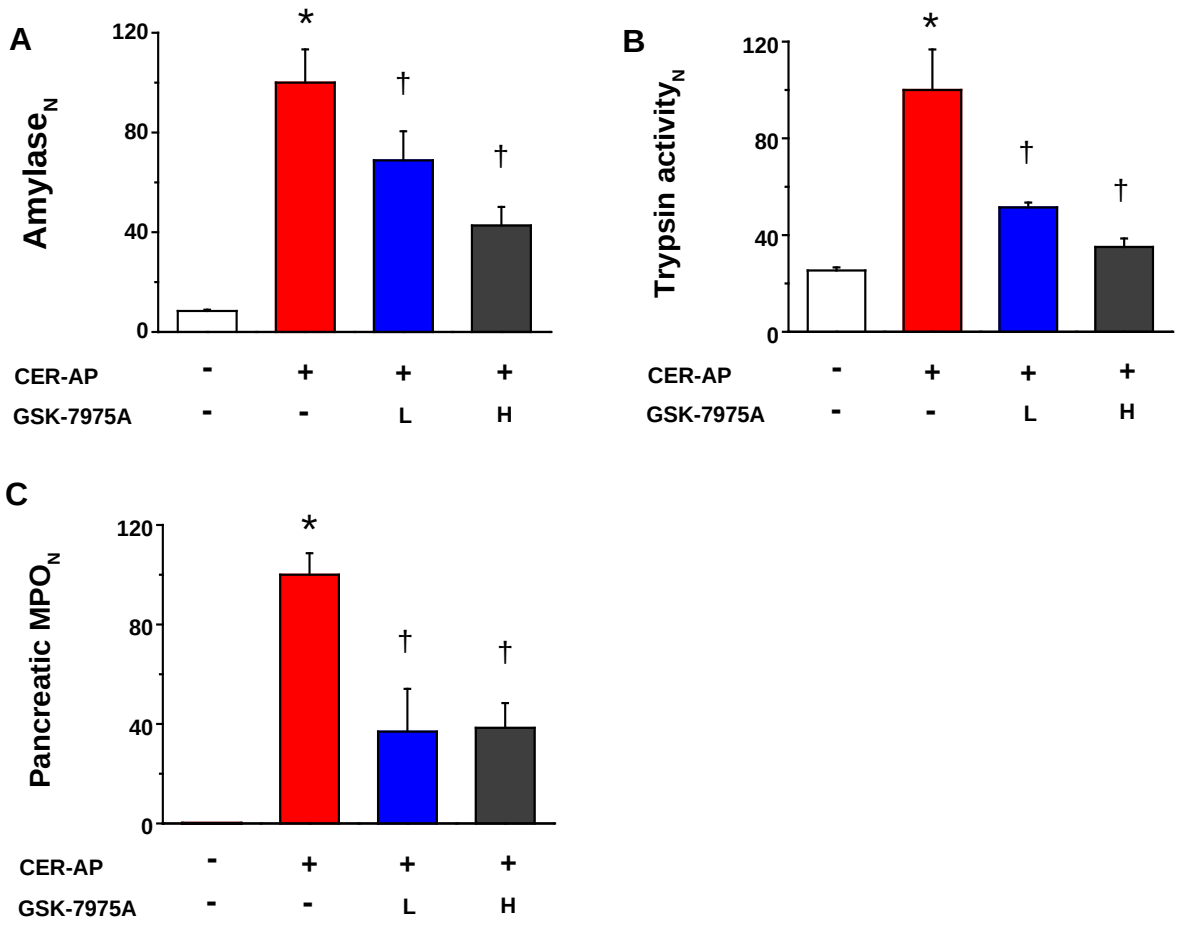

Figure 4.2 Effects of GSK-7975A on pancreatic parameters in CER-AP. CER-AP resulted in substantial elevation of **(A)** serum amylase, **(B)** pancreatic trypsin activity and **(C)** pancreatic myeloperoxidase (MPO) activity. Subcutaneous administration of GSK-7975A given as prodrug GSK-6288B at the low (L) and high (H) doses significantly reduced all parameters, with more marked reduction of serum amylase and pancreatic trypsin activity at the high dose. Data were normalised to CER-AP at 100, N suffix indicating normalisation applied for each parameter (mean ± s.e.m., ≥6 mice/group; *p<0.05, control vs CER-AP; †p<0.05 CER-AP vs CER-AP plus GSK-7975A).

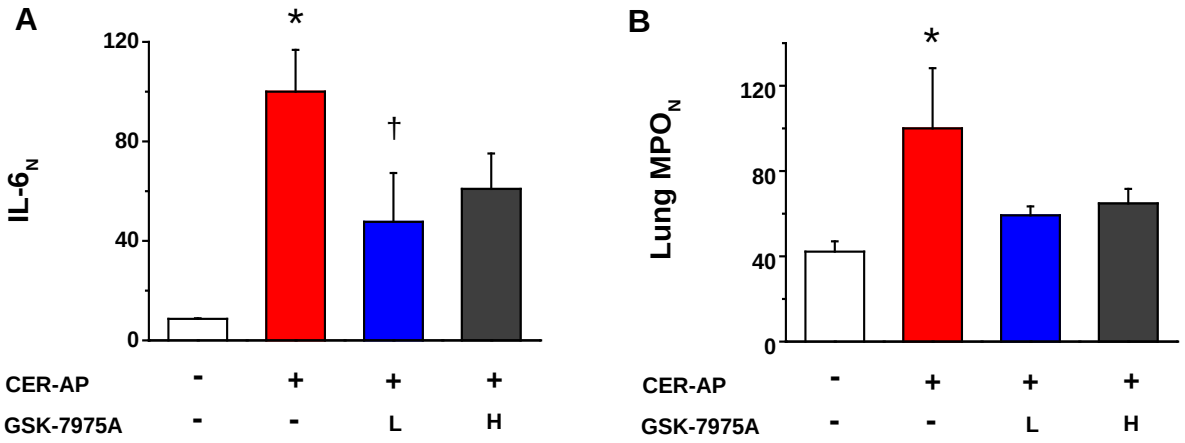

Figure 4.3 Effects of GSK-7975A on systemic biochemical parameters. CER-AP resulted in substantial elevation of **(A)** IL-6 and **(B)** lung myeloperoxidase (MPO) activity. Subcutaneous administration of GSK-7975A given as prodrug GSK-6288B at the low (L) and high (H) doses significantly reduced IL-6 at the low dose, but not at the high dose and neither doses significantly reduced lung MPO activity. Data were normalised to CER-AP at 100, N suffix indicating normalisation applied for each parameter (mean ± s.e.m., ≥6 mice/group; *p<0.05, control vs CER-AP; †p<0.05 CER-AP vs CER-AP plus GSK-7975A).

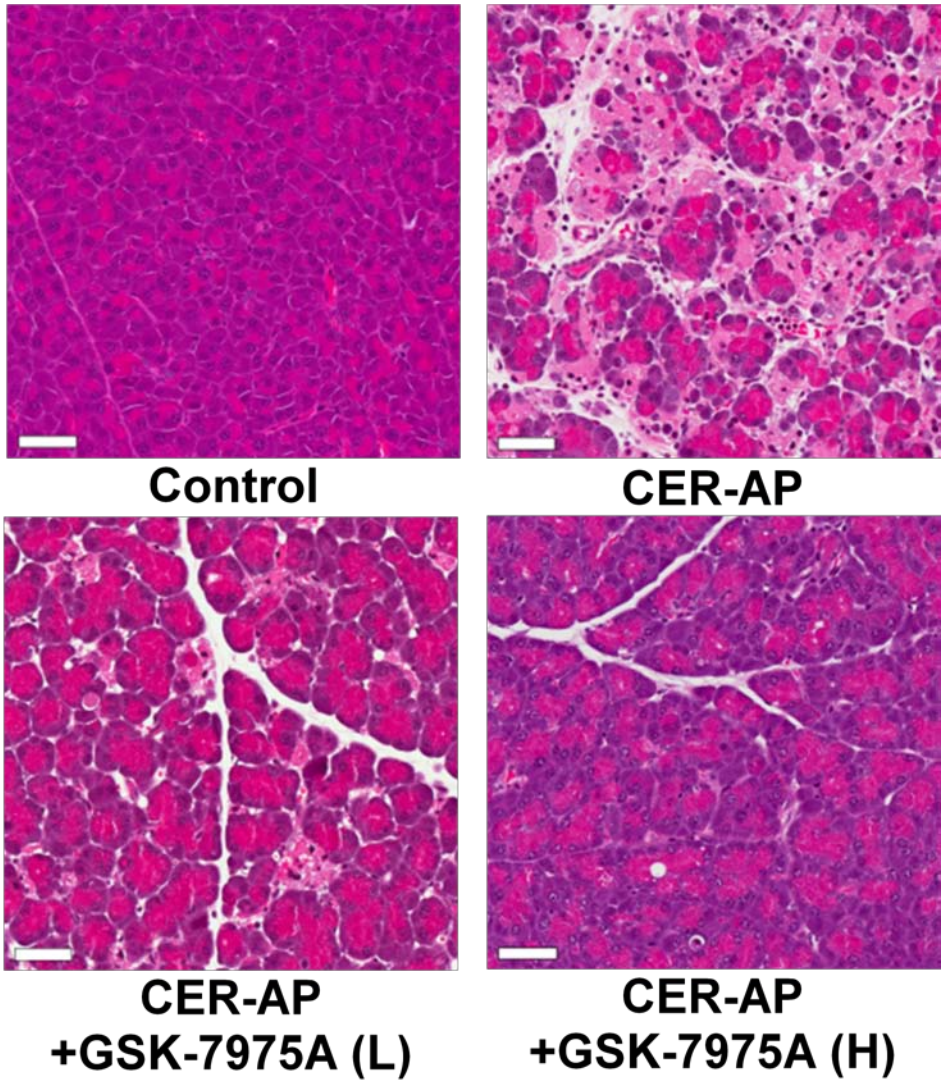

Figure 4.4 Typical histopathology from CER-AP. Representative histological images showing normal pancreatic histology, typical histopathology from CER-AP and typical histopathology from CER-AP after treatment with GSK-7975A at the low (L) and high (H) doses (H&E, Haematoxylin and Eosin; scale bar= 50 µM).

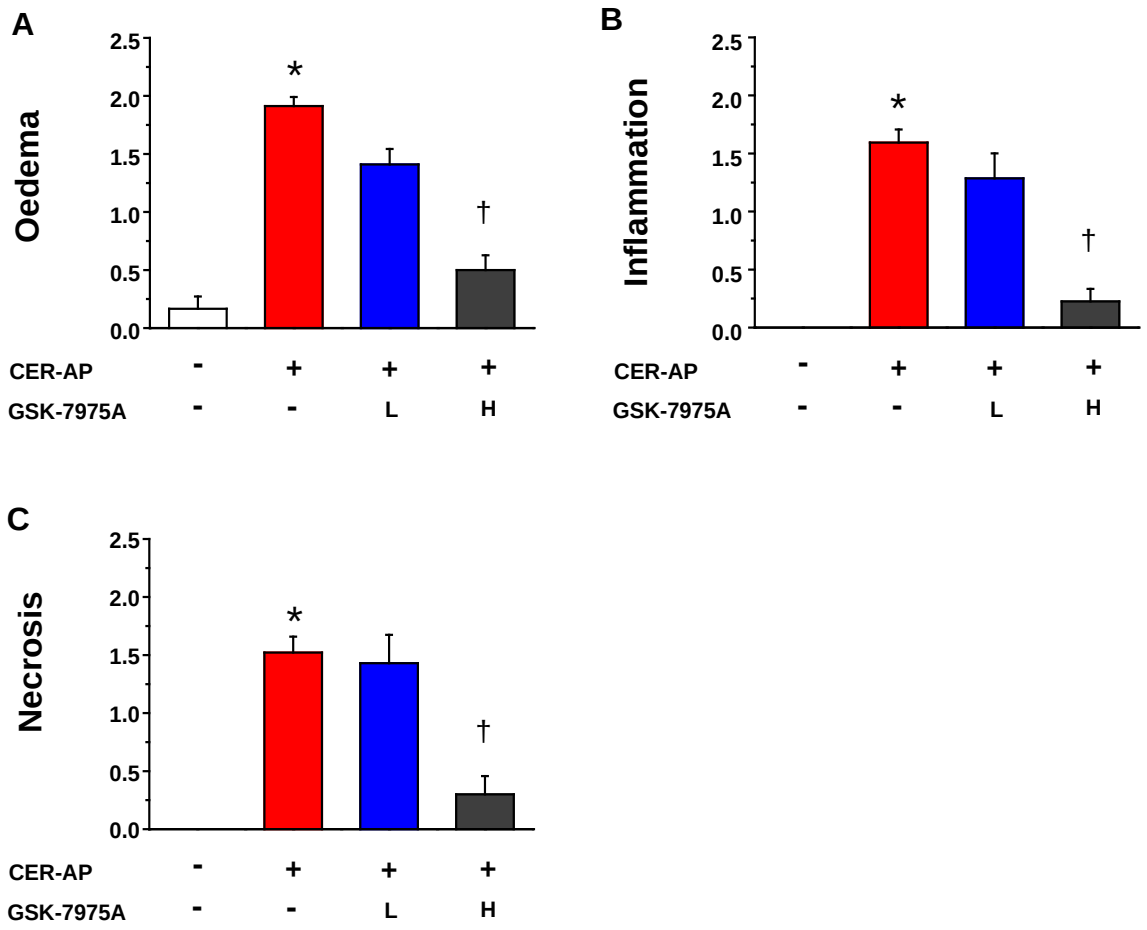

Figure 4.5 Histopathological scores from CER-AP. CER-AP results in substantial increase in **(A)** oedema, **(B)** inflammation and **(C)** necrosis. Subcutaneous administration of GSK-7975A given as prodrug GSK-6288B at the high (H) dose significantly reduced pancreatic damage, approaching control levels (mean ± s.e.m., ≥6 mice/group; *p<0.05, control vs CER-AP; †p<0.05 CER-AP vs CER-AP plus GSK-7975A).

4.3.4 Effects of GSK-7975A on disease severity in two clinical representative models.

To fully investigate potential clinical significance using murine models, the effects of GSK-7975A were studied in TLCS-AP and FAEE-AP, which mimic biliary and alcoholic AP respectively. GSK-7975A administered subcutaneously 30 min after TLCS-AP induction and 1 h after FAEE-AP significantly reduced all pancreatic (see **Figure 4.6**) and systemic biochemical parameters (see **Figure 4.7**), with more pronounced reduction at the high dose in serum amylase, pancreatic trypsin activity and IL-6 ($p<0.05$). Similar significant improvements were observed in pancreatic histopathology, with the high dose showing more marked reduction (see **Figure 4.8** and **Figure 4.9**).

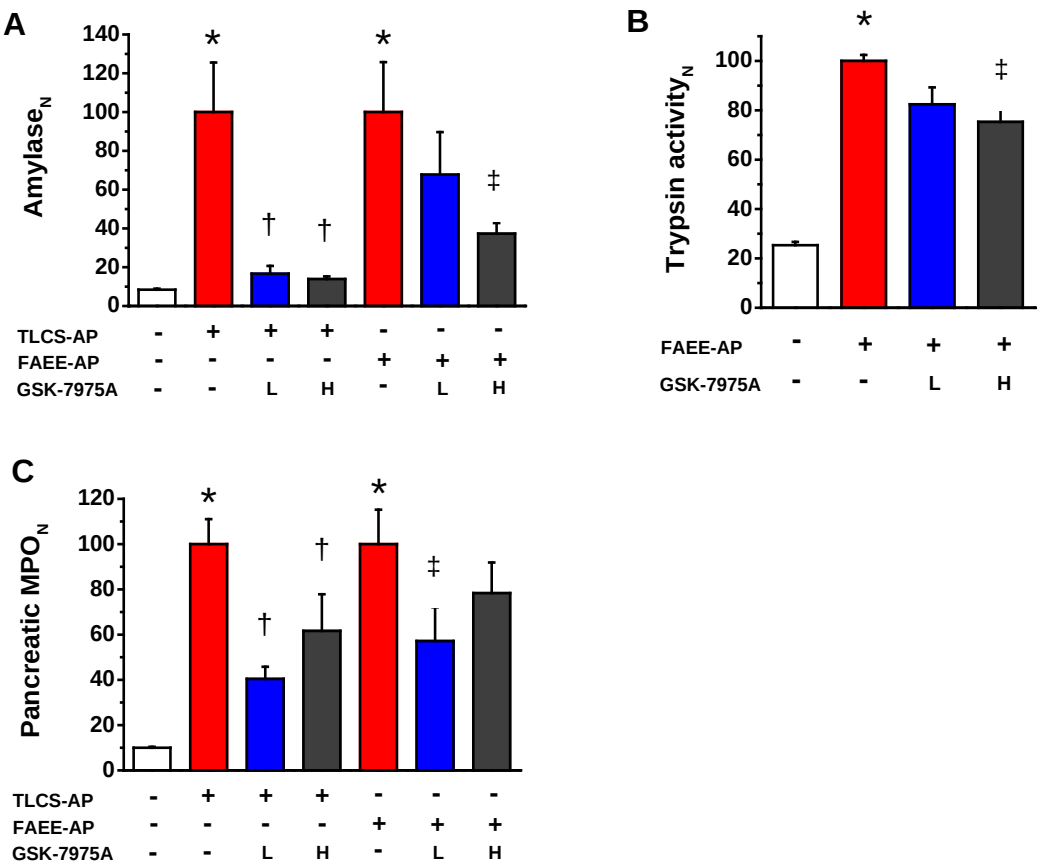

Figure 4.6 Effects of GSK-7975A on pancreatic parameters in TLCS-AP and FAEE-AP. Two models resulted in substantial elevation of **(A)** serum amylase, **(B)** pancreatic trypsin activity and **(C)** pancreatic myeloperoxidase (MPO) activity. Subcutaneous administration of GSK-7975A given as pro-drug GSK-6288B at either low (L) or high (H) doses significantly reduced all parameters, with more marked reduction of serum amylase and pancreatic trypsin activity at the high dose. Data were normalised to TLCS-AP or FAEE-AP at 100, N suffix indicating normalisation applied for each parameter (mean ± s.e.m., ≥6 mice/group; *p<0.05, control vs two models; †p<0.05, TLCS-AP vs TLCS-AP plus GSK-7975A; ‡p<0.05, FAEE-AP vs FAEE-AP plus GSK-7975A).

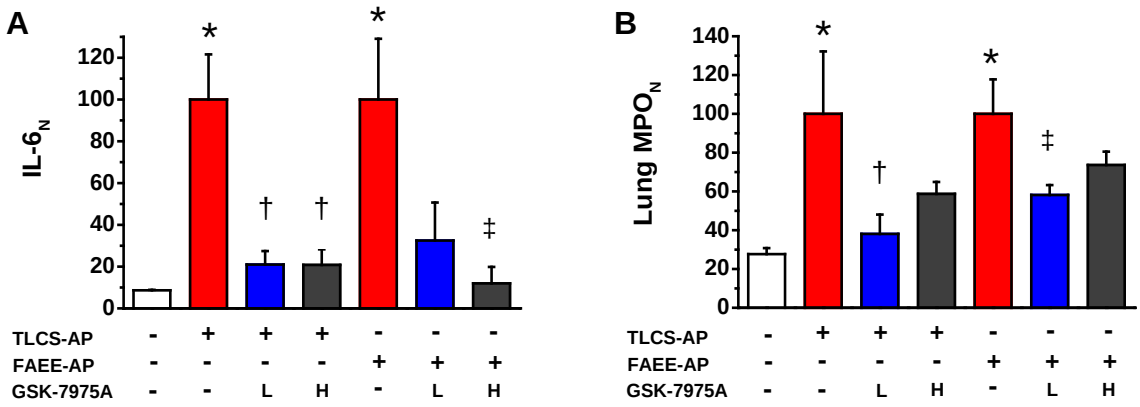

Figure 4.7 Effects of GSK-7975A on systemic biochemical parameters in TLCS-AP and FAEE-AP. Two models resulted in substantial elevation of **(A)** IL-6 and **(B)** lung myeloperoxidase (MPO) activity. Subcutaneous administration of GSK-7975A given as pro-drug GSK-6288B at the low (L) and high (H) doses significantly reduced all parameters, with more marked reduction of lung MPO activity at the low dose. Data were normalised to TLCS-AP or FAEE-AP at 100, N suffix indicating normalisation applied for each parameter (mean ± s.e.m., ≥6 mice/group; *p<0.05, control vs two models; †p<0.05, TLCS-AP vs TLCS-AP plus GSK-7975A; ‡p<0.05, FAEE-AP vs FAEE-AP plus GSK-7975A).

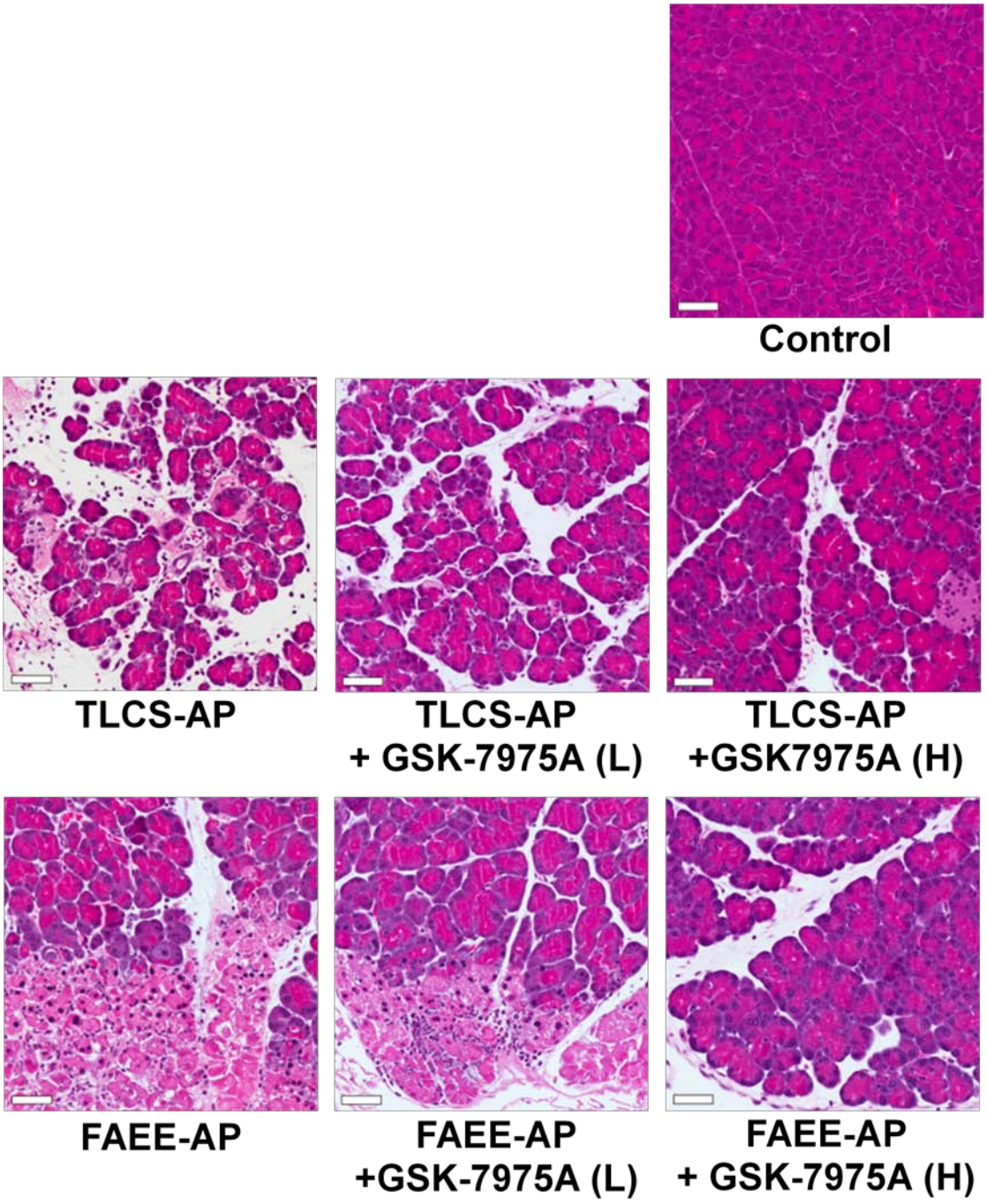

Figure 4.8 Typical histopathology from TLCS-AP and FAEE-AP. Representative histological images showing normal pancreatic histology, typical histopathology from two models and typical histopathology from two models after treatment with GSK-7975A at low (L) and high (H) doses (H&E, Haematoxylin and Eosin; scale bar= 50 µM)

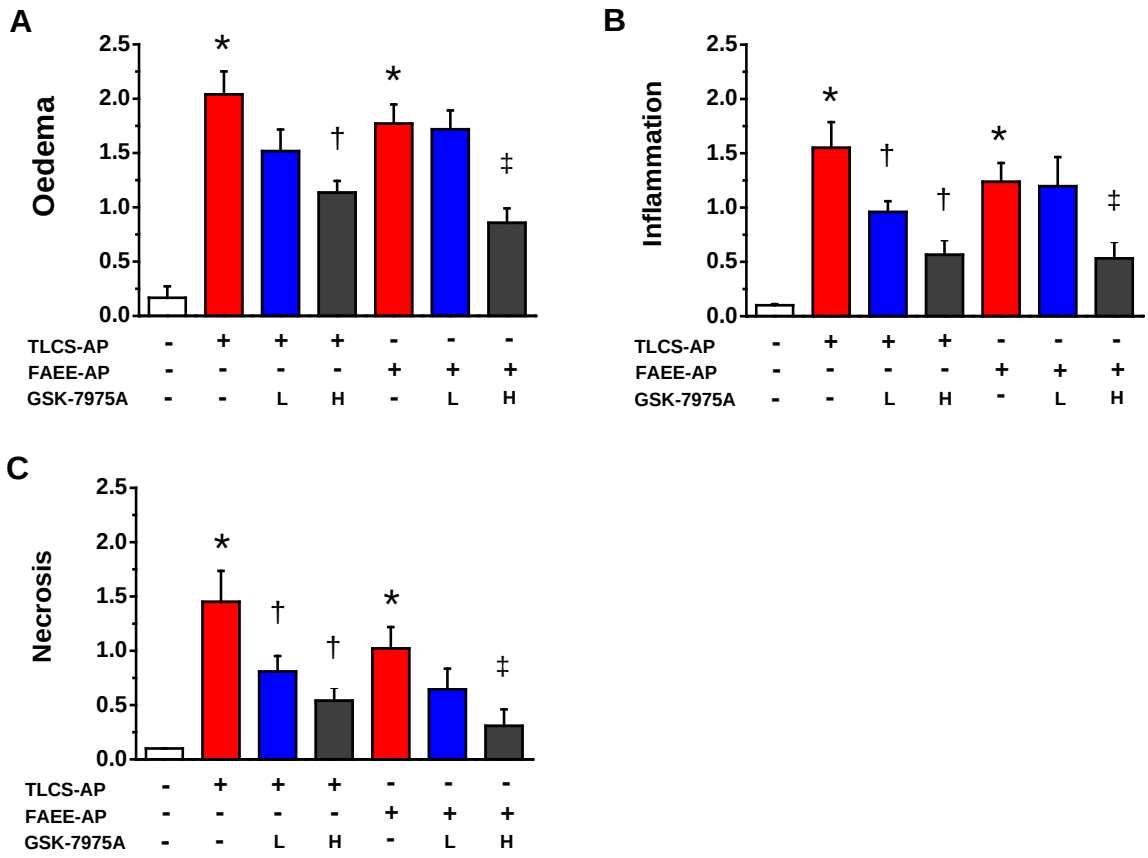

Figure 4.9 Histopathological scores from TLCS-AP and FAEE-AP. The two models resulted in substantial increases in **(A)** oedema, **(B)** inflammation and **(C)** necrosis scores. Subcutaneous administration of GSK-7975A given as pro-drug GSK-6288B at either low (L) or high (H) doses significantly reduced pancreatic damage, with more marked reduction at the high dose (mean ± s.e.m., ≥6 mice/group; *p<0.05, control vs two models; †p<0.05, TLCS-AP vs TLCS-AP plus GSK-7975A; ‡p<0.05, FAEE-AP vs FAEE-AP plus GSK-7975A).

4.4 Discussion

Subcutaneous administration of GSK-7975A at the low and high doses 30-60 min after disease induction was markedly effective across a representative range of local and systemic biochemical, immunological and histological disease responses in three diverse, clinically representative models of AP. In all models, GSK-7975A at the high dose showed more pronounced reduction in pancreatic injury biochemically and histologically. On the other hand, GSK-7975A at the low dose was generally as effective as the high dose in reducing IL-6, which contributes to lung injury and lethality (Zhang et al., 2013), and pancreatic and lung MPO. These data are consistent with the lower IC_{50} of GSK-7975A on Orai channel SOCE in leukocytes (~1 μM for T lymphocytes) (Derler et al., 2013, Rice et al., 2013) compared to that in PACs (3.4 μM) (Gerasimenko et al., 2013).

Measurement of blood and tissue levels of GSK-7975A after induction of experimental AP established an appropriate dosing regimen (110 mg/kg/h via minipump) for maximum effect, at a steady state of 10-15 μM in the blood and ~50 μM in the pancreas, with <10% free GSK-7975A. *In vitro* cell data indicated that at 50 μM, GSK-7975A had no loss of effect, and the concentration of free compound *in vivo* was significantly lower. At this dose, however, GSK-7975A was highly effective in reducing all measures of disease response in three clinically representative models of AP (CER-AP, TLCS-AP and FAEE-AP), and more so than at a lower dose (28 mg/kg/h). These data provide robust confirmation of the hypothesis that cytosolic Ca^{2+} overload is a critical trigger for AP and inhibition of SOCE via Orai channels is a potential intervention for AP.

In clinical practice how soon after the onset of symptoms that patients with AP present to hospital varies from hours to days. Whether all patients can benefit from such treatment as tested here is uncertain, as the treatment was administered quite early (30-60 min) after disease induction in these preclinical evaluation settings. Whether there would be protective effects if the treatment were to be started late after disease induction remains to be determined.

4.5 Summary

The data described in this chapter demonstrate that the Orai inhibitor GSK-7975A is highly effective in protecting against experimental AP. Subcutaneous administration of GSK-7975A (as the prodrug GSK-6288B) at the low and high doses markedly reduced all local and systemic parameters, with more pronounced reduction at the high dose across three diverse, clinical representative experimental AP models (CER-AP, TLCS-AP and FAEE-AP).

Results: Chapter 5

Effects of GSK-7975A administered late in experimental acute pancreatitis

5.1 Introduction

Pancreatitis-toxins such as bile acids and ethanol metabolites cause PAC injury through aberrant intracellular calcium signalling, nuclear factor kappa B activation, trypsinogen activation, mitochondrial dysfunction, lysosomal dysfunction, impaired autophagy flux and endoplasmic reticulum stress (Petersen and Sutton, 2006, Sah et al., 2012, Lankisch et al., 2015). The timeline of these major cellular events is not fully understood. Cytosolic Ca^{2+} overload is the earliest intra-pancreatic acinar cellular event and is a critical trigger of AP (Ward et al., 1995, Sutton et al., 2003). Ca^{2+} entry through SOCE is the rate-limiting step in mediating pancreatic acinar cell injury during AP. In Chapter 4, GSK-7975A, an Orai inhibitor was shown to be highly effective when first administered early after disease induction, with a higher dose showing more marked efficacy. However, whether later administration of this or other compounds results in similar efficacy in experimental AP has not been extensively studied.

Over the last three decades, several studies have investigated the effects of agents applied at different time points in murine experimental models. **Table 5.1** shows a summary of agents administered prophylactically and therapeutically in mouse and rat experimental AP models. The modes of action of these agents are diverse, including anti-inflammatory, anti-oxidant, anti-secretory and microcirculatory effects. In 13 out of 21 studies, the beneficial effects were observed when the agents were given prophylactically, which would not be possible in the majority of patients developing AP as they present after the disease has begun. Among these 13 studies, 5 studies only compared one parameter (mortality, single biochemical or single histological parameter) between groups. Interestingly, two agents, caffeic acid

phenethyl ester (CAPE) and propolis given prophylactically had less effects on reducing pancreatic damage in four hourly injections of caerulein model, compared to the agents administered 12 h after then last injections of caerulein.

Moreover, only six studies (out of a total of over 300 studies) have compared the effects of agents applied therapeutically at different time points in murine experimental AP, **Table 5.2** summarizes these studies. Except one study was in mouse model, all other studies were using AP models in rats with the majority being bile acid-induced AP. This simplex experimental AP models used in the previous publications did not fully represent different causes of human AP. 5 out of these 6 studies showed the protective effects were observed when tested agents begun early after disease induction, with two studies only comparing a single outcome measure between groups. Also, the different efficacy between early versus late time points were generally not significant for most if not all parameters compared with the majority showing the trend that agents given early was better. Interestingly, one agent, caspase1/interleukin-1β-converting enzyme (ICE) inhibitor showed similar efficacy for reducing biochemical (amylase), immunological (peripheral white blood cell counts and myeloperoxidase activity) and histological (pancreatic necrosis and pulmonary structure and inflammation) parameters measured when given 6 h and 12 h after disease induction. All these previous publications did not provide robust and valid evidence of the exact therapeutic time window for the therapies tested.

Table 5.1 Summary of agents applied prophylactically and therapeutically in murine experimental AP

No.	Agents	Species	EAP model	Timing of therapeutical application	Outcome	Ref.
1	PPAR-γ agonist	Mouse	Caerulein	3 h after the last injection of caerulein	Equally effective*	(Rollins et al., 2006)
2	Thalidomide analog, pomalidomide	Mouse	Caerulein	1 h after the last injection of caerulein	More effective when given prophylactically	(Tsai et al., 2011)
3	HO-1 metabolites	Mouse	Bile salt	4 h after the induction	More effective when given prophylactically	(Nuhn et al., 2013)
4	PAR-2 inhibitor	Mouse	Bile salt	2 h or 5 h after the induction	Effective when given prophylactically or 2 h after*	(Michael et al., 2013)
5	CCK receptor antagonist, CR 1392	Rat	Caerulein	30 min after the last injection of caerulein	More effective when given prophylactically	(Otsuki et al., 1989)
6	Octreotide	Rat	Bile salt	5 min after the induction	Effective only when given prophylactically	(Zhu et al., 1991)
7	Antithrombin III	Rat	Bile salt	2 or 5 h after the induction	Effective when given prophylactically or 2 h after†	(Bleeker et al., 1992)
8	Prostaglandin E1	Rat	Trypsin and Bile salt	Immediately after the induction	More effective when given prophylactically‡	(Sakai et al., 1992)
9	Protease inhibitor, E3123	Rat	Caerulein	30 min after caerulein infusion	More effective when give prophylactically*	(Sata et al., 1994)
10	Tetraprenylacetone	Rat	Caerulein	Immediately after the last injection of caerulein	More effective when given prophylactically	(Tachibana et al., 1995)
11	MCl-727	Rat	Caerulein	Immediately after the last injection of caerulein	More effective when given prophylactically	(Tachibana et al., 1996)
12	IL-10	Rat	Caerulein	2 h after caerulein infusion	More effective when given prophylactically	(Rongione et al., 1997)

13	Octreotide	Rat	Bile salt	5 h after the induction	Equally effective on reducing amylase, pancreatic damage and mortality	(Chen et al., 1998)
14	$sPLA_2$ inhibitor	Rat	Bile salt	1 min or 1 h after the induction	More effective when given prophylactically†	(Tomita et al., 2004)
15	AT receptor antagonist	Rat	Caerulein	30 min after the last injection of caerulein	Equally effective	(Tsang et al., 2004)
16	Inosine	Rat	Bile salt plus caerulein	3 h after the induction	More effective when given prophylactically	(Schneider et al., 2006)
17	Relaxin	Rat	BPDOE-CDL	1 h or 4 h after the induction	More effective when given prophylactically	(Cosen-Binker et al., 2006)
18	Polyamine analog, Me_2Spm	Rat	Bile salt	4 h after the induction	More effective when given prophylactically	(Jin et al., 2008)
19	Dexamethasone	Rat	Bile salt	1 h after the induction	More effective when given prophylactically	(Yubero et al., 2009)
20	CAPE	Rat	Caerulein	12 h after the last injection of caerulein	Less effective when given prophylactically	(Buyukberber et al., 2009a)
21	Propolis	Rat	Caerulein	12 h after the last injection of caerulein	Less effective when given prophylactically	(Buyukberber et al., 2009b)

Note: prophylactically- given before or at the time of disease induction; *only one (either biochemical or histological) parameter was compared between groups; †only mortality was compared between groups; ‡therapeutical administration only improved mortality, but not other parameters.
Abbreviation: EAP, experimental AP; CER, caerulein; IL1R, interleukin-1 receptor; MCl-727, (Z)-2-(4-methylpiperazin-1-yl)-1-[4-(2-phenyl-ethyl)phenyl]-eth anone oxime hydrochloride monohydrate; IL-10, Interleukin-10; TNF receptor-bp, tumor necrosis factor receptor binding protein; PPAR, Peroxisome proliferator-activated receptor; CCK, Cholecystokinin; ICE, interleukin 1β-converting enzyme; HO-1, heme oxygenase-1; AT, angiotensin; $sPLA_2$, secretory phospholipase A_2; Me_2Spm, bismethylspermine; PAR-2, proteinase-activated receptor-2; CAPE, caffeic acid phenethyl ester.

Table 5.2 Summary of agents administered therapeutically at early or late after disease induction in murine experimental AP

No.	Agents	Species	EAP model	Timing of the treatment	Outcome	Ref.
1	PAR-2 inhibitor	Mouse	Bile salt	Early-2 h after the induction Late- 5 h after the induction	Effective when given early in reducing pancreatic acinar injury	(Michael et al., 2013)
2	Antithrombin III	Rat	Bile salt	Early-2 h after induction Late-5 h after induction	Effective when given early in reducing mortality*	(Bleeker et al., 1992)
3	ICE inhibitor	Rat	Bile salt	Early-6 h after the induction Late-12 h after the induction	Equally effective in biochemical and histological parameters measured	(Paszkowski et al., 2002)
4	Multiple antioxidant	Rat	L-arginine	Early- 6 h after the induction Late-24 h after the induction	Effective when given early in reducing biochemical and histological parameters measured†	(Hardman et al., 2005)
5	Relaxin	Rat	BPDOE-CDL	Early-1 h after the induction Late- 4 h after the induction	More Effective when given early in reducing biochemical and histological parameters measured	(Cosen-Binker et al., 2006)
6	Octreotide	Rat	Bile salt	Early-6 h after the induction Late-14 h after the induction	Effective when given early in reducing biochemical and histological parameters measured	(Wenger et al., 2007)

Note: Multiple antioxidants contain selenium, ascorbate and N-acetylcystein. *only mortality was compared between early versus late group; †L-arginine started to damage the pancreas at least 24 h after the induction in rat (Hegyi et al., 2004); even after 48 h in mouse (Dawra et al., 2007)
Abbreviation: EAP, experimental AP; PAR-2, proteinase-activated receptor-2; BPDOE-CDL, Bilio-pancreatic-duct-outlet-exclusion closed-duodenal-loops; ICE, interleukin 1β-converting enzyme.

The study described in this chapter was designed to determine the effects of delayed therapy using GSK-7975A in experimental AP, compared to earlier administration described in Chapter 4. This included assessment of control groups with AP at the time point when delayed administration of GSK-7975A would otherwise have been started.

5.2 Methods

5.2.1 Induction of experimental AP

Experimental AP (TLCS-AP and FAEE-AP) was induced as previously described in 2.6.

5.2.2 Administration of GSK-7975A

GSK-7975A was given subcutaneously as the pro-drug GSK-6288B at high dose (110 mg/kg/h) by minipump insertion, starting 6 h after TLCS-AP or FAEE-AP induction.

5.2.3 Assessment of experimental AP severity

Standard biochemical parameters and blinded histopathology were used, as previously described in 2.7.

5.2.4 Statistical analysis

Statistical evaluation was performed using OriginPro 9 (OriginLab corporation, USA), comparison was made by two-tailed Student's t-test or χ^2 test with p values <0.05 considered significant.

5.3 Results

5.3.1 Effects of GSK-7975A administered late on disease severity in TLCS-AP

To examine the effects of GSK-7975A begun 6 h after disease induction (late), GSK-7975A at high dose was tested in TLCS-AP, representative of gallstone AP. GSK-7975A administered late after TLCS-AP induction was less protective on all tested parameters than when begun 30 min after disease induction (early); the data for the latter administration are the same as those presented in Chapter 4 and are included here to assist with comparisons. Treatment with GSK-7975A starting late still caused marked reduction of serum amylase (significantly less effective, although both $p<0.05$), but did not improve other local and systemic biochemical parameters (see **Figure 5.1** and **Figure 5.2**). Similarly, GSK-7975A administered late was less protective on pancreatic histopathology, showing significantly less efficacy in reducing oedema, inflammatory infiltration and overall histopathology scores (see **Figure 5.3** and **Figure 5.4**).

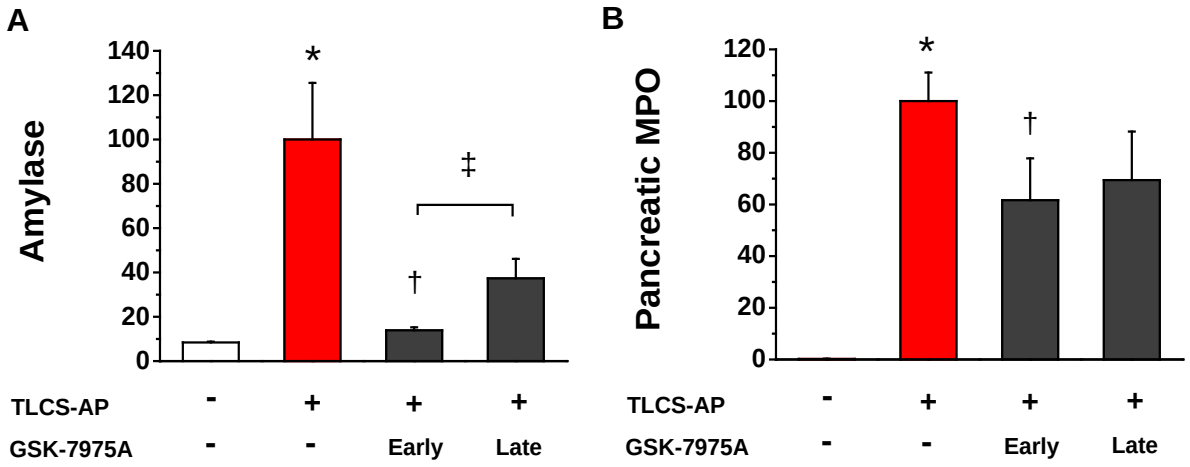

Figure 5.1 Effects of GSK-7975A administered late on pancreatic parameters in TLCS-AP. TLCS-AP resulted in substantial elevations of **(A)** serum amylase and **(B)** pancreatic myeloperoxidase (MPO) activity. Subcutaneous osmotic minipump administration of GSK-7975A given as the pro-drug GSK-6288B at high dose started at a late time point (6 h) was less protective than when begun early (30 min; mean ± s.e.m. ≥6 mice/group; *p<0.05, control vs TLCS-AP; †p<0.05 TLCS-AP vs TLCS-AP plus GSK-7975A; ‡p<0.05 GSK-7975A early vs late).

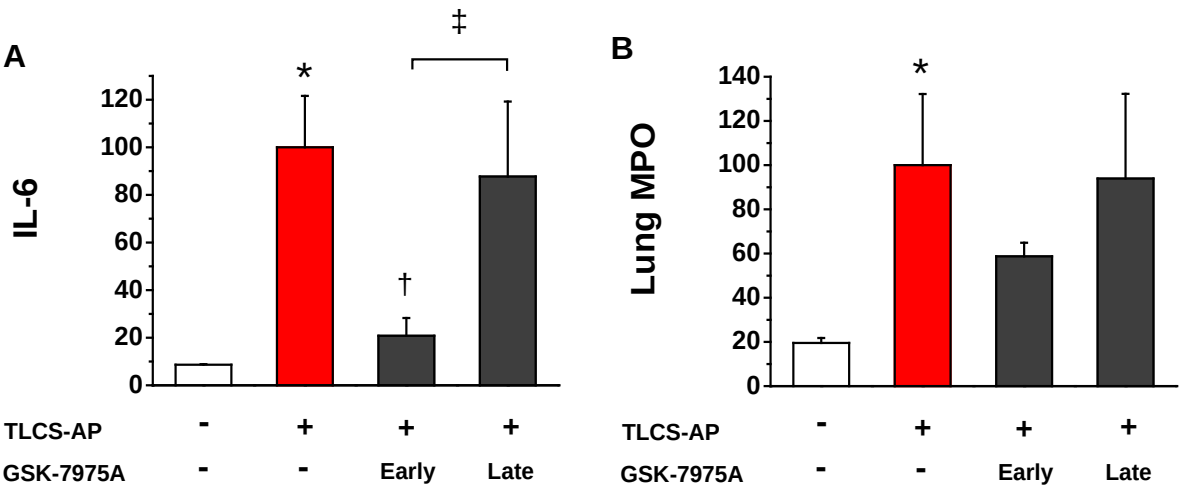

Figure 5.2 Effects of GSK-7975A administered late on systemic biochemical parameters in TLCS-AP. TLCS-AP resulted in substantial elevations of **(A)** IL-6 and **(B)** Lung MPO activity. Subcutaneous osmotic minipump administration of GSK-7975A given as the pro-drug GSK-6288B at high dose from a late time point (6 h) was less protective than when begun early (30 min; mean ± s.e.m. ≥6 mice/group; *p<0.05, control vs TLCS-AP; †p<0.05 TLCS-AP vs TLCS-AP plus GSK-7975A; ‡p<0.05 GSK-7975A early vs late).

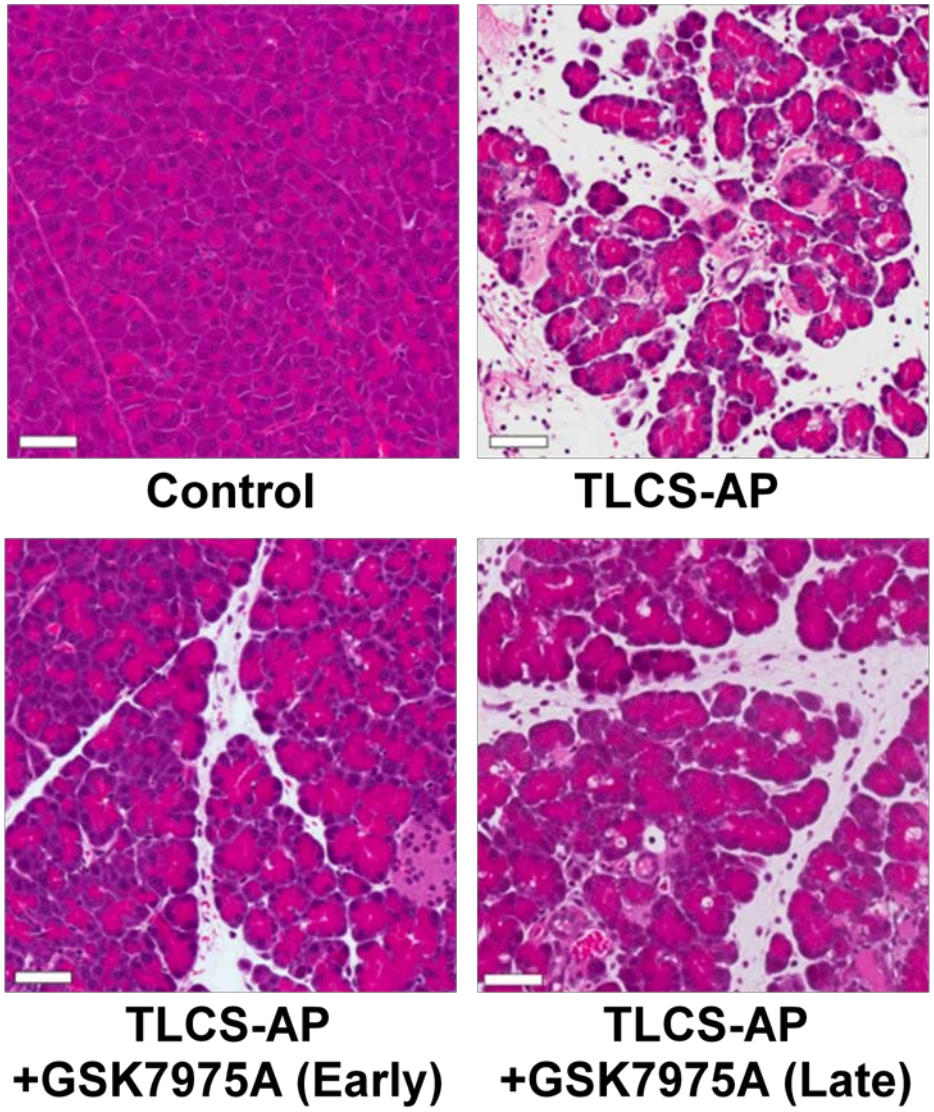

Figure 5.3 Typical histopathology of TLCS-AP following late administration of GSK-7975A. Representative histological images showing normal pancreatic histology, typical histopathology from TLCS-AP and typical histopathology from TLCS-AP after treatment with GSK-7975A early (30 min) or late (6 h) after disease induction (Haematoxylin and Eosin, H&E; scale bar= 50 µM).

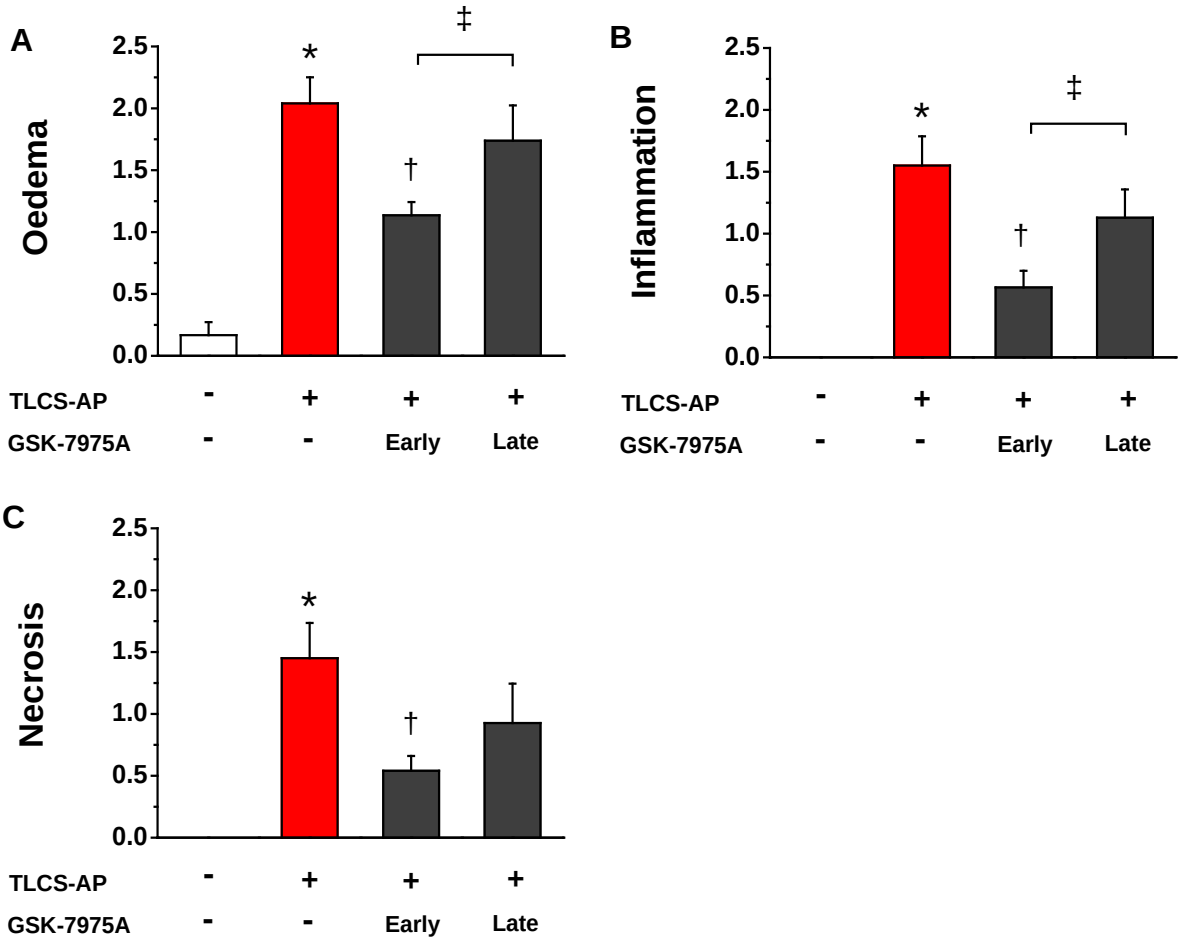

Figure 5.4 Histopathological scores of TLCS-AP comparing early versus late administration of GSK-7975A. TLCS-AP resulted in substantial increases in **(A)** oedema, **(B)** inflammation and **(C)** necrosis scores. Subcutaneous administration of GSK-7975A given as the pro-drug GSK-6288B at high dose administered from a late time point (6 h) was less effective that when begun early (30 min; mean ± s.e.m. ≥6 mice/group; *p<0.05, control vs TLCS-AP; †p<0.05 TLCS-AP vs TLCS-AP plus GSK-7975A; ‡p<0.05 GSK-7975A early vs late).

5.3.2 Effects of GSK-7975A administered late on disease severity in FAEE-AP

GSK-7975A applied 6 h after disease induction (late) was also tested in FAEE-AP, which mimics alcoholic acute pancreatitis. Consistent with the results in TLCS-AP, GSK-7975A administered late was less protective on all tested parameters than when begun early (1 h), showing significant less effect on reducing serum amylase ($p<0.05$) (see **Figure 5.5** and **Figure 5.6**). Similarly, GSK-7975A administered late was less protective on pancreatic histopathology, showing significantly less efficacy on oedema and overall histopathology scores (see **Figure 5.7** and **Figure 5.8**).

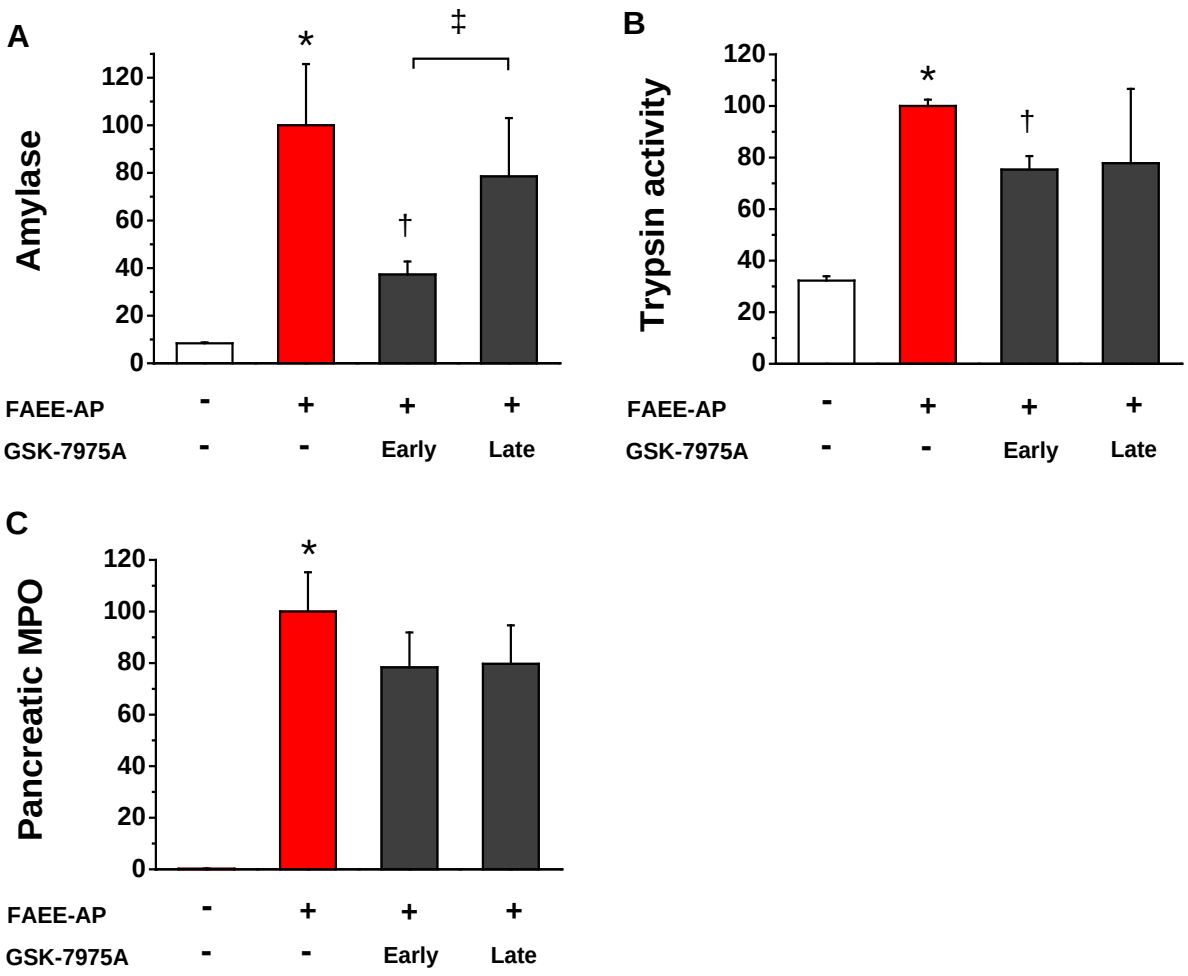

Figure 5.5 Effects of GSK-7975A administered late on pancreatic parameters in FAEE-AP. FAEE-AP resulted in substantial elevations of **(A)** serum amylase, **(B)** pancreatic trypsin and **(C)** pancreatic myeloperoxidase (MPO) activity. Subcutaneous administration of GSK-7975A given as pro-drug GSK-6288B at high dose from a late time point (6 h) less effective than when given early (1 h; mean ± s.e.m. ≥6 mice/group; *p<0.05, control vs FAEE-AP; †p<0.05 FAEE-AP vs FAEE-AP plus GSK-7975A; ‡p<0.05 GSK-7975A early vs late).

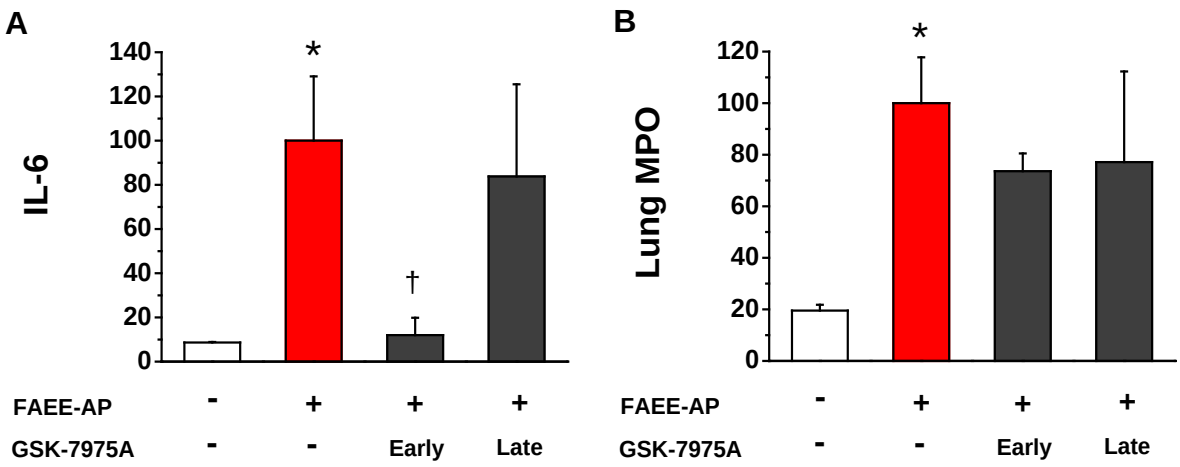

Figure 5.6 Effects of GSK-7975A administered late on systemic biochemical parameters in FAEE-AP. FAEE-AP resulted in substantial elevations of **(A)** IL-6 and **(B)** lung MPO activity. Subcutaneous administration of GSK-7975A given as the pro-drug GSK-6288B at high dose from a later time point (6 h) was significantly less effective than when given early (1 h; mean ± s.e.m. ≥6 mice/group; *p<0.05, control vs FAEE-AP; †p<0.05 FAEE-AP vs FAEE-AP plus GSK-7975A; ‡p<0.05 GSK-7975A early vs late).

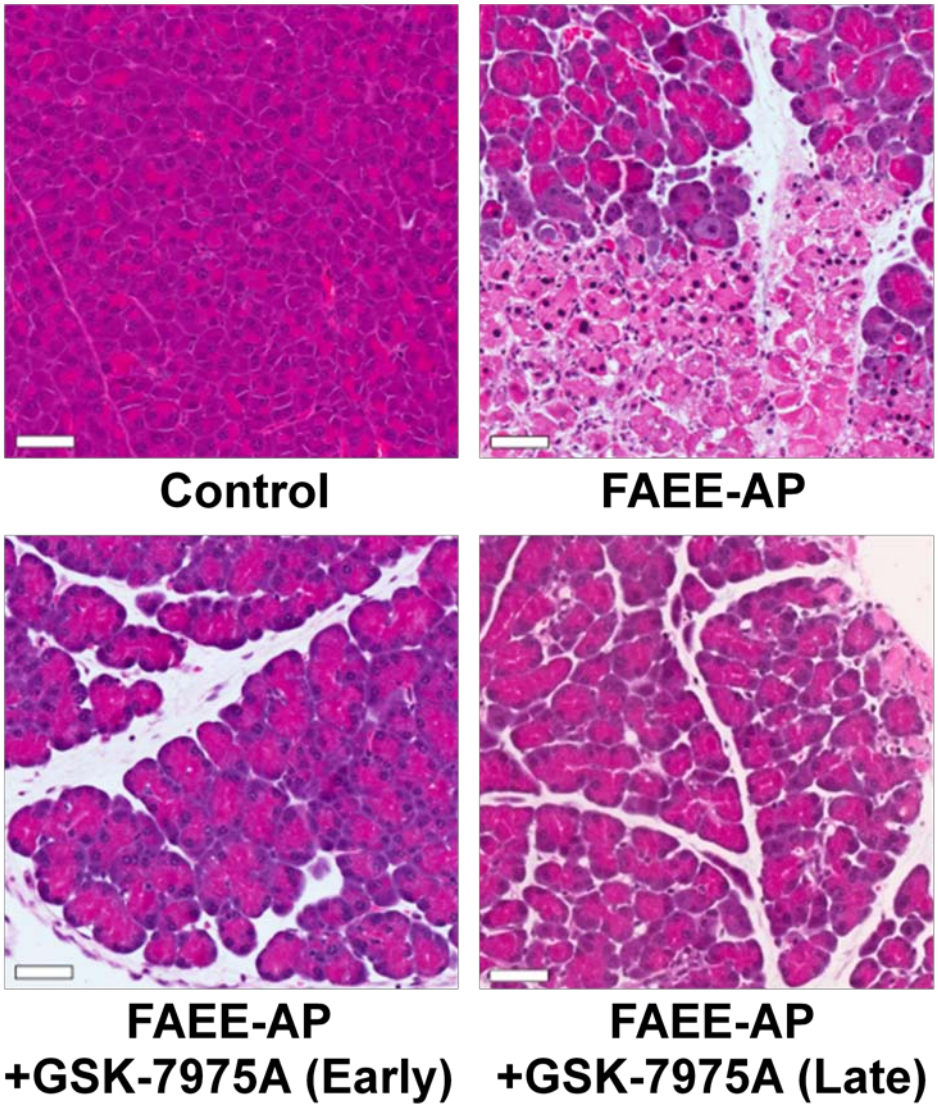

Figure 5.7 Typical histopathology of FAEE-AP following late administration of GSK-7975A. Representative histological images showing normal pancreatic histology, typical histopathology from FAEE-AP and typical histopathology from FAEE-AP after treatment with GSK-7975A early (1 h) and late (6 h) after disease induction (Haematoxylin and Eosin, H&E; scale bar= 50 µM).

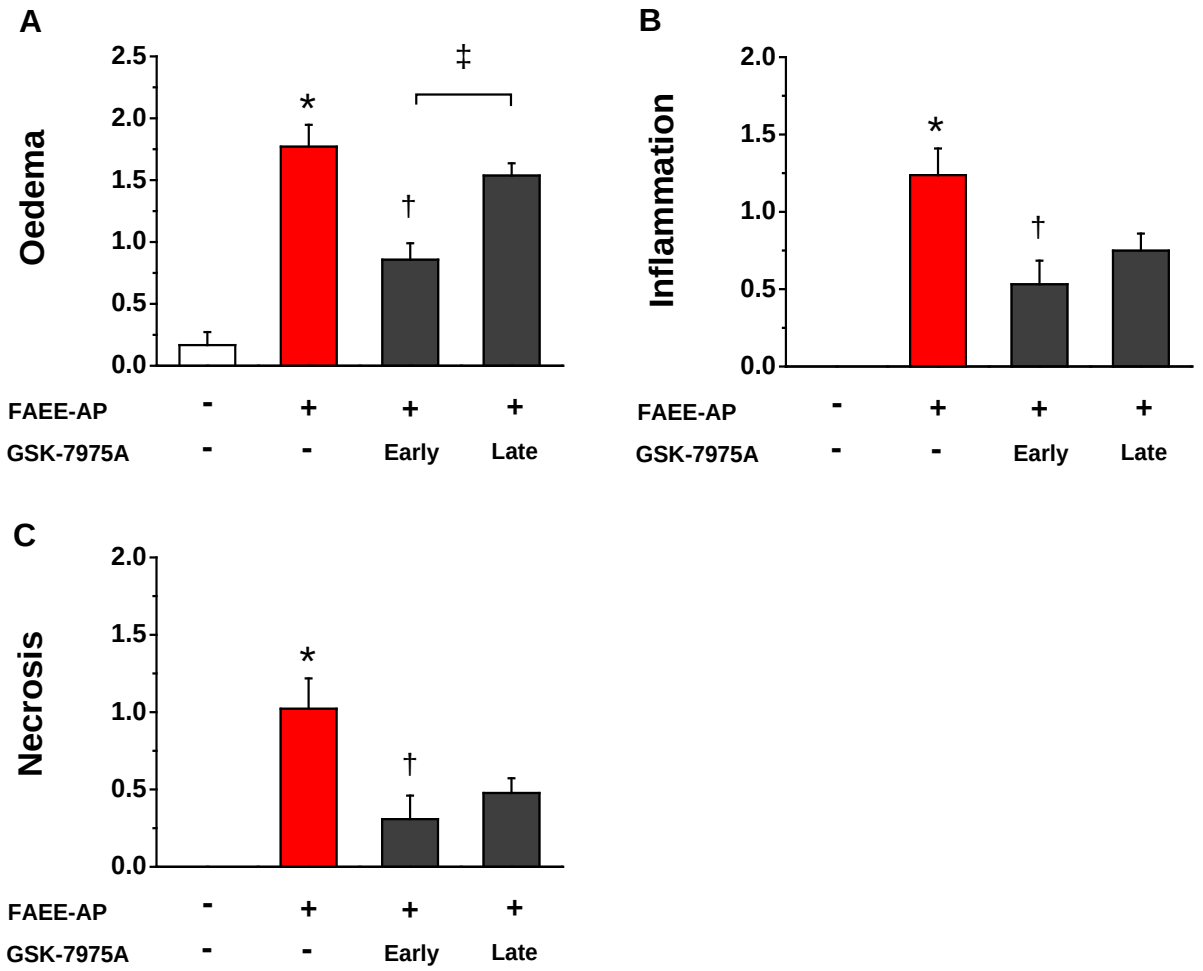

Figure 5.8 Histological scores of FAEE-AP comparing early versus late administration of GSK-7975A. FAEE-AP results in substantial increases in **(A)** oedema, **(B)** inflammation and **(C)** necrosis scores. Subcutaneous administration of GSK-7975A given as the pro-drug GSK-6288B at high dose from a later time point (6 h) was significantly less effective that when begun early (1 h; mean ± s.e.m. ≥6 mice/group; *p<0.05, control vs FAEE-AP; †p<0.05 FAEE-AP vs FAEE-AP plus GSK-7975A; ‡p<0.05 GSK-7975A early vs late).

5.3.3 The extent of experimental AP when late administration of GSK-7975A was begun

To determine the extent of experimental AP established by the time that late administration of GSK-7975A was begun (6 h after the start of disease induction) acute pancreatitis was induced in control mice for assessment at 6 h after the start of disease induction, using standard biochemical parameters and histopathology. The data already presented earlier in this Chapter on the effects of late administration of GSK-7975A are also given below in the figures for ease of comparison, especially comparison with disease severity at 6 h after the start of disease induction. Pancreatic parameters from TLCS-AP and FAEE-AP at 6 h markedly increased compared to control without disease induction ($p<0.05$); the values further increased at 24 h, with pancreatic MPO being significant ($p<0.05$) (see **Figure 5.9**). Systemic biochemical parameters from these two models at 6 h were markedly elevated compared to control without disease induction ($p<0.05$), with significantly higher levels of IL-6 and lung MPO in FAEE-AP at 6 h compared with the values at 24 h (see **Figure 5.10**). GSK-7975A started 6 h after disease induction did not reduce biochemical parameters compared to the scores at 6 h, except for amylase (TLCS-AP), IL-6 (FAEE-AP) and lung MPO (FAEE-AP) being significantly reduced.

Pancreatic injury at 6 h and 24 h evaluated by histopathology progressively increased, with significant progression of inflammation, necrosis and overall histopathology scores at 24 h ($p<0.05$). GSK-7975A started 6 h after disease induction did not reduce pancreatic histopathology scores compared to the scores at 6 h (see **Figure 5.11** and **Figure 5.12**).

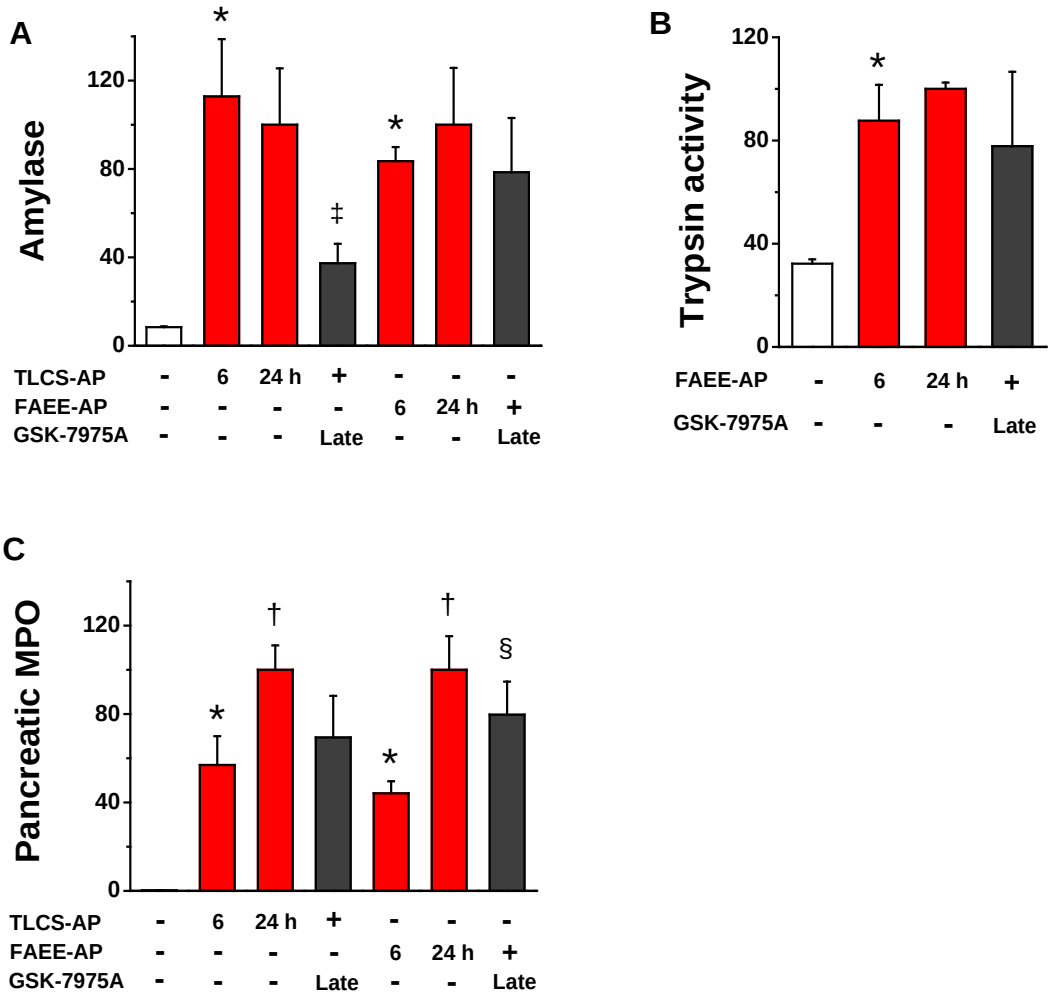

Figure 5.9 Pancreatic parameters at 6 h and 24 h in TLCS-AP and FAEE-AP. The two models at 6 h and 24 h resulted in substantial elevations of **(A)** serum amylase, **(B)** pancreatic trypsin and **(C)** myeloperoxidase (MPO) activity, with more markedly elevation of pancreatic trypsin and MPO activity at 24 h. Subcutaneous administration of GSK-7975A at the high dose begun at 6 h after the start of disease induction (late) significantly reduced serum amylase from levels at 6 h, but not other parameters (mean ± s.e.m. ≥6 mice/group; *p<0.05, control vs two models at 6 h; †p<0.05, two models at 6 h vs 24 h; ‡p<0.05, TLCS-AP at 6 h vs TLCS-AP plus GSK-7976A; §p<0.05, FAEE-AP at 6 h vs FAEE-AP plus GSK-7975A).

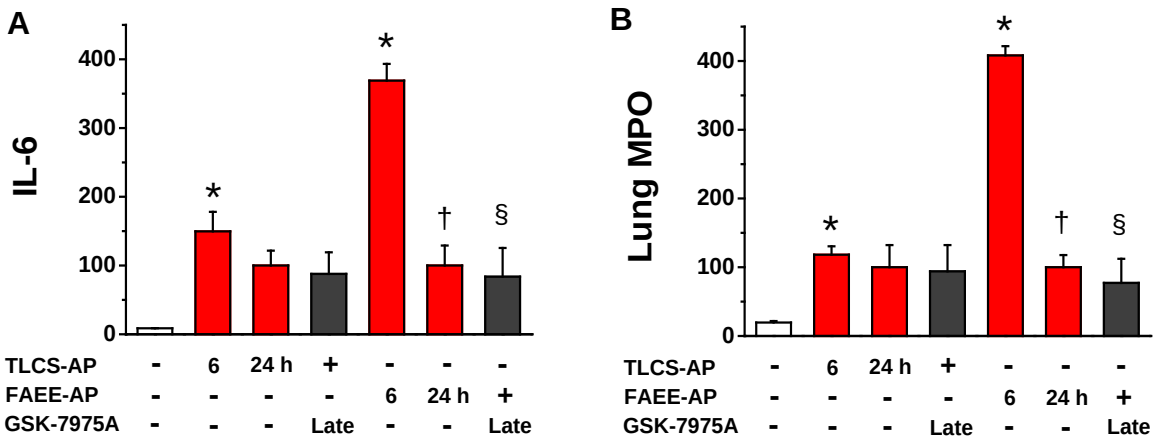

Figure 5.10 Systemic biochemical parameters at 6 h and 24 h in TLCS-AP and FAEE-AP. The two models at 6 h and 24 h resulted in substantial elevation of **(A)** serum amylase and **(B)** lung myeloperoxidase (MPO) activity, with more marked elevation of both at 6 h. Subcutaneous administration of GSK-7975A at high dose administered late (6 h) significantly reduced both IL-6 and Lung MPO from levels at 6 h in TLCS-AP, but not in FAEE-AP (mean ± s.e.m. ≥6 mice/group; *p<0.05, control vs two models at 6 h; †p<0.05, two models at 6 h vs 24 h; §p<0.05, FAEE-AP at 6 h vs FAEE-AP plus GSK-7975A).

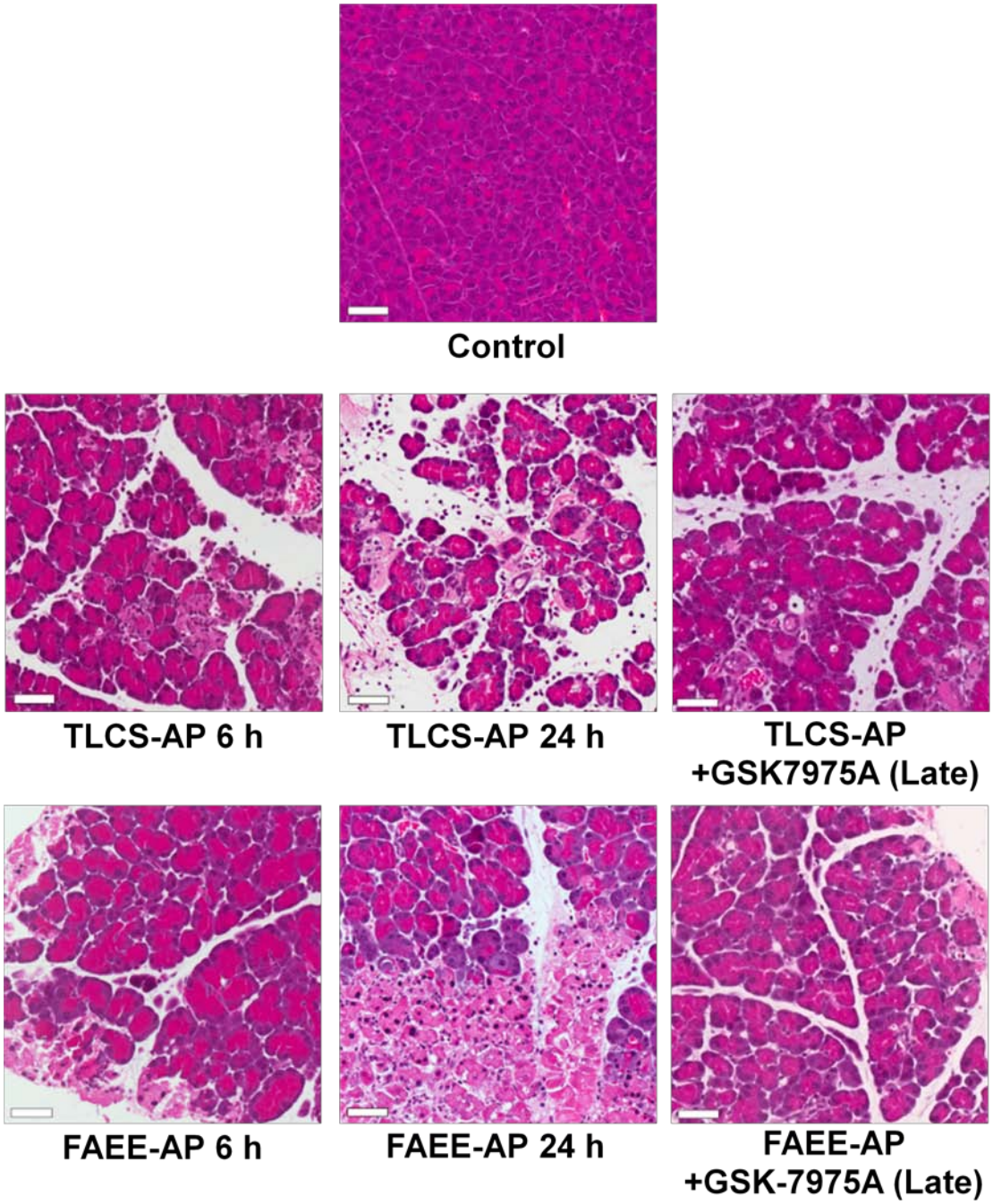

Figure 5.11 Typical histopathology at 6 h and 24 h from TLCS-AP and FAEE-AP including effects of late administration of GSK-7975A. Representative histological images showing normal pancreatic histology, typical histopathology from two models at 6 h and 24 h and typical histopathology from two models after treatment with GSK-7975A begun 6 h after disease induction (late) (H&E; scale bar= 50 µM).

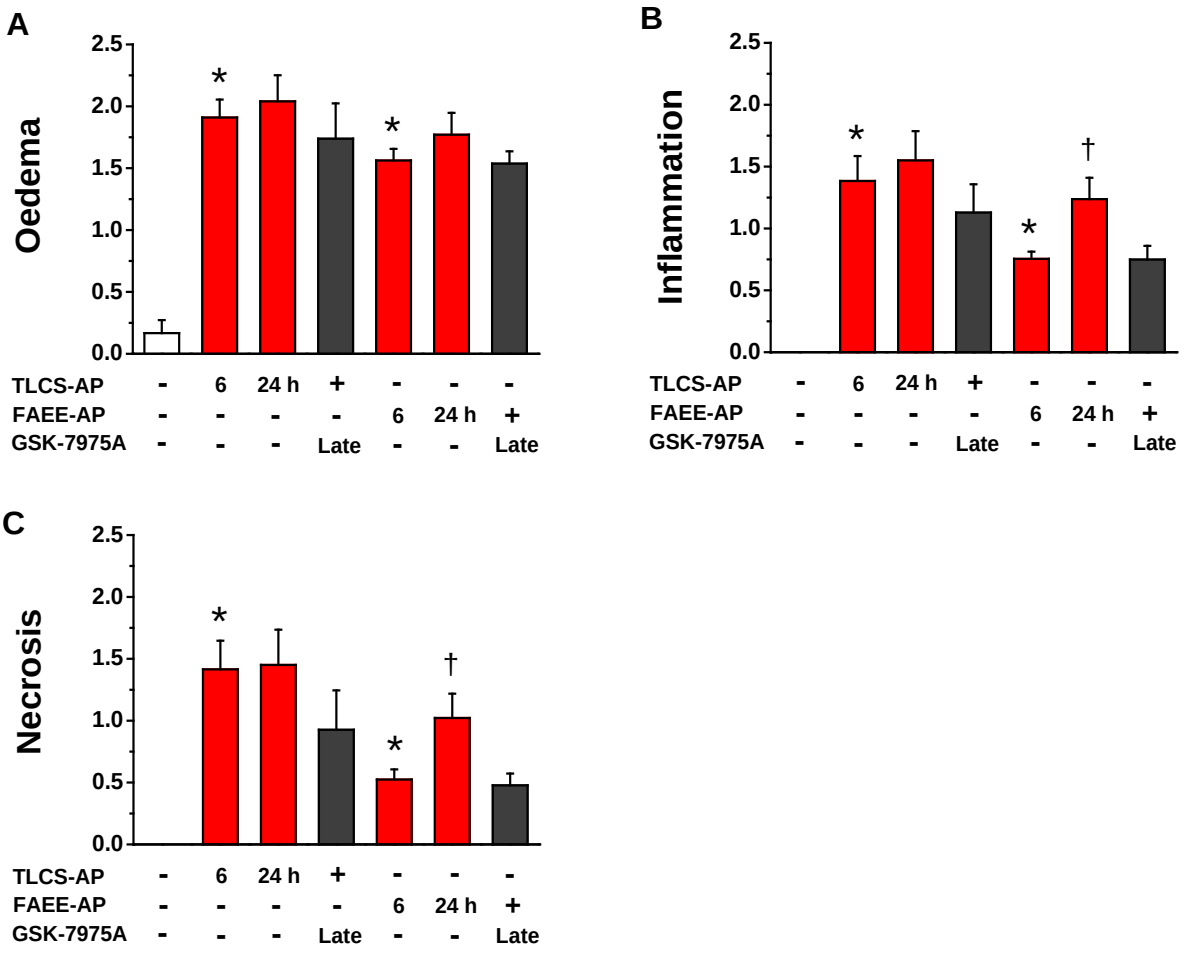

Figure 5.12 Histopathological scores at 6 h and 24 h in TLCS-AP and FAEE-AP, including effects of late administration of GSK-7975A. The two models at 6 h and 24 h resulted in progressive increases in **(A)** oedema, **(B)** inflammation and **(C)** necrosis scores, with more marked elevation of all scores at 24 h. Subcutaneous administration of GSK-7975A begun 6 h after disease induction (late) did not reduce any score significantly from levels at 6 h (mean ± s.e.m. ≥6 mice/group; *$p<0.05$, control vs two models at 6 h; †$p<0.05$, two models at 6 h vs 24 h).

5.4 Discussion

Subcutaneous administration of GSK-7975A at high dose from a late time point (6 h) after disease induction was significantly less protective across a broad range of pancreatic and systemic parameters in two clinically representative models of acute pancreatitis, significantly so for amylase (TLCS-AP and FAEE-AP), IL-6 (TLCS-AP), oedema (TLCS-AP and FAEE-AP), inflammatory infiltrate (TLCS-AP) and total histolopathology score (TLCS-AP and FAEE-AP). It is notable that the same dose administered early after disease induction was found to be highly effective in three representative models of acute pancreatitis (see Chapter 4).

GSK-7975A was administered after disease induction to model the potential treatment of clinical acute pancreatitis, but the delay in administration of GSK-7975A to six hours after disease induction resulted in diminished efficacy. Biological time courses including that of acute pancreatitis are longer in humans than mice, with pancreatic necrosis typically detected within days rather than hours. Nevertheless human pancreatic acinar necrotic cell death pathway activation may begin in clinical AP at an early stage after disease onset, shown here in mouse models within six hours of onset.

Door-to-needle times of less than 60 minutes are established in guidelines for patients with acute myocardial infarction (30 min)(O'Gara et al., 2013) and acute ischaemic stroke (60 min)(Jauch et al., 2013), making every second count, with national and international quality improvement initiatives underway towards fully achieving these (Fonarow et al., 2014). Although pancreatic necrosis has a less rapid time course and is not the result of major arterial occlusion (Lankisch et al.,

2015), the translational implication from here is that door-to-needle time is an important issue in administration of any treatment for acute pancreatitis that targets the pathogenesis of pancreatic injury, which drives the disease.

5.5 Summary

In this chapter the data demonstrated that delayed administration of GSK-7975A resulted in diminished efficacy in two clinical representative models of AP. Subcutaneous administration of GSK-7975A from a late time point (6 h after disease induction) was significantly less protective across a broad range of parameters, suggesting the timing of treatment that targets pancreatic injury is an important issue in future endeavour to gain optimal benefits from any drug treatment.

Results: Chapter 6

Effects of CM_128, a novel Orai inhibitor,

in experimental acute pancreatitis

6.1 Introduction

CM_128 is a new molecular entity that has been shown to inhibit Orai1, discovered and patented by CalciMedica. Confidential unpublished data from CalciMedica demonstrate that Orai channels are the targets of CM_128, not STIM1; CM_128 has 10-20 fold greater potency on Orai1 compared to Orai2. CM_128 inhibits thapsigargin-induced SOCE in both mouse and human PACs (Chapter 3). CM_128 concentration-dependently inhibited cyclopiazonic acid-induced Ca^{2+} entry in mouse PACs, with IC_{50} of ~0.7 μM (Wen et al., 2015). Moreover, confidential unpublished data from CalciMedica showed CM_128 also blocks CCK and TLCS-induced SOCE in mouse PACs, with complete inhibition at 10 μM for CCK and at 1 or 3 μM for TLCS. Patch clamp recordings demonstrated that CM_128 concentration-dependently inhibited I_{CRAC} in HEK 293 cells transfected with human Orai1 and human STIM1, with IC_{50} of ~0.1 μM and a complete inhibition at 1 μM (Wen et al., 2015). CM_128 protected against necrotic cell death pathway activation in mouse and human PACs (Chapter 3). Furthermore, intraperitoneal administration of CM_128 significantly reduced serum amylase and lipase, pancreatic weight and pancreatic damage in a dose-dependent manner, showing maximal efficacy at 20 mg/kg in mouse CER-AP model (confidential unpublished data from CalciMedica).

CM2489 is a closely related analogue of CM_128 that has been tested in a Phase I clinical trial for the treatment of moderate-to-severe plaque psoriasis; CM2489 is the first CRAC inhibitor to be tested in human (Jairaman and Prakriya, 2013). In the multiple ascending dose Phase I study of CM2489 this drug was shown to be safe, well-tolerated and well-behaved with evidence of clinical improvement

(www.calcimedica.com), suggesting the potential for clinical application of CRAC inhibitors.

The study described in this chapter was designed to investigate the effects of CM_128 begun one and six hours after disease induction in two clinically representative models of experimental AP. The work included assessment of CM_128 administration at both early and late time points (as in Chapters 4 and 5 for GSK-7975A) as well as comparison with the severity of AP at 6 h after disease induction.

6.2 Methods

6.2.1 Measurement of CM_128 *in vivo*

Sampling of CM_128 from three mice was made at the same time point when drug efficacy was assessed. Immediately following humane killing, 0.5 µL of blood was collected in a heparinised tube containing 10 U of heparin; centrifuged at 7,600 rpm for 7 min to obtain the plasma; the pancreas and lung were removed, processed in a Mini-Beadbeater (Biospec) containing glass beads and mixed with plasma matrix (1:4). Levels of CM_128 were determined by liquid chromatography mass spectrometry (LC-MS/MS; Varian 500-MS with Varian 212 LC and Phenomenex C8 column).

6.2.2 Protein binding of CM_128

The protein binding of CM_128 in plasma (from Bioreclamation, Inc.,Westbury, NY) was determined at 30 µM and 50 µM by equilibrium dialysis using a high throughput dialysis Teflon block (HTDialysis, LLC, Gales Ferry, CT) and dialysis membrane

strips. Plasma was dialyzed against phosphate buffered saline (PBS, pH 7.4 from Invitrogen/Gibco, Carlsbad, CA) in a buffer chamber, shaking gently at 37ºC overnight. After equilibrium, samples from both sample chamber and buffer chamber were collected in a matrix-match manner and analyzed by LC-MS/MS (Varian 500-MS with Varian 212 LC and Phenomenex C8 column). Experiments were carried out in triplicate. The percentage of CM_128 bound was calculated by the equation: % bound= ($[CM\_128]_a$- $[CM\_128]_b$)/ [CM_128]a ×100%, where $[CM\_128]_a$ was the concentration of CM_128 in the sample chamber and $[CM\_128]_b$ was the concentration of CM_128 in the buffer chamber.

6.2.3 Induction of experimental AP

Experimental AP (TLCS-AP and FAEE-AP) was induced as previously described in 2.5.

6.2.4 Administration of CM_128

Preliminary *in vivo* experiments indicated CM_128 has a significantly longer half-life than GSK-7975A, suitable for intraperitoneal dosing every 12 hours to achieve sustained blood levels. 20 mg/kg CM_128 was administered intraperitoneally every 12 hours in TLCS-AP and FAEE-AP; treatment of CM_128 was begun either one or six hours after disease induction.

6.2.5 Assessment of experimental AP severity

Standard biochemical parameters and blinded histopathology scoring systems were used, as previously described in 2.6.

6.2.6 Statistical analysis

Statistical evaluation was performed using OriginPro 9 (OriginLab corporation, USA); comparison was made by two-tailed Student's t-test or χ^2 test with p values <0.05 considered significant.

6.3 Results

6.3.1 Effects of CM_128 administered 1 h or 6 h after disease induction on disease severity in TLCS-AP and FAEE-AP

Preliminary *in vivo* experiments undertaken by Calcimedica indicated that CM_128 has a long half-life, suitable for intraperitoneal dosing every 12 hours to achieve sustained blood levels with >99% bound (free fraction in murine plasma 0.33%; when added to human plasma 0.16%). Levels of CM_128 in the plasma, pancreas and lung were measured (see **Figure 6.1**), showing ~7.5 µM in blood, ~50 µM in the pancreas and ~30 µM in the lung.

Since high dose GSK-7975A demonstrated greater efficacy *in vivo* than with low dose GSK-7975A (Chapter 4), and *in vitro* data obtained with CM_128 did not suggest loss of efficacy at high concentrations (Wen et al., 2015) and also that CM_128 at 20 mg/kg previously showed to have maximal efficacy in CER-AP, 20 mg/kg CM_128 was administered every 12 hours to test efficacy of this agent in TLCS-AP and FAEE-AP. High dose GSK-7975A administered 6 h after disease induction resulted in diminished protective effects, compared with treatment starting early after disease induction (Chapter 5). Therefore the relative efficacy of CM_128 administered either 1 h or 6 h after disease induction was determined in both models.

CM_128 started 1 h after disease induction significantly reduced all pancreatic and systemic biochemical parameters in TLCS-AP and FAEE-AP (see **Figure 6.2** and **Figure 6.3**). Similar effects on pancreatic histopathology were observed, showing significant reduction of oedema, inflammation, necrosis and total histopathological scores (see **Figure 6.4** and **Figure 6.5**). CM_128 begun 6 h after disease induction was less effective across a broad range of biochemical parameters (see **Figure 6.2** and **Figure 6.3**), significantly so for pancreatic MPO (FAEE-AP), lung MPO (TLCS-AP) and IL-6 (TLCS-AP), although significant reductions were still seen in amylase (TLCS-AP and FAEE-AP) and lung MPO (TLCS-AP). CM_128 begun 6 h after disease induction was less protective on pancreatic histopathology (see **Figure 6.4** and **Figure 6.5**), although significant reductions were still observed in oedema (TLCS-AP and FAEE-AP), inflammation (FAEE-AP), necrosis (FAEE-AP) and total histological scores (FAEE-AP).

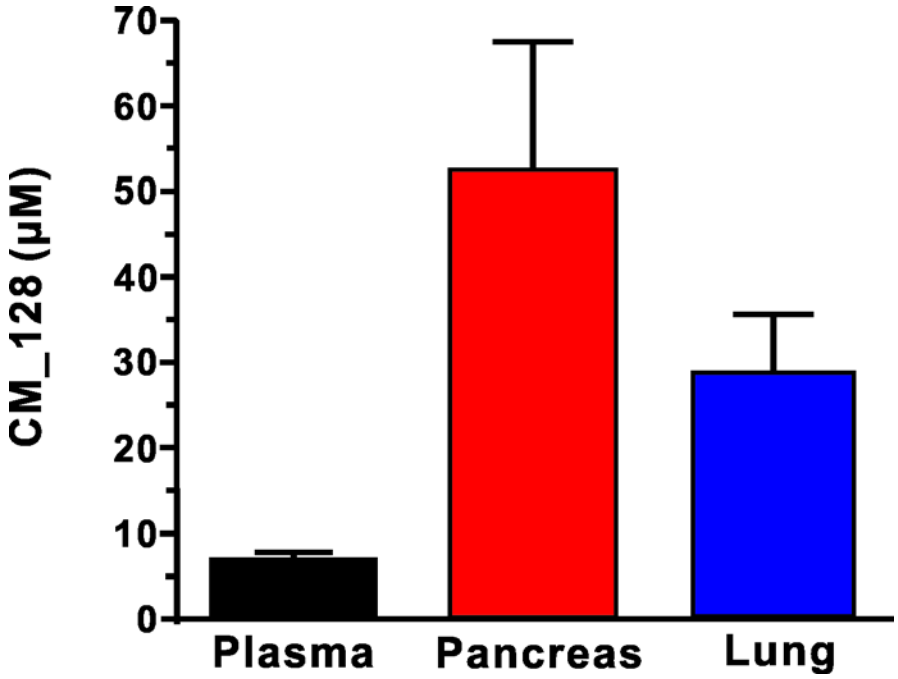

Figure 6.1 Levels of CM_128 in the plasma, pancreas and lung. Mean (± s.e.m) plasma, pancreas and lung levels following administration of CM_128 at 20 mg/kg, sampling at the time point when drug efficacy was assessed; these were ~10 µM, ~50 µM and ~ 30 µM respectively.

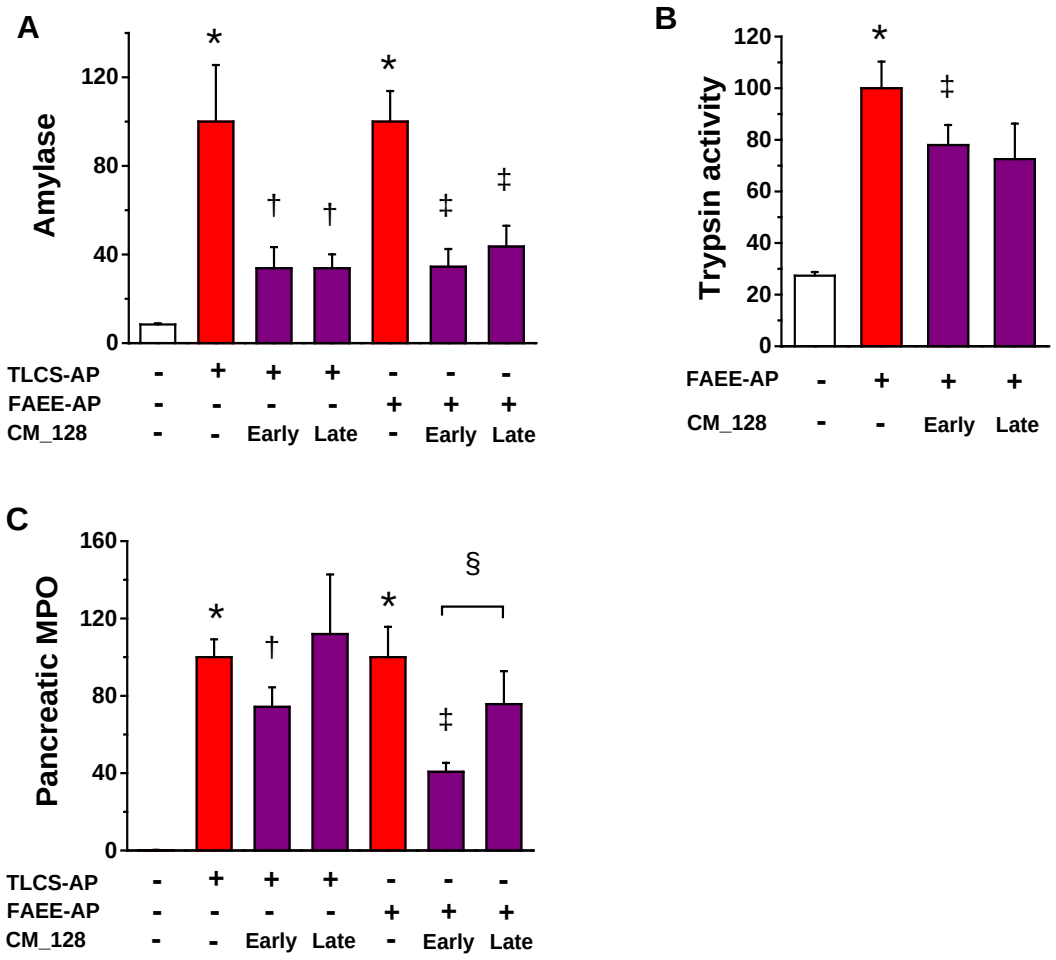

Figure 6.2 Effects of CM_128 administered early or late on pancreatic parameters in TLCS-AP and FAEE-AP. The two models resulted in substantial elevations of **(A)** serum amylase, **(B)** pancreatic trypsin activity and **(C)** pancreatic myeloperoxidase (MPO) activity. Intraperitoneal administration of CM_128 at 20 mg/kg given at 1 h after disease induction (early) or 6 h after (late) significantly reduced all parameters, with more marked reduction of pancreatic MPO activity when CM_128 was administered early (mean ± s.e.m., ≥6 mice/group; *p<0.05, control vs TLCS-AP; †p<0.05 TLCS-AP vs TLCS-AP plus CM_128; ‡p<0.05 FAEE-AP vs FAEE-AP plus CM_128; §P<0.05 CM_128 early vs late).

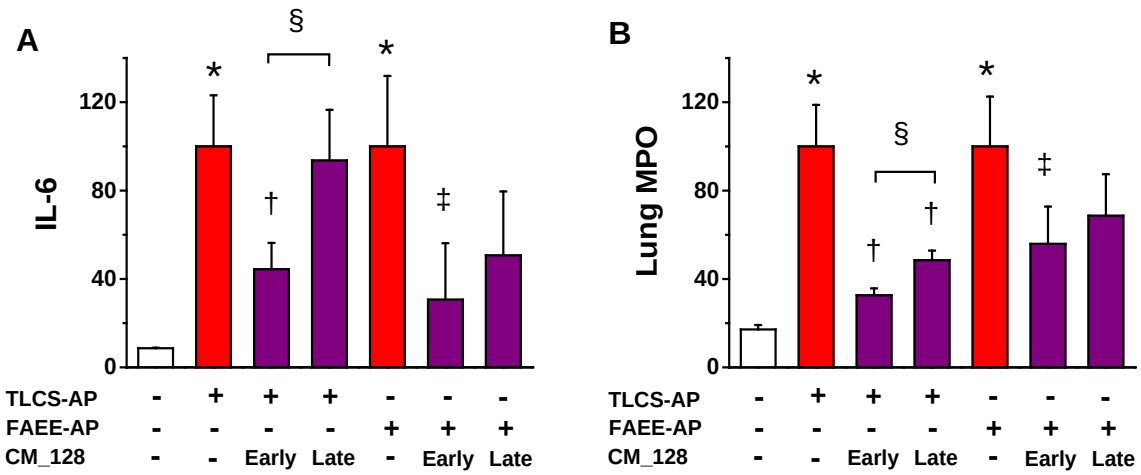

Figure 6.3 Effects of CM_128 administered early or late on systemic biochemical parameters in TLCS-AP and FAEE-AP. The two models resulted in substantial elevation of **(A)** IL-6 and **(B)** lung myeloperoxidase (MPO) activity. Intraperitoneal administration of CM_128 at 20 mg/kg given at 1 h after disease induction (early) or 6 h after (late) significantly reduced all parameters, with more marked reduction when CM_128 was administered early (mean ± s.e.m., ≥6 mice/group; *p<0.05, control vs TLCS-AP; †p<0.05 TLCS-AP vs TLCS-AP plus CM_128; ‡p<0.05 FAEE-AP vs FAEE-AP plus CM_128; §P<0.05 CM_128 early vs late).

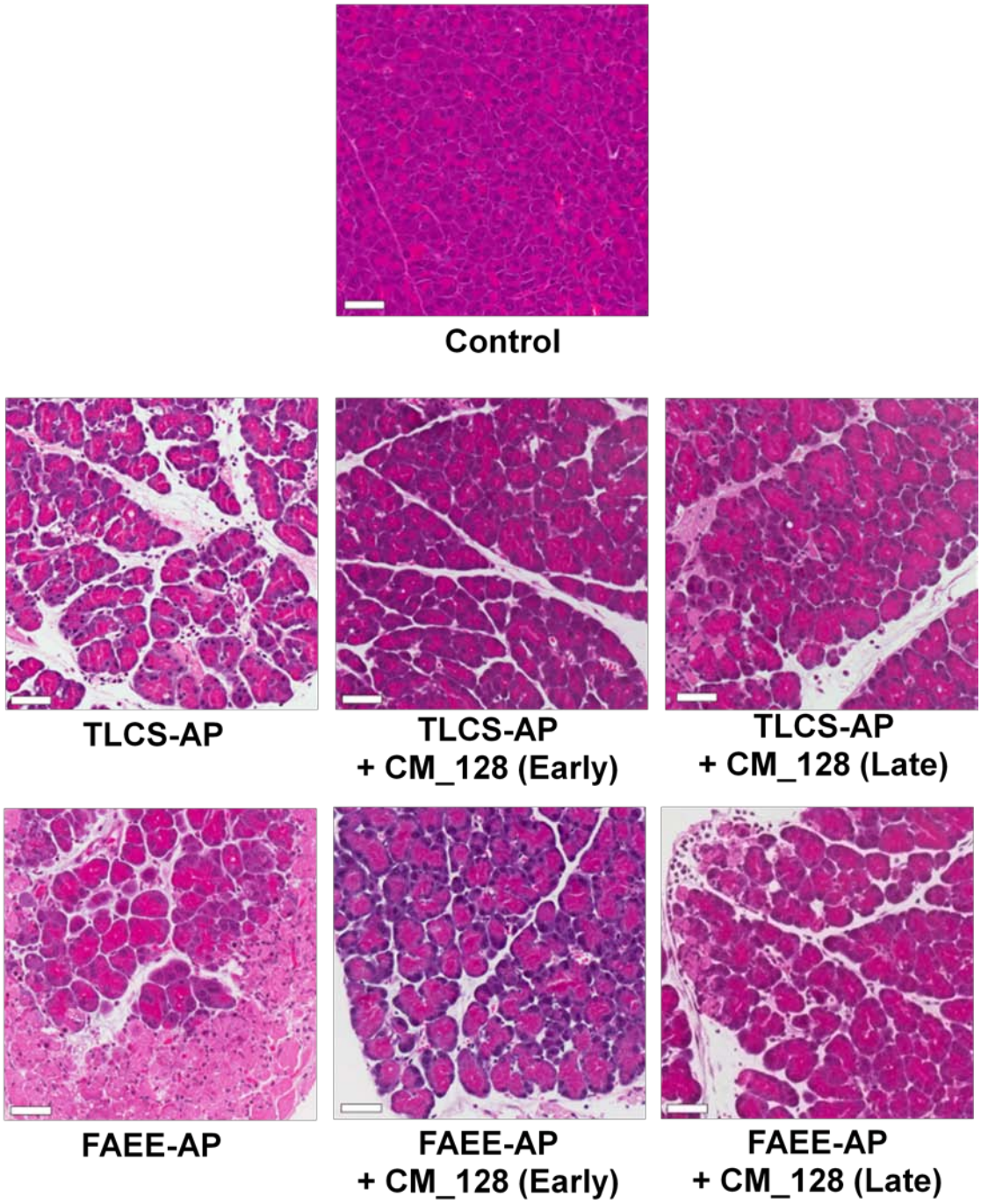

Figure 6.4 Typical histopathology from TLCS-AP and FAEE-AP following early or late administration of CM_128. Representative histological images showing normal pancreatic histology, typical histopathology from two models and typical histopathology from two models after treatment with CM_128 early or late after disease induction (Haematoxylin and Eosin, H&E; scale bar= 50 µM).

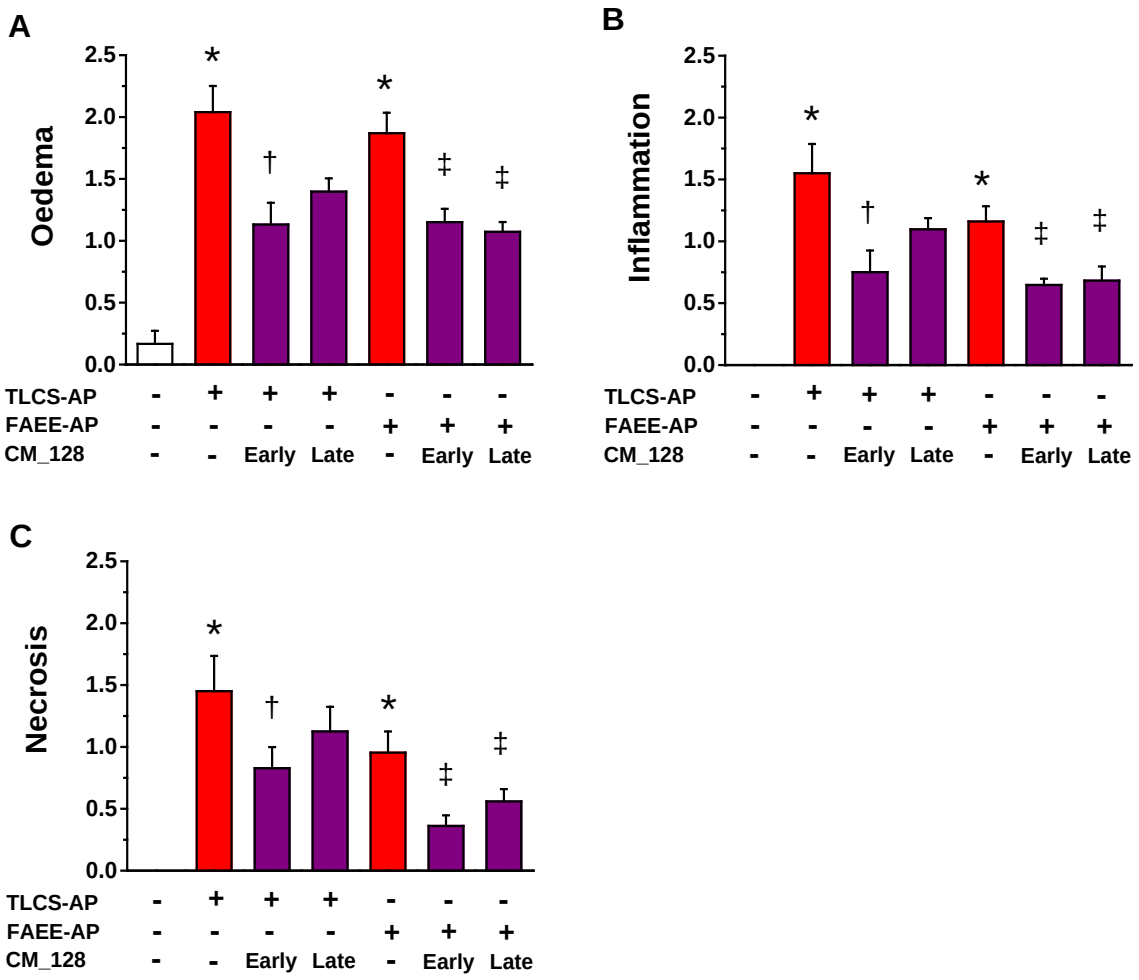

Figure 6.5 Histopathological scores of CM_128 administered early or late in TLCS-AP and FAEE-AP. Both models resulted in substantial increases in **(A)** oedema, **(B)** inflammation, **(C)** necrosis and **(D)** total histology score. Intraperitoneal administration of CM_128 at 20 mg/kg given at 1 h after disease induction (early) or 6 h after (late) significantly reduced all parameters, with more marked reduction when CM_128 was administered early (mean ± s.e.m. ≥6 mice/group; *p<0.05, control vs TLCS-AP; †p<0.05 TLCS-AP vs TLCS-AP plus CM_128; ‡p<0.05 FAEE-AP vs FAEE-AP plus CM_128; §P<0.05 CM_128 early vs late).

6.3.2 The extent of experimental AP when late administration of CM_128 was begun

To determine the extent to which disease was established at 6 h after disease induction, and the effect of CM_128 begun then, all parameters were assessed at 6 h and compared with values at 24 hours. The data already presented earlier in this Chapter on the effects of late administration of CM_128 are also given below in the figures for ease of comparison, especially comparison with disease severity at 6 h after the start of disease induction. Pancreatic parameters from TLCS-AP and FAEE-AP at 6 h markedly increased compared to control without disease induction ($p<0.05$); the values further increased at 24 h, with pancreatic MPO being significant ($p<0.05$) (See **Figure 6.6**). Systemic biochemical parameters from the two models at 6 h were markedly elevated compared to controls without disease induction ($p<0.05$); there were significantly higher levels of IL-6 and lung MPO in FAEE-AP at 6 h compared with the values at 24 h (See **Figure 6.7**). Pancreatic injury at 6 h and 24 h evaluated by histopathology progressively increased, with significant progression of inflammation, necrosis and overall histopathology scores at 24 h ($p<0.05$) (See **Figure 6.8** and **Figure 6.9**). These data demonstrated that by 24 h there was no significant improvement of parameters as measured at six hours as a result of CM_128 administration begun at six hours, confirming delay in therapy to be disadvantageous, although CM_128 appeared to prevent these parameters from increasing.

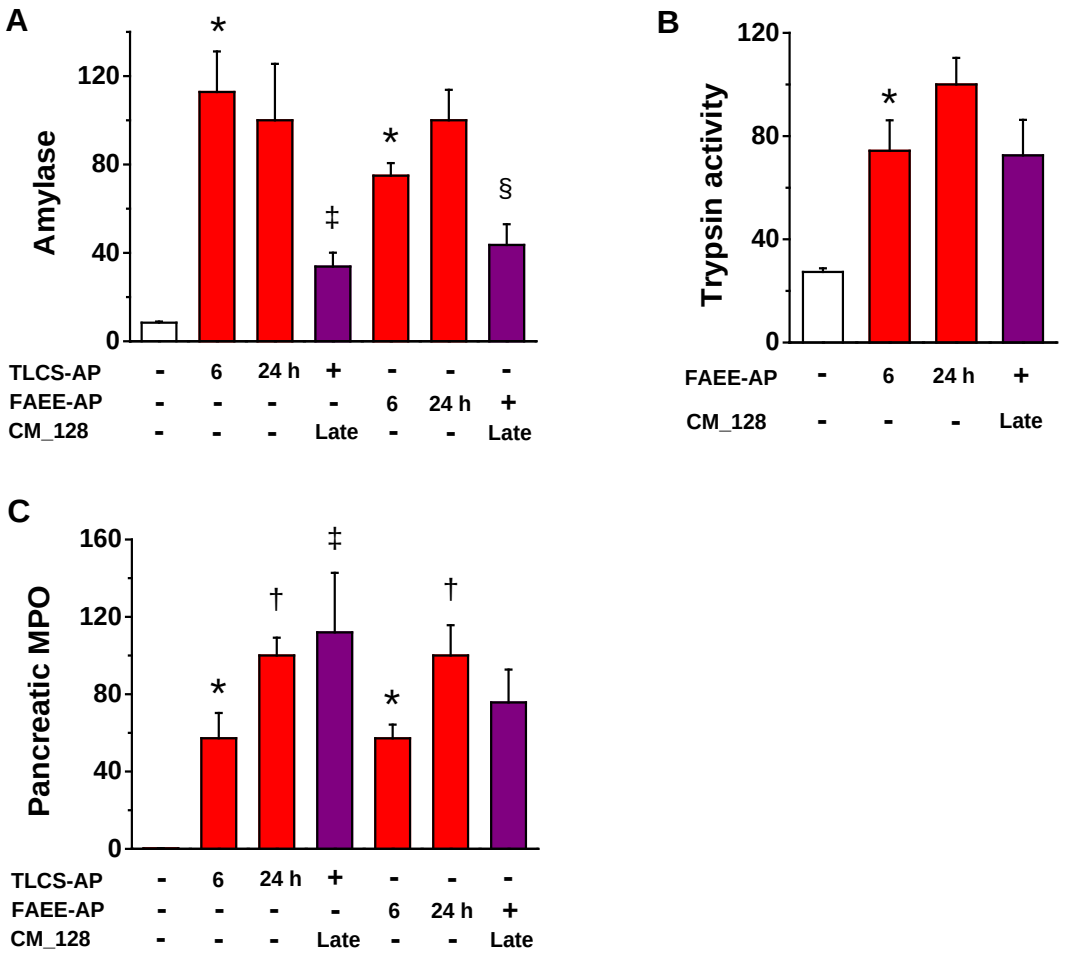

Figure 6.6 Pancreatic parameters at 6 h and 24 h in TLCS-AP and FAEE-AP. The two models at 6 h and 24 h resulted in substantial elevations of **(A)** serum amylase, **(B)** pancreatic trypsin activity and **(C)** pancreatic myeloperoxidase (MPO) activity, with more marked elevation of pancreatic trypsin and MPO activity at 24 h. Intraperitoneal administration of CM_128 at 20 mg/kg late significantly reduced all parameters from levels at 6 h (mean ± s.e.m., ≥6 mice/group; *p<0.05, control vs two models at 6 h; †p<0.05 two models at 6 h vs at 24 h; ‡p<0.05 TLCS-AP at 6 h vs TLCS-AP plus CM_128; §P<0.05 FAEE-AP at 6 h vs FAEE-AP plus CM_128).

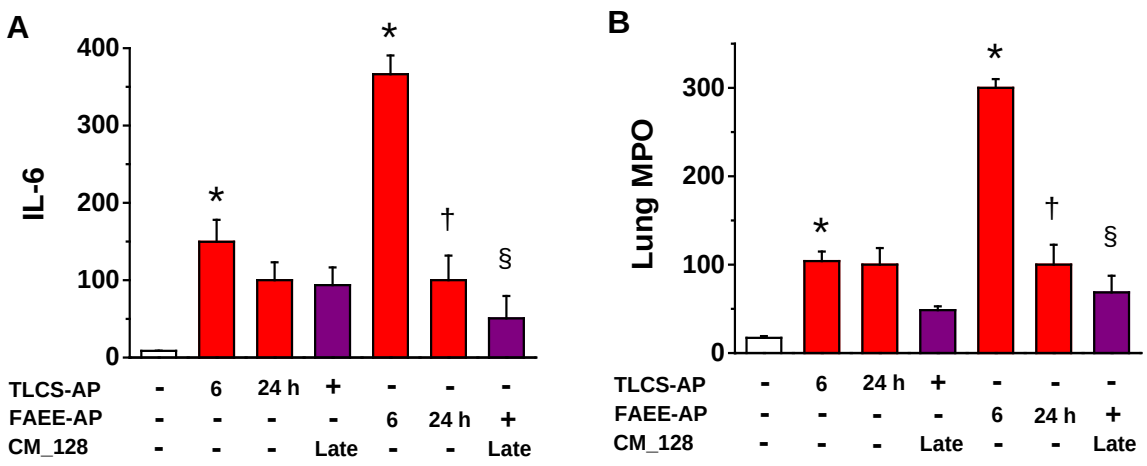

Figure 6.7 Systemic biochemical parameters at 6 h and 24 h in TLCS-AP and FAEE-AP. The two models at 6 h and 24 h resulted in substantial elevations of **(A)** IL-6 and **(B)** lung myeloperoxidase (MPO) activity, with more elevation at 6 h. Intraperitoneal administration of CM_128 at 20 mg/kg late significantly reduced all parameters from levels at 6 h (mean ± s.e.m. ≥6 mice/group; *p<0.05, control vs two models at 6 h; †p<0.05 two models at 6 h vs at 24 h; ‡p<0.05 TLCS-APO at 6 h vs TLCS-AP plus CM_128; §P<0.05 FAEE-AP at 6 h vs FAEE-AP plus CM_128).

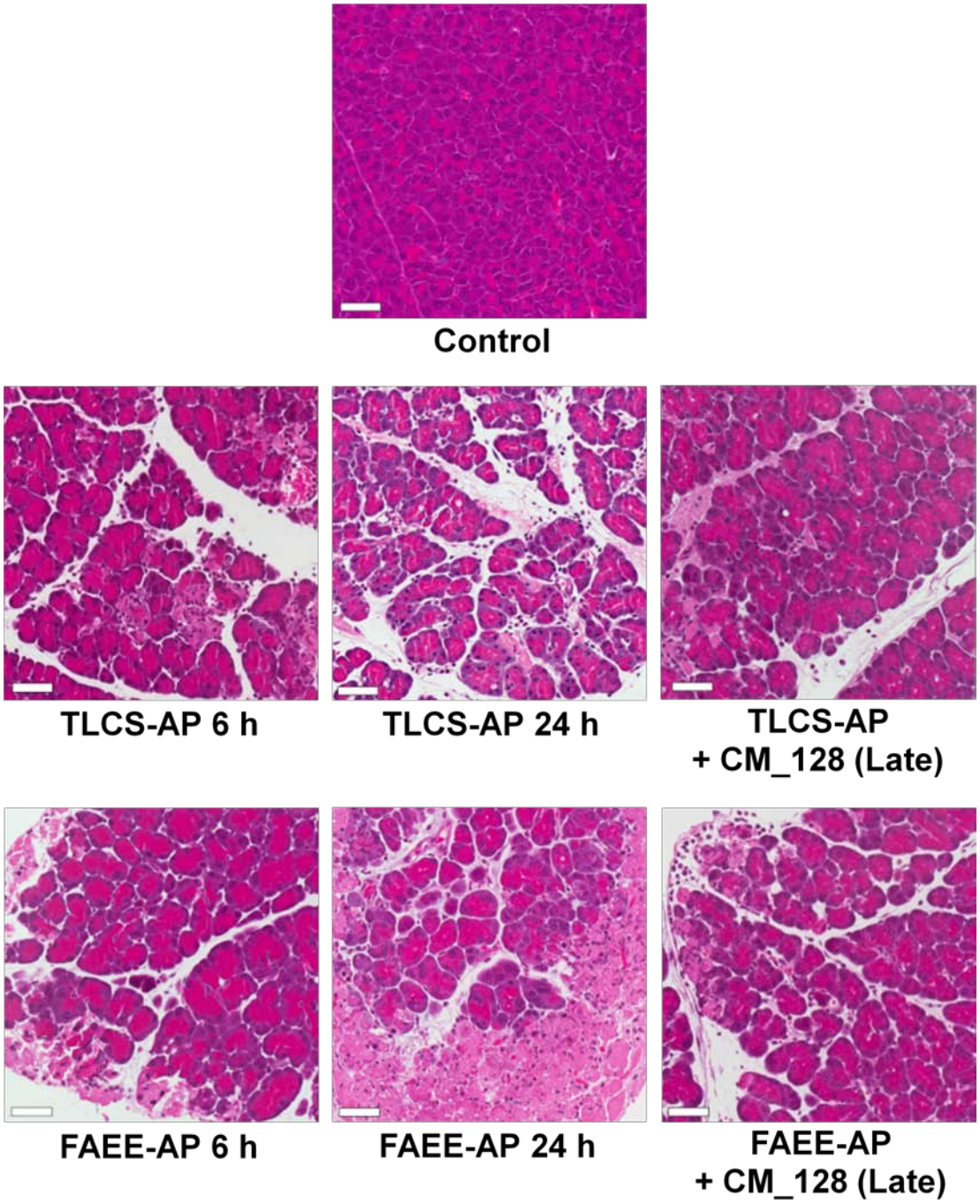

Figure 6.8 Typical histopathology from TLCS-AP and FAEE-AP showing extent of injury at 6 h and following late administration of CM_128. Representative histological images showing normal pancreatic histology, typical histopathology from two models at 6 h and 24 h and typical histopathology from two models after treatment with CM_128 late after disease induction (Haematoxylin and Eosin, H&E; scale bar= 50 µM).

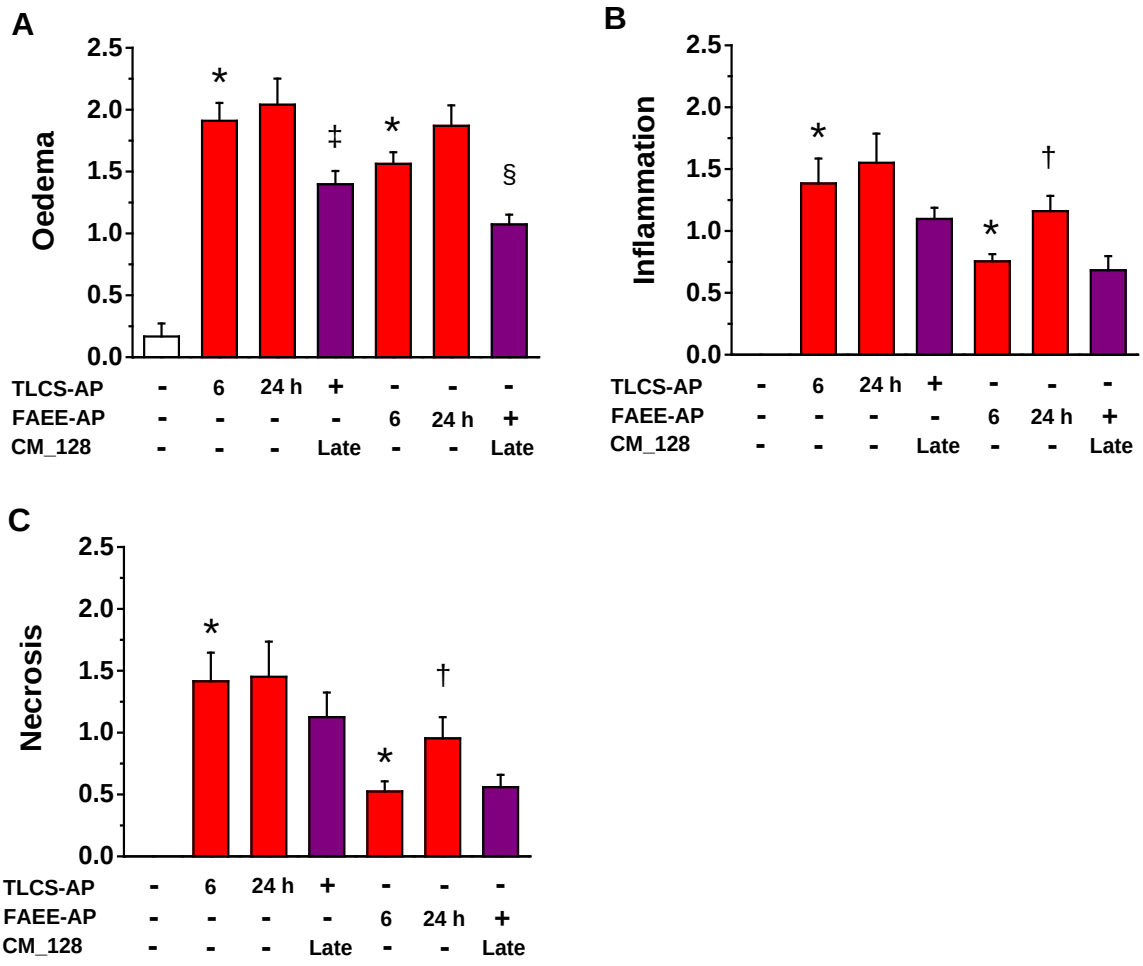

Figure 6.9 Histopathological scores of TLCS-AP and FAEE-AP showing extent of injury at 6 h and following late administration of CM_128. The two models at 6 h and 24 h resulted in substantially progressive increases in **(A)** oedema, **(B)** inflammation and **(C)** necrosis scores, with more marked elevation of all scores at 24 h. Intraperitoneal administration of CM_128 at 20 mg/kg from 6 h after disease induction significantly reduced oedema, but not inflammation, necrosis and total histopathology scores at 6 h (mean ± s.e.m., ≥6 mice/group; *p<0.05, control vs two models at 6 h; †p<0.05 two models at 6 h vs at 24 h; ‡p<0.05 TLCS-AP at 6 h vs TLCS-AP plus CM_128; §P<0.05 FAEE-AP at 6 h vs FAEE-AP plus CM_128).

6.4 Discussion

Intraperitoneal administration of CM_128 at 20 mg/kg significantly reduced a broad range of biochemical, immunological and histopathological disease parameters in TLCS-AP and FAEE-AP, which are representative models of gallstone and alcoholic acute pancreatitis (Lerch and Gorelick, 2013, Huang et al., 2014). These findings are consistent with previously findings *in vitro* (Chapter 3, data from CalciMedica and (Wen et al., 2015)), in CER-AP (data from CalciMedica) and with GSK-7975A in three models of experimental acute pancreatitis (Chapter 4 and 5). CM_128 is highly potent but with high levels of plasma and tissue binding; the pharmacokinetic study indicated that CM_128 levels are ~10 µM in blood, ~50 µM in the pancreas and ~30 µM in the lung 11 h after the last dose, levels which were highly effective in reducing all disease parameters. These data provide robust preclinical validation of SOCE inhibition by CM_128 as a therapeutic approach for treating AP.

Treatment of CM_128 begun late was less protective in both models, although it did prevent parameters from increasing. Consistently with the findings from experiments with GSK-7975A, both compounds were administered after disease induction to model treatment of clinical acute pancreatitis, but delay in administration of either compound to 6 h after disease induction resulted in diminished efficacy. As concluded in Chapter 5, these data also strongly suggest that door-to-needle time is an important issue in administration of any treatment for acute pancreatitis that targets the pathogenesis of pancreatic injury. To minimise the initiation of a treatment, a quicker approach to recruit patient is required for trials of any therapy, such as that offered here with Orai inhibition by CM_128, a novel molecular entity currently undergoing preclinical toxicological evaluation prior to Phase I trials.

6.5 Summary

The data presented in this Chapter demonstrate that intraperitoneal administration of CM_128, a novel Orai inhibitor, at 20 mg/kg 1 h (early) and 6 h (late) after disease induction significantly reduced disease severity in two clinically representative models of acute pancreatitis. Treatment with CM_128 begun early showed more marked reduction of all parameters than that begun late. These data confirm the hypothesis that cytosolic Ca^{2+} overload is a critical trigger of AP and indicate that door-to-needle time is an important issue. Since an analogue of CM_128 has been tested in humans and been found to be safe, CM_128 would appear to have significant potential as a treatment for human acute pancreatitis.

Chapter 7

Overview

7.1 Targeting Ca^{2+} signalling to treat AP

Intracellular Ca^{2+} overload plays a central role in a variety of diseases, such as myocardial infarction (Garcia-Dorado et al., 2012), cardiac hypertrophy and vascular proliferative disease (Lompre et al., 2013), acute ischemic stroke (Tuttolomondo et al., 2009), Alzheimer disease (Demuro et al., 2010), atherosclerosis (Prendergast et al., 2014) and AP (Lankisch et al., 2015). Cautions should be taken as cells from different systems have their unique set of components from the Ca^{2+}-signalling toolkit to regulate cytosolic Ca^{2+} overload in response to toxins and to mediate subsequent pathophysiological processes (Berridge et al., 2003). Better understanding of the unique pathogenesis of each disease is required to search suitable therapeutic targets for preventing Ca^{2+} overload in the cytosol. For instance, targeting neuronal voltage-gated cation channels, particularly blockers of calcium and sodium channels may be beneficial following ischemic stroke *in vitro* and *in vivo*, but have yet yielded a significant clinical benefit (Tuttolomondo et al., 2009). Targeting the late sodium current (I_{Na}) could reduce Ca^{2+} overload after myocardial ischemia with a successful translation into clinical as an anti-ischemic agent (Madonna et al., 2013). Targeting SOCE via Orai1 channels as described in this thesis could prevent cytosolic Ca^{2+} overload induced by toxins in PACs and protect against AP.

Mounting evidence suggests that cytosolic Ca^{2+} overload is the key trigger and early common mechanism for PAC injury in most if not all forms of AP (Ward et al., 1995, Lankisch et al., 2015). It has been noted for many years that SOCE is the rate-limiting step for abnormal Ca^{2+} signal generation in PACs induced by pancreatitis toxins (Petersen and Sutton, 2006). Molecular components (Orai1 and STIM1) of this

Ca^{2+} entry pathway have been identified (Liou et al., 2005, Prakriya et al., 2006) and pharmacological Orai channel inhibitors have emerged during recent years (Sweeney et al., 2009, Parekh, 2010, Jairaman and Prakriya, 2013). These advances make it possible to investigate the roles of SOCE in AP and various other diseases. The studies described in this thesis have successfully demonstrated SOCE via Orai channels plays a pivotal role in the pathogenesis of AP and confirmed the hypothesis that prolonged elevation of $[Ca^{2+}]_c$ is toxic and is the key trigger of AP (Ward et al., 1995), providing a valid therapeutic tool for treating human AP.

SOCE is the principle mechanism of Ca^{2+} influx in non-excitable cells (Abdullaev et al., 2008). The critical role of Orai channels in the pathogenesis of several other diseases has been noted. For instance, McCarl *et al* demonstrated the important *in vitro* and *in vivo* role of Orai1 channel for T cell-mediated autoimmunity and allograft rejection using T cells from SCID patients and mice expressing non-functional Orai-R91W protein, respectively (McCarl et al., 2010). Vig *et al* showed Orai1 deficient mice exhibited defective mast cell effector function and the inhibition of allergic reaction elicited (Vig et al., 2008). Braun *et al* showed Orai1 is strongly expressed in human and mouse platelets and Orai1 deficiency in mice resulted in resistance to pulmonary thromboembolism, arterial thrombosis and ischemic brain infarction with only mild bleeding time prolongation (Braun et al., 2009). Yang *et al* demonstrated SOCE mediated via Orai1 and STIM1 is essential for breast tumor cell migration *in vitro* and tumor metastasis *in vivo* (Yang et al., 2009). SOCE via Orai1 channel was the predominant mechanism that mediates neutrophil recruitment in response to acute inflammation (Schaff et al., 2010). Moreover, the protective effects of Orai1

inhibition by 2-APB or GSK-7975A/Synta-66 have also been observed *in vitro* and *in vivo* models of the diseases, such as allergic rhinitis (Lin et al., 2011), stroke (van Kruchten et al., 2012) and asthma (Ashmole et al., 2012). Together with the observations in this thesis, all these investigations indicate much broader potential applications of Orai1 inhibitors with significant clinical impact.

Orai1 was firstly discovered from the patients with hereditary SCID syndrome, who presented as infants with a marked propensity for fungal and viral infections and had the defect in SOCE and CRAC channel function (Feske et al., 2006). Orai1 knockout ($Orai1^{-/-}$) mice were smaller in size and exhibited clinical relevant phenotypes about immunodeficiency with defective T- and B-cell function, impaired mast cell function (Vig et al., 2008, Gwack et al., 2008). Gwack *et al* found $Orai1^{-/-}$ mice with the inbred C57BL/6 background were perinatal lethality, which could overcome by crossing them to outbred ICR mice and had eyelid irritation and sporadic hair loss (Gwack et al., 2008). Since immunological events are known to be one critical component in the development and progression of AP, targeting Orai1 channels could be an attractive strategy for treating AP on the one hand. There are clear evidences indicating the inflammatory cells and their functions are critical determinants of AP severity. Depletion of neutrophil markedly reduced the severity of caerulein-, CDE diet-induced AP (Sandoval et al., 1996, Frossard et al., 1999, Gukovskaya et al., 2002). Demols *et al* showed AP severity significantly decreased in nude mice and CD4+ (but not CD8+)-depleted mice, suggesting T cells-predominantly CD4+ T cells play a pivotal role in the development of experimental AP (Demols et al., 2000). Moreover, platelet activation significantly enhanced in AP patients and was associated with AP severity with a more pronounced increase in more severe form of the disease

(Mimidis et al., 2004, Beyazit et al., 2012, Osada et al., 2012). Depletion of platelet protected against caerulein- and L-arginine-induced experimental AP with decreased neutrophil infiltration (Abdulla et al., 2011) . The functions of neutrophils, T-cells and platelets all can possibly be altered by inhibition of Orai1, which was expected to ameliorate disease severity to some extent during AP. On the other hand, phenotypic data from SCID patient and Orai1-deficient mice highlights the importance of CRAC channel function for immune defence, especially for lymphocyte activation. Moreover, the normal function of immune defence at the late stage of AP is certainly important in mediating the morbidity and mortality since the death at the late stage of AP is mainly caused by infected necrosis (Raraty et al., 2004, Petrov et al., 2010).

Apart from inhibition of SOCE via Orai1 channels to prevent Ca^{2+} overload, inhibition of primary Ca^{2+} release through IP_3Rs and RyRs has been shown to be protective *in vitro* and *in vivo* models of AP (Husain et al., 2005, Gerasimenko et al., 2009, Orabi et al., 2012, Husain et al., 2012), but ubiquitous expression of IP_3Rs and RyRs and their physiological important roles preclude them to be translated as a safe therapeutic tool. Ca^{2+} extrusion from PACs is largely dependent on PMCA pump activity since Na^{+}-Ca^{2+} exchanger is of little quantitative importance (Petersen and Sutton, 2006). Highly ATP-dependent PAC Ca^{2+} extrusion highlights mitochondrial protection as a potentially useful approach for efficient Ca^{2+} handling in the development of AP.

Pancreatitis toxins caused mitochondrial Ca^{2+} overload as a result of cytosolic Ca^{2+} overload, leading to $\Delta\Psi_M$ depletion, uncoupling of oxidative phosphorylation and

impairment of ATP production (Voronina et al., 2002, Criddle et al., 2004, Criddle et al., 2006, Mukherjee et al., 2008). Cyp D a mitochondrial matrix protein encoded by *Ppif* gene, is the key regulator of MPTP opening. Compared with Orai1 knockout phenotypes, Cyp D-deficient (*Ppif*$^{-/-}$) mice are viable, fertile and have no obvious abnormalities. Accumulative evidences showed Cyp D-dependent MPTP plays critical role in acute cellular injuries such as cardiac and cerebral I/R injury (Baines et al., 2005, Nakagawa et al., 2005). Two studies demonstrated genetic deletion and pharmacological inhibition of Cyp D markedly reduced AP severity *in vitro* and *in vivo* (Shalbueva et al., 2013, Mukherjee et al., 2015). Development of specific Cyp D inhibitors has much wider clinical applications. The agents currently in the market are all general cyclophilin inhibitors with specificity lack for Cyp D. Moreover, preservation of mitochondrial function may have a much broader therapeutic window and also have more potential for preserving other vital organ function (not only the pancreas) than targeting Ca^{2+} overload. Experimental evidence suggested mitochondrial respiration rates are affected at different time points after the onset of AP; 6 h after in the pancreas, 24 h after in the kidney and 48 h after in the lung, respectively (Trumbeckaite et al., 2013). The duration of mitochondrial function stays intact after disease onset offers good opportunity for the drug that preserves mitochondrial function to exert its roles.

7.2 Other strategies to treat AP

The exocrine pancreas is the organ within the whole body that has the highest level of protein synthesis and secretion. Maintaining ER homeostasis is of particularly importance for pancreatic physiology and unfolded protein responses (UPRs) as a copying mechanism of ER stress play a critical role in the disease status (Logsdon

and Ji, 2013). UPRs are mediated by three distinct ER-transmembrane protein sensors, namely double strand RNA-activated protein kinase-like ER kinase (PERK), inositol-requiring kinase 1 alpha (IRE1α) and activating transcription factor (ATF) 6. ER chaperones BiP (immunoglobulin heavy chain binding protein, also known as GRP78) dissociates from these sensors and binds to unfolded/misfolded polypeptide in the ER lumen(Austin, 2009, Kim et al., 2008, Zhang and Kaufman, 2008). ER stress-induced cell death (apoptosis mainly) is mediated largely by C/EBP homologous protein (CHOP), which is a critical downstream component of ER-stress pathways at the convergence of PERK-eIF2α-ATF4, IRE1α and ATF6 pathways (Kim et al., 2008). Early massive dilatation of rough ER has been observed in experimental models of AP (Aho and Nevalainen, 1980, Lerch et al., 1992), indicating ER stress is an early event in the pathogenesis of AP. ER-stress related processes, including PERK phosphorylation, eIF2α phosphorylastion, BiP upregulation, X box binding protein (XBP1) splicing, CHOP expression and caspase 12 activation, have been detected during hyperstimulation *in vitro* and L-arginine-induced *in vivo* models of AP (Kubisch et al., 2006, Kubisch and Logsdon, 2007). Emerging evidences suggest alteration of some components such as BiP, XBP1 and CHOP in the UPR pathway can affect the severity of AP (Suyama et al., 2008, Ye et al., 2010, Lugea et al., 2011). Thus, the strategies that enhance the efficacy or sustain the ability of UPR could be potential approach for overcoming the disease induced by defective ER stress.

The hallmark of AP is premature digestive enzyme activation and loss-of-function mutation in PRSS1 was associated with hereditary pancreatitis (Whitcomb et al., 1996), providing further confirmation. Mice lacking trypsinogen isoform 7 (T7) gene

exhibited a 50% reduction in acinar necrosis during AP (Dawra et al., 2011), suggesting inhibition of trypsinogen activation could be beneficial. Early NF-κB activation was detectable and most previous studies indicated the blockage of NF-κB activation is beneficial in several experimental AP models (Rakonczay et al., 2008). On the other hand, Algul *et al* showed constitutive deletion of pancreas-specific RelA lead to more severe pancreatic damage and systemic complications (Algul et al., 2007); Huang *et al* recently demostrated co-expression of IKKβ and p65 results in more severe form of caerulein-induced panceatitis (Huang et al., 2013). All these observation implied NF-κB activation paly multideimensional roles in the pathogenesis of AP, suggesting cautions should be taken into account for targeting NF-κB activation. Pancreatic ductal cells also as the initial site of injury could be another potential target for preventing AP (Hegyi and Petersen, 2013).

Immune responses are one independent, but synergic determinant of AP severity. Tissue injuries caused by toxins use the same set of the immune sensors and initiators, such as toll-like receptors (TLRs), nucleotide-binding domain (NOD)-like receptors (NLRs) and receptor for advanced glycation end-products (RAGE), to initiate sterile inflammation (Chen and Nunez, 2010). There are emerging evidences indicated targeting these inflammatory sensors, such as TLR4 and TLR9 to prevent inflammation initiation could be protective in AP (Sharif et al., 2009, Hoque et al., 2011). On the other hand, cell death (RCD) in parenchymal cells can promote inflammation by the release of pro-inflammatory cytokines and/or DAMPs. Following an initial event, cell death and inflammation can induce and amplify each other to exaggerate the disease (Linkermann et al., 2014). Necroptosis is activated by death receptor, including tumor necrosis factor receptor 1 (TNFR1) and is dependent on

receptor-interacting protein kinase (RIP) and mixed lineage kinase domain-like protein (MLKL)(Sun et al., 2012, Vandenabeele et al., 2010, Linkermann and Green, 2014). Genetic deletion of TNFR1 and RIP3 protected from experimental AP (Denham et al., 1997, He et al., 2009), suggesting some role of necroptosis in the pathogenesis of AP, though further investigations are required. Thus, targeting the upstream sensor of inflammation and/or the key components from RCD pathway can be potential therapeutic strategies for modulating the inflammation to prevent the progression of AP.

There are several potentially useful approaches that can be investigated from either intra-acinar pathways or immunological pathways, leading to search a cure for human AP. The studies presented in this thesis confirmed that inhibition of Orai1 channels to prevent Ca^{2+} overload is a valid therapeutic strategy for human AP. The experiments designed here have addressed several critical aspects concerning the development of clinically applicable Orai channel inhibitors, which will be discussed in this chapter.

7.3 SOCE mediated via Orai1 is a valid drug target for protecting against AP

The Orai1 channel fulfils several key criteria required of an ideal drug target, such as it is the principal channel for SOCE in PACs (Gerasimenko et al., 2013, Lur et al., 2009); it is proximal to the initiation of AP; it plays a pivotal role and acts as the key regulator in aberrant intracellular Ca^{2+} signalling during AP; possibly potential side effects can be favourably predicted according to its phenotype data. Well-established, diverse, *in vitro* and *in vivo* models of experimental AP were used in the studies

described in this thesis to validate the capability of Orai1 channel as a potential target for the treatment of AP.

Firstly, the effects of Orai inhibition was investigated in freshly isolated PACs, comprising the bulk of the pancreas and, together with ductal cells, the initial site of injury during AP (Sutton et al., 2003, Hegyi and Rakonczay, 2015). Clearly, GSK-7975A and the new molecular entity CM_128 markedly inhibit toxin-induced SOCE in murine and human PACs in a concentration-dependent manner, exceeding >90% block of relative control values in some protocols. It has been known for a long time that the severity of pancreatic damage correlates directly with the extent of necrosis *in vitro* as well as in distinct *in vivo* models of experimental AP (Kaiser et al., 1995, Criddle et al., 2007). In the studies here, GSK-7975A and CM_128 significantly reduced necrotic cell death pathway activation in murine and human PACs exposed to TLCS, which induces acute pancreatitis *in vivo* (Laukkarinen et al., 2007). The effects of GSK-7975A have been described on thapsigargin- and POAEE-induced SOCE as well as necrotic cell death pathway activation in murine PACs (Gerasimenko et al., 2013, Voronina et al., 2015). Here, GSK-7975A had a similarly critical effects on TLCS- and CCK-induced SOCE in murine PACs, as well as thapsigargin-induced SOCE and TLCS-induced necrotic cell death pathway activation in human PACs. CM_128 showed higher potency (IC_{50} ~0.1 µM from Orai1/STIM1-transfected HEK 293 cell patch clamp data) (Wen et al., 2015) and unlike GSK-7975A, no loss of efficacy at high doses. Administration of either compound within one hour following disease induction was markedly effective across a representative range of local and systemic biochemical, immunological and histopathological disease responses.

Orai channels also contribute to inflammatory cell responses, including neutrophil migration and activation (Bergmeier et al., 2013); inhibition of innate immune responses significantly reduces the severity of experimental AP (Gukovskaya et al., 2002), thus there may be a contribution here from Orai inhibition of immune cells. Nevertheless while knockout of Orai1/STIM1 SOCE inhibits neutrophils functions, it does not prevent all (Bergmeier et al., 2013); also data obtained in the NIHR Pancreas Biomedical Research Unit (not shown in this thesis) show that polymorphonuclear leukocyte reactive oxygen species (ROS) production is significantly reduced, but not abrogated, by Orai blockade with GSK-7975A. So the primary contribution of Orai blockade in this study is likely to have been in the pancreas. Orai blockade has less effect on other cell types in which Orai channels have less prominent roles, such as electrically excitable cells in which other ion channels, e.g. non-selective cation channels, have a larger role in Ca^{2+} entry (Choi et al., 2014). Non-selective cation channels permit limited SOCE into PACs (Gerasimenko et al., 2013, Kim et al., 2009) that could sustain essential Ca^{2+} entry.

7.4 Inhibitors of Orai1 have translational potential as a treatment for human AP

Previous work in Liverpool demonstrated that CCK-8 can directly act on murine and human PACs by activation of the CCK receptor (Murphy et al., 2008, Criddle et al., 2009), providing explannation for the use of CCK-8 *in vitro* and caerulein *in vivo* hyperstimulation models in this study. The hyperstimulation model also draws a parallel with human pancreatitis following scorpion bites from *Tityus trinitatis* (Bartholomew, 1970). TLCS-AP and FAEE-AP have been used in this study,

paralleling with two major causes - gallstone and alcohol abuse of AP, respectively. The reflux of bile plays a crucial role in the pathogenesis of human AP, which was firstly suggested by Opie (Opie, 1901). Subsequent study indicated it may not be bile acid alone, but ductal pressure or a combination that causes actual damage in human AP (Lerch and Gorelick, 2013). Effects of TLCS *in vitro* (Voronina et al., 2002) and *in vivo* (Laukkarinen et al., 2007, Perides et al., 2010) are stable, well-characterised and well-established. Non-oxidative metabolites of ethanol are key toxic components in alcohol-induced pancreatic damage *in vitro* (Criddle et al., 2004, Criddle et al., 2006). A combined application of ethanol and fatty acids, providing the fuel to form fatty acid ethyl esters within the pancreas, causes pancreatitis *in vivo* (Huang et al., 2014).

Both GSK-7975A and CM_128 blocked SOCE promptly, shown to result in complete block of human Orai1 by CM_128 at 1 µM (Wen et al., 2015). Both compounds protected against necrotic cell death pathway activation induced by TLCS, showing the same effects on murine and human PACs. Moreover, CM_128 at 1 µM significantly inhibited thapsigargin-induce SOCE, showing the same effects on murine and human PACs. These novel human data support the potential applicability of Orai1 inhibition as a treatment for clinical AP. Either compound has been administered after disease induction, showing pronounced protection in experimental models of AP.

7.5 Door-to-needle time is critical for the treatment of AP

Here both compounds were administered after disease induction to model treatment of clinical AP, but delay in administration of either compound to six hours after

disease induction resulted in diminished efficacy, dependent on the endpoint measured and the model employed. While biological time courses including that of AP are longer in humans than mice, with pancreatic necrosis typically detected within days rather than hours, human pancreatic acinar necrotic cell death pathway activation may begin in clinical pancreatitis at the early stage after disease onset, shown here in mouse models within six hours of onset.

Door-to-needle times of less than 60 minutes are established in guidelines for patients with acute myocardial infarction (30 min)(O'Gara et al., 2013) and acute ischaemic stroke (60 min) (Jauch et al., 2013), making every second count, with national and international quality improvement initiatives underway towards fully achieving these (Fonarow et al., 2014). Although pancreatic necrosis has a less rapid time course and is not the result of major arterial occlusion (Lankisch et al., 2015), the translational implication of the work presented here is that door-to-needle time is an important issue in administration of any treatment for acute pancreatitis. Previously clinical trials of treatments for acute pancreatitis have ‘enriched’ recruitment with patients predicted to have severe disease (often with recruitment up to 72 h after admission) (Lankisch et al., 2015, Villatoro et al., 2010), which delays initiation of therapy. Furthermore, the expansion of disease categories from the original Atlanta Classification (mild and severe)(Bradley, 1993) into the RAC (mild, moderate and severe)(Banks et al., 2013) and DBC (mild, moderate, severe, critical)(Dellinger et al., 2012), further complicates patient selection from among these potentially overlapping sub-groups.

Numerous compounds have been assessed in Phase II or Phase III clinical trials, but with rather disappointing outcomes. None of these compounds have become licensed drugs for treating AP. Understanding causes of failure could inform and guide us to improve trial design in the future. Implications of the work described in this thesis for clinical trial design is that the timing to initiate the treatment would be the key to gain the maximal therapeutic benefits, see **Figure 7.1**.

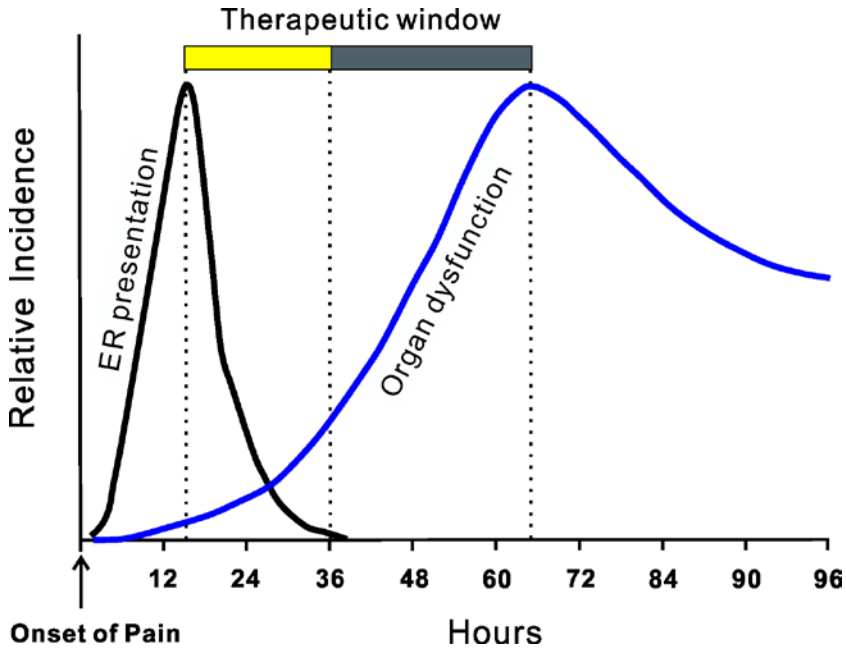

Figure 7.1. Optimal therapeutic window for the drug that targets the pathogenesis of AP. This plot indicates a potential therapeutic window for therapies targeting the pathogenesis of pancreatitis. The duration from emergency presentation to the established organ dysfunction allows for specific targeted treatment to be administered. Implications of the work in this thesis suggested initiation of certain treatment within the time that yellow bar indicated could gain the better therapeutic benefits than within the time that grew bar indicated. *Adapted from* (Norman, 1998)

7.6 Conclusion

Significant progresses have made for understanding the molecular mechanisms of AP and identifying the molecular components/regulators of each pathway. Novel insights into intracellular and immunological pathways, including the understanding of Ca^{2+} overload, mitochondrial dysfunction, ER stress and inflammation provide opportunities to identify/select promising therapeutic approaches. These potential strategies can be explored, confirmed and translated for human AP. The studies in this thesis firstly validate the hypothesis that cytosolic Ca^{2+} overload plays a pivotal role in the pathogenesis of AP; secondly provide a comprehensive preclinical validation of Orai1 channel inhibition as the treatment using *in vitro* and three diverse, clinically representative *in vivo* models of AP. Novel human data strongly suggested the translational potential of Orai channel inhibitors. The comparison of drug efficacy between early versus late time point indicated the door-to-needle time is an important issue for such treatment.

Implications from the work here are 1) the precise understanding of the mechanism is critically important for successfully identifying the therapeutic target; 2) the optimal therapeutic window time is much earlier than it is accepted for treatment that targets the pathogenesis of AP. Efforts should be made to minimise any delay of the initiation of the treatment in order to gain therapeutic benefit. Continuing basic research into the mechanism of AP will never end, continuously serving to exploit novel therapeutic strategies in the future. Ideas from other diseases that share similar pathophysiological processes could broad the exploration of novel drug targets for treating AP. The hope will be that a new specific targeted therapy for

treating AP will soon be translated into clinical usage, bringing benefits to our patients. Inhibition of Orai as described here could be such a treatment.

References

ABDULLA, A., AWLA, D., HARTMAN, H., RAHMAN, M., JEPPSSON, B., REGNER, S. & THORLACIUS, H. 2011. Role of platelets in experimental acute pancreatitis. *Br J Surg,* 98**,** 93-103.

ABDULLAEV, I. F., BISAILLON, J. M., POTIER, M., GONZALEZ, J. C., MOTIANI, R. K. & TREBAK, M. 2008. Stim1 and Orai1 mediate CRAC currents and store-operated calcium entry important for endothelial cell proliferation. *Circ Res,* 103**,** 1289-99.

AHO, H. J. & NEVALAINEN, T. J. 1980. Experimental pancreatitis in the rat. Ultrastructure of sodium taurocholate-induced pancreatic lesions. *Scand J Gastroenterol,* 15**,** 417-24.

AL-OMRAN, M., ALBALAWI, Z. H., TASHKANDI, M. F. & AL-ANSARY, L. A. 2010. Enteral versus parenteral nutrition for acute pancreatitis. *Cochrane Database Syst Rev***,** CD002837.

ALAVIAN, K. N., BEUTNER, G., LAZROVE, E., SACCHETTI, S., PARK, H. A., LICZNERSKI, P., LI, H., NABILI, P., HOCKENSMITH, K., GRAHAM, M., PORTER, G. A., JR. & JONAS, E. A. 2014. An uncoupling channel within the c-subunit ring of the F1FO ATP synthase is the mitochondrial permeability transition pore. *Proc Natl Acad Sci U S A,* 111**,** 10580-5.

ALGUL, H., TREIBER, M., LESINA, M., NAKHAI, H., SAUR, D., GEISLER, F., PFEIFER, A., PAXIAN, S. & SCHMID, R. M. 2007. Pancreas-specific RelA/p65 truncation increases susceptibility of acini to inflammation-associated cell death following cerulein pancreatitis. *J Clin Invest,* 117**,** 1490-501.

ASHMOLE, I., DUFFY, S. M., LEYLAND, M. L., MORRISON, V. S., BEGG, M. & BRADDING, P. 2012. CRACM/Orai ion channel expression and function in human lung mast cells. *J Allergy Clin Immunol,* 129**,** 1628-35 e2.

ASRANI, V., CHANG, W. K., DONG, Z., HARDY, G., WINDSOR, J. A. & PETROV, M. S. 2013. Glutamine supplementation in acute pancreatitis: a meta-analysis of randomized controlled trials. *Pancreatology,* 13**,** 468-74.

AUSTIN, R. C. 2009. The unfolded protein response in health and disease. *Antioxid Redox Signal,* 11**,** 2279-87.

BAINES, C. P., KAISER, R. A., PURCELL, N. H., BLAIR, N. S., OSINSKA, H., HAMBLETON, M. A., BRUNSKILL, E. W., SAYEN, M. R., GOTTLIEB, R. A., DORN, G. W., ROBBINS, J. & MOLKENTIN, J. D. 2005. Loss of cyclophilin D reveals a critical role for mitochondrial permeability transition in cell death. *Nature,* 434**,** 658-62.

BAINES, C. P., KAISER, R. A., SHEIKO, T., CRAIGEN, W. J. & MOLKENTIN, J. D. 2007. Voltage-dependent anion channels are dispensable for mitochondrial-dependent cell death. *Nat Cell Biol,* 9**,** 550-5.

BAKKER, O. J., ISSA, Y., VAN SANTVOORT, H. C., BESSELINK, M. G., SCHEPERS, N. J., BRUNO, M. J., BOERMEESTER, M. A. & GOOSZEN, H. G. 2014. Treatment options for acute pancreatitis. *Nat Rev Gastroenterol Hepatol,* 11**,** 462-9.

BAKKER, O. J., VAN SANTVOORT, H. C., VAN BRUNSCHOT, S., GESKUS, R. B., BESSELINK, M. G., BOLLEN, T. L., VAN EIJCK, C. H., FOCKENS, P., HAZEBROEK, E. J., NIJMEIJER, R. M., POLEY, J. W., VAN RAMSHORST, B., VLEGGAAR, F. P., BOERMEESTER, M. A., GOOSZEN, H. G., WEUSTEN, B. L., TIMMER, R. & DUTCH PANCREATITIS STUDY, G. 2012.

Endoscopic transgastric vs surgical necrosectomy for infected necrotizing pancreatitis: a randomized trial. *JAMA,* 307**,** 1053-61.

BANKS, P. A., BOLLEN, T. L., DERVENIS, C., GOOSZEN, H. G., JOHNSON, C. D., SARR, M. G., TSIOTOS, G. G., VEGE, S. S. & ACUTE PANCREATITIS CLASSIFICATION WORKING, G. 2013. Classification of acute pancreatitis--2012: revision of the Atlanta classification and definitions by international consensus. *Gut,* 62**,** 102-11.

BARR, V. A., BERNOT, K. M., SRIKANTH, S., GWACK, Y., BALAGOPALAN, L., REGAN, C. K., HELMAN, D. J., SOMMERS, C. L., OH-HORA, M., RAO, A. & SAMELSON, L. E. 2008. Dynamic movement of the calcium sensor STIM1 and the calcium channel Orai1 in activated T-cells: puncta and distal caps. *Mol Biol Cell,* 19**,** 2802-17.

BARTHOLOMEW, C. 1970. Acute scorpion pancreatitis in Trinidad. *Br Med J,* 1**,** 666-8.

BERGMEIER, W., WEIDINGER, C., ZEE, I. & FESKE, S. 2013. Emerging roles of store-operated Ca(2)(+) entry through STIM and ORAI proteins in immunity, hemostasis and cancer. *Channels (Austin),* 7**,** 379-91.

BERRIDGE, M. J., BOOTMAN, M. D. & RODERICK, H. L. 2003. Calcium signalling: dynamics, homeostasis and remodelling. *Nat Rev Mol Cell Biol,* 4**,** 517-29.

BEYAZIT, Y., SAYILIR, A., TORUN, S., SUVAK, B., YESIL, Y., PURNAK, T., OZTAS, E., KURT, M., KEKILLI, M. & IBIS, M. 2012. Mean platelet volume as an indicator of disease severity in patients with acute pancreatitis. *Clin Res Hepatol Gastroenterol,* 36**,** 162-8.

BHATIA, M. 2005. Inflammatory response on the pancreatic acinar cell injury. *Scand J Surg,* 94**,** 97-102.

BLEEKER, W. K., AGTERBERG, J., RIGTER, G., HACK, C. E. & GOOL, J. V. 1992. Protective effect of antithrombin III in acute experimental pancreatitis in rats. *Dig Dis Sci,* 37**,** 280-5.

BOOTH, D. M., MUKHERJEE, R., SUTTON, R. & CRIDDLE, D. N. 2011. Calcium and reactive oxygen species in acute pancreatitis: friend or foe? *Antioxid Redox Signal,* 15**,** 2683-98.

BOOTMAN, M. D., COLLINS, T. J., MACKENZIE, L., RODERICK, H. L., BERRIDGE, M. J. & PEPPIATT, C. M. 2002. 2-aminoethoxydiphenyl borate (2-APB) is a reliable blocker of store-operated Ca2+ entry but an inconsistent inhibitor of InsP3-induced Ca2+ release. *FASEB J,* 16**,** 1145-50.

BRADLEY, E. L., 3RD 1993. A clinically based classification system for acute pancreatitis. Summary of the International Symposium on Acute Pancreatitis, Atlanta, Ga, September 11 through 13, 1992. *Arch Surg,* 128**,** 586-90.

BRAUN, A., VARGA-SZABO, D., KLEINSCHNITZ, C., PLEINES, I., BENDER, M., AUSTINAT, M., BOSL, M., STOLL, G. & NIESWANDT, B. 2009. Orai1 (CRACM1) is the platelet SOC channel and essential for pathological thrombus formation. *Blood,* 113**,** 2056-63.

BUYUKBERBER, M., SAVAS, M. C., BAGCI, C., KORUK, M., GULSEN, M. T., TUTAR, E., BILGIC, T. & CEYLAN, N. O. 2009a. Therapeutic effect of caffeic acid phenethyl ester on cerulein-induced acute pancreatitis. *World J Gastroenterol,* 15**,** 5181-5.

BUYUKBERBER, M., SAVAS, M. C., BAGCI, C., KORUK, M., GULSEN, M. T., TUTAR, E., BILGIC, T., DEVECI, R. & KUCUK, C. 2009b. The beneficial effect of propolis on cerulein-induced experimental acute pancreatitis in rats. *Turk J Gastroenterol,* 20**,** 122-8.

CHAUDHARI, S., WU, P., WANG, Y., DING, Y., YUAN, J., BEGG, M. & MA, R. 2014. High glucose and diabetes enhanced store-operated Ca(2+) entry and increased expression of its signaling proteins in mesangial cells. *Am J Physiol Renal Physiol,* 306**,** F1069-80.

CHEN, C. C., WANG, S. S., TSAY, S. H., LEE, F. Y., WU, S. L., LU, R. H., CHANG, F. Y. & LEE, S. D. 1998. Effects of high dose octreotide on retrograde bile salt-induced pancreatitis in rats. *Peptides,* 19**,** 543-7.

CHEN, G., PANICKER, S., LAU, K. Y., APPARSUNDARAM, S., PATEL, V. A., CHEN, S. L., SOTO, R., JUNG, J. K., RAVINDRAN, P., OKUHARA, D., BOHNERT, G., CHE, Q., RAO, P. E., ALLARD, J. D., BADI, L., BITTER, H. M., NUNN, P. A., NARULA, S. K. & DEMARTINO, J. A. 2013. Characterization of a novel CRAC inhibitor that potently blocks human T cell activation and effector functions. *Mol Immunol,* 54**,** 355-67.

CHEN, G. Y. & NUNEZ, G. 2010. Sterile inflammation: sensing and reacting to damage. *Nat Rev Immunol,* 10**,** 826-37.

CHOI, S., MALETH, J., JHA, A., LEE, K. P., KIM, M. S., SO, I., AHUJA, M. & MUALLEM, S. 2014. The TRPCs-STIM1-Orai interaction. *Handb Exp Pharmacol,* 223**,** 1035-54.

COSEN-BINKER, L. I., BINKER, M. G., COSEN, R., NEGRI, G. & TISCORNIA, O. 2006. Relaxin prevents the development of severe acute pancreatitis. *World J Gastroenterol,* 12**,** 1558-68.

CRIDDLE, D. N., BOOTH, D. M., MUKHERJEE, R., MCLAUGHLIN, E., GREEN, G. M., SUTTON, R., PETERSEN, O. H. & REEVE, J. R., JR. 2009. Cholecystokinin-58 and cholecystokinin-8 exhibit similar actions on calcium

signaling, zymogen secretion, and cell fate in murine pancreatic acinar cells. *Am J Physiol Gastrointest Liver Physiol,* 297**,** G1085-92.

CRIDDLE, D. N., GERASIMENKO, J. V., BAUMGARTNER, H. K., JAFFAR, M., VORONINA, S., SUTTON, R., PETERSEN, O. H. & GERASIMENKO, O. V. 2007. Calcium signalling and pancreatic cell death: apoptosis or necrosis? *Cell Death Differ,* 14**,** 1285-94.

CRIDDLE, D. N., MURPHY, J., FISTETTO, G., BARROW, S., TEPIKIN, A. V., NEOPTOLEMOS, J. P., SUTTON, R. & PETERSEN, O. H. 2006. Fatty acid ethyl esters cause pancreatic calcium toxicity via inositol trisphosphate receptors and loss of ATP synthesis. *Gastroenterology,* 130**,** 781-93.

CRIDDLE, D. N., RARATY, M. G., NEOPTOLEMOS, J. P., TEPIKIN, A. V., PETERSEN, O. H. & SUTTON, R. 2004. Ethanol toxicity in pancreatic acinar cells: mediation by nonoxidative fatty acid metabolites. *Proc Natl Acad Sci U S A,* 101**,** 10738-43.

DAWRA, R., KU, Y. S., SHARIF, R., DHAULAKHANDI, D., PHILLIPS, P., DUDEJA, V. & SALUJA, A. K. 2008. An improved method for extracting myeloperoxidase and determining its activity in the pancreas and lungs during pancreatitis. *Pancreas,* 37**,** 62-8.

DAWRA, R., SAH, R. P., DUDEJA, V., RISHI, L., TALUKDAR, R., GARG, P. & SALUJA, A. K. 2011. Intra-acinar trypsinogen activation mediates early stages of pancreatic injury but not inflammation in mice with acute pancreatitis. *Gastroenterology,* 141**,** 2210-2217 e2.

DAWRA, R., SHARIF, R., PHILLIPS, P., DUDEJA, V., DHAULAKHANDI, D. & SALUJA, A. K. 2007. Development of a new mouse model of acute

pancreatitis induced by administration of L-arginine. *Am J Physiol Gastrointest Liver Physiol,* 292**,** G1009-18.

DELLINGER, E. P., FORSMARK, C. E., LAYER, P., LEVY, P., MARAVI-POMA, E., PETROV, M. S., SHIMOSEGAWA, T., SIRIWARDENA, A. K., UOMO, G., WHITCOMB, D. C., WINDSOR, J. A., PANCREATITIS ACROSS NATIONS CLINICAL, R. & EDUCATION, A. 2012. Determinant-based classification of acute pancreatitis severity: an international multidisciplinary consultation. *Ann Surg,* 256**,** 875-80.

DEMOLS, A., LE MOINE, O., DESALLE, F., QUERTINMONT, E., VAN LAETHEM, J. L. & DEVIERE, J. 2000. CD4(+)T cells play an important role in acute experimental pancreatitis in mice. *Gastroenterology,* 118**,** 582-90.

DEMURO, A., PARKER, I. & STUTZMANN, G. E. 2010. Calcium signaling and amyloid toxicity in Alzheimer disease. *J Biol Chem,* 285**,** 12463-8.

DENHAM, W., YANG, J., FINK, G., DENHAM, D., CARTER, G., WARD, K. & NORMAN, J. 1997. Gene targeting demonstrates additive detrimental effects of interleukin 1 and tumor necrosis factor during pancreatitis. *Gastroenterology,* 113**,** 1741-6.

DERLER, I., SCHINDL, R., FRITSCH, R., HEFTBERGER, P., RIEDL, M. C., BEGG, M., HOUSE, D. & ROMANIN, C. 2013. The action of selective CRAC channel blockers is affected by the Orai pore geometry. *Cell Calcium,* 53**,** 139-51.

DJURIC, S. W., BAMAUNG, N. Y., BASHA, A., LIU, H., LULY, J. R., MADAR, D. J., SCIOTTI, R. J., TU, N. P., WAGENAAR, F. L., WIEDEMAN, P. E., ZHOU, X., BALLARON, S., BAUCH, J., CHEN, Y. W., CHIOU, X. G., FEY, T., GAUVIN, D., GUBBINS, E., HSIEH, G. C., MARSH, K. C., MOLLISON, K. W., PONG, M., SHAUGHNESSY, T. K., SHEETS, M. P., SMITH, M., TREVILLYAN, J. M.,

WARRIOR, U., WEGNER, C. D. & CARTER, G. W. 2000. 3,5-Bis(trifluoromethyl)pyrazoles: a novel class of NFAT transcription factor regulator. *J Med Chem,* 43**,** 2975-81.

FERDEK, P. E., GERASIMENKO, J. V., PENG, S., TEPIKIN, A. V., PETERSEN, O. H. & GERASIMENKO, O. V. 2012. A novel role for Bcl-2 in regulation of cellular calcium extrusion. *Curr Biol,* 22**,** 1241-6.

FESKE, S., GWACK, Y., PRAKRIYA, M., SRIKANTH, S., PUPPEL, S. H., TANASA, B., HOGAN, P. G., LEWIS, R. S., DALY, M. & RAO, A. 2006. A mutation in Orai1 causes immune deficiency by abrogating CRAC channel function. *Nature,* 441**,** 179-85.

FONAROW, G. C., ZHAO, X., SMITH, E. E., SAVER, J. L., REEVES, M. J., BHATT, D. L., XIAN, Y., HERNANDEZ, A. F., PETERSON, E. D. & SCHWAMM, L. H. 2014. Door-to-needle times for tissue plasminogen activator administration and clinical outcomes in acute ischemic stroke before and after a quality improvement initiative. *JAMA,* 311**,** 1632-40.

FROSSARD, J. L., SALUJA, A., BHAGAT, L., LEE, H. S., BHATIA, M., HOFBAUER, B. & STEER, M. L. 1999. The role of intercellular adhesion molecule 1 and neutrophils in acute pancreatitis and pancreatitis-associated lung injury. *Gastroenterology,* 116**,** 694-701.

FUTATSUGI, A., NAKAMURA, T., YAMADA, M. K., EBISUI, E., NAKAMURA, K., UCHIDA, K., KITAGUCHI, T., TAKAHASHI-IWANAGA, H., NODA, T., ARUGA, J. & MIKOSHIBA, K. 2005. IP3 receptor types 2 and 3 mediate exocrine secretion underlying energy metabolism. *Science,* 309**,** 2232-4.

GARCIA-DORADO, D., RUIZ-MEANA, M., INSERTE, J., RODRIGUEZ-SINOVAS, A. & PIPER, H. M. 2012. Calcium-mediated cell death during myocardial reperfusion. *Cardiovasc Res,* 94**,** 168-80.

GASHAW, I., ELLINGHAUS, P., SOMMER, A. & ASADULLAH, K. 2011. What makes a good drug target? *Drug Discov Today,* 16**,** 1037-43.

GERASIMENKO, J. V., FLOWERDEW, S. E., VORONINA, S. G., SUKHOMLIN, T. K., TEPIKIN, A. V., PETERSEN, O. H. & GERASIMENKO, O. V. 2006. Bile acids induce Ca2+ release from both the endoplasmic reticulum and acidic intracellular calcium stores through activation of inositol trisphosphate receptors and ryanodine receptors. *J Biol Chem,* 281**,** 40154-63.

GERASIMENKO, J. V., GRYSHCHENKO, O., FERDEK, P. E., STAPLETON, E., HEBERT, T. O., BYCHKOVA, S., PENG, S., BEGG, M., GERASIMENKO, O. V. & PETERSEN, O. H. 2013. Ca2+ release-activated Ca2+ channel blockade as a potential tool in antipancreatitis therapy. *Proc Natl Acad Sci U S A,* 110**,** 13186-91.

GERASIMENKO, J. V., LUR, G., SHERWOOD, M. W., EBISUI, E., TEPIKIN, A. V., MIKOSHIBA, K., GERASIMENKO, O. V. & PETERSEN, O. H. 2009. Pancreatic protease activation by alcohol metabolite depends on Ca2+ release via acid store IP3 receptors. *Proc Natl Acad Sci U S A,* 106**,** 10758-63.

GERASIMENKO, O. V. & GERASIMENKO, J. V. 2012. Mitochondrial function and malfunction in the pathophysiology of pancreatitis. *Pflugers Arch,* 464**,** 89-99.

GIORGIO, V., VON STOCKUM, S., ANTONIEL, M., FABBRO, A., FOGOLARI, F., FORTE, M., GLICK, G. D., PETRONILLI, V., ZORATTI, M., SZABO, I., LIPPE, G. & BERNARDI, P. 2013. Dimers of mitochondrial ATP synthase form the permeability transition pore. *Proc Natl Acad Sci U S A,* 110**,** 5887-92.

GOLDACRE, M. J. & ROBERTS, S. E. 2004. Hospital admission for acute pancreatitis in an English population, 1963-98: database study of incidence and mortality. *Bmj,* 328**,** 1466-1469.

GOMATOS, I. P., XIAODONG, X., GHANEH, P., HALLORAN, C., RARATY, M., LANE, B., SUTTON, R. & NEOPTOLEMOS, J. P. 2014. Prognostic markers in acute pancreatitis. *Expert Rev Mol Diagn,* 14**,** 333-46.

GOTO, J., SUZUKI, A. Z., OZAKI, S., MATSUMOTO, N., NAKAMURA, T., EBISUI, E., FLEIG, A., PENNER, R. & MIKOSHIBA, K. 2010. Two novel 2-aminoethyl diphenylborinate (2-APB) analogues differentially activate and inhibit store-operated Ca(2+) entry via STIM proteins. *Cell Calcium,* 47**,** 1-10.

GROSS, S. A., WISSENBACH, U., PHILIPP, S. E., FREICHEL, M., CAVALIE, A. & FLOCKERZI, V. 2007. Murine ORAI2 splice variants form functional Ca2+ release-activated Ca2+ (CRAC) channels. *J Biol Chem,* 282**,** 19375-84.

GUKOVSKAYA, A. S., GUKOVSKY, I., ZANINOVIC, V., SONG, M., SANDOVAL, D., GUKOVSKY, S. & PANDOL, S. J. 1997. Pancreatic acinar cells produce, release, and respond to tumor necrosis factor-alpha. Role in regulating cell death and pancreatitis. *J Clin Invest,* 100**,** 1853-62.

GUKOVSKAYA, A. S., VAQUERO, E., ZANINOVIC, V., GORELICK, F. S., LUSIS, A. J., BRENNAN, M. L., HOLLAND, S. & PANDOL, S. J. 2002. Neutrophils and NADPH oxidase mediate intrapancreatic trypsin activation in murine experimental acute pancreatitis. *Gastroenterology,* 122**,** 974-84.

GUKOVSKY, I., PANDOL, S. J. & GUKOVSKAYA, A. S. 2011. Organellar dysfunction in the pathogenesis of pancreatitis. *Antioxid Redox Signal,* 15**,** 2699-710.

GWACK, Y., SRIKANTH, S., OH-HORA, M., HOGAN, P. G., LAMPERTI, E. D., YAMASHITA, M., GELINAS, C., NEEMS, D. S., SASAKI, Y., FESKE, S., PRAKRIYA, M., RAJEWSKY, K. & RAO, A. 2008. Hair loss and defective T- and B-cell function in mice lacking ORAI1. *Mol Cell Biol,* 28**,** 5209-22.

HARDMAN, J., SHIELDS, C., SCHOFIELD, D., MCMAHON, R., REDMOND, H. P. & SIRIWARDENA, A. K. 2005. Intravenous antioxidant modulation of end-organ damage in L-arginine-induced experimental acute pancreatitis. *Pancreatology,* 5**,** 380-6.

HARTMANN, J., DRAGICEVIC, E., ADELSBERGER, H., HENNING, H. A., SUMSER, M., ABRAMOWITZ, J., BLUM, R., DIETRICH, A., FREICHEL, M., FLOCKERZI, V., BIRNBAUMER, L. & KONNERTH, A. 2008. TRPC3 channels are required for synaptic transmission and motor coordination. *Neuron,* 59**,** 392-8.

HE, S., WANG, L., MIAO, L., WANG, T., DU, F., ZHAO, L. & WANG, X. 2009. Receptor interacting protein kinase-3 determines cellular necrotic response to TNF-alpha. *Cell,* 137**,** 1100-11.

HEGYI, P., PANDOL, S., VENGLOVECZ, V. & RAKONCZAY, Z., JR. 2011. The acinar-ductal tango in the pathogenesis of acute pancreatitis. *Gut,* 60**,** 544-52.

HEGYI, P. & PETERSEN, O. H. 2013. The exocrine pancreas: the acinar-ductal tango in physiology and pathophysiology. *Rev Physiol Biochem Pharmacol,* 165**,** 1-30.

HEGYI, P. & RAKONCZAY, Z., JR. 2015. The role of pancreatic ducts in the pathogenesis of acute pancreatitis. *Pancreatology*.

HEGYI, P., RAKONCZAY, Z., JR., SARI, R., GOG, C., LONOVICS, J., TAKACS, T. & CZAKO, L. 2004. L-arginine-induced experimental pancreatitis. *World J Gastroenterol,* 10**,** 2003-9.

HOQUE, R., MALIK, A. F., GORELICK, F. & MEHAL, W. Z. 2012. Sterile inflammatory response in acute pancreatitis. *Pancreas,* 41**,** 353-7.

HOQUE, R., SOHAIL, M., MALIK, A., SARWAR, S., LUO, Y., SHAH, A., BARRAT, F., FLAVELL, R., GORELICK, F., HUSAIN, S. & MEHAL, W. 2011. TLR9 and the NLRP3 inflammasome link acinar cell death with inflammation in acute pancreatitis. *Gastroenterology,* 141**,** 358-69.

HOTCHKISS, R. S., STRASSER, A., MCDUNN, J. E. & SWANSON, P. E. 2009. Cell death. *N Engl J Med,* 361**,** 1570-83.

HOU, X., PEDI, L., DIVER, M. M. & LONG, S. B. 2012. Crystal structure of the calcium release-activated calcium channel Orai. *Science,* 338**,** 1308-13.

HUANG, H., LIU, Y., DANILUK, J., GAISER, S., CHU, J., WANG, H., LI, Z. S., LOGSDON, C. D. & JI, B. 2013. Activation of nuclear factor-kappaB in acinar cells increases the severity of pancreatitis in mice. *Gastroenterology,* 144**,** 202-10.

HUANG, W., BOOTH, D. M., CANE, M. C., CHVANOV, M., JAVED, M. A., ELLIOTT, V. L., ARMSTRONG, J. A., DINGSDALE, H., CASH, N., LI, Y., GREENHALF, W., MUKHERJEE, R., KAPHALIA, B. S., JAFFAR, M., PETERSEN, O. H., TEPIKIN, A. V., SUTTON, R. & CRIDDLE, D. N. 2014. Fatty acid ethyl ester synthase inhibition ameliorates ethanol-induced Ca2+-dependent mitochondrial dysfunction and acute pancreatitis. *Gut,* 63**,** 1313-24.

HUSAIN, S. Z., ORABI, A. I., MUILI, K. A., LUO, Y., SARWAR, S., MAHMOOD, S. M., WANG, D., CHOO-WING, R., SINGH, V. P., PARNESS, J.,

ANANTHANARAVANAN, M., BHANDARI, V. & PERIDES, G. 2012. Ryanodine receptors contribute to bile acid-induced pathological calcium signaling and pancreatitis in mice. *Am J Physiol Gastrointest Liver Physiol,* 302**,** G1423-33.

HUSAIN, S. Z., PRASAD, P., GRANT, W. M., KOLODECIK, T. R., NATHANSON, M. H. & GORELICK, F. S. 2005. The ryanodine receptor mediates early zymogen activation in pancreatitis. *Proc Natl Acad Sci U S A,* 102**,** 14386-91.

ISHIKAWA, J., OHGA, K., YOSHINO, T., TAKEZAWA, R., ICHIKAWA, A., KUBOTA, H. & YAMADA, T. 2003. A pyrazole derivative, YM-58483, potently inhibits store-operated sustained Ca2+ influx and IL-2 production in T lymphocytes. *J Immunol,* 170**,** 4441-9.

JAIRAMAN, A. & PRAKRIYA, M. 2013. Molecular pharmacology of store-operated CRAC channels. *Channels (Austin),* 7**,** 402-14.

JAUCH, E. C., SAVER, J. L., ADAMS, H. P., JR., BRUNO, A., CONNORS, J. J., DEMAERSCHALK, B. M., KHATRI, P., MCMULLAN, P. W., JR., QURESHI, A. I., ROSENFIELD, K., SCOTT, P. A., SUMMERS, D. R., WANG, D. Z., WINTERMARK, M., YONAS, H., AMERICAN HEART ASSOCIATION STROKE, C., COUNCIL ON CARDIOVASCULAR, N., COUNCIL ON PERIPHERAL VASCULAR, D. & COUNCIL ON CLINICAL, C. 2013. Guidelines for the early management of patients with acute ischemic stroke: a guideline for healthcare professionals from the American Heart Association/American Stroke Association. *Stroke,* 44**,** 870-947.

JI, B., GAISER, S., CHEN, X., ERNST, S. A. & LOGSDON, C. D. 2009. Intracellular trypsin induces pancreatic acinar cell death but not NF-kappaB activation. *J Biol Chem,* 284**,** 17488-98.

JI, W., XU, P., LI, Z., LU, J., LIU, L., ZHAN, Y., CHEN, Y., HILLE, B., XU, T. & CHEN, L. 2008. Functional stoichiometry of the unitary calcium-release-activated calcium channel. *Proc Natl Acad Sci U S A,* 105**,** 13668-73.

JIN, H. T., LAMSA, T., HYVONEN, M. T., SAND, J., RATY, S., GRIGORENKO, N., KHOMUTOV, A. R., HERZIG, K. H., ALHONEN, L. & NORDBACK, I. 2008. A polyamine analog bismethylspermine ameliorates severe pancreatitis induced by intraductal infusion of taurodeoxycholate. *Surgery,* 144**,** 49-56.

JONES, B. F., BOYLES, R. R., HWANG, S. Y., BIRD, G. S. & PUTNEY, J. W. 2008. Calcium influx mechanisms underlying calcium oscillations in rat hepatocytes. *Hepatology,* 48**,** 1273-81.

KAISER, A. M., SALUJA, A. K., SENGUPTA, A., SALUJA, M. & STEER, M. L. 1995. Relationship between severity, necrosis, and apoptosis in five models of experimental acute pancreatitis. *Am J Physiol,* 269**,** C1295-304.

KIM, I., XU, W. & REED, J. C. 2008. Cell death and endoplasmic reticulum stress: disease relevance and therapeutic opportunities. *Nat Rev Drug Discov,* 7**,** 1013-30.

KIM, J. Y., KIM, K. H., LEE, J. A., NAMKUNG, W., SUN, A. Q., ANANTHANARAYANAN, M., SUCHY, F. J., SHIN, D. M., MUALLEM, S. & LEE, M. G. 2002. Transporter-mediated bile acid uptake causes Ca2+-dependent cell death in rat pancreatic acinar cells. *Gastroenterology,* 122**,** 1941-53.

KIM, K. D., SRIKANTH, S., TAN, Y. V., YEE, M. K., JEW, M., DAMOISEAUX, R., JUNG, M. E., SHIMIZU, S., AN, D. S., RIBALET, B., WASCHEK, J. A. & GWACK, Y. 2014. Calcium signaling via Orai1 is essential for induction of the

nuclear orphan receptor pathway to drive Th17 differentiation. *J Immunol,* 192**,** 110-22.

KIM, M. S., HONG, J. H., LI, Q., SHIN, D. M., ABRAMOWITZ, J., BIRNBAUMER, L. & MUALLEM, S. 2009. Deletion of TRPC3 in mice reduces store-operated Ca2+ influx and the severity of acute pancreatitis. *Gastroenterology,* 137**,** 1509-17.

KIM, M. S., LEE, K. P., YANG, D., SHIN, D. M., ABRAMOWITZ, J., KIYONAKA, S., BIRNBAUMER, L., MORI, Y. & MUALLEM, S. 2011. Genetic and pharmacologic inhibition of the Ca2+ influx channel TRPC3 protects secretory epithelia from Ca2+-dependent toxicity. *Gastroenterology,* 140**,** 2107-15, 2115 e1-4.

KOKOSZKA, J. E., WAYMIRE, K. G., LEVY, S. E., SLIGH, J. E., CAI, J., JONES, D. P., MACGREGOR, G. R. & WALLACE, D. C. 2004. The ADP/ATP translocator is not essential for the mitochondrial permeability transition pore. *Nature,* 427**,** 461-5.

KROEMER, G., GALLUZZI, L. & BRENNER, C. 2007. Mitochondrial membrane permeabilization in cell death. *Physiol Rev,* 87**,** 99-163.

KUBISCH, C. H. & LOGSDON, C. D. 2007. Secretagogues differentially activate endoplasmic reticulum stress responses in pancreatic acinar cells. *Am J Physiol Gastrointest Liver Physiol,* 292**,** G1804-12.

KUBISCH, C. H., SANS, M. D., ARUMUGAM, T., ERNST, S. A., WILLIAMS, J. A. & LOGSDON, C. D. 2006. Early activation of endoplasmic reticulum stress is associated with arginine-induced acute pancreatitis. *Am J Physiol Gastrointest Liver Physiol,* 291**,** G238-45.

KWONG, J. Q., DAVIS, J., BAINES, C. P., SARGENT, M. A., KARCH, J., WANG, X., HUANG, T. & MOLKENTIN, J. D. 2014. Genetic deletion of the mitochondrial phosphate carrier desensitizes the mitochondrial permeability transition pore and causes cardiomyopathy. *Cell Death Differ,* 21**,** 1209-17.

LANKISCH, P. G., APTE, M. & BANKS, P. A. 2015. Acute pancreatitis. *Lancet*.

LAUKKARINEN, J. M., VAN ACKER, G. J., WEISS, E. R., STEER, M. L. & PERIDES, G. 2007. A mouse model of acute biliary pancreatitis induced by retrograde pancreatic duct infusion of Na-taurocholate. *Gut,* 56**,** 1590-8.

LEE, K. P., CHOI, S., HONG, J. H., AHUJA, M., GRAHAM, S., MA, R., SO, I., SHIN, D. M., MUALLEM, S. & YUAN, J. P. 2014. Molecular determinants mediating gating of Transient Receptor Potential Canonical (TRPC) channels by stromal interaction molecule 1 (STIM1). *J Biol Chem,* 289**,** 6372-82.

LERCH, M. M. & GORELICK, F. S. 2013. Models of acute and chronic pancreatitis. *Gastroenterology,* 144**,** 1180-93.

LERCH, M. M., SALUJA, A. K., DAWRA, R., RAMARAO, P., SALUJA, M. & STEER, M. L. 1992. Acute necrotizing pancreatitis in the opossum: earliest morphological changes involve acinar cells. *Gastroenterology,* 103**,** 205-13.

LIN, L., ZHENG, C., ZHANG, L., DA, C. & ZHAO, K. 2011. 2-Aminoethoxydiphenyl borate administration into the nostril alleviates murine allergic rhinitis. *Am J Otolaryngol,* 32**,** 318-28.

LINKERMANN, A. & GREEN, D. R. 2014. Necroptosis. *N Engl J Med,* 370**,** 455-65.

LINKERMANN, A., STOCKWELL, B. R., KRAUTWALD, S. & ANDERS, H. J. 2014. Regulated cell death and inflammation: an auto-amplification loop causes organ failure. *Nat Rev Immunol,* 14**,** 759-67.

LIOU, J., KIM, M. L., HEO, W. D., JONES, J. T., MYERS, J. W., FERRELL, J. E., JR. & MEYER, T. 2005. STIM is a Ca2+ sensor essential for Ca2+-store-depletion-triggered Ca2+ influx. *Curr Biol,* 15**,** 1235-41.

LIOUDYNO, M. I., KOZAK, J. A., PENNA, A., SAFRINA, O., ZHANG, S. L., SEN, D., ROOS, J., STAUDERMAN, K. A. & CAHALAN, M. D. 2008. Orai1 and STIM1 move to the immunological synapse and are up-regulated during T cell activation. *Proc Natl Acad Sci U S A,* 105**,** 2011-6.

LOGSDON, C. D. & JI, B. 2013. The role of protein synthesis and digestive enzymes in acinar cell injury. *Nat Rev Gastroenterol Hepatol,* 10**,** 362-70.

LOMPRE, A. M., BENARD, L., SALIBA, Y., AUBART, F., FAUCONNIER, J. & HULOT, J. S. 2013. STIM1 and Orai in cardiac hypertrophy and vascular proliferative diseases. *Front Biosci (Schol Ed),* 5**,** 766-73.

LOWENFELS, A. B., MAISONNEUVE, P. & SULLIVAN, T. 2009. The changing character of acute pancreatitis: epidemiology, etiology, and prognosis. *Current gastroenterology reports,* 11**,** 97-103.

LUGEA, A., TISCHLER, D., NGUYEN, J., GONG, J., GUKOVSKY, I., FRENCH, S. W., GORELICK, F. S. & PANDOL, S. J. 2011. Adaptive unfolded protein response attenuates alcohol-induced pancreatic damage. *Gastroenterology,* 140**,** 987-97.

LUIK, R. M., WU, M. M., BUCHANAN, J. & LEWIS, R. S. 2006. The elementary unit of store-operated Ca2+ entry: local activation of CRAC channels by STIM1 at ER-plasma membrane junctions. *J Cell Biol,* 174**,** 815-25.

LUR, G., HAYNES, L. P., PRIOR, I. A., GERASIMENKO, O. V., FESKE, S., PETERSEN, O. H., BURGOYNE, R. D. & TEPIKIN, A. V. 2009. Ribosome-

free terminals of rough ER allow formation of STIM1 puncta and segregation of STIM1 from IP(3) receptors. *Curr Biol,* 19**,** 1648-53.

MADONNA, R., CEVIK, C. & NASSER, M. 2013. Electrical plasticity and cardioprotection in myocardial ischemia--role of selective sodium channel blockers. *Clin Cardiol,* 36**,** 255-61.

MALETH, J., RAKONCZAY, Z., JR., VENGLOVECZ, V., DOLMAN, N. J. & HEGYI, P. 2013. Central role of mitochondrial injury in the pathogenesis of acute pancreatitis. *Acta Physiol (Oxf),* 207**,** 226-35.

MANKAD, P., JAMES, A., SIRIWARDENA, A. K., ELLIOTT, A. C. & BRUCE, J. I. 2012. Insulin protects pancreatic acinar cells from cytosolic calcium overload and inhibition of plasma membrane calcium pump. *J Biol Chem,* 287**,** 1823-36.

MARENINOVA, O. A., HERMANN, K., FRENCH, S. W., O'KONSKI, M. S., PANDOL, S. J., WEBSTER, P., ERICKSON, A. H., KATUNUMA, N., GORELICK, F. S., GUKOVSKY, I. & GUKOVSKAYA, A. S. 2009. Impaired autophagic flux mediates acinar cell vacuole formation and trypsinogen activation in rodent models of acute pancreatitis. *J Clin Invest,* 119**,** 3340-55.

MARSHALL, J. C., COOK, D. J., CHRISTOU, N. V., BERNARD, G. R., SPRUNG, C. L. & SIBBALD, W. J. 1995. Multiple organ dysfunction score: a reliable descriptor of a complex clinical outcome. *Crit Care Med,* 23**,** 1638-52.

MCCARL, C. A., KHALIL, S., MA, J., OH-HORA, M., YAMASHITA, M., ROETHER, J., KAWASAKI, T., JAIRAMAN, A., SASAKI, Y., PRAKRIYA, M. & FESKE, S. 2010. Store-operated Ca2+ entry through ORAI1 is critical for T cell-mediated autoimmunity and allograft rejection. *J Immunol,* 185**,** 5845-58.

MENG, W., YUAN, J., ZHANG, C., BAI, Z., ZHOU, W., YAN, J. & LI, X. 2013. Parenteral analgesics for pain relief in acute pancreatitis: a systematic review. *Pancreatology,* 13**,** 201-6.

MICHAEL, E. S., KULIOPULOS, A., COVIC, L., STEER, M. L. & PERIDES, G. 2013. Pharmacological inhibition of PAR2 with the pepducin P2pal-18S protects mice against acute experimental biliary pancreatitis. *Am J Physiol Gastrointest Liver Physiol,* 304**,** G516-26.

MIMIDIS, K., PAPADOPOULOS, V., KOTSIANIDIS, J., FILIPPOU, D., SPANOUDAKIS, E., BOURIKAS, G., DERVENIS, C. & KARTALIS, G. 2004. Alterations of platelet function, number and indexes during acute pancreatitis. *Pancreatology,* 4**,** 22-7.

MOHSENI SALEHI MONFARED, S. S., VAHIDI, H., ABDOLGHAFFARI, A. H., NIKFAR, S. & ABDOLLAHI, M. 2009. Antioxidant therapy in the management of acute, chronic and post-ERCP pancreatitis: a systematic review. *World J Gastroenterol,* 15**,** 4481-90.

MOUNZER, R. & WHITCOMB, D. C. 2013. Genetics of acute and chronic pancreatitis. *Curr Opin Gastroenterol,* 29**,** 544-51.

MUIK, M., SCHINDL, R., FAHRNER, M. & ROMANIN, C. 2012. Ca(2+) release-activated Ca(2+) (CRAC) current, structure, and function. *Cell Mol Life Sci,* 69**,** 4163-76.

MUKHERJEE, R., CRIDDLE, D. N., GUKOVSKAYA, A., PANDOL, S., PETERSEN, O. H. & SUTTON, R. 2008. Mitochondrial injury in pancreatitis. *Cell Calcium,* 44**,** 14-23.

MUKHERJEE, R., MARENINOVA, O. A., ODINOKOVA, I. V., HUANG, W., MURPHY, J., CHVANOV, M., JAVED, M. A., WEN, L., BOOTH, D. M., CANE,

M. C., AWAIS, M., GAVILLET, B., PRUSS, R. M., SCHALLER, S., MOLKENTIN, J. D., TEPIKIN, A. V., PETERSEN, O. H., PANDOL, S. J., GUKOVSKY, I., CRIDDLE, D. N., GUKOVSKAYA, A. S., SUTTON, R. & AND, N. P. B. R. U. 2015. Mechanism of mitochondrial permeability transition pore induction and damage in the pancreas: inhibition prevents acute pancreatitis by protecting production of ATP. *Gut*.

MURPHY, J. A., CRIDDLE, D. N., SHERWOOD, M., CHVANOV, M., MUKHERJEE, R., MCLAUGHLIN, E., BOOTH, D., GERASIMENKO, J. V., RARATY, M. G., GHANEH, P., NEOPTOLEMOS, J. P., GERASIMENKO, O. V., TEPIKIN, A. V., GREEN, G. M., REEVE, J. R., JR., PETERSEN, O. H. & SUTTON, R. 2008. Direct activation of cytosolic Ca2+ signaling and enzyme secretion by cholecystokinin in human pancreatic acinar cells. *Gastroenterology,* 135**,** 632-41.

NAKAGAWA, T., SHIMIZU, S., WATANABE, T., YAMAGUCHI, O., OTSU, K., YAMAGATA, H., INOHARA, H., KUBO, T. & TSUJIMOTO, Y. 2005. Cyclophilin D-dependent mitochondrial permeability transition regulates some necrotic but not apoptotic cell death. *Nature,* 434**,** 652-8.

NATHAN, J. D., ROMAC, J., PENG, R. Y., PEYTON, M., MACDONALD, R. J. & LIDDLE, R. A. 2005. Transgenic expression of pancreatic secretory trypsin inhibitor-I ameliorates secretagogue-induced pancreatitis in mice. *Gastroenterology,* 128**,** 717-27.

NILIUS, B., OWSIANIK, G., VOETS, T. & PETERS, J. A. 2007. Transient receptor potential cation channels in disease. *Physiol Rev,* 87**,** 165-217.

NORMAN, J. 1998. The role of cytokines in the pathogenesis of acute pancreatitis. *Am J Surg,* 175**,** 76-83.

NUHN, P., MITKUS, T., CEYHAN, G. O., KUNZLI, B. M., BERGMANN, F., FISCHER, L., GIESE, N., FRIESS, H. & BERBERAT, P. O. 2013. Heme oxygenase 1-generated carbon monoxide and biliverdin attenuate the course of experimental necrotizing pancreatitis. *Pancreas,* 42**,** 265-71.

O'GARA, P. T., KUSHNER, F. G., ASCHEIM, D. D., CASEY, D. E., JR., CHUNG, M. K., DE LEMOS, J. A., ETTINGER, S. M., FANG, J. C., FESMIRE, F. M., FRANKLIN, B. A., GRANGER, C. B., KRUMHOLZ, H. M., LINDERBAUM, J. A., MORROW, D. A., NEWBY, L. K., ORNATO, J. P., OU, N., RADFORD, M. J., TAMIS-HOLLAND, J. E., TOMMASO, C. L., TRACY, C. M., WOO, Y. J., ZHAO, D. X., ANDERSON, J. L., JACOBS, A. K., HALPERIN, J. L., ALBERT, N. M., BRINDIS, R. G., CREAGER, M. A., DEMETS, D., GUYTON, R. A., HOCHMAN, J. S., KOVACS, R. J., KUSHNER, F. G., OHMAN, E. M., STEVENSON, W. G., YANCY, C. W. & AMERICAN COLLEGE OF CARDIOLOGY FOUNDATION/AMERICAN HEART ASSOCIATION TASK FORCE ON PRACTICE, G. 2013. 2013 ACCF/AHA guideline for the management of ST-elevation myocardial infarction: a report of the American College of Cardiology Foundation/American Heart Association Task Force on Practice Guidelines. *Circulation,* 127**,** e362-425.

ODINOKOVA, I. V., SUNG, K. F., MARENINOVA, O. A., HERMANN, K., GUKOVSKY, I. & GUKOVSKAYA, A. S. 2008. Mitochondrial mechanisms of death responses in pancreatitis. *J Gastroenterol Hepatol,* 23 Suppl 1**,** S25-30.

ORABI, A. I., LUO, Y., AHMAD, M. U., SHAH, A. U., MANNAN, Z., WANG, D., SARWAR, S., MUILI, K. A., SHUGRUE, C., KOLODECIK, T. R., SINGH, V. P., LOWE, M. E., THROWER, E., CHEN, J. & HUSAIN, S. Z. 2012. IP3 receptor

type 2 deficiency is associated with a secretory defect in the pancreatic acinar cell and an accumulation of zymogen granules. *PLoS One,* 7**,** e48465.

ORABI, A. I., SHAH, A. U., AHMAD, M. U., CHOO-WING, R., PARNESS, J., JAIN, D., BHANDARI, V. & HUSAIN, S. Z. 2010. Dantrolene mitigates caerulein-induced pancreatitis in vivo in mice. *Am J Physiol Gastrointest Liver Physiol,* 299**,** G196-204.

OSADA, J., WERESZCZYNSKA-SIEMIATKOWSKA, U., DABROWSKI, A. & DABROWSKA, M. I. 2012. Platelet activation in acute pancreatitis. *Pancreas,* 41**,** 1319-24.

OTSUKI, M., TANI, S., OKABAYSHI, Y., NAKAMURA, T., FUJII, M., FUJISAWA, T., BABA, S. & ITOH, H. 1989. Effect of a new cholecystokinin receptor antagonist CR 1392 on caerulein-induced acute pancreatitis in rats. *Pancreas,* 4**,** 237-43.

PANDOL, S. J., SALUJA, A. K., IMRIE, C. W. & BANKS, P. A. 2007. Acute pancreatitis: bench to the bedside. *Gastroenterology,* 132**,** 1127-51.

PAREKH, A. B. 2010. Store-operated CRAC channels: function in health and disease. *Nat Rev Drug Discov,* 9**,** 399-410.

PAREKH, A. B. & PUTNEY, J. W., JR. 2005. Store-operated calcium channels. *Physiol Rev,* 85**,** 757-810.

PARK, C. Y., HOOVER, P. J., MULLINS, F. M., BACHHAWAT, P., COVINGTON, E. D., RAUNSER, S., WALZ, T., GARCIA, K. C., DOLMETSCH, R. E. & LEWIS, R. S. 2009. STIM1 clusters and activates CRAC channels via direct binding of a cytosolic domain to Orai1. *Cell,* 136**,** 876-90.

PARK, M. K., ASHBY, M. C., ERDEMLI, G., PETERSEN, O. H. & TEPIKIN, A. V. 2001. Perinuclear, perigranular and sub-plasmalemmal mitochondria have

distinct functions in the regulation of cellular calcium transport. *EMBO J,* 20**,** 1863-74.

PASZKOWSKI, A. S., RAU, B., MAYER, J. M., MOLLER, P. & BEGER, H. G. 2002. Therapeutic application of caspase 1/interleukin-1beta-converting enzyme inhibitor decreases the death rate in severe acute experimental pancreatitis. *Ann Surg,* 235**,** 68-76.

PEERY, A. F., DELLON, E. S., LUND, J., CROCKETT, S. D., MCGOWAN, C. E., BULSIEWICZ, W. J., GANGAROSA, L. M., THINY, M. T., STIZENBERG, K., MORGAN, D. R., RINGEL, Y., KIM, H. P., DIBONAVENTURA, M. D., CARROLL, C. F., ALLEN, J. K., COOK, S. F., SANDLER, R. S., KAPPELMAN, M. D. & SHAHEEN, N. J. 2012. Burden of gastrointestinal disease in the United States: 2012 update. *Gastroenterology,* 143**,** 1179-87 e1-3.

PENNA, A., DEMURO, A., YEROMIN, A. V., ZHANG, S. L., SAFRINA, O., PARKER, I. & CAHALAN, M. D. 2008. The CRAC channel consists of a tetramer formed by Stim-induced dimerization of Orai dimers. *Nature,* 456**,** 116-20.

PERIDES, G., VAN ACKER, G. J., LAUKKARINEN, J. M. & STEER, M. L. 2010. Experimental acute biliary pancreatitis induced by retrograde infusion of bile acids into the mouse pancreatic duct. *Nat Protoc,* 5**,** 335-41.

PETERSEN, O. H. 2005. Ca2+ signalling and Ca2+-activated ion channels in exocrine acinar cells. *Cell Calcium,* 38**,** 171-200.

PETERSEN, O. H. 2012. Specific mitochondrial functions in separate sub-cellular domains of pancreatic acinar cells. *Pflugers Arch,* 464**,** 77-87.

PETERSEN, O. H. & SUTTON, R. 2006. Ca2+ signalling and pancreatitis: effects of alcohol, bile and coffee. *Trends Pharmacol Sci,* 27**,** 113-20.

PETERSEN, O. H., SUTTON, R. & CRIDDLE, D. N. 2006. Failure of calcium microdomain generation and pathological consequences. *Cell Calcium,* 40**,** 593-600.

PETERSEN, O. H. & TEPIKIN, A. V. 2008. Polarized calcium signaling in exocrine gland cells. *Annu Rev Physiol,* 70**,** 273-99.

PETERSEN, O. H., TEPIKIN, A. V., GERASIMENKO, J. V., GERASIMENKO, O. V., SUTTON, R. & CRIDDLE, D. N. 2009. Fatty acids, alcohol and fatty acid ethyl esters: toxic Ca2+ signal generation and pancreatitis. *Cell Calcium,* 45**,** 634-42.

PETROV, M. S., PYLYPCHUK, R. D. & EMELYANOV, N. V. 2008. Systematic review: nutritional support in acute pancreatitis. *Aliment Pharmacol Ther,* 28**,** 704-12.

PETROV, M. S., PYLYPCHUK, R. D. & UCHUGINA, A. F. 2009. A systematic review on the timing of artificial nutrition in acute pancreatitis. *Br J Nutr,* 101**,** 787-93.

PETROV, M. S., SHANBHAG, S., CHAKRABORTY, M., PHILLIPS, A. R. & WINDSOR, J. A. 2010. Organ failure and infection of pancreatic necrosis as determinants of mortality in patients with acute pancreatitis. *Gastroenterology,* 139**,** 813-20.

POROPAT, G., GILJACA, V., HAUSER, G. & STIMAC, D. 2015. Enteral nutrition formulations for acute pancreatitis. *Cochrane Database Syst Rev,* 3**,** CD010605.

PRAKRIYA, M., FESKE, S., GWACK, Y., SRIKANTH, S., RAO, A. & HOGAN, P. G. 2006. Orai1 is an essential pore subunit of the CRAC channel. *Nature,* 443**,** 230-3.

PRENDERGAST, C., QUAYLE, J., BURDYGA, T. & WRAY, S. 2014. Atherosclerosis affects calcium signalling in endothelial cells from apolipoprotein E knockout mice before plaque formation. *Cell Calcium,* 55**,** 146-54.

RAKONCZAY, Z., JR., HEGYI, P., TAKACS, T., MCCARROLL, J. & SALUJA, A. K. 2008. The role of NF-kappaB activation in the pathogenesis of acute pancreatitis. *Gut,* 57**,** 259-67.

RARATY, M., WARD, J., ERDEMLI, G., VAILLANT, C., NEOPTOLEMOS, J. P., SUTTON, R. & PETERSEN, O. H. 2000. Calcium-dependent enzyme activation and vacuole formation in the apical granular region of pancreatic acinar cells. *Proc Natl Acad Sci U S A,* 97**,** 13126-31.

RARATY, M. G., CONNOR, S., CRIDDLE, D. N., SUTTON, R. & NEOPTOLEMOS, J. P. 2004. Acute pancreatitis and organ failure: pathophysiology, natural history, and management strategies. *Curr Gastroenterol Rep,* 6**,** 99-103.

RARATY, M. G., MURPHY, J. A., MCLOUGHLIN, E., SMITH, D., CRIDDLE, D. & SUTTON, R. 2005. Mechanisms of acinar cell injury in acute pancreatitis. *Scand J Surg,* 94**,** 89-96.

RICE, L. V., BAX, H. J., RUSSELL, L. J., BARRETT, V. J., WALTON, S. E., DEAKIN, A. M., THOMSON, S. A., LUCAS, F., SOLARI, R., HOUSE, D. & BEGG, M. 2013. Characterization of selective Calcium-Release Activated Calcium channel blockers in mast cells and T-cells from human, rat, mouse and guinea-pig preparations. *Eur J Pharmacol,* 704**,** 49-57.

ROBERTS-THOMSON, S. J., PETERS, A. A., GRICE, D. M. & MONTEITH, G. R. 2010. ORAI-mediated calcium entry: mechanism and roles, diseases and pharmacology. *Pharmacol Ther,* 127**,** 121-30.

ROBERTS, S., WILLIAMS, J., MEDDINGS, D. & GOLDACRE, M. 2008. Incidence and case fatality for acute pancreatitis in England: geographical variation, social deprivation, alcohol consumption and aetiology–a record linkage study. *Alimentary pharmacology & therapeutics,* 28**,** 931-941.

ROLLINS, M. D., SUDARSHAN, S., FIRPO, M. A., ETHERINGTON, B. H., HART, B. J., JACKSON, H. H., JACKSON, J. D., EMERSON, L. L., YANG, D. T., MULVIHILL, S. J. & GLASGOW, R. E. 2006. Anti-inflammatory effects of PPAR-gamma agonists directly correlate with PPAR-gamma expression during acute pancreatitis. *J Gastrointest Surg,* 10**,** 1120-30.

RONGIONE, A. J., KUSSKE, A. M., KWAN, K., ASHLEY, S. W., REBER, H. A. & MCFADDEN, D. W. 1997. Interleukin 10 reduces the severity of acute pancreatitis in rats. *Gastroenterology,* 112**,** 960-7.

ROOS, J., DIGREGORIO, P. J., YEROMIN, A. V., OHLSEN, K., LIOUDYNO, M., ZHANG, S., SAFRINA, O., KOZAK, J. A., WAGNER, S. L., CAHALAN, M. D., VELICELEBI, G. & STAUDERMAN, K. A. 2005. STIM1, an essential and conserved component of store-operated Ca2+ channel function. *J Cell Biol,* 169**,** 435-45.

SAH, R. P., GARG, P. & SALUJA, A. K. 2012. Pathogenic mechanisms of acute pancreatitis. *Curr Opin Gastroenterol,* 28**,** 507-15.

SAKAI, Y., HAYAKAWA, T., KONDO, T., SHIBATA, T., KITAGAWA, M., SOBAJIMA, H., NARUSE, S. & OHNISHI, S. T. 1992. Protective effects of a prostaglandin E1 oligomer on taurocholate-induced rat pancreatitis. *J Gastroenterol Hepatol,* 7**,** 591-5.

SALUJA, A. K., LERCH, M. M., PHILLIPS, P. A. & DUDEJA, V. 2007. Why does pancreatic overstimulation cause pancreatitis? *Annu Rev Physiol,* 69**,** 249-69.

SAMAD, A., JAMES, A., WONG, J., MANKAD, P., WHITEHOUSE, J., PATEL, W., ALVES-SIMOES, M., SIRIWARDENA, A. K. & BRUCE, J. I. 2014. Insulin protects pancreatic acinar cells from palmitoleic acid-induced cellular injury. *J Biol Chem,* 289**,** 23582-95.

SANDOVAL, D., GUKOVSKAYA, A., REAVEY, P., GUKOVSKY, S., SISK, A., BRAQUET, P., PANDOL, S. J. & POUCELL-HATTON, S. 1996. The role of neutrophils and platelet-activating factor in mediating experimental pancreatitis. *Gastroenterology,* 111**,** 1081-91.

SATA, N., ATOMI, Y., KIMURA, W., KURODA, A., MUTO, T. & MINEO, C. 1994. Intracellular action of an exogenous low-molecular-weight synthetic protease inhibitor, E3123, in cerulein-induced acute pancreatitis in rats. *Int J Pancreatol,* 15**,** 119-27.

SCHAFF, U. Y., DIXIT, N., PROCYK, E., YAMAYOSHI, I., TSE, T. & SIMON, S. I. 2010. Orai1 regulates intracellular calcium, arrest, and shape polarization during neutrophil recruitment in shear flow. *Blood,* 115**,** 657-66.

SCHINZEL, A. C., TAKEUCHI, O., HUANG, Z., FISHER, J. K., ZHOU, Z., RUBENS, J., HETZ, C., DANIAL, N. N., MOSKOWITZ, M. A. & KORSMEYER, S. J. 2005. Cyclophilin D is a component of mitochondrial permeability transition and mediates neuronal cell death after focal cerebral ischemia. *Proc Natl Acad Sci U S A,* 102**,** 12005-10.

SCHNEIDER, L., PIETSCHMANN, M., HARTWIG, W., MARCOS, S. S., HACKERT, T., GEBHARD, M. M., UHL, W., BUCHLER, M. W. & WERNER, J. 2006. Inosine reduces microcirculatory disturbance and inflammatory organ damage in experimental acute pancreatitis in rats. *Am J Surg,* 191**,** 510-4.

SHALBUEVA, N., MARENINOVA, O. A., GERLOFF, A., YUAN, J., WALDRON, R. T., PANDOL, S. J. & GUKOVSKAYA, A. S. 2013. Effects of oxidative alcohol metabolism on the mitochondrial permeability transition pore and necrosis in a mouse model of alcoholic pancreatitis. *Gastroenterology,* 144**,** 437-446 e6.

SHARIF, R., DAWRA, R., WASILUK, K., PHILLIPS, P., DUDEJA, V., KURT-JONES, E., FINBERG, R. & SALUJA, A. 2009. Impact of toll-like receptor 4 on the severity of acute pancreatitis and pancreatitis-associated lung injury in mice. *Gut,* 58**,** 813-9.

SHIM, A. H., TIRADO-LEE, L. & PRAKRIYA, M. 2015. Structural and functional mechanisms of CRAC channel regulation. *J Mol Biol,* 427**,** 77-93.

SIMMONS, D. L. 2006. What makes a good anti-inflammatory drug target? *Drug Discov Today,* 11**,** 210-9.

SIRIWARDENA, A. K., MASON, J. M., BALACHANDRA, S., BAGUL, A., GALLOWAY, S., FORMELA, L., HARDMAN, J. G. & JAMDAR, S. 2007. Randomised, double blind, placebo controlled trial of intravenous antioxidant (n-acetylcysteine, selenium, vitamin C) therapy in severe acute pancreatitis. *Gut,* 56**,** 1439-44.

STATHOPULOS, P. B., ZHENG, L., LI, G. Y., PLEVIN, M. J. & IKURA, M. 2008. Structural and mechanistic insights into STIM1-mediated initiation of store-operated calcium entry. *Cell,* 135**,** 110-22.

SUN, L., WANG, H., WANG, Z., HE, S., CHEN, S., LIAO, D., WANG, L., YAN, J., LIU, W., LEI, X. & WANG, X. 2012. Mixed lineage kinase domain-like protein mediates necrosis signaling downstream of RIP3 kinase. *Cell,* 148**,** 213-27.

SUTTON, R., CRIDDLE, D., RARATY, M. G., TEPIKIN, A., NEOPTOLEMOS, J. P. & PETERSEN, O. H. 2003. Signal transduction, calcium and acute pancreatitis. *Pancreatology,* 3**,** 497-505.

SUYAMA, K., OHMURAYA, M., HIROTA, M., OZAKI, N., IDA, S., ENDO, M., ARAKI, K., GOTOH, T., BABA, H. & YAMAMURA, K. 2008. C/EBP homologous protein is crucial for the acceleration of experimental pancreatitis. *Biochem Biophys Res Commun,* 367**,** 176-82.

SWEENEY, Z. K., MINATTI, A., BUTTON, D. C. & PATRICK, S. 2009. Small-molecule inhibitors of store-operated calcium entry. *ChemMedChem,* 4**,** 706-18.

TACHIBANA, I., WATANABE, N., SHIROHARA, H., AKIYAMA, T., NAKANO, S. & OTSUKI, M. 1996. Effects of MCI-727 on pancreatic exocrine secretion and acute pancreatitis in two experimental rat models. *Pancreas,* 12**,** 165-72.

TACHIBANA, I., WATANABE, N., SHIROHARA, H., AKIYAMA, T., NANANO, S. & OTSUKI, M. 1995. Effects of tetraprenylacetone on pancreatic exocrine secretion and acute pancreatitis in two experimental models in rats. *Int J Pancreatol,* 17**,** 147-54.

TAKESHIMA, H., IINO, M., TAKEKURA, H., NISHI, M., KUNO, J., MINOWA, O., TAKANO, H. & NODA, T. 1994. Excitation-contraction uncoupling and muscular degeneration in mice lacking functional skeletal muscle ryanodine-receptor gene. *Nature,* 369**,** 556-9.

TENNER, S., BAILLIE, J., DEWITT, J., VEGE, S. S. & AMERICAN COLLEGE OF, G. 2013. American College of Gastroenterology guideline: management of acute pancreatitis. *Am J Gastroenterol,* 108**,** 1400-15; 1416.

TOLHURST, G., CARTER, R. N., AMISTEN, S., HOLDICH, J. P., ERLINGE, D. & MAHAUT-SMITH, M. P. 2008. Expression profiling and electrophysiological studies suggest a major role for Orai1 in the store-operated Ca2+ influx pathway of platelets and megakaryocytes. *Platelets,* 19**,** 308-13.

TOMITA, Y., KUWABARA, K., FURUE, S., TANAKA, K., YAMADA, K., UENO, M., ONO, T., MARUYAMA, T., AJIKI, T., ONOYAMA, H., YAMAMOTO, M. & HORI, Y. 2004. Effect of a selective inhibitor of secretory phospholipase A2, S-5920/LY315920Na, on experimental acute pancreatitis in rats. *J Pharmacol Sci,* 96**,** 144-54.

TRUMBECKAITE, S., KULIAVIENE, I., DEDUCHOVAS, O., KINCIUS, M., BANIENE, R., VIRKETYTE, S., BUKAUSKAS, D., JANSEN, E., KUPCINSKAS, L., BORUTAITE, V. & GULBINAS, A. 2013. Experimental acute pancreatitis induces mitochondrial dysfunction in rat pancreas, kidney and lungs but not in liver. *Pancreatology,* 13**,** 216-24.

TSAI, M. J., CHEN, C., CHEN, S. H., HUANG, Y. T. & CHIU, T. H. 2011. Pomalidomide suppresses cerulein-induced acute pancreatitis in mice. *J Gastroenterol,* 46**,** 822-33.

TSANG, S. W., IP, S. P. & LEUNG, P. S. 2004. Prophylactic and therapeutic treatments with AT 1 and AT 2 receptor antagonists and their effects on changes in the severity of pancreatitis. *Int J Biochem Cell Biol,* 36**,** 330-9.

TSE, F. & YUAN, Y. 2012. Early routine endoscopic retrograde cholangiopancreatography strategy versus early conservative management strategy in acute gallstone pancreatitis. *Cochrane Database Syst Rev,* 5**,** CD009779.

TUTTOLOMONDO, A., DI SCIACCA, R., DI RAIMONDO, D., ARNAO, V., RENDA, C., PINTO, A. & LICATA, G. 2009. Neuron protection as a therapeutic target in acute ischemic stroke. *Curr Top Med Chem,* 9**,** 1317-34.

VAN KRUCHTEN, R., BRAUN, A., FEIJGE, M. A., KUIJPERS, M. J., RIVERA-GALDOS, R., KRAFT, P., STOLL, G., KLEINSCHNITZ, C., BEVERS, E. M., NIESWANDT, B. & HEEMSKERK, J. W. 2012. Antithrombotic potential of blockers of store-operated calcium channels in platelets. *Arterioscler Thromb Vasc Biol,* 32**,** 1717-23.

VAN SANTVOORT, H. C., BAKKER, O. J., BOLLEN, T. L., BESSELINK, M. G., AHMED ALI, U., SCHRIJVER, A. M., BOERMEESTER, M. A., VAN GOOR, H., DEJONG, C. H., VAN EIJCK, C. H., VAN RAMSHORST, B., SCHAAPHERDER, A. F., VAN DER HARST, E., HOFKER, S., NIEUWENHUIJS, V. B., BRINK, M. A., KRUYT, P. M., MANUSAMA, E. R., VAN DER SCHELLING, G. P., KARSTEN, T., HESSELINK, E. J., VAN LAARHOVEN, C. J., ROSMAN, C., BOSSCHA, K., DE WIT, R. J., HOUDIJK, A. P., CUESTA, M. A., WAHAB, P. J., GOOSZEN, H. G. & DUTCH PANCREATITIS STUDY, G. 2011. A conservative and minimally invasive approach to necrotizing pancreatitis improves outcome. *Gastroenterology,* 141**,** 1254-63.

VAN SANTVOORT, H. C., BESSELINK, M. G., BAKKER, O. J., HOFKER, H. S., BOERMEESTER, M. A., DEJONG, C. H., VAN GOOR, H., SCHAAPHERDER, A. F., VAN EIJCK, C. H., BOLLEN, T. L., VAN RAMSHORST, B., NIEUWENHUIJS, V. B., TIMMER, R., LAMERIS, J. S., KRUYT, P. M., MANUSAMA, E. R., VAN DER HARST, E., VAN DER SCHELLING, G. P., KARSTEN, T., HESSELINK, E. J., VAN LAARHOVEN, C. J., ROSMAN, C.,

BOSSCHA, K., DE WIT, R. J., HOUDIJK, A. P., VAN LEEUWEN, M. S., BUSKENS, E., GOOSZEN, H. G. & DUTCH PANCREATITIS STUDY, G. 2010. A step-up approach or open necrosectomy for necrotizing pancreatitis. *N Engl J Med,* 362**,** 1491-502.

VANDENABEELE, P., GALLUZZI, L., VANDEN BERGHE, T. & KROEMER, G. 2010. Molecular mechanisms of necroptosis: an ordered cellular explosion. *Nat Rev Mol Cell Biol,* 11**,** 700-14.

VIG, M., DEHAVEN, W. I., BIRD, G. S., BILLINGSLEY, J. M., WANG, H., RAO, P. E., HUTCHINGS, A. B., JOUVIN, M. H., PUTNEY, J. W. & KINET, J. P. 2008. Defective mast cell effector functions in mice lacking the CRACM1 pore subunit of store-operated calcium release-activated calcium channels. *Nat Immunol,* 9**,** 89-96.

VIG, M., PEINELT, C., BECK, A., KOOMOA, D. L., RABAH, D., KOBLAN-HUBERSON, M., KRAFT, S., TURNER, H., FLEIG, A., PENNER, R. & KINET, J. P. 2006. CRACM1 is a plasma membrane protein essential for store-operated Ca2+ entry. *Science,* 312**,** 1220-3.

VILLATORO, E., MULLA, M. & LARVIN, M. 2010. Antibiotic therapy for prophylaxis against infection of pancreatic necrosis in acute pancreatitis. *Cochrane Database Syst Rev***,** CD002941.

VINCENT, J. L., MORENO, R., TAKALA, J., WILLATTS, S., DE MENDONCA, A., BRUINING, H., REINHART, C. K., SUTER, P. M. & THIJS, L. G. 1996. The SOFA (Sepsis-related Organ Failure Assessment) score to describe organ dysfunction/failure. On behalf of the Working Group on Sepsis-Related Problems of the European Society of Intensive Care Medicine. *Intensive Care Med,* 22**,** 707-10.

VONLAUFEN, A., APTE, M. V., IMHOF, B. A. & FROSSARD, J. L. 2007. The role of inflammatory and parenchymal cells in acute pancreatitis. *J Pathol,* 213**,** 239-48.

VORONINA, S., COLLIER, D., CHVANOV, M., MIDDLEHURST, B., BECKETT, A. J., PRIOR, I. A., CRIDDLE, D. N., BEGG, M., MIKOSHIBA, K., SUTTON, R. & TEPIKIN, A. V. 2015. The role of Ca2+ influx in endocytic vacuole formation in pancreatic acinar cells. *Biochem J,* 465**,** 405-12.

VORONINA, S., LONGBOTTOM, R., SUTTON, R., PETERSEN, O. H. & TEPIKIN, A. 2002. Bile acids induce calcium signals in mouse pancreatic acinar cells: implications for bile-induced pancreatic pathology. *J Physiol,* 540**,** 49-55.

WARD, J. B., PETERSEN, O. H., JENKINS, S. A. & SUTTON, R. 1995. Is an elevated concentration of acinar cytosolic free ionised calcium the trigger for acute pancreatitis? *Lancet,* 346**,** 1016-9.

WEN, L., VORONINA, S., JAVED, M. A., AWAIS, M., SZATMARY, P., LATAWIEC, D., CHVANOV, M., COLLIER, D., BARRETT, J., BEGG, M., STAUDERMAN, K., ROOS, J., GRIGORYEV, S., RAMOS, S., ROGERS, E., WHITTEN, J., VELICELEBI, G., DUNN, M., TEPIKIN, A. V., CRIDDLE, D. N. & SUTTON, R. 2015. Inhibitors of ORAI1 Prevent Cytosolic Calcium-associated Injury of Human Pancreatic Acinar Cells and Acute Pancreatitis in 3 Mouse Models. *Gastroenterology*.

WENGER, F. A., KILIAN, M., HEUKAMP, I., FOITZIK, T., JACOBI, C. A., GUSKI, H., SCHIMKE, I. & MULLER, J. M. 2007. Effects of octreotide in acute hemorrhagic necrotizing pancreatitis in rats. *J Gastroenterol Hepatol,* 22**,** 1872-6.

WHITCOMB, D. C., GORRY, M. C., PRESTON, R. A., FUREY, W., SOSSENHEIMER, M. J., ULRICH, C. D., MARTIN, S. P., GATES, L. K., JR., AMANN, S. T., TOSKES, P. P., LIDDLE, R., MCGRATH, K., UOMO, G., POST, J. C. & EHRLICH, G. D. 1996. Hereditary pancreatitis is caused by a mutation in the cationic trypsinogen gene. *Nat Genet,* 14**,** 141-5.

WILDI, S., KLEEFF, J., MAYERLE, J., ZIMMERMANN, A., BOTTINGER, E. P., WAKEFIELD, L., BUCHLER, M. W., FRIESS, H. & KORC, M. 2007. Suppression of transforming growth factor beta signalling aborts caerulein induced pancreatitis and eliminates restricted stimulation at high caerulein concentrations. *Gut,* 56**,** 685-92.

WINDSOR, J. A., JOHNSON, C. D., PETROV, M. S., LAYER, P., GARG, P. K. & PAPACHRISTOU, G. I. 2015. Classifying the severity of acute pancreatitis: Towards a way forward. *Pancreatology*.

WORKING GROUP, I. A. P. A. P. A. A. P. G. 2013. IAP/APA evidence-based guidelines for the management of acute pancreatitis. *Pancreatology,* 13**,** e1-15.

WU, B. U. & BANKS, P. A. 2013. Clinical management of patients with acute pancreatitis. *Gastroenterology,* 144**,** 1272-81.

WU, B. U., HWANG, J. Q., GARDNER, T. H., REPAS, K., DELEE, R., YU, S., SMITH, B., BANKS, P. A. & CONWELL, D. L. 2011. Lactated Ringer's solution reduces systemic inflammation compared with saline in patients with acute pancreatitis. *Clin Gastroenterol Hepatol,* 9**,** 710-717 e1.

YANG, S., ZHANG, J. J. & HUANG, X. Y. 2009. Orai1 and STIM1 are critical for breast tumor cell migration and metastasis. *Cancer Cell,* 15**,** 124-34.

YE, R., MARENINOVA, O. A., BARRON, E., WANG, M., HINTON, D. R., PANDOL, S. J. & LEE, A. S. 2010. Grp78 heterozygosity regulates chaperone balance in exocrine pancreas with differential response to cerulein-induced acute pancreatitis. *Am J Pathol,* 177**,** 2827-36.

YEROMIN, A. V., ZHANG, S. L., JIANG, W., YU, Y., SAFRINA, O. & CAHALAN, M. D. 2006. Molecular identification of the CRAC channel by altered ion selectivity in a mutant of Orai. *Nature,* 443**,** 226-9.

YUBERO, S., RAMUDO, L., MANSO, M. A. & DE DIOS, I. 2009. Targeting peripheral immune response reduces the severity of necrotizing acute pancreatitis. *Crit Care Med,* 37**,** 240-5.

ZHANG, H., NEUHOFER, P., SONG, L., RABE, B., LESINA, M., KURKOWSKI, M. U., TREIBER, M., WARTMANN, T., REGNER, S., THORLACIUS, H., SAUR, D., WEIRICH, G., YOSHIMURA, A., HALANGK, W., MIZGERD, J. P., SCHMID, R. M., ROSE-JOHN, S. & ALGUL, H. 2013. IL-6 trans-signaling promotes pancreatitis-associated lung injury and lethality. *J Clin Invest,* 123**,** 1019-31.

ZHANG, K. & KAUFMAN, R. J. 2008. From endoplasmic-reticulum stress to the inflammatory response. *Nature,* 454**,** 455-62.

ZHANG, S. L., YU, Y., ROOS, J., KOZAK, J. A., DEERINCK, T. J., ELLISMAN, M. H., STAUDERMAN, K. A. & CAHALAN, M. D. 2005. STIM1 is a Ca2+ sensor that activates CRAC channels and migrates from the Ca2+ store to the plasma membrane. *Nature,* 437**,** 902-5.

ZHU, Z. H., HOLT, S., EL-LBISHI, M. S., GRADY, T., TAYLOR, T. V. & POWERS, R. E. 1991. A somatostatin analogue is protective against retrograde bile salt-induced pancreatitis in the rat. *Pancreas,* 6**,** 609-13.

Publications arising from work in this thesis:

Li Wen, Svetlana Voronina, Muhammad A Javed, Muhammad Awais, Peter Szatmary Diane Latawiec, Michael Chvanov, David Collier, Wei Huang, John Barrett, Malcolm Begg, Ken Stauderman, Jack Roos, Sergey Grigoryev, Evan Roger, Jeffrey Whitten, Gonul Velicelibi, Michael Dunn, Alexei Tepikin, David. N. Criddle and Robert Sutton. ***Inhibitors of ORAI1 prevent cytosolic calcium-associated injury of human pancreatic acinar cells and acute pancreatitis in 3 mouse models.*** **Gastroenterology** 2015;149(2):481-492.

Gastroenterology 2015;149:481–492

BASIC AND TRANSLATIONAL—PANCREAS

Inhibitors of ORAI1 Prevent Cytosolic Calcium-Associated Injury of Human Pancreatic Acinar Cells and Acute Pancreatitis in 3 Mouse Models

Li Wen,[1,3] Svetlana Voronina,[2] Muhammad A. Javed,[1,2] Muhammad Awais,[1] Peter Szatmary,[1,2] Diane Latawiec,[1] Michael Chvanov,[2] David Collier,[2] Wei Huang,[1] John Barrett,[4] Malcolm Begg,[4] Ken Stauderman,[5] Jack Roos,[5] Sergey Grigoryev,[5] Stephanie Ramos,[5] Evan Rogers,[5] Jeff Whitten,[5] Gonul Velicelebi,[5] Michael Dunn,[5] Alexei V. Tepikin,[2] David N. Criddle,[2] and Robert Sutton[1]

[1]Pancreas Biomedical Research Unit, National Institute for Health Research Liverpool, Royal Liverpool University Hospital, [2]Department of Molecular and Cellular Physiology, Institute of Translational Medicine, University of Liverpool, Liverpool, United Kingdom; [3]Department of Integrated Traditional and Western Medicine, Sichuan Provincial Pancreatitis Centre, West China Hospital, Sichuan University, Chengdu, People's Republic of China; [4]Respiratory Therapy Area Unit, Medicines Research Centre, GlaxoSmithKline, Stevenage, United Kingdom; [5]CalciMedica, La Jolla, California

BACKGROUND & AIMS: Sustained activation of the cytosolic calcium concentration induces injury to pancreatic acinar cells and necrosis. The calcium release–activated calcium modulator ORAI1 is the most abundant Ca^{2+} entry channel in pancreatic acinar cells; it sustains calcium overload in mice exposed to toxins that induce pancreatitis. We investigated the roles of ORAI1 in pancreatic acinar cell injury and the development of acute pancreatitis in mice. **METHODS:** Mouse and human acinar cells, as well as HEK 293 cells transfected to express human ORAI1 with human stromal interaction molecule 1, were hyperstimulated or incubated with human bile acid, thapsigargin, or cyclopiazonic acid to induce calcium entry. GSK-7975A or CM_128 were added to some cells, which were analyzed by confocal and video microscopy and patch clamp recordings. Acute pancreatitis was induced in C57BL/6J mice by ductal injection of taurolithocholic acid 3-sulfate or intravenous' administration of cerulein or ethanol and palmitoleic acid. Some mice then were given GSK-7975A or CM_128, which inhibit ORAI1, at different time points to assess local and systemic effects. **RESULTS:** GSK-7975A and CM_128 each separately inhibited toxin-induced activation of ORAI1 and/or activation of Ca^{2+} currents after Ca^{2+} release, in a concentration-dependent manner, in mouse and human pancreatic acinar cells (inhibition >90% of the levels observed in control cells). The ORAI1 inhibitors also prevented activation of the necrotic cell death pathway in mouse and human pancreatic acinar cells. GSK-7975A and CM_128 each inhibited all local and systemic features of acute pancreatitis in all 3 models, in dose- and time-dependent manners. The agents were significantly more effective, in a range of parameters, when given at 1 vs 6 hours after induction of pancreatitis. **CONCLUSIONS:** Cytosolic calcium overload, mediated via ORAI1, contributes to the pathogenesis of acute pancreatitis. ORAI1 inhibitors might be developed for the treatment of patients with pancreatitis.

Keywords: STIM1; SOCE; Calcium Entry Inhibition; Drug Development; Experimental Pancreatitis.

Sustained increase of the cytosolic calcium concentration ($[Ca^{2+}]_C$) is a critical trigger for pancreatic acinar cell injury and necrosis, which depends on store-operated calcium entry (SOCE).[1–4] ORAI1 is the principal SOCE channel in the pancreatic acinar cell,[5] the opening of which is coordinated by stromal interaction molecule (STIM)1 and STIM2, after decreases in endoplasmic reticulum calcium store concentrations.[3,5–7] GSK-7975A and CM_128 were developed independently by GlaxoSmithKline (Stevenage, United Kingdom)[3,7,8] and CalciMedica (La Jolla, CA), respectively, to block ORAI1 channels, although only CM_128 continues toward clinical development. GSK-7975A inhibits SOCE induced by thapsigargin in isolated murine pancreatic acinar cells over the range of 1–50 μmol/L (half-maximal inhibitory concentration [IC_{50}], ~3.4 μmol/L),[3] inhibits endocytic vacuole formation[9] and reduces necrosis induced by toxins that cause acute pancreatitis.[3,9] CM_128 is a new molecular entity. ORAI1 inhibition could inhibit SOCE and necrosis in human pancreatic acinar cells and ameliorate acute pancreatitis.

Genetic knockout of the transient receptor potential canonical 3 channel,[10] a nonselective cation channel regulated in part by STIM1 via transient receptor potential canonical 1,[11] resulted in an approximately 50% reduction of in vivo serum amylase increase and edema formation induced by 4 injections of cerulein.[10] These experiments supported some role for SOCE in acute pancreatitis, but in a single mild model with few parameters of response.

Abbreviations used in this paper: **AP, acute pancreatitis; $[Ca^{2+}]_C$, cytosolic calcium concentration; CCK, cholecystokinin; CER, cerulein; FAEE, fatty acid ethyl ester; IC_{50}, half-maximal inhibitory concentration; I_{CRAC}, Ca^{2+} release-activated Ca^{2+} currents; IL, interleukin; MPO, myeloperoxidase; PI, propidium iodide; SOCE, store-operated calcium entry; STIM, stromal interaction molecule; TLCS, taurolithocholate acid sulfate.**

0016-5085/$36.00
http://dx.doi.org/10.1053/j.gastro.2015.04.015

Here, we defined the concentration-dependent inhibitory effects of GSK-7975A and CM_128 on SOCE and necrosis in murine and human pancreatic acinar cells induced by taurolithocholic acid 3-sulfate (TLCS)[2,12] or cholecystokinin (CCK) 8.[1,10] The effects of CM_128 on ORAI1 were substantiated by examination of its effect on Ca^{2+} release-activated Ca^{2+} currents (I_{CRAC})[3,6,7] in ORAI1/STIM1-transfected HEK 293 cells.[7] Our in vitro work informed in vivo pharmacokinetic analysis. GSK-7975A was given at selected doses after induction of acute pancreatitis (AP) with TLCS (TLCS-AP),[13] 7 injections of cerulein (CER-AP)[14] or ethanol and palmitoleic acid (FAEE-AP).[15] Because GSK-7975A markedly reduced all parameters of pathobiologic response in a dose-dependent manner, a high dose of GSK-7975A and separately CM_128 was begun at 2 different time points after disease induction to determine the effect of early vs late drug administration. Drug administration that was begun 1 hour after disease induction was highly effective in reducing parameters of pathobiologic response, significantly more so than when begun 6 hours after disease induction, in all models. These data provide thorough preclinical validation for ORAI channel inhibition as a potential early treatment for acute pancreatitis.

Materials and Methods

Human Specimen Sampling

Human pancreas was sampled and cells were isolated as described.[16] The time from sampling to the start of cell isolation was fewer than 10 minutes.

Cell Culture and Transfection

HEK 293 cells were cultured and transfected as described.[7] HEK 293 cells stably transfected with complementary DNAs encoding human ORAI1 and STIM1 were used in patch-clamp recording.

Animals

CD-1 and C57BL/6J mice were from Charles River UK, Ltd (Margate, Kent, UK). Pancreatic acinar cells were isolated from CD-1 mice as described.[1,3,12,15] For in vivo experiments, 10-week-old male C57BL/6J mice (25 g) were used.

Confocal Fluorescence Microscopy and Video Imaging

Isolated pancreatic acinar cells were imaged using a Till Photonics System (Munich, Germany) to assess $[Ca^{2+}]_C$ with Fura-2 (5 μmol/L; excitation, 340 and 380 nm; emission, >490 nm; ratio of fluorescence recorded from excitation, 340 and 380 nm) and using LSM710 systems (Carl Zeiss, Jena GmbH) to assess necrotic cell death pathway activation with propidium iodide (PI) (1 μmol/L; excitation, 488 nm; emission, 630–693 nm).

Necrotic Cell Death Pathway Activation Measurement

Cells were treated with GSK-7975A or CM_128 together with TLCS (500 μmol/L) for 30 minutes, gently shaking at 1000 rpm at room temperature. After washing, cells were stained with PI and Hoechst 33342, distributed into 96-well glass bottom plates (150 μL/well), and imaged using LSM710 systems. Hoechst 33342 (50 μg/mL; excitation, 364 nm; emission, 405–450 nm) was used to stain nuclei and count the total number of cells. PI was used to assess plasma membrane rupture: the total number of cells showing PI uptake was counted in 3 or more wells and in 12 or more random fields of each differently treated group of each isolate to provide a percentage, averaged across fields, as the mean ± SEM field percentage PI uptake with 3 or more isolates per group, except where stated.

Patch-Clamp Current Recording

The whole-cell configuration was used to record I_{CRAC} from hORAI1/hSTIM1 HEK 293 cells.[7] Patch pipettes were pulled from borosilicate glass capillaries (Sutter Instruments) with a resistance of 2–5 MΩ when filled with an extracellular solution of 120 mmol/L NaCl; 10 mmol/L TEA-Cl; 10 mmol/L HEPES; 10 or 0 mmol/L $CaCl_2$; 2 or 12 mmol/L $MgCl_2$, and 10 mmol/L glucose, pH 7.2. I_{CRAC} was activated by passive depletion of intracellular Ca^{2+} stores using the intracellular solution of 105 mmol/L Cs-glutamate; 10 mmol/L HEPES; 20 mmol/L 1,2-bis(o-aminophenoxy)ethane-N,N,N′,N′-tetraacetic acid; 8 mmol/L $MgCl_2$, pH 7.2. Patched cells were exposed to Ca^{2+}-free buffer to establish stable baseline (for 5 min), then 10 mmol/L $CaCl_2$ to develop I_{CRAC} (for 10 min), and then CM_128 (0.001, 0.01, 0.1, and 1 μmol/L for 10 min). External recording saline with no Ca^{2+} then was perfused for 2 minutes to determine the background current in the absence of I_{CRAC}. Whole-cell currents were sampled at 10 KHz and filtered at 2 KHz (Multiclamp 700B amplifier and PClamp software; Axon Instruments). The voltage clamp protocol included a cycle of steps to 0 mV (for 10 ms to evaluate zero current), then -100 mV (for 10 ms to measure I_{CRAC}), and a ramp from -100 mV to +100 mV over 50 ms for I-V relationship followed by step to +50 mV (for 10 ms to estimate leak current). The voltage between sweeps was +30 mV (for 12 s). Whole-cell capacitive compensation was used. Data analysis was performed using Clampfit software. I_{CRAC} was measured at -100 mV and current was measured at approximately 6 minutes and was used as the baseline control. The current measured after a 10-minute application of test compound was normalized to the baseline current (expressed as the percentage of control). The current measured in zero Ca^{2+} buffer was used to subtract the background leak current. Data points were fitted by nonlinear regression analysis with variable slope (SigmaPlot software) to determine the IC_{50} and Hill slope. The IC_{50} was taken as the point on the nonlinear regression halfway between the extrapolated baseline (control) and maximum inhibition produced by the compound.

Experimental Acute Pancreatitis

TLCS-AP was induced by retrograde pancreatic ductal injection with 3 mmol/L TLCS (5 μL/min over 10 minutes by infusion pump)[13]; humane killing was 6 or 24 hours later. CER-AP was induced by 7 hourly intraperitoneal cerulein injections (50 μg/kg)[14]; humane killing was 12 hours after the first. FAEE-AP was induced by 2 hourly intraperitoneal injections of 150 mg/kg palmitoleic acid and 1.35 g/kg ethanol[15]; humane killing was 6 or 24 hours later. GSK-6288B, the prodrug of

GSK-7975A, was administered by minipump; CM_128 was administered by intraperitoneal injection (≥6 mice/group).

Enzyme Activity and Interleukin 6 Measurement

Trypsin activity was measured as described[17] in homogenized tissue (Boc-Gln-Ala-Arg-MCA substrate; excitation, 380 nm; emission, 440 nm). Responses without treatment were normalized to 100 with SEM to compare different doses of either drug at different time points across models. Serum amylase was determined by a Roche Analyzer (Roche); interleukin (IL)6 was determined by enzyme-linked immunosorbent assay (R&D Systems).

Myeloperoxidase Activity

Myeloperoxidase (MPO) activity was determined as described.[18] Pancreatic or lung tissue was homogenized, resuspended in 100 mmol/L phosphate buffer (pH 5.4) containing 0.5% hexadecyltrimethyl ammonium bromide, 10 mmol/L EDTA and protease inhibitors, freeze-thawed 3 times, sonicated for 30 seconds, and centrifuged for 15 minutes at 16,000 × g. MPO activity was measured in supernatants (3,3,5,5-tetramethylbenzidine substrate with 0.01% H_2O_2). Absorbance was measured at 655 nm and MPO was calculated as the difference between absorbance at 0 and 3 minutes.

Histology

Pancreatic tissue was fixed in 10% formalin, embedded in paraffin, and stained (H&E). Evaluation was performed on 10 random fields (×200) by 2 blinded independent investigators grading (scale, 0–3) edema, inflammatory cell infiltration, and acinar necrosis, calculating the means ± SEM (≥6 mice/group).

Chemicals, Reagents, and Minipumps

CCK-8 was from American Peptide; fluorescent dyes were from Molecular Probes; Boc-Gln-Ala-Arg-MCA was from the Peptide Institute (Osaka, Japan); protease inhibitors were from Roche GmbH (Mannheim, Germany); IL6 quantikine enzyme-linked immunosorbent assay kit was from R&D Systems; and other reagents were from Sigma (Dorset, United Kingdom). 2,6-difluoro-N-(1-(4-hydroxy-2-(trifluoromethyl)benzyl)-1H-pyrazol-3-yl)benzamide (GSK-7975A) and pro-drug GSK-6288B were a gift from GlaxoSmithKline. CM_128 was a gift from CalciMedica. ALZET osmotic mini-pumps (2001D) were from Charles River UK, Ltd.

Statistical Analysis

Data are presented as means ± SEM. Comparisons were performed by the 2-tailed Student *t* test or chi-squared test, and *P* values less than .05 were considered significant.

Study Approval

Human pancreatic samples were obtained with informed consent as approved by the Liverpool Adult Local Research Ethics Committee (ref: 03/12/242/A). All animal studies were ethically reviewed and conducted according to UK Animals (Scientific Procedures) Act of 1986, approved by the UK Home Office (PPL 40/3320, renewed as 70/8109).

Results

Effects of GSK-7975A and CM_128 on Human Pancreatic Acinar Cells

Potential translational applications of SOCE inhibition as a treatment for clinical acute pancreatitis were evaluated by examination of the effects of GSK-7975A or CM_128 on isolated human pancreatic acinar cells.[16] Thapsigargin was used in zero external Ca^{2+} to empty Ca^{2+} stores, stimulate STIM-mediated Orai pore formation, and permit SOCE by the re-introduction of external Ca^{2+}. GSK-7975A (10–50 μmol/L) inhibited SOCE in these cells (Figure 1*A* and *B*). CM_128 also was found to inhibit SOCE in human pancreatic acinar cells at lower concentrations (Figure 1*C*). Both GSK-7975A (30 μmol/L) and CM_128 (1 μmol/L) inhibited necrotic cell death pathway activation in these cells (Figure 1*D*). To verify that CM_128 inhibits human ORAI1, HEK 293 cells transfected with ORAI1/STIM1[7] were patched in zero extracellular Ca^{2+} to measure I_{CRAC} in response to extracellular addition of 10 mmol/L Ca^{2+}, and the effect of a range of concentrations of CM_128 tested. CM_128 was found to inhibit I_{CRAC} in a direct concentration-dependent manner, with IC_{50} at approximately 0.1 μmol/L and no loss of effect at high concentrations (10 μmol/L) (Figure 1*E* and *F*). These findings were confirmed over the same concentration range with FLIPR technology (data not shown).

Effects of GSK-7975A on Murine Pancreatic Acinar Cells

Isolated murine pancreatic acinar cells maintained in 5 mmol/L external Ca^{2+} were perfused with TLCS (500 μmol/L) or supramaximal CCK (1 nmol/L) to induce sustained increases of $[Ca^{2+}]_C$ dependent on SOCE.[1,3,6,10] Once a stable plateau in $[Ca^{2+}]_C$ had formed, a range of fixed concentrations (0–100 μmol/L) of GSK-7975A were added. Increasing concentrations of GSK-7975A decreased the $[Ca^{2+}]_C$ plateau progressively and increasingly rapidly (Figure 2*A*–*D*). With TLCS, suppression of $[Ca^{2+}]_C$ toward the initial baseline approached 80% using 30 μmol/L GSK-7975A; with CCK, more than 95% using 15 μmol/L GSK-7975A, an effect also seen when cells were maintained in 1.8 mmol/L external Ca^{2+} (Supplementary Figure 1*A*). At 100 μmol/L GSK-7975A, but not at 50 μmol/L GSK-7975A, there was a loss of effect through an unknown mechanism (Supplementary Figure 1*B*–*E*). Necrotic cell death pathway activation was reduced markedly in murine pancreatic acinar cells by GSK-7975A (Figure 2*E*).

Effects of CM_128 on Murine Pancreatic Acinar Cells

To determine the effect of CM_128 on SOCE into isolated murine pancreatic acinar cells, thapsigargin was used to empty Ca^{2+} stores and initiate STIM-mediated ORAI pore formation, while maintaining cells in zero external Ca^{2+} until Ca^{2+} was re-introduced to enable SOCE.[1,3] Application of this protocol showed that CM_128 reduced SOCE markedly, at a lower dose than that of GSK-7975A (1 μmol/L)

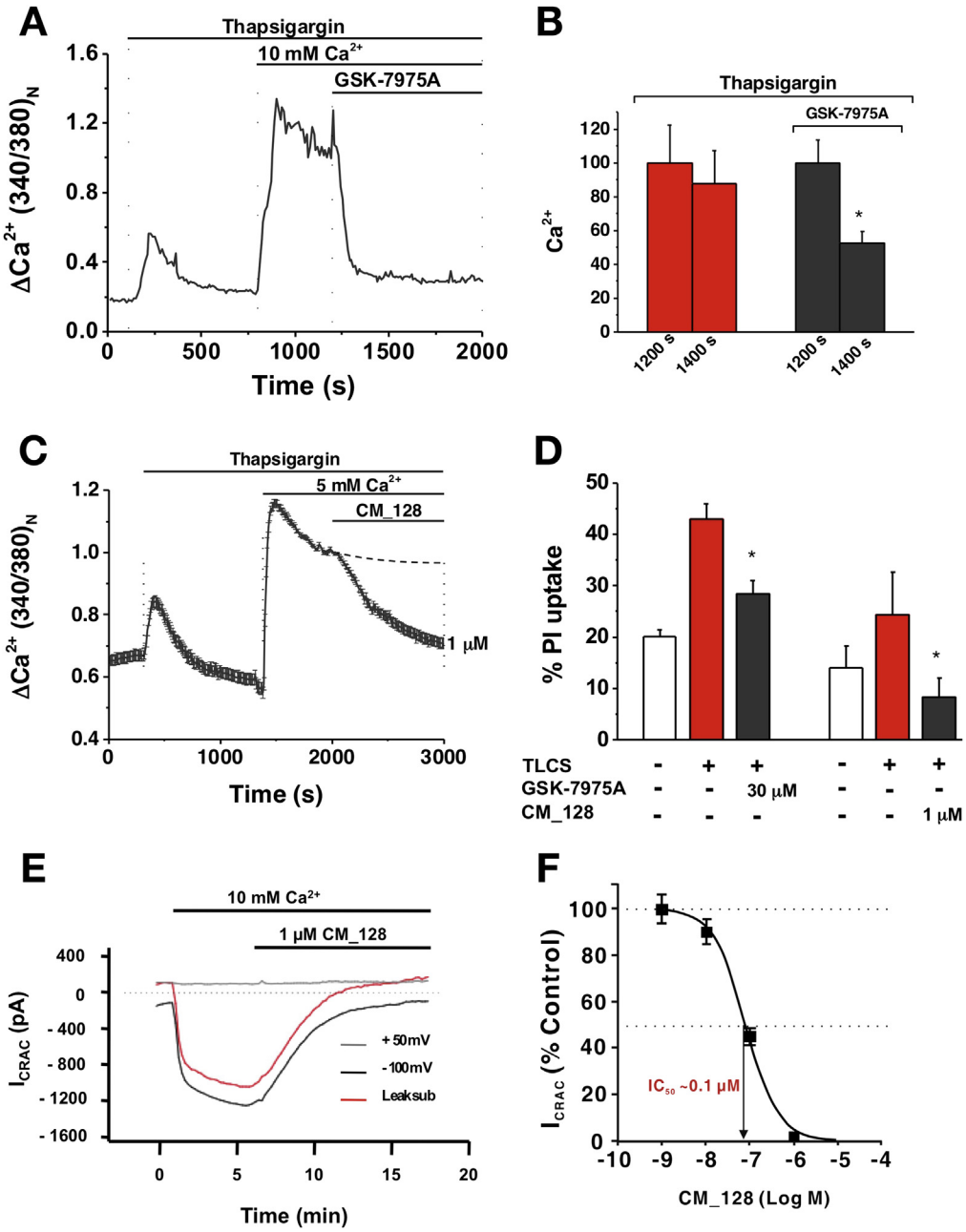

Figure 1. GSK-7975A and CM_128 inhibit CRAC entry (Fura-2 340:380 normalized at 1200 or 2000 s) and necrosis (PI uptake) in human pancreatic acinar cells and CM_128 concentration-dependently inhibits I_{CRAC} in hORAI1/hSTIM1 HEK 293 cells. (*A*) Typical trace showing the inhibitory effect of GSK-7975A (50 μmol/L) on thapsigargin-induced Ca^{2+} influx. (*B*) Mean (±SEM) $[Ca^{2+}]_C$ at 1200 and 1400 s from thapsigargin and thapsigargin plus GSK-7975A traces, showing a marked reduction with GSK-7975A ($\geq$20 cells/group; *$P < .001$; thapsigargin vs thapsigargin plus GSK-7975A at 1400 s). (*C*) Changes in human pancreatic acinar $[Ca^{2+}]_C$ induced by thapsigargin (Fura-2 340:380 normalized at 2000 s), showing the inhibitory effect of 1 μmol/L CM_128. (*D*) GSK-7975A and CM_128 protected isolated human pancreatic acinar cells from necrotic cell death pathway activation induced by TLCS (500 μmol/L) (mean ± SEM; 3 experiments/group for GSK-7975A; *$P < .05$, TLCS vs TLCS plus GSK-7975A and 1 experiment/group [4 wells and 16 high-power fields each; total. 172 control cells, 97 TLCS, 110 TLCS, and CM_128] for CM_128; *$P < .05$, TLCS vs TLCS plus CM_128). (*E*) Typical trace showing I_{CRAC} current in response to Ca^{2+}-depletion protocol with 1 μmol/L CM_128 in hORAI1/hSTIM1 HEK 293 cells. (*F*) Concentration-dependent inhibitory effects of CM_128 on I_{CRAC} current.

(Figure 3*A* and *B*); this same dose also was effective in significantly reducing necrotic cell death pathway activation by TLCS in these cells (Figure 3*C*). To confirm the effect of CM_128 on SOCE and to determine dose-dependency, cyclopiazonic acid was used to empty Ca^{2+} stores within murine pancreatic acinar cells[10] (maintained in zero external Ca^{2+}) to stimulate STIM-mediated ORAI opening. Upon reintroduction of external Ca^{2+} (1.8 mmol/L), the rate

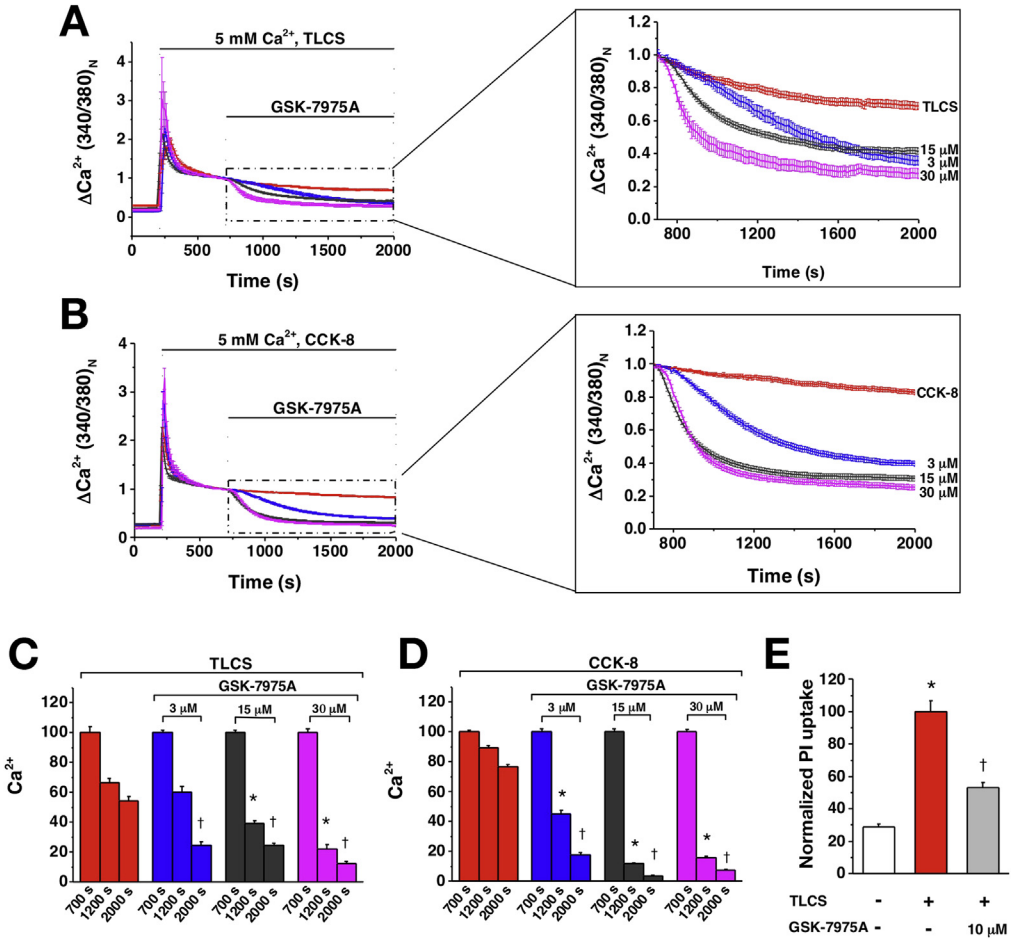

Figure 2. GSK-7975A concentration-dependently inhibits CRAC entry (Fura-2 340:380 normalized at 700 s) and necrosis (PI uptake). Changes in mouse pancreatic acinar $[Ca^{2+}]_C$ induced by (*A*) TLCS (500 μmol/L) and (*B*) CCK (1 nmol/L) showing effects of GSK-7975A from 700 s, expanded. (*C* and *D*) Mean (±SEM) $[Ca^{2+}]_C$ at 700, 1200, and 2000 s from panels *A* and *B*, showing progressive reduction with increasing GSK-7975A (≥19 cells/group; **P* < .001, toxin vs toxin plus GSK-7975A at 1200 s; †*P* < .001 at 2000 s). (*E*) GSK-7975A protected isolated murine pancreatic acinar cells from necrotic cell death pathway activation induced by TLCS (500 μmol/L) (mean ± SEM, normalized to TLCS at 100; ≥3 experiments/group; **P* < .001, control vs TLCS; †*P* < .001, TLCS vs TLCS plus GSK-7975A).

of Ca^{2+} entry showed concentration-dependent log proportionality, with the IC_{50} at approximately 0.7 μmol/L and no loss of effect at high concentrations (10 μmol/L) (Figure 3*D* and *E*).

Effects of GSK-7975A on Experimental Acute Pancreatitis

To ensure consistent delivery of GSK-7975A in vivo we tested subcutaneous minipump administration of GSK-7975A against a background of CER-AP. Because of the modest aqueous solubility of GSK-7975A, we used a phosphate prodrug (GSK-6288B) that is cleaved rapidly in vivo to liberate GSK-7975A. Blood and pancreatic levels of GSK-7975A reached a steady state within 4 hours at all doses tested (Supplementary Figure 2). GSK-7975A at 28 (low) and 110 (high) mg/kg/h achieved steady-state blood concentrations of approximately 4.3 μmol/L and approximately 13.3 μmol/L, and pancreatic concentrations of approximately 8.9 μmol/L and approximately 49.3 μmol/L, respectively, with no detectable prodrug at all doses and time points.

GSK-7975A was tested in 3 clinically representative mouse models of acute pancreatitis. TLCS-AP, which is representative of acute biliary pancreatitis from ampullary gallstone obstruction, was induced by pancreatic ductal infusion of TLCS[13] and minipumps inserted 30 minutes later. At both doses GSK-7975A significantly reduced increases in serum amylase, IL6, and pancreatic MPO levels; lung MPO was reduced significantly by low dose only (Figure 4). There were consistent reductions in pancreatic edema, inflammatory cell infiltration, and acinar cell necrosis, with a marked reduction in overall histopathology score in the GSK-7975A–treated groups; inflammatory cell infiltration and histopathology score were reduced significantly more by the higher dose (Figure 5).

CER-AP is the most widely used model that is representative of acute pancreatitis induced by hyperstimulation,[14] such as from anticholinesterase insecticides or *Tityus* species scorpion stings.[19] In CER-AP, minipumps were inserted with the third of 7 cerulein injections. At both doses GSK-7975A significantly reduced the increases in serum amylase, pancreatic trypsin, and MPO levels, with the low dose resulting in significant reductions in IL6 and lung MPO levels (Figure 4). Pancreatic histopathology showed a trend toward a reduction in the low-dose group; at the high dose, there were significant marked reductions in all measures of pancreatic histopathology, approaching control levels (Figure 5).

FAEE-AP parallels acute alcoholic pancreatitis through in vivo formation of toxic ethanol metabolites.[15] Minipumps

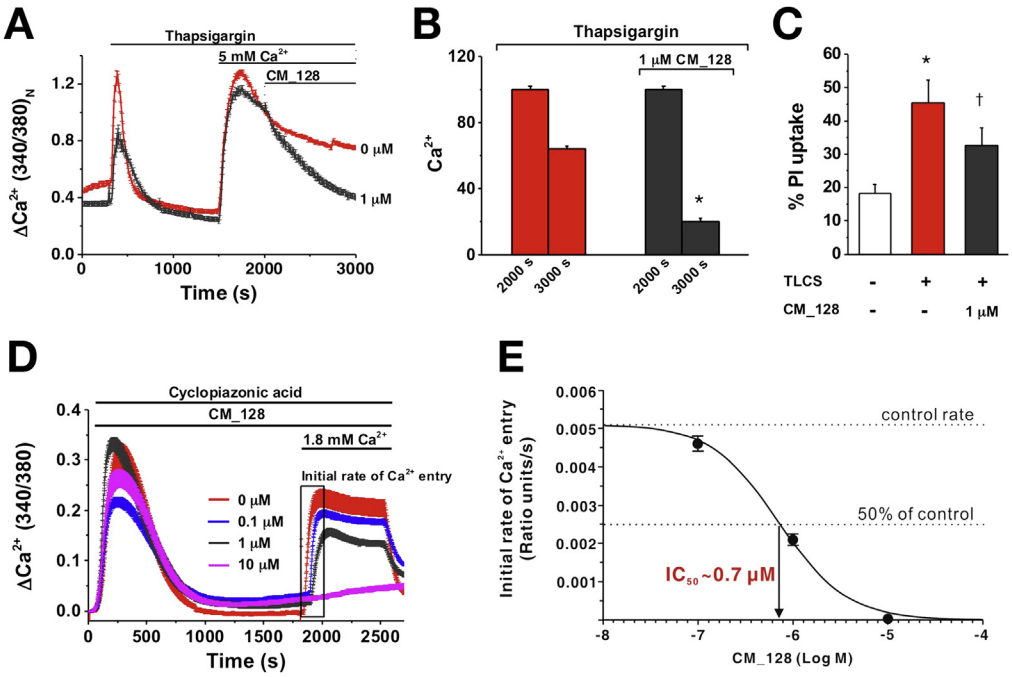

Figure 3. CM_128 concentration-dependently inhibits CRAC entry and necrosis (PI uptake). (*A*) Changes in mouse pancreatic acinar $[Ca^{2+}]_C$ induced by thapsigargin (Fura-2 340:380 normalized at 2000 s), showing effect of 1 μmol/L CM_128. (*B*) Mean (±SEM) $[Ca^{2+}]_C$ at 2000 and 3000 s from panel *A*, showing a marked reduction with 1 μmol/L CM_128 (≥62 cells/group; *$P <$ .001, thapsigargin vs thapsigargin plus CM_128 at 3000 s). (*C*) CM_128 protected isolated murine pancreatic acinar cells from necrotic cell death pathway activation induced by TLCS (500 μmol/L) (mean ± SEM; ≥3 experiments/group; *$P <$ .001, TLCS vs control; †$P <$ .05, TLCS vs TLCS plus CM_128). (*D*) Concentration-dependent inhibitory effects of CM_128 on cyclopiazonic acid–induced Ca^{2+} influx, showing a progressive reduction of the initial rate of Ca^{2+} entry and plateau with increasing CM_128, with complete inhibition of Ca^{2+} entry at 10 μmol/L (≥17 cells/group). (*E*) Concentration-dependent inhibitory effects of CM_128 on the initial rate of Ca^{2+} entry.

were inserted in FAEE-AP at 1 hour after the second of 2 intraperitoneal injections of ethanol and palmitoleic acid. GSK-7975A reduced the increases in all parameters, with pancreatic and lung MPO levels significantly reduced at the low dose; serum amylase level, IL6 level, pancreatic trypsin level, and histopathology were reduced significantly at the high dose (Figures 4 and 5). There were significantly greater reductions in edema, inflammation, and the overall histopathology score at the high dose, with levels of necrosis approaching control levels (Figure 5). In all models, low-dose GSK-7975A was generally as effective as the high dose in reducing IL6, which contributes to lung injury and lethality,[20] and MPO. These data are consistent with the lower IC_{50} of GSK-7975A on ORAI channel SOCE in leukocytes (~1 μmol/L for T lymphocytes)[7,8] than in pancreatic acinar cells (3.4 μmol/L).[3]

Effects of CM_128 on Experimental Acute Pancreatitis

Preliminary in vivo experiments indicated that CM_128 has a significantly longer half-life than GSK-7975A, and is suitable for intraperitoneal dosing every 12 hours to achieve sustained blood levels with more than 99% bound (free fraction in murine plasma, 0.33%; when added to human plasma, 0.16%). Because our work with high-dose GSK-7975A showed greater efficacy in vivo than with low-dose GSK-7975A, and in vitro data obtained with CM_128 did not suggest loss of efficacy at high concentrations (10 μmol/L), we administered 20 mg/kg CM_128 every 12 hours to test the efficacy of this agent in TLCS-AP and FAEE-AP. We also determined the relative efficacy of CM_128 administered either 1 or 6 hours after induction of either model of acute pancreatitis. CM_128 begun 1 hour after disease induction significantly reduced all parameters of both TLCS-AP and FAEE-AP, including all local and systemic biochemical, immunologic, and histopathologic measures (Figures 6 and 7). CM_128 begun 6 hours after disease induction was less effective across a broad range of parameters (Figures 6 and 7), significantly so for IL6 (TLCS-AP), pancreatic MPO (FAEE-AP), and lung MPO (TLCS-AP), although significant reductions still were seen in amylase (TLCS-AP and FAEE-AP), lung MPO (TLCS-AP), edema (TLCS-AP and FAEE-AP), inflammation (FAEE-AP), necrosis (FAEE-AP), and total histopathology score (FAEE-AP). To determine the extent to which disease was established at 6 hours after disease induction, and the effect of CM_128 begun at that time, all parameters were assessed at 6 hours and compared with values at 24 hours. These data showed that by 24 hours there was no significant improvement of parameters as measured at 6 hours as a result of CM_128 administration begun at 6 hours (Supplementary Figures 3 and 4), confirming delay in therapy to be disadvantageous; although CM_128 appeared to prevent these

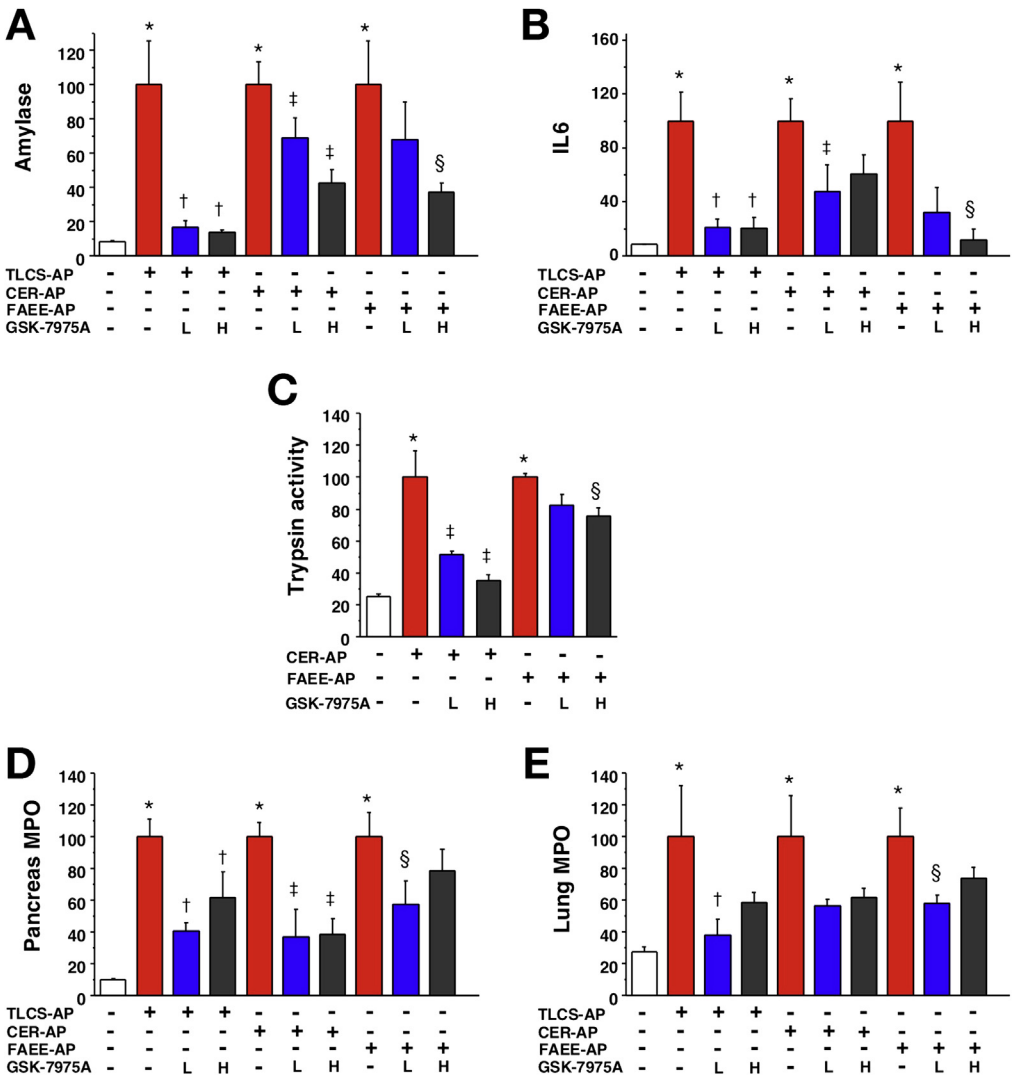

Figure 4. GSK-7975A markedly reduces all biochemical responses of TLCS-AP, CER-AP, and FAEE-AP. All models resulted in substantial increases of (*A*) serum amylase, (*B*) IL6, (*C*) pancreatic trypsin activity, (*D*) pancreatic activity, and (*E*) lung MPO activity. Subcutaneous osmotic minipump administration of GSK-7975A given as prodrug GSK-6288B at low (L) or high (H) doses significantly reduced all parameters, with a more marked reduction of serum amylase and IL6, pancreatic trypsin at the high dose (mean ± SEM ≥6 mice/group; $^{*}P < .05$, control vs 3 models; $^{\dagger}P < .05$ TLCS-AP vs TLCS-AP plus GSK-7975A; $^{\ddagger}P < .05$, CER-AP vs CER-AP plus GSK-7975A; and $^{\S}P < .05$, FAEE-AP vs FAEE-AP plus GSK-7975A).

parameters from increasing. To further explore the effect of delay in dosing, the effect of high-dose GSK-7975A on disease responses also was tested at 1 and 6 hours after induction. Similar to CM_128, GSK-7975A begun 6 hours after disease induction was less effective across a broad range of parameters (Supplementary Figures 5 and 6), significantly so for amylase (TLCS-AP and FAEE-AP), IL6 (TLCS-AP), edema (TLCS-AP and FAEE-AP), inflammatory infiltrate (TLCS-AP), and total histopathology score (TLCS-AP and FAEE-AP).

Discussion

We found GSK-7975A and the new molecular entity CM_128 to inhibit toxin-induced SOCE into murine and human pancreatic acinar cells in a concentration-dependent manner, exceeding more than 90% block of relative control values in some protocols. We also found both GSK-7975A and CM_128 to reduce significantly the necrotic cell death pathway activation in murine and human pancreatic acinar cells exposed to TLCS, which induces acute pancreatitis in vivo.[13,14] Although effects of GSK-7975A have been described on thapsigargin- and palmitoleic acid ethyl ester–induced murine pancreatic acinar SOCE,[3] our study found GSK-7975A to have a similarly critical effect on TLCS- and CCK-induced murine pancreatic acinar SOCE, as well as thapsigargin-induced human pancreatic acinar SOCE and TLCS-induced human pancreatic acinar necrotic cell death pathway activation. CM_128 showed a higher potency (IC_{50} ~0.1 μmol/L from ORAI1/STIM1-transfected HEK 293 cell patch-clamp data), and unlike GSK-7975A, no loss of efficacy at high doses. Comprehensive in vivo evaluation using 3 diverse, clinically representative models of acute pancreatitis[14] with prior pharmacokinetic assessment showed the validity of SOCE inhibition as a therapeutic approach. Thus, administration of either compound within 1 hour after disease induction was markedly effective across a representative range of local and systemic biochemical, immunologic, and histologic disease responses.

Our novel human data support the potential applicability of SOCE inhibition as a treatment for clinical acute

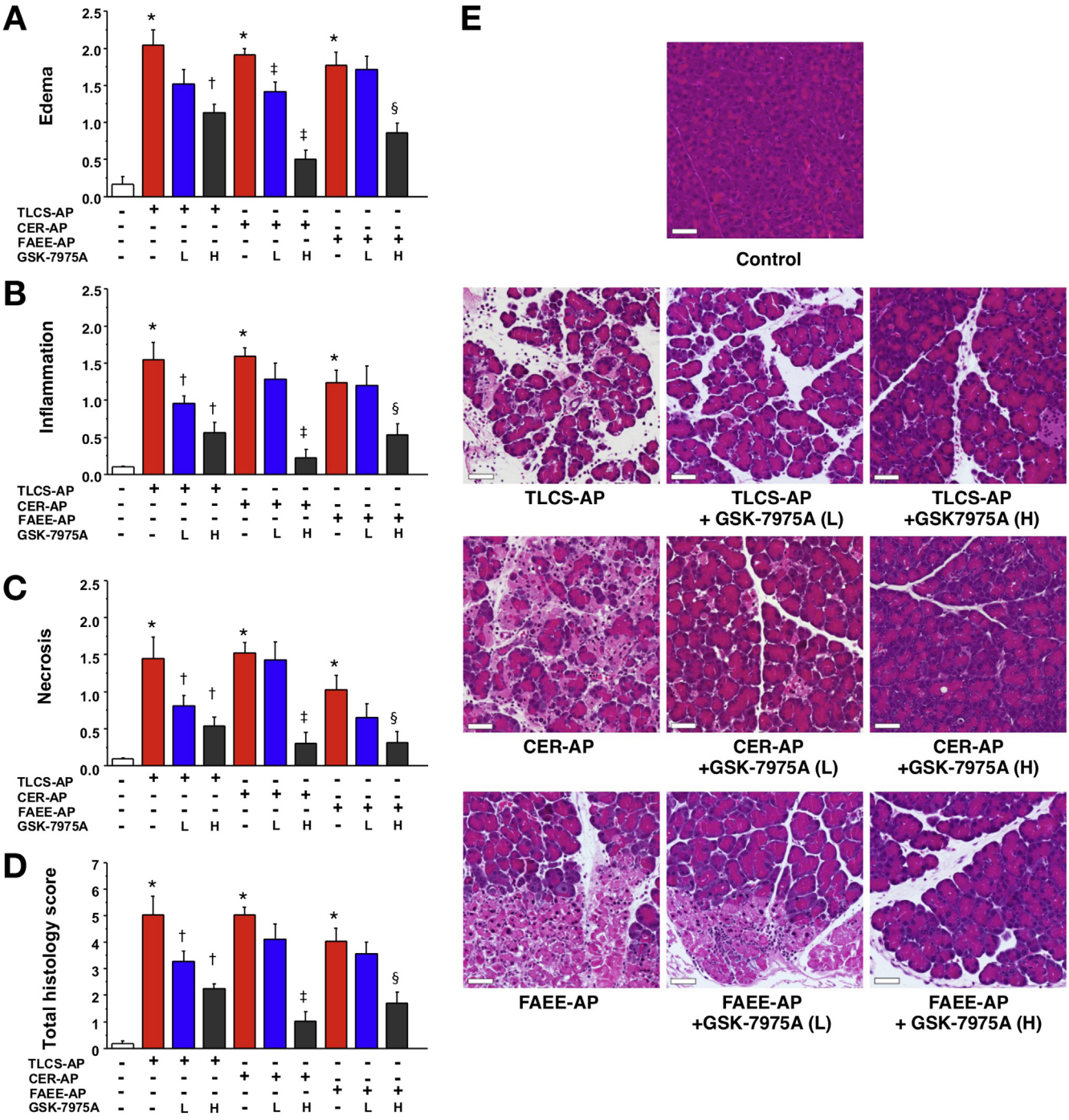

Figure 5. GSK-7975A markedly reduces pancreatic histopathology in TLCS-AP, CER-AP, and FAEE-AP. All models resulted in substantial increases in (*A*) edema, (*B*) inflammation, (*C*) necrosis, and (*D*) total histology score. Subcutaneous osmotic minipump administration of GSK-7975A given as prodrug GSK-6288B at low (L) or high (H) doses markedly reduced pancreatic damage, with more marked reduction at high dose (mean ± SEM ≥6 mice/group; $^{*}P < .05$ control vs 3 models; $^{\dagger}P < .05$, TLCS-AP vs TLCS-AP plus GSK-7975A; $^{\ddagger}P < .05$, CER-AP vs CER-AP plus GSK-7975A; and $^{\S}P < .05$, FAEE-AP vs FAEE-AP plus GSK-7975A). (*E*) Representative images showing normal pancreatic histology, typical histopathology from all 3 models, and typical histopathology from all 3 models after treatment with GSK-7975A at low (L) or high (H) doses (H&E; *scale bar*: 50 μm).

pancreatitis. Both GSK-7975A and CM_128 blocked SOCE promptly, shown here to result in complete block of human ORAI1 by CM_128. Although an action on other ORAI channels cannot be excluded and could be desirable, ORAI1 is the primary channel for SOCE into pancreatic acinar cells,[3,5] blocked by both compounds. ORAI channels also contribute to inflammatory cell responses, including neutrophil migration and activation[21]; inhibition of innate

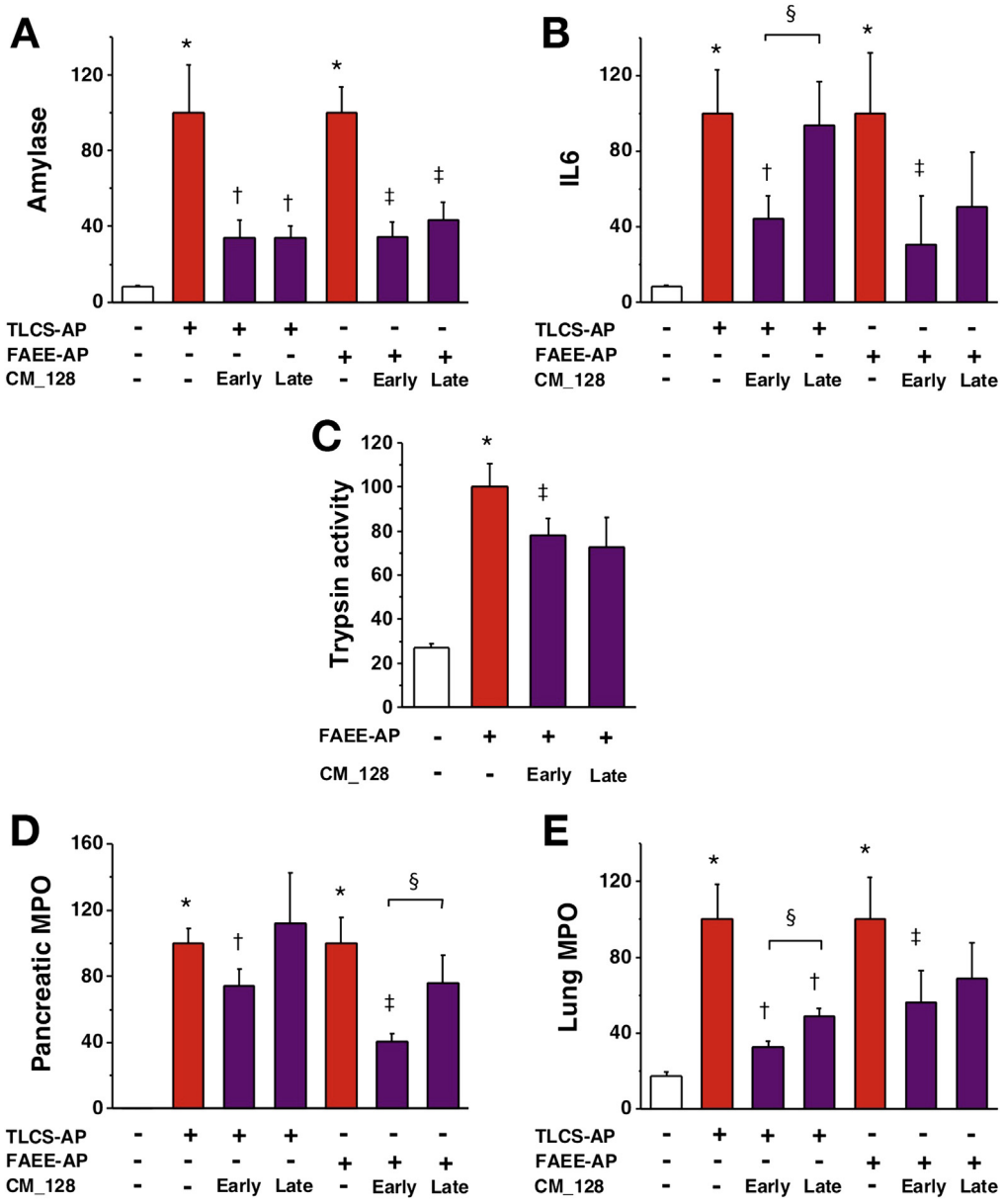

Figure 6. CM_128 markedly reduces all biochemical responses of TLCS-AP and FAEE-AP. Two models resulted in substantial increases of (*A*) serum amylase, (*B*) IL6, (*C*) pancreatic trypsin activity, (*D*) pancreatic activity, and (*E*) lung MPO activity. Intraperitoneal administration of CM_128 at 20 mg/kg given at 1 hour after disease induction (early) and 6 hours after (late) significantly reduced all parameters, with more marked reduction of IL6, pancreatic activity, and lung MPO activity when CM_128 was administered early (mean ± SEM ≥6 mice/group; $^{*}P < .05$, control vs 2 models; $^{\dagger}P < .05$ TLCS-AP vs TLCS-AP plus CM_128; $^{\ddagger}P < .05$, FAEE-AP vs FAEE-AP plus CM_128; and $^{\S}P < .05$, CM_128 early vs late).

immune responses significantly reduces the severity of experimental acute pancreatitis,[22] thus there may be a contribution here from ORAI inhibition of immune cells. Nevertheless, although knockout of ORAI1/STIM1 SOCE inhibits neutrophil functions, it does not prevent all functions,[21] so the primary contribution of ORAI blockade in our experiments is likely to have been in the pancreas. Furthermore, because SOCE inhibition for clinical acute pancreatitis would necessarily be short term, inhibition of the adaptive immune system[21] also would be short term. ORAI blockade has less effect on other cell types in which ORAI channels have a less prominent role, such as electrically excitable cells in which other ion channels (eg, nonselective cation channels) have a larger role in Ca^{2+} entry.[23] Nonselective cation channels, however, permit limited SOCE into pancreatic acinar cells[3,10] that could sustain essential Ca^{2+} entry.[23] Without such Ca^{2+} entry, continued activation of the plasma membrane Ca^{2+}-adenosine triphosphatase pump upon secretagogue- or toxin-mediated release of Ca^{2+} from intracellular stores could deplete these stores to deleterious levels, inducing or exacerbating endoplasmic reticulum stress.[24]

Measurement of blood and tissue levels of GSK-7975A after induction of experimental acute pancreatitis established an appropriate dosing regimen (110 mg/kg/h via minipump) for maximum effect, at a steady state of 10–15 μmol/L in blood and approximately 50 μmol/L in the pancreas, with less than 10% free GSK-7975A. Our cell data indicated that at 50 μmol/L, GSK-7975A had no loss of effect, and the concentration of free compound in vivo was significantly lower. At this dose, however, GSK-7975A was highly effective in reducing all measures of disease response in 3 clinically representative models of acute pancreatitis (TLCS-AP, CER-AP, and FAEE-AP), and more so than at a

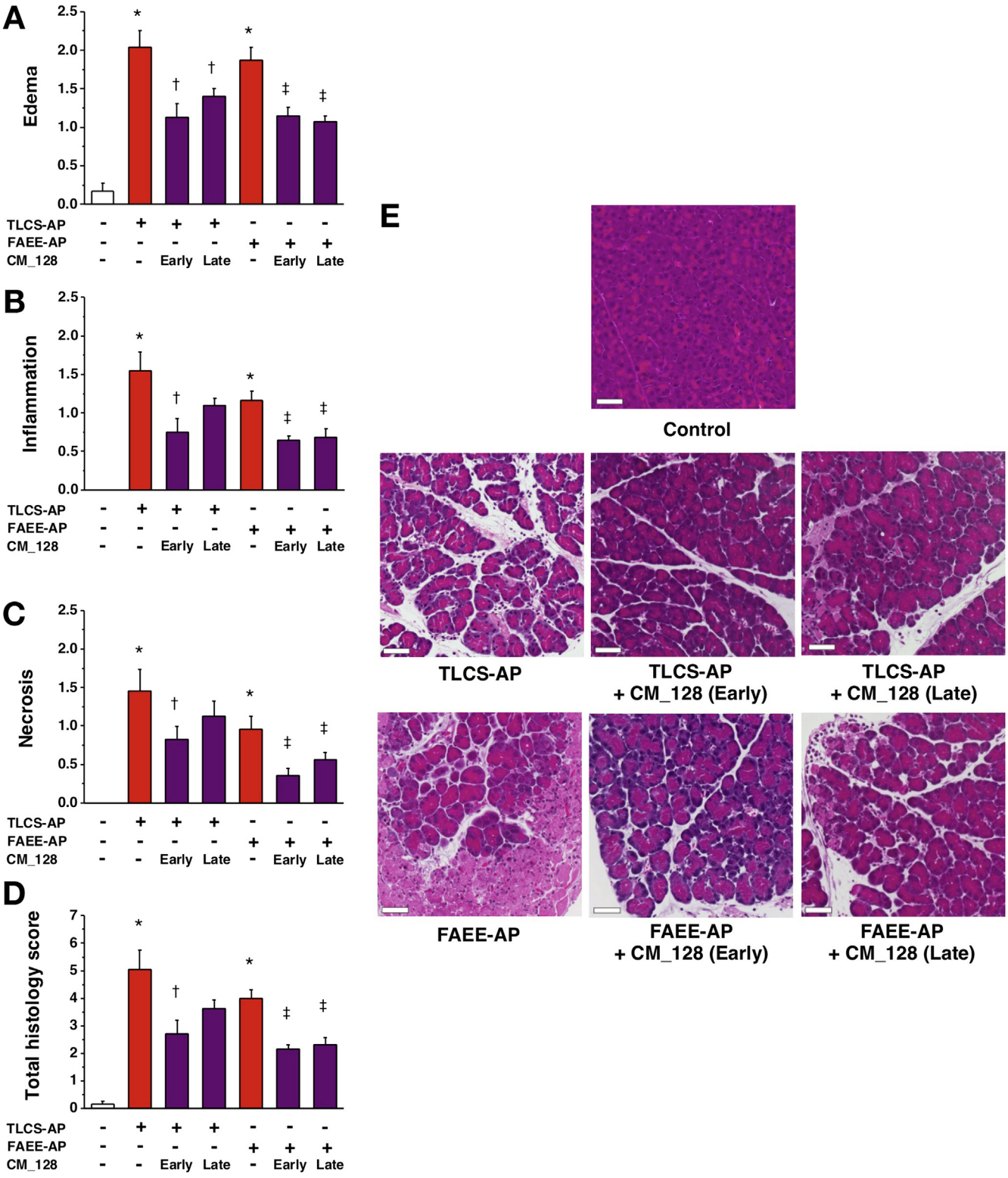

Figure 7. CM_128 markedly reduces pancreatic histopathology in TLCS-AP and FAEE-AP. Both models resulted in substantial increases in (*A*) edema, (*B*) inflammation, (*C*) necrosis, and (*D*) total histology score. Intraperitoneal administration of CM_128 at 20 mg/kg given at 1 hour after disease induction (early) and 6 hours after (late) significantly reduced all parameters, with a more marked reduction when CM_128 was administered early (mean ± SEM ≥6 mice/group; $^{*}P < .05$, control vs 2 models; $^{\dagger}P < .05$ TLCS-AP vs TLCS-AP plus CM_128; $^{\ddagger}P < .05$, FAEE-AP vs FAEE-AP plus CM_128; and $^{\S}P < .05$, CM_128 early vs late). (*E*) Representative images showing normal pancreatic histology, typical histopathology from 2 models, and typical histopathology from 2 models after treatment with CM_128 early and late after disease induction (H&E; *scale bar*: 50 μm).

lower dose (28 mg/kg/h). CM_128, with higher potency than GSK-7975A but higher levels of plasma and tissue binding, was tested at 20 mg/kg given every 12 hours via intraperitoneal injection in TLCS-AP and FAEE-AP, representative of gallstone and alcoholic acute pancreatitis,[14,15] the most common forms of the disease.[4] This resulted in CM_128 levels greater than 7 μmol/L in blood and approximately 50 μmol/L in the pancreas 11 hours after the last dose, levels that were highly effective in reducing all disease parameters. These data provide robust confirmation of the hypothesis that cytosolic Ca^{2+} overload is a critical trigger of acute pancreatitis.[25]

Both compounds were administered after disease induction to model treatment of clinical acute pancreatitis, but a delay in administration of either compound to 6 hours after disease induction resulted in diminished efficacy, dependent on the end point measured and the model used. Although biological time courses including that of acute pancreatitis are longer in human beings than in mice,[4,14,26] with pancreatic necrosis typically detected within days rather than hours,[4,27] human pancreatic acinar necrotic cell death pathway activation may begin in clinical acute pancreatitis at an early stage after disease onset, shown here in mouse models within 6 hours of onset. Door-to-needle times of less than 60 minutes are established guidelines for patients with acute myocardial infarction (30 min)[28] and acute ischemic stroke (60 min),[29] making every second count, with national and international quality-improvement initiatives underway toward fully achieving these.[30] Although pancreatic necrosis has a less rapid time course and is not the result of major arterial occlusion,[4] the translational implication of our work is that door-to-needle time is an important issue in administration of any treatment for acute pancreatitis that targets the pathogenesis of pancreatic injury, which drives the disease. Previously, clinical trials of treatments for acute pancreatitis "enriched" recruitment with patients predicted to have severe disease (often with recruitment up to 72 h after admission),[4,31] which delays the initiation of therapy. Furthermore, the expansion of disease categories from the original Atlanta Classification (mild and severe)[32] into the revised Atlanta (mild, moderate, and severe)[33] and Determinants-Based (mild, moderate, severe, and critical)[34] classification, further complicates patient selection from among these potentially overlapping subgroups. To minimize door-to-needle time, a quicker and more accurate approach to the selection of patients is required for trials of any therapy, such as that offered here with ORAI inhibition by CM_128, a novel molecular entity currently undergoing preclinical toxicologic evaluation before phase I trials.

Supplementary Material

Note: To access the supplementary material accompanying this article, visit the online version of *Gastroenterology* at www.gastrojournal.org, and at http://dx.doi.org/10.1053/j.gastro.2015.04.015.

References

1. Raraty M, Ward J, Erdemli G, et al. Calcium-dependent enzyme activation and vacuole formation in the apical granular region of pancreatic acinar cells. Proc Natl Acad Sci U S A 2000;97:13126–13131.
2. Petersen OH, Sutton R. Ca2+ signalling and pancreatitis: effects of alcohol, bile and coffee. Trends Pharmacol Sci 2006;27:113–120.
3. **Gerasimenko JV, Gryshchenko O, Ferdek PE**, et al. Ca2+ release-activated Ca2+ channel blockade as a potential tool in antipancreatitis therapy. Proc Natl Acad Sci U S A 2013;110:13186–13191.
4. Lankisch PG, Apte M, Banks PA. Acute pancreatitis. Lancet 2015. Epub ahead of print.
5. Lur G, Haynes LP, Prior IA, et al. Ribosome-free terminals of rough ER allow formation of STIM1 puncta and segregation of STIM1 from IP(3) receptors. Curr Biol 2009;19:1648–1653.
6. Muik M, Schindl R, Fahrner M, et al. Ca(2+) release-activated Ca(2+) (CRAC) current, structure, and function. Cell Mol Life Sci 2012;69:4163–4176.
7. Derler I, Schindl R, Fritsch R, et al. The action of selective CRAC channel blockers is affected by the Orai pore geometry. Cell Calcium 2013;53:139–151.
8. Rice LV, Bax HJ, Russell LJ, et al. Characterization of selective calcium-release activated calcium channel blockers in mast cells and T-cells from human, rat, mouse and guinea-pig preparations. Eur J Pharmacol 2013;704:49–57.
9. **Voronina S, Collier D**, Chvanov M, et al. The role of Ca2+ influx in endocytic vacuole formation in pancreatic acinar cells. Biochem J 2015;465:405–412.
10. Kim MS, Hong JH, Li Q, et al. Deletion of TRPC3 in mice reduces store-operated Ca2+ influx and the severity of acute pancreatitis. Gastroenterology 2009;137:1509–1517.
11. **Lee KP, Choi S**, Hong JH, et al. Molecular determinants mediating gating of transient receptor potential canonical (TRPC) channels by stromal interaction molecule 1 (STIM1). J Biol Chem 2014;289:6372–6382.
12. Voronina S, Longbottom R, Sutton R, et al. Bile acids induce calcium signals in mouse pancreatic acinar cells: implications for bile-induced pancreatic pathology. J Physiol 2002;540:49–55.
13. Laukkarinen JM, Van Acker GJ, Weiss ER, et al. A mouse model of acute biliary pancreatitis induced by retrograde pancreatic duct infusion of Na-taurocholate. Gut 2007;56:1590–1598.
14. Lerch MM, Gorelick FS. Models of acute and chronic pancreatitis. Gastroenterology 2013;144:1180–1193.
15. **Huang W, Booth DM**, Cane MC, et al. Fatty acid ethyl ester synthase inhibition ameliorates ethanol-induced Ca2+-dependent mitochondrial dysfunction and acute pancreatitis. Gut 2014;63:1313–1324.
16. Murphy JA, Criddle DN, Sherwood M, et al. Direct activation of cytosolic Ca2+ signaling and enzyme secretion by cholecystokinin in human pancreatic acinar cells. Gastroenterology 2008;135:632–641.
17. Nathan JD, Romac J, Peng RY, et al. Transgenic expression of pancreatic secretory trypsin inhibitor-I ameliorates

secretagogue-induced pancreatitis in mice. Gastroenterology 2005;128:717–727.
18. Dawra R, Ku YS, Sharif R, et al. An improved method for extracting myeloperoxidase and determining its activity in the pancreas and lungs during pancreatitis. Pancreas 2008;37:62–68.
19. Gallagher S, Sankaran H, Williams JA. Mechanism of scorpion toxin-induced enzyme secretion in rat pancreas. Gastroenterology 1981;80:970–973.
20. **Zhang H, Neuhofer P**, Song L, et al. IL-6 trans-signaling promotes pancreatitis-associated lung injury and lethality. J Clin Invest 2013;123:1019–1031.
21. Bergmeier W, Weidinger C, Zee I, et al. Emerging roles of store-operated Ca^{2+} entry through STIM and ORAI proteins in immunity, hemostasis and cancer. Channels (Austin) 2013;7:379–391.
22. Gukovskaya AS, Vaquero E, Zaninovic V, et al. Neutrophils and NADPH oxidase mediate intrapancreatic trypsin activation in murine experimental acute pancreatitis. Gastroenterology 2002;122:974–984.
23. Choi S, Maleth J, Jha A, et al. The TRPCs-STIM1-Orai interaction. Handb Exp Pharmacol 2014;223:1035–1054.
24. **Mekahli D, Bultynck G**, Parys JB, et al. Endoplasmic-reticulum calcium depletion and disease. Cold Spring Harb Perspect Biol 2011;3:6.
25. Ward JB, Petersen OH, Jenkins SA, et al. Is an elevated concentration of acinar cytosolic free ionised calcium the trigger for acute pancreatitis? Lancet 1995;346:1016–1019.
26. Demetrius L, Legendre S, Harremöes P. Evolutionary entropy: a predictor of body size, metabolic rate and maximal life span. Bull Math Biol 2009;71:800–818.
27. Spanier BW, Nio Y, van der Hulst RW, et al. Practice and yield of early CT scan in acute pancreatitis: a Dutch Observational Multicenter Study. Pancreatology 2010;10:222–228.
28. O'Gara PT, Kushner FG, Ascheim DD, et al. 2013 ACCF/AHA guideline for the management of ST-elevation myocardial infarction: a report of the American College of Cardiology Foundation/American Heart Association Task Force on Practice Guidelines. Circulation 2013;127:e362–e425.
29. Jauch EC, Saver JL, Adams HP Jr, et al. Guidelines for the early management of patients with acute ischemic stroke: a guideline for healthcare professionals from the American Heart Association/American Stroke Association. Stroke 2013;44:870–947.
30. Fonarow GC, Zhao X, Smith EE, et al. Door-to-needle times for tissue plasminogen activator administration and clinical outcomes in acute ischemic stroke before and after a quality improvement initiative. JAMA 2014;311:1632–1640.
31. Villatoro E, Mulla M, Larvin M. Antibiotic therapy for prophylaxis against infection of pancreatic necrosis in acute pancreatitis. Cochrane Database Syst Rev 2010;5:CD002941.
32. Bradley EL 3rd. A clinically based classification system for acute pancreatitis. Arch Surg 1993;128:586–590.
33. Banks PA, Bollen TL, Dervenis C, et al. Classification of acute pancreatitis 2012: revision of the Atlanta classification and definitions by international consensus. Gut 2013;62:102–111.
34. Dellinger EP, Forsmark CE, Layer P, et al. Determinant-based classification of acute pancreatitis severity: an international multidisciplinary consultation. Ann Surg 2012;256:875–880.

Author names in bold designate shared co-first authors.

Received July 24, 2014. Accepted April 20, 2015.

Reprint requests
Address requests for reprints to: Robert Sutton, MB, BS, DPhil, FRCS, National Institute for Health Research Pancreas Biomedical Research Unit, NIHR Royal Liverpool University Hospital, Liverpool L69 3GA, United Kingdom. e-mail: r.sutton@liverpool.ac.uk; fax: (44)151-706-5826.

Acknowledgments
The authors are grateful to Paula Ghaneh, Chris Halloran, John Neoptolemos, Michael Raraty, and Rajesh Satchidanand who assisted in provision of human pancreatic tissue samples.

Conflicts of interest
These authors disclose the following: John Barrett and Malcolm Begg are employees of GlaxoSmithKline, who supplied GSK-7975A and GSK-6288B; Ken Stauderman, Jack Roos, Sergey Grigoryev, Stephanie Ramos, Evan Rogers, Jeff Whitten, Gonul Velicelebi, and Michael Dunn are or were at the time of these studies employees of CalciMedica, who undertook/supervised experiments with or supplied CM_128; and Robert Sutton has received funding from CalciMedica. The remaining authors disclose no conflicts.

Funding
Supported by a Liverpool China Scholarship Council Award (L.W.), State Administration of Traditional Chinese Medicine Key Discipline Construction Project, China (W.H.), the UK Medical Research Council (S.V., M.C., D.N.C., R.S., and A.V.T.), CORE, UK and the Royal College of Surgeons of England (M.A.J.), a Liverpool-RIKEN Studentship (D.C.), CalciMedica (M.D., K.S. J.R., S.G., S.R., E.R., J.W., G.V.), and the UK National Institute for Health Research (M.A., A.V.T., D.N.C., R.S.).

Supplementary Materials and Methods

Measurements of GSK-7975A and CM_128 In Vivo

Sampling of GSK-7975A was at 1, 2, 4, 10, and 22 hours after osmotic minipump insertion from 3 mice/time point. Immediately after humane killing, blood was collected into a heparinized tube, diluted 1:1 with sterile water, and the pancreas was removed and homogenized in 2 mL Covaris tubes containing ceramic beads. Standards and study samples (50 μL from blood and 100 μL from pancreas) were extracted by protein precipitation and centrifuged. Supernatants were dried under heated nitrogen (40°C). Levels of GSK-7975A and GSK-6288B were determined by LC-MS/MS (API4000 with Jasco X-LC and Ascentis express C18 column), as were levels of CM_128 in plasma and pancreas (Varian 500-MS with Varian 212 LC and Phenomenex C8 column), sampling from 3 mice at the same time point when drug efficacy was assessed.

Protein Binding of GSK-7975A and CM_128

The protein binding of GSK-7975A in the blood and pancreas was determined at 1 μg/mL using a dialysis Teflon block (HTDialysis, LLC, Gales Ferry, CT) with dialysis membrane strips and a rapid equilibrium dialysis device (Thermo Scientific), respectively. The protein binding of CM_128 in plasma (from Bioreclamation, Inc, Westbury, NY) was determined at 30 μmol/L or 50 μmol/L by equilibrium dialysis using a high-throughput dialysis Teflon block (HTDialysis, LLC) and dialysis membrane strips. Blood was collected into a heparin precoated tube and diluted 1:1 with phosphate-buffered saline (pH 7.4). Pancreas was homogenized in 500 μL phosphate-buffered saline, diluted 1:10. Blood, pancreas, homogenate, and plasma were dialyzed against phosphate-buffered saline in a buffer chamber, shaking gently at 37°C for 5 hours (blood), 4 hours (pancreas homogenate), and overnight (plasma). After equilibrium, samples from both the sample chamber and the buffer chamber of the rapid equilibrium dialysis plate were collected in a matrix-match manner and analyzed by liquid chromatography–mass spectrometry (AP14000; Applied Biosystems; or Varian 500-MS with Varian 212 LC and Phenomenex C8 column). Experiments were performed in triplicate. The percentage of GSK-7975A bound was calculated by the following equation: % bound= $([\text{GSK-7975A}]_a - [\text{GSK-7975A}]_b)/[\text{GSK-7975A}]_a \times 100\%$, where $[\text{GSK-7975A}]_a$ was the concentration of GSK-7975A in the sample chamber and $[\text{GSK-7975A}]_b$ was the concentration of GSK-7975A in the buffer chamber. The same equation was applied to calculate CM_128 binding.

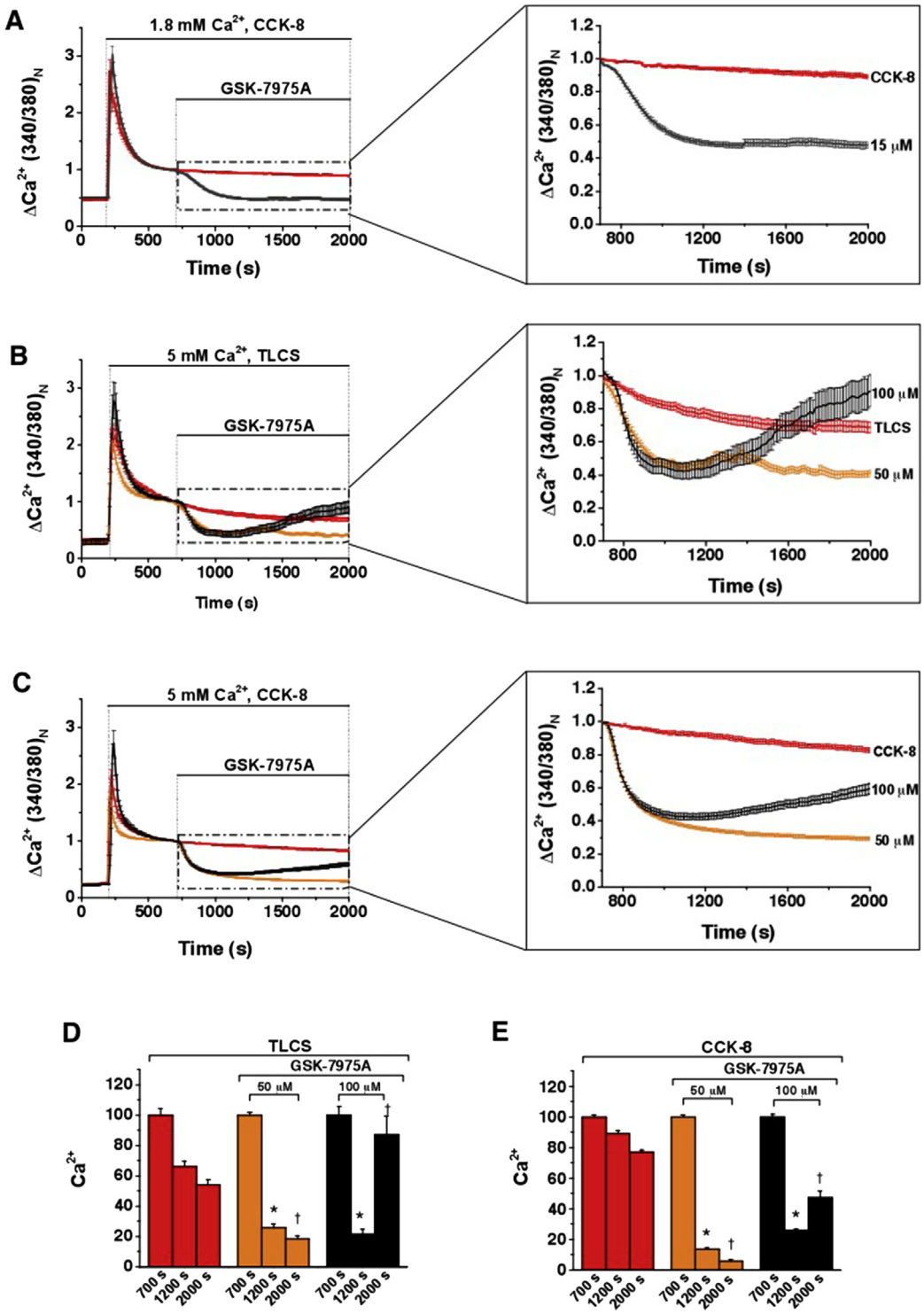

Supplementary Figure 1. GSK-7975A inhibits CRAC entry (Fura-2 340:380 normalized at 700 s). (*A*) Changes in mouse pancreatic acinar $[Ca^{2+}]_C$ induced by CCK (1 nmol/L) with external physiological $[Ca^{2+}]$ (1.8 mmol/L) applied, showing the effect of 15 μmol/L GSK-7975A from 700 seconds, expanded ($\geq$79 cells/group). Changes in mouse pancreatic acinar $[Ca^{2+}]_C$ induced by (*B*) TLCS (500 μmol/L) and (*C*) CCK (1 nmol/L), showing effects of 50 and 100 μmol/L GSK-7975A from 700 seconds, expanded. (*D* and *E*) Mean ($\pm$SEM) $[Ca^{2+}]_C$ at 700, 1200, and 2000 seconds from panels *B* and *C*, showing a marked reduction with 50 μmol/L GSK-7975A, but not 100 μmol/L GSK-7975A ($\geq$27 cells/group; $^*P < .001$, toxin vs toxin plus GSK-7975A at 1200 s; $^{\dagger}P < .001$, at 2000 s).

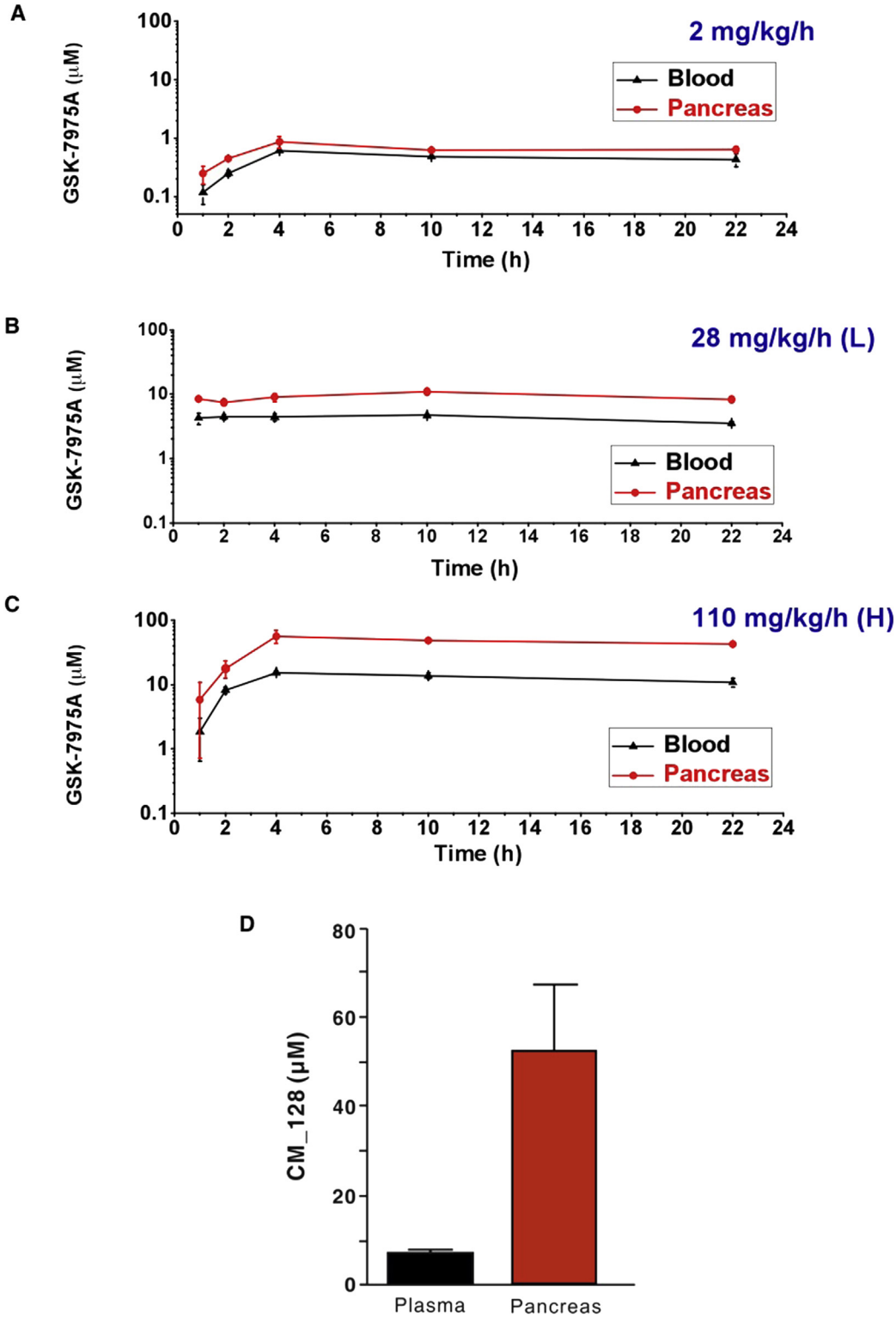

Supplementary Figure 2. GSK-7975A given as prodrug GSK-6288B administered by a subcutaneous osmotic minipump can be delivered consistently to each mouse and maintained throughout the experimental period. There was no detectable GSK-6288B in the blood or pancreas, suggesting complete conversion into GSK-7975A. (*A*) Blood and pancreas levels of GSK-7975A after administration of 2 mg/kg/h GSK-6288B showing a steady state 4 hours after minipump implantation, when the mean concentrations in blood and pancreas were approximately 0.4 and approximately 0.6 μmol/L respectively. (*B*) Blood and pancreas levels of GSK-7975A at the (lower) dose of 28 mg/kg/h GSK 6288B (L) reached a steady state 1 hour after minipump implantation, when the mean concentrations in blood and pancreas were approximately 5 and approximately 10 μmol/L, respectively. (*C*) Blood and pancreas levels of GSK-7975A at the (higher) dose of 110 mg/kg/h GSK-6288B (H) reached a steady state 4 hours after minipump implantation, when the mean concentrations in blood and pancreas were approximately 15 and approximately 50 μmol/L, respectively. (*D*) Mean (±SEM) plasma and pancreas levels of CM_128 at 20 mg/kg sampling at the time point when drug efficacy was assessed, were approximately 10 and approximately 50 μmol/L, respectively.

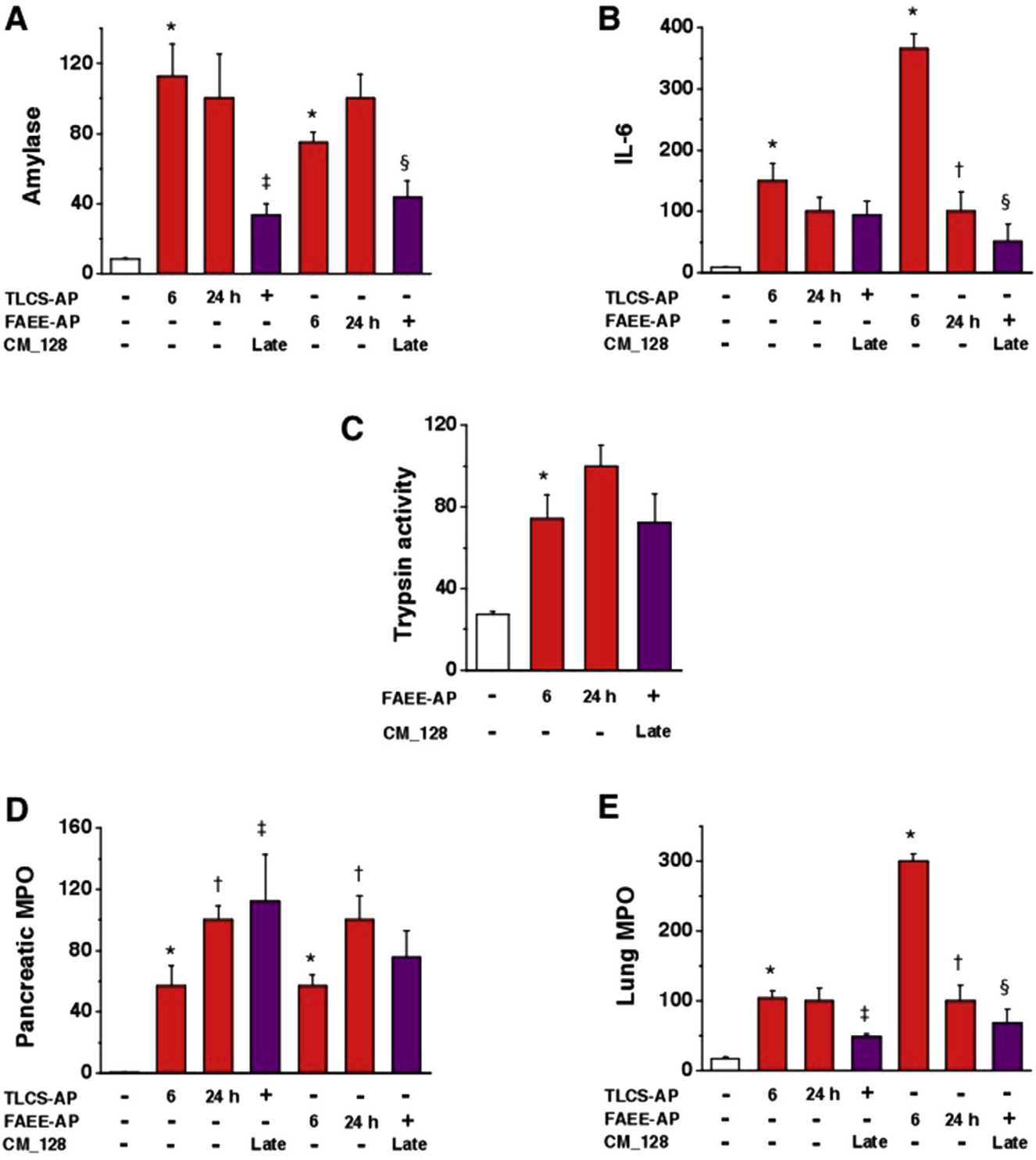

Supplementary Figure 3. CM_128 administered from 6 hours after disease induction (late) markedly reduced biochemical responses in TLCS-AP and FAEE-AP. Two models at 6 and 24 hours resulted in substantial increase of (*A*) serum amylase, (*B*) IL6, (*C*) pancreatic trypsin activity, (*D*) pancreatic activity, and (*E*) lung MPO activity, with more marked increase of IL6 and lung MPO activity at 6 hours, but of pancreatic trypsin and MPO activity at 24 hours. Intraperitoneal administration of CM_128 at 20 mg/kg late significantly reduced all parameters from levels at 6 hours (mean ± SEM ≥6 mice/group; $^{*}P < .05$, control vs 2 models at 6 h; $^{\dagger}P < .05$ 2 models at 6 vs 24 h; $^{\ddagger}P < .05$, TLCS-AP at 6 h vs TLCS-AP plus CM_128; $^{\S}P < .05$, FAEE-AP at 6 h vs FAEE-AP plus CM_128).

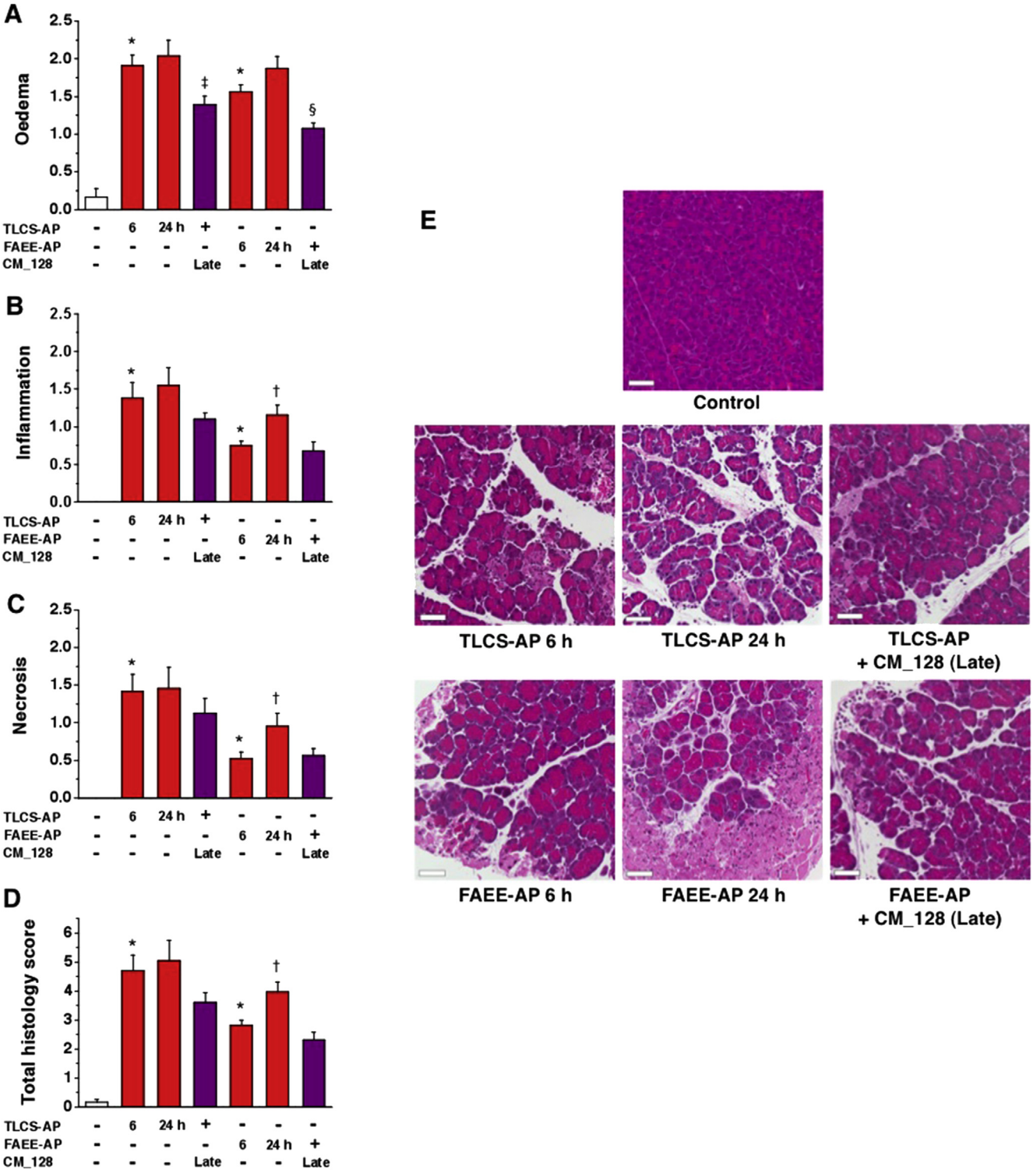

Supplementary Figure 4. CM_128 administered from 6 hours after disease induction (late) markedly reduced pancreatic histopathology in TLCS-AP and FAEE-AP. Two models at 6 and 24 hours resulted in substantially progressive increases in (*A*) edema, (*B*) inflammation, (*C*) necrosis, and (*D*) total histology score, with more marked increase of all scores at 24 hours. Intraperitoneal administration of CM_128 at 20 mg/kg from 6 hours after disease induction significantly reduced edema, but not inflammation, necrosis, or total histology scores at 6 hours (mean ± SEM ≥6 mice/group; $^{*}P < .05$, control vs 2 models at 6 hours; $^{\dagger}P < .05$ 2 models at 6 vs 24 hours; $^{\ddagger}P < .05$, TLCS-AP at 6 h vs TLCS-AP plus CM_128; $^{\S}P < .05$, FAEE-AP at 6 h vs FAEE-AP plus CM_128). (*E*) Representative images showing normal pancreatic histology, typical histopathology from 2 models at 6 and 24 hours, and typical histopathology from 2 models after treatment with CM_128 administered late after disease induction (H&E; *scale bar*: 50 μm).

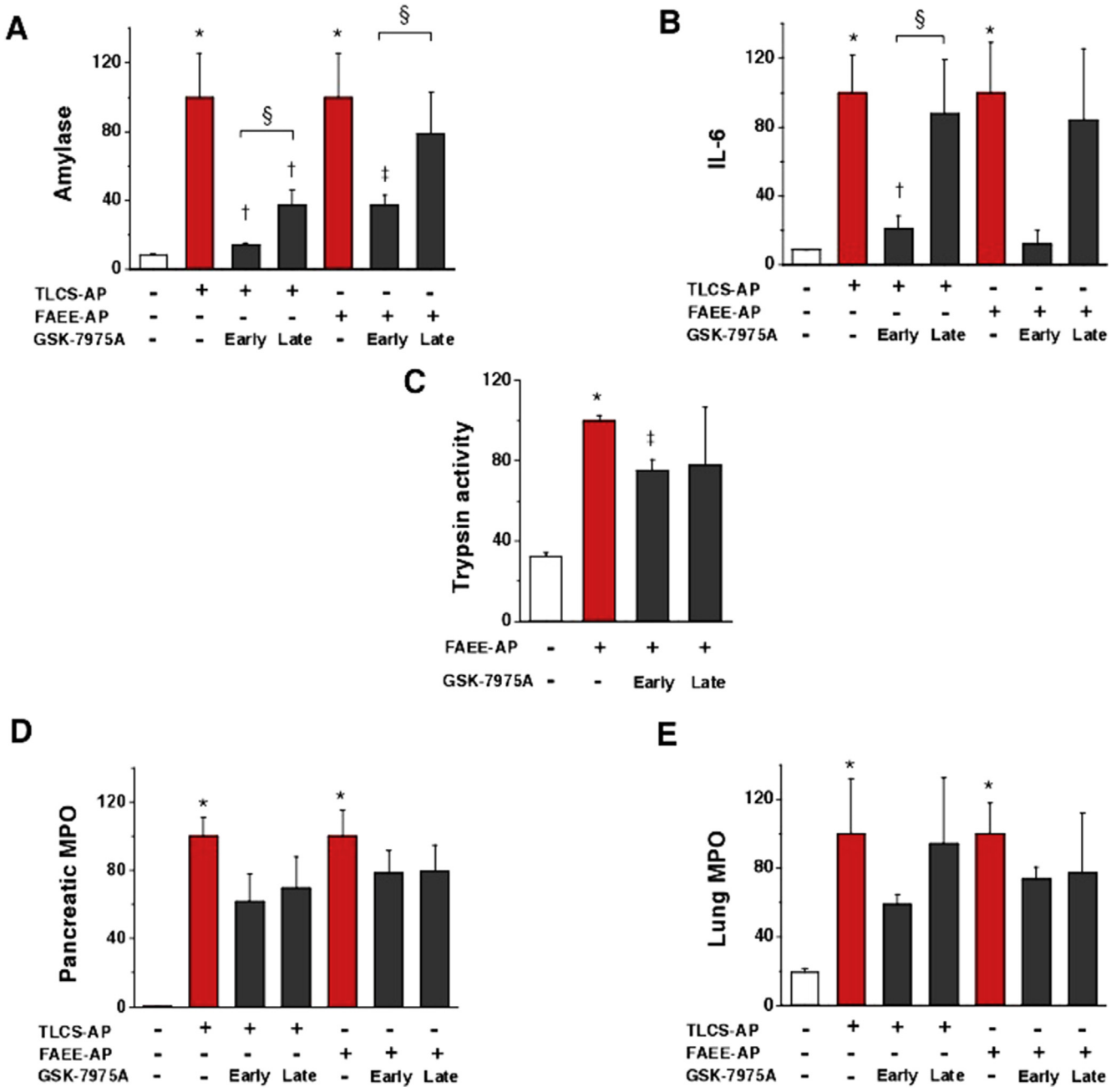

Supplementary Figure 5. GSK-7975A administered from 6 hours after disease induction (late) less effectively reduced biochemical responses of TLCS-AP and FAEE-AP. Two models resulted in substantial increases of (*A*) serum amylase, (*B*) IL6, (*C*) pancreatic trypsin activity, (*D*) pancreatic activity, and (*E*) lung MPO activity. Subcutaneous osmotic minipump administration of GSK-7975A given as prodrug GSK-6288B at high dose administered from a late time point was less protective than when given early (mean ± SEM ≥6 mice/group; $^{*}P < .05$, control vs 2 models; $^{\dagger}P < .05$ TLCS-AP vs TLCS-AP plus GSK-7975A; $^{\ddagger}P < .05$, FAEE-AP vs FAEE-AP plus GSK-7975A; and $^{\S}P < .05$, GSK-7975A early vs GSK-7975A late).

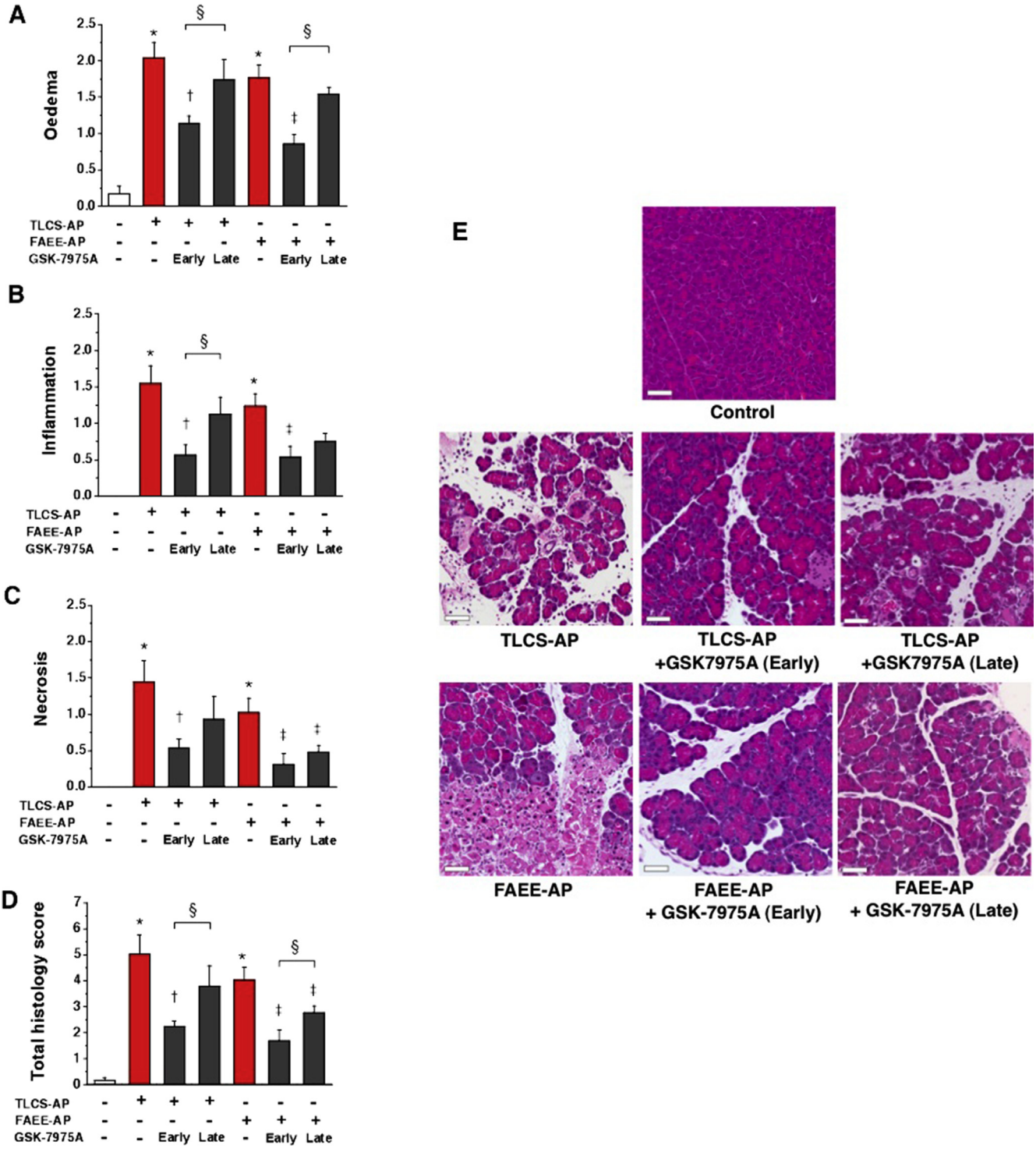

Supplementary Figure 6. GSK-7975A administered from 6 hours after disease induction (late) less effectively reduced pancreatic histopathology in TLCS-AP and FAEE-AP. Two models resulted in substantial increases in (*A*) edema, (*B*) inflammation, (*C*) necrosis, and (*D*) total histology score. Subcutaneous osmotic minipump administration of GSK-7975A given as prodrug GSK-6288B at high dose administered from a late time point was less effective that when begun early (mean ± SEM ≥6 mice/group; $^{*}P < .05$, control vs 2 models; $^{\dagger}P < .05$ TLCS-AP vs TLCS-AP plus GSK-7975A; $^{\ddagger}P < .05$, FAEE-AP vs FAEE-AP plus GSK-7975A, and $^{\S}P < .05$, GSK-7975A early vs GSK-7975A late). (*E*) Representative images showing normal pancreatic histology, typical histopathology from 2 models, and typical histopathology from 2 models after treatment with GSK-7975A administered early and late after disease induction (H&E; *scale bar*: 50 μm).